### INFORMATION TO USERS

While the most advanced technology has been used to photograph and reproduce this manuscript, the quality of the reproduction is heavily dependent upon the quality of the material submitted. For example:

- Manuscript pages may have indistinct print. In such cases, the best available copy has been filmed.
- Manuscripts may not always be complete. In such cases, a note will indicate that it is not possible to obtain missing pages.
- Copyrighted material may have been removed from the manuscript. In such cases, a note will indicate the deletion.

Oversize materials (e.g., maps, drawings, and charts) are photographed by sectioning the original, beginning at the upper left-hand corner and continuing from left to right in equal sections with small overlaps. Each oversize page is also filmed as one exposure and is available, for an additional charge, as a standard 35mm slide or as a 17"x 23" black and white photographic print.

Most photographs reproduce acceptably on positive microfilm or microfiche but lack the clarity on xerographic copies made from the microfilm. For an additional charge, 35mm slides of 6"x 9" black and white photographic prints are available for any photographs or illustrations that cannot be reproduced satisfactorily by xerography.

		·	

# Al-Soboh, Ghassan

# A SIMULATION STUDY OF THE DISPLACEMENT BEHAVIOR OF A TRUNK SHAKER SYSTEM DURING CHERRY HARVEST

Michigan State University

Ph.D. 1986

University
Microfilms
International 300 N. Zeeb Road, Ann Arbor, MI 48106

# **PLEASE NOTE:**

In all cases this material has been filmed in the best possible way from the available copy. Problems encountered with this document have been identified here with a check mark  $\sqrt{\phantom{a}}$ .

1.	Glossy photographs or pages
2.	Colored illustrations, paper or print
3.	Photographs with dark background
4.	lilustrations are poor copy
5.	Pages with black marks, not original copy
6.	Print shows through as there is text on both sides of page
7.	Indistinct, broken or small print on several pages
8.	Print exceeds margin requirements
9.	Tightly bound copy with print lost in spine
10.	Computer printout pages with indistinct print
11.	Page(s) lacking when material received, and not available from school or author.
12.	Page(s) seem to be missing in numbering only as text follows.
13.	Two pages numbered Text follows.
14.	Curling and wrinkled pages
15.	Dissertation contains pages with print at a slant, filmed as received
16.	Other

University
Microfilms
International

# A SIMULATION STUDY OF THE DISPLACEMENT BEHAVIOR OF A TRUNK SHAKER SYSTEM DURING CHERRY HARVEST

BY

Ghassan Al-Soboh

### A DISSERTATION

Submitted to
Michigan State University
in partial fullfillment of the requirements
for the degree of

DOCTOR OF PHILOSOPHY

Department of Agricultural Engineering

#### ABSTRACT

# A SIMULATION STUDY OF THE DISPLACEMENT BEHAVIOR OF A TRUNK SHAKER SYSTEM DURING CHERRY HARVEST

BY

### GHASSAN AL-SOBOH

Mechanical harvesting is now the only method for harvesting the sweet or sour cherries for processing that are grown in Michigan. Nearly all mechanical harvesting systems use a trunk shaker. Currently, growers are reporting an increased problem with bark damage due to trunk shaking. Many believe bark damage contributes to cherry tree decline (early loss of tree vigor and yield).

With the goal of identifying some shaker design or operational changes that would help reduce physical damage to the tree bark, a simulation study of the vibrational behavior of a trunk shaker was conducted. The Integrated Mechanisms Program (IMP) was selected as the tool for computer modeling, and the Friday C-clamp trunk shaker was modeled since it is widely used for cherry harvesting.

During the study, the required physical properties of the shaker and young cherry trees were measured, analyzed and used in the IMP program. Through free-shake simulation runs, the IMP program successfuly predicted dynamic shaker displacement behavior similar to that observed in field tests.

The simulated shaker displacement behavior during free-shake conditions (no tree clamped in the shaker) was found to shift and gallop (large displacements) during startup, and then to drift when operated at harvesting frequency. These conditions are believed to create excessive stress on the tree bark.

Shaker physical properties changes (housing mass, eccentric rotating mass, and rotating mass eccentricity) and changes in rotating mass accelerations and starting phase angles were studied to find ways to reduce the undesirable shaker displacements.

The undesirable displacements were eliminated when the eccentricity of the rotating masses was initially set at zero then increased to cause the desired shaking action, or when a particular rotating mass position was used in which the starting phase angle between the two masses was 225 degrees. Such changes in the shaker design and operation should reduce undesirable displacements and thereby reduce bark damage. Tests with a modified shaker will be required to verify these simulation results.

#### ACKNOWLEDGMENTS

I thank my god who gave me the health and the power to accomplish this work successfully.

I thank my family, my loving wife Nuha, my son Yasser, and my daughter Noor, for their encouragement, support and patience during my study.

The author would like to express his deepest gratitude to the following persons and organizations for the contribution to this study:

To Dr. Galen K. Brown (Research Leader, Fruit and Vegetable Harvesting, U.S Department of Agriculture), my major professor, for his professional guidance, cooperation, support, and editorial help provided throughout the duration of my Ph.D program.

To Dr. Gary L. Cloud (Professor Metallurgy, Mechanics and Materials Science), Dr. Gary R. Van Ee (Assistant Professor Agricultural Engineering), and Dr. Clyde Burton (Assistant Professor U.S. Department of Agriculture) for their time, enstructive counsel, and professional interest.

To Henry Affeldt (Ph.D Gradute Student), Tom Eash (Ph.D Gradute Student), and Dale Marshall (Agricultural Engineer USDA), for their contribution of valuable assistance and experience to the project during the experimental stage.

To AID program, and U.S. Department of Agriculture for

their educational and financial assistance during my study in the United States.

To Dr. Kenneth Ebert (Specialist, International Student Dean) for his time and effort with the USDA and the university to keep the program going successfully.

To my family in Syria, and my friends who have been a continuing source of strength and encourgement.

# TABLE OF CONTENTS

ACKNOWLEDGEMENTS. iii LIST OF TABLES. viii LIST OF FIGURES. ix  CHAPTER 1:  1. INTRODUCTION. 1  1.1 Cherry Production 5  1.2 Mechanical Harvesting. 10  1.3 The Bark Damage Problem 14  1.4 The Need For A Shaker Model 16  1.5 Objective Of The Study 18  CHAPTER 2:  2. LITERATURE REVIEW. 20  2.1 Bark Damage And Causes. 20  2.2 Bark Structure And Strength. 27  2.3 Shaker Pads, Forces, And Pressures 32  2.4 Dynamic Response Of Trees 35  CHAPTER 3:  3. COMPUTER MODELING. 46  3.1 IMP Program. 46  3.2.1 Model Assumptions 48  3.2.2 Model Development 55  Trunk Shaker. 52  3.2.3 Model Development Of C-Clamp  Trunk Shaker. 52  3.2.3 Model Development Of C-Clamp Trunk  58	PAGE
1. INTRODUCTION	LIST OF TABLES viii
1.1 Cherry Production	CHAPTER 1:
1.2 Mechanical Harvesting. 10 1.3 The Bark Damage Problem. 14 1.4 The Need For A Shaker Model. 16 1.5 Objective Of The Study. 18  CHAPTER 2:  2. LITERATURE REVIEW. 20 2.1 Bark Damage And Causes. 20 2.2 Bark Structure And Strength. 27 2.3 Shaker Pads, Forces, And Pressures. 32 2.4 Dynamic Response Of Trees. 35  CHAPTER 3:  3. COMPUTER MODELING. 46 3.1 IMP Program. 46 3.2 Model Development 48 3.2.1 Model Assumptions. 48 3.2.2 Model Development Of C-Clamp Trunk Shaker. 52 3.2.3 Model Development Of C-Clamp Trunk	1. INTRODUCTION
2. LITERATURE REVIEW	1.2 Mechanical Harvesting
2.1 Bark Damage And Causes	CHAPTER 2:
2.2 Bark Structure And Strength	2. LITERATURE REVIEW
3. COMPUTER MODELING	2.2 Bark Structure And Strength
3.1 IMP Program	HAPTER 3:
3.2 Model Development	3. COMPUTER MODELING
Trunk Shaker	3.2 Model Development
	Trunk Shaker

# CHAPTER 4:

4.	EXPI	ERIMENTAL MEASUREMENTS	1
	4.1	Tree Measurements	1
		Gravity, And Mass Measurements 6	2
	4.2	4.1.2 Stiffness And Damping Measurements 8 Trunk Shaker Description	5
	4.3	Trunk Shaker Physical Properties	
	4.4	Rotating Mass Velocity Measurements 10	1
CHAP	TER	5 <b>:</b>	
5.	SHAI	KER DISPLACEMENT RESULTS	
		Free-Shake Vibration 10	
		Shaker-Tree Vibration System	
	5.5	model verilication	0
CHAP	TER	6:	
6.	SENS	SITIVITY ANALYSIS STUDY OF DISPLACEMENT	
	6.1	Variation Of The Magnitude Of The Shaker	_
	6.2	Housing Mass 13 Variation Of The Magnitude of the Rotating	U
		Masses 13	
		Variation of The Rotating Mass Acceleration 14	
		Variation Of The Rotating Masses Eccentricity 14 Variation Of The Rotating Mass Phase Angle 15	
		variation of the negating has industrial	Ī
СНАР	TER	7:	
7.	SUM	MARY AND CONCLUSIONS	
		Summary 20	
	7.2	Conclusions	
		7.2.1 Scope And Limitations	9
			_
REFE	RENC	CES	1

APPENDIX	A	
	Free-Shake C-Clamp Trunk Shaker Model	A.1
APPENDIX	В	
	Shaker-Tree C-Clamp Trunk Shaker Model	B.1
APPENDIX	c	
	Optical Free-Shake Displacement Results	C.1
APPENDIX	D	
	Optical Shaker-Tree Displacement Results	D.1

# LIST OF TABLES

TABLE		PAGE
1.1	Michigan Sour Cherry Production And Utilization	6
1.2	Michigan Sweet Cherry Production And Utilization	8
4.1	Linear Stiffness And Damping Properties Of The Sour Cherry Tree	76
4.2	Rotary Stiffness And Damping Properties Of The Sour Cherry Tree	83
4.3	Shaker Moment Of Inertia Determined By Swinging	92
4.4	Stiffness And Damping Constants For Shaker Mounts	100
4.5	Summary Of The Physical Properties Of Friday C-Clamp Trunk Shaker And A 63 mm Sweet Cherry Tree Used In IMP Model	107
6.1	Summary Of The Simulated Displacement Results At Different Rotating Mass Starting Phase Angles	180

# LIST OF FIGURES

FIGU	RE ·	PAGE
1.1	Sour Cherry Production In Michigan Between 1981 To 1985	7
1.2	Sweet Cherry Production In Michigan Between 1981 to 1985	8
2.1	Bark Damage On A Cherry Tree Trunk As A Result Of Mechanical harvesting	21
3.1	Top View Of Friday C-Clamp Trunk Shaker As Defined For The IMP Model	53
3.2	Side View Of C-Clamp Trunk Shaker As Defined For The IMP Model	54
3.3	Top View Of Friday C-Clamp Trunk Shaker-Tree System As Defined For The IMP Model	60
4.1	Sweet Cherry Tree Height Vs. Tree Trunk Diameter	63
4.2	Sour Cherry Tree Height Vs. Tree Trunk Diameter	64
4.3	Sweet Cherry Tree Center Of Gravity Vs. Tree Trunk Diameter	66
4.4	Sour Cherry Tree Center Of Gravity Vs. Tree Trunk Diameter	67
4.5	Sweet Cherry Tree Mass Vs. Tree Trunk Diameter	68
4.6	Sour Cherry Tree Mass Vs. Tree Trunk Diameter	69
4.7	Tree Pull Test Setup For Linear Stiffness	72
4.8	Linear Displacements Measurements Of A 63 mm Diameter Cherry Tree Trunk	74
4.9	Linear Force Measurements Of A 63 mm Diameter Cherry Tree Trunk Versus Time	75
4.10	Tree Twister Setup For Rotary Stiffness	78

4.11	Angular Displacements Versus Time Of A 63 mm Diameter Cherry Tree Trunk	80
4.12	Experimental Torque Measurements Of A 63 mm Diameter Cherry Tree Trunk	81
4.13	Friday C-Clamp Trunk Shaker	86
4.14	Shaker Physical Dimensions	89
4.15	LVDT Locations And Damping Measurements Of The Trunk Shaker	99
4.16	Inside Rotating Mass Frequency Of A Free Shaker	103
4.17	Outside Rotating Mass Frequency Of A Free Shaker	104
4.18	Inside Rotating Mass Frequency Of A Shaker Attached To A 63 mm Diameter Cherry Tree Trunk	105
4.19	Outside Rotating Mass Frequency Of A Shaker Attached To A 63 mm Diameter Cherry Tree Trunk	106
5.1	Free Shaking Displacement Vs. Time At A Mass Rotating Frequency Of 5 Hz	113
5.2	Free Shaking Displacement Vs. Time At A Mass Rotating Frequency Of 10 Hz	114
5.3	Free Shaking Displacement Vs. Time At A Mass Rotating Frequency Of 15 Hz	115
5.4	Rotating Masses Are Running According To Simulated Transient Velocity Function	116
5.5	Tree Displacement At A Mass Rotating Frequency Of 5 Hz With No Tree Stiffness Or Damping	119
5.6	Tree Displacement At A Mass Rotating Frequency Of 10 Hz With No Tree Stiffness Or Damping	120
5.7	Tree Displacement At A Mass Rotating Frequency Of 15 Hz With No Tree Stiffness Or Damping	121
5.8	Tree Displacement At A Shaker Rotating Mass Frequency Of 15 Hz	123
6.1	Rotating Masses Are Running According To Simulated Velocity Function For A Shaker Housing Mass Of 317 kg	133

6.2	Free Shaking Displacement Vs. Time At A Mass Rotating Frequency Of 15 Hz, And Shaker Housing Mass Of 317 kg	134
6.3	Rotating Masses Are Running According To Simulated Transient Velocity Function For A Shaker Housing Mass Of 226.5 kg	135
6.4	Free Shaking Displacement Vs. Time At Mass Rotating Frequency Of 15 Hz And Shaker Housing Mass Of 226.5 kg	136
6.5	Rotating Masses Are Running According To Simulated Velocity Function For A Mass Of 31.7 kg	139
6.6	Free Shaking Displacement Vs. Time At Frequency Of 15 Hz And Shaker Rotating Mass Of 31.7 kg	140
6.7	Rotating Masses Are Running According To Simulated Transient Velocity Function For A A Mass Of 18.12 kg	141
6.8	Free Shaking Displacement Vs. Time At Frequency Of 15 Hz And Shaker Rotating Mass Of 18.12 kg	142
6.9	Rotating Masses Are Running According To Simulated Transient Velocity Function For Two Different Acceleration Levels, 280 And 270 rad/s.s	145
6.10	Rotating Masses Are Running According To Simulated Transient Velocity Function For Two Different Acceleration Levels, 280 And 260 rad/s.s	146
	Rotating Masses Are Running According To Simulated Transient Velocity Function For Two Different Acceleration Levels, 328 And 246 rad/s.s	147
	Sliding Rotating Mass Model	
6.14	Rotating Masses Are Running According To	

	Simulated Transient Velocity Function With Moving Eccentricity At Rate Of 190 mm/s	153
6.15	Rotating Masses Are Running According To Simulated Transient Velocity Function With Moving Eccentricity At Rate Of 165 mm/s	154
6.16	Rotating Masses Are Running At Steady Frequency Of 5 Hz With Moving Eccentricity At Rate Of 217 mm/s	155
6.17	Rotating Masses Are Running At Steady Frequency Of 10 Hz With Moving Eccentricity At Rate Of 217 mm/s	1,56
6.18	Rotating Masses Are Running At Steady Frequency Of 15 Hz With Moving Eccentricity At Rate Of 217 mm/s	157
6.19	Shaker Displacement In The x Direction. Masses Are Running At Accelerations Of 328 And 246 rad/s.s. At A Starting Phase Angle Of 0 Degrees	160
6.20	Shaker Displacement In The y Direction. Masses Are Running At Accelerations Of 328 And 246 rad/s.s. At A Starting Phase Angle Of 0 Degrees	161
6.21	Shaker Displacement In The x-y Plane. Masses Are Running At Accelerations Of 328 And 246 rad/s.s. At A Starting Phase Angle Of O Degrees	162
6.22	Shaker Displacement In The x Direction. Masses Are Running At Accelerations Of 328 And 246 rad/s.s. At A Starting Phase Angle Of 45 Degrees	163
	Shaker Displacement In The y Direction. Masses Are Running At Accelerations Of 328 And 246 rad/s.s. At A Starting Phase Angle Of 45 Degrees	164
6.24	Shaker Displacement In The x-y Plane. Masses Are Running At Accelerations Of 328 And 246 rad/s.s. At A Starting Phase Angle Of 45 Degrees	165
6 25	Shakan Dicalegement In The v Direction Massas	

	Are Running At Accelerations Of 328 And 246 rad/s.s. At A Starting Phase Angle Of 90 Degrees	166
6.26	Shaker Displacement In The y Direction. Masses Are Running At Accelerations Of 328 And 246 rad/s.s. At A Starting Phase Angle Of 90 Degrees	167
6.27	Shaker Displacement In The x-y Plane. Masses Are Running At Accelerations Of 328 And 246 rad/s.s. At A Starting Phase Angle Of 90 Degrees	168
6.28	Shaker Displacement In The x Direction. Masses Are Running At Accelerations Of 328 And 246 rad/s.s. At A Starting Phase Angle Of 135 Degrees	170
6.29	Shaker Displacement In The y Direction. Masses Are Running At Accelerations Of 328 And 246 rad/s.s. At A Starting Phase Angle Of 135 Degrees	171
6.30	Shaker Displacement In The x-y Plane. Masses Are Running At Accelerations Of 328 And 246 rad/s.s. At A Starting Phase Angle Of 135 Degrees	172
6.31	Shaker Displacement In The x Direction. Masses Are Running At Accelerations Of 328 And 246 rad/s.s. At A Starting Phase Angle Of 180 Degrees	173
6.32	Shaker Displacement In The y Direction. Masses Are Running At Accelerations Of 328 And 246 rad/s.s. At A Starting Phase Angle Of 180 Degrees	174
6.33	Shaker Displacement In The x-y Plane. Masses Are Running At Accelerations Of 328 And 246 rad/s.s. At A Starting Phase Angle Of 180 Degrees	175
6.34	Shaker Displacement In The x Direction. Masses Are Running At Accelerations Of 328 And 246 rad/s.s. At A Starting Phase Angle Of 225 Degrees	176
6.35	Shaker Displacement In The v Direction, Masses	

	Are Running At Accelerations Of 328 And 246 rad/s.s. At A Starting Phase Angle Of 225 Degrees	177
6.36	Shaker Displacement In The x-y Plane. Masses Are Running At Accelerations Of 328 And 246 rad/s.s. At A Starting Phase Angle Of 225 Degrees	178
6.37	Shaker Displacement In The x Direction. Masses Are Running At Accelerations Of 328 And 246 rad/s.s. At A Starting Phase Angle Of 270 Degrees	181
6.38	Shaker Displacement In The y Direction. Masses Are Running At Accelerations Of 328 And 246 rad/s.s. At A Starting Phase Angle Of 270 Degrees	182
6.39	Shaker Displacement In The x-y Plane. Masses Are Running At Accelerations Of 328 And 246 rad/s.s. At A Starting Phase Angle Of 270 Degrees	183
6.40	Shaker Displacement In The x Direction. Masses Are Running At Accelerations Of 328 And 246 rad/s.s. At A Starting Phase Angle Of 315 Degrees	184
6.41	Shaker Displacement In The y Direction. Masses Are Running At Accelerations Of 328 And 246 rad/s.s. At A Starting Phase Angle Of 315 Degrees	185
6.42	Shaker Displacement In The x-y Plane. Masses Are Running At Accelerations Of 328 And 246 rad/s.s. At A Starting Phase Angle Of 315 Degrees	186
6.43	Shaker Displacement In The x Direction. Masses Are Running At Accelerations Of 358 And 276 rad/s.s. At A Starting Phase Angle Of 225 Degrees	189
6.44	Shaker Displacement In The y Direction. Masses Are Running At Accelerations Of 358 And 276 rad/s.s. At A Starting Phase Angle Of 225 Degrees	190
6.45	Shaker Displacement In The x-y Plane. Masses	

	Are Running At Accelerations Of 358 And 276
	rad/s.s. At A Starting Phase Angle Of
	225 Degrees 191
6.46	Shaker Displacement In The x Direction. Masses
	Are Running At Accelerations Of 358 And 276
	rad/s.s. At A Starting Phase Angle Of
	0 Degrees 192
6.47	Shaker Displacement In The y Direction. Masses
	Are Running At Accelerations Of 358 And 276
	rad/s.s. At A Starting Phase Angle Of
	0 Degrees 193
6.48	Shaker Displacement In The x-y Plane. Masses
	Are Running At Accelerations Of 358 And 276
	rad/s.s. At A Starting Phase Angle Of
	0 Degrees 194
6.49	Shaker Displacement In The x Direction. Masses
	Are Running At Accelerations Of 298 And 216
	rad/s.s. At A Starting Phase Angle Of
	225 Degrees 195
6.50	Shaker Displacement In The y Direction. Masses
	Are Running At Accelerations Of 298 And 216
	rad/s.s. At A Starting Phase Angle Of
	225 Degrees
6.51	Shaker Displacement In The x-y Plane. Masses
	Are Running At Accelerations Of 298 And 216
	rad/s.s. At A Starting Phase Angle Of
	225 Degrees 197
6 52	Shaker Displacement In The x Direction. Masses
0.52	Are Running At Accelerations Of 298 And 216
	rad/s.s. At A Starting Phase Angle Of
	O Degrees
	v begrees
6.53	Shaker Displacement In The y Direction. Masses
	Are Running At Accelerations Of 298 And 216
	rad/s.s. At A Starting Phase Angle Of
	0 Degrees 199
6.54	Shaker Displacement In The x-y Plane. Masses
	Are Running At Accelerations Of 298 And 216
	rad/s.s. At A Starting Phase Angle Of
	0 Degrees 200

### CHAPTER 1

### 1. INTRODUCTION

Mechanical harvesting of cherries has played an important role in cherry production areas in Michigan, where over 95% of the sour and sweet cherry trees are being harvested mechanically using shake-and-catch harvesting systems. Nearly all of these systems use trunk shakers, because they provide faster harvest and lower harvest cost than limb shakers.

Over the years, mechanical tree shakers have improved from a simple push boom or pull cable attached to a crank mechanism on a tractor to inertia machines providing programmed options for shaking stroke, force, direction and frequency. Today, powerful trunk shakers are available, and the shaker clamp systems have been enlarged and improved.

In recent years, growers have reported that cherry tree decline (loss of vigor and yield, early replacement of the orchard) is an increasing problem where the mechanical harvesting of cherries is being practiced. Internal tree damage has been found, and a possible cause of this damage is high dynamic forces during shaker operation.

At present there is a need to analyze the trunk shaker design used for cherry harvesting, with the goal of

identifying design changes that would help reduce physical damage to the tree bark system of young trees. The cherry tree trunk diameters considered in this study ranged from 63 mm (2.5 in.) to 165 mm (6.5 in.).

The startup phase and the stopping phase of tree shaking have been observed to be most likely times for bark damage to occur. Large unstable displacements have been observed that can result in large shear and compression forces and stresses being transmitted to the bark. If these large displacements can be eliminated, the large forces and stresses should also be eliminated. Thus, bark damage should be reduced. The startup and steady state phases of the shaker operation were studied. The stopping phase was not studied, although that may be a source of serious damage since the shaker is not in a controlled (powered) state at that time.

To study the displacement behavior and identify design changes that would help eliminate large undesirable displacement, computer program entitled 8. Integrated Mechanisms Program (IMP) was selected as a tool for mechanical system simulation . The IMP program is capable of simulating two-or three-dimensional rigid link mechanical systems having single or multiple degrees of freedom. different modes can be simulated by this program: kinematic (geometric), static (equilibrium), or dynamic (time response). With these considerations in mind, a free-shake model was developed and used in the IMP program to study the dynamic behavior of a C-clamp trunk shaker as a function of time. Through this approach, possible design changes were introduced and evaluated for their ability to reduce conditions likely to cause bark damage.

A shaker-tree model was also developed and used in the program to simulate the displacement behavior of a trunk attached to the Friday C-clamp trunk shaker. The tree properties of mass, damping and stiffness were measured for use in this model. In the first modeling stage, the mass and inertia properties of a 63 mm (2.5 in.) diameter sour cherry tree trunk were introduced in the IMP model, but the stiffness or damping were omitted. The simulated tree displacement results were close to those measured in experimental field tests. In a second modeling stage, the tree stiffness and damping properties were added in the IMP model. Unfortunately, the simulated tree displacements were not realistic and the simulation aborted due to some problems in the stiffness matrix of the IMP program. Consequently, the simulation results presented in this study deal with the free-shake displacement behavior of the These results are believed to be very indicative of shaker. the actual displacement behavior of the shaker when clamped to young trees having trunk of 63 to 114 mm (2.5 to 4.5 in.)

diameter. In the future, the stiffness and damping properties can be added to the shaker-tree model when IMP program has been corrected.

### 1.1 Cherry Production

Cherry production has continued to play an important role in Michigan agricultural production. Production of sour cherries, Montmorency variety, in Michigan was up slightly in 1985 while the main varieties for sweet (Napoleon, Golds, Schmidt, Emperor Francis, Hedelfingen, Windsor, and others) declined marginally from 1984 levels. In Michigan, the nation's leading sour cherry producing state, the 1985 production estimate was 97,523 tonnes (215,000,000 lbs). Trees planted in the late 1970's are now bearing and will help sustain future production at present levels. Perfect weather conditions prevailed throughout much of the growing season in 1985. Only intermittent hailstorms and windstorms affected production and quality. Utilized production was about 95,255 tonnes (210,000,000 lbs) in 1985 and had a farm gate value of \$52,395,000. A summary Michigan sour cherry production in the last 5 years is presented in Table 1.1 and Figure 1.1.

Sweet cherry production was about 28,860 tonnes (62,000,000 lbs) in 1985 and had a farm gate value of \$15,128,000. A summery of Michigan sweet cherry production in the last 5 years is presented in Table 1.2 and Figure 1.2.

Table 1.1 Michigan Sour Cherry Production

And Utilization.

CROP	TOTAL PRODUCTION* (Tonnes)	UTILIZED PRODUCTION	
YEAR		FRESH (Tonnes)	PROCESSED (Tonnes)
1985	99,660	2,265	97,395
1984	95,130	2,265	88,335
1983	39,410	905	38,500
1982	117,780	2,265	86,070
1981	39,865	905	38,958

<sup>\*</sup> Total production defined as production avilable for harvest.

Source: Michigan Agricultural Statistics, 1985.

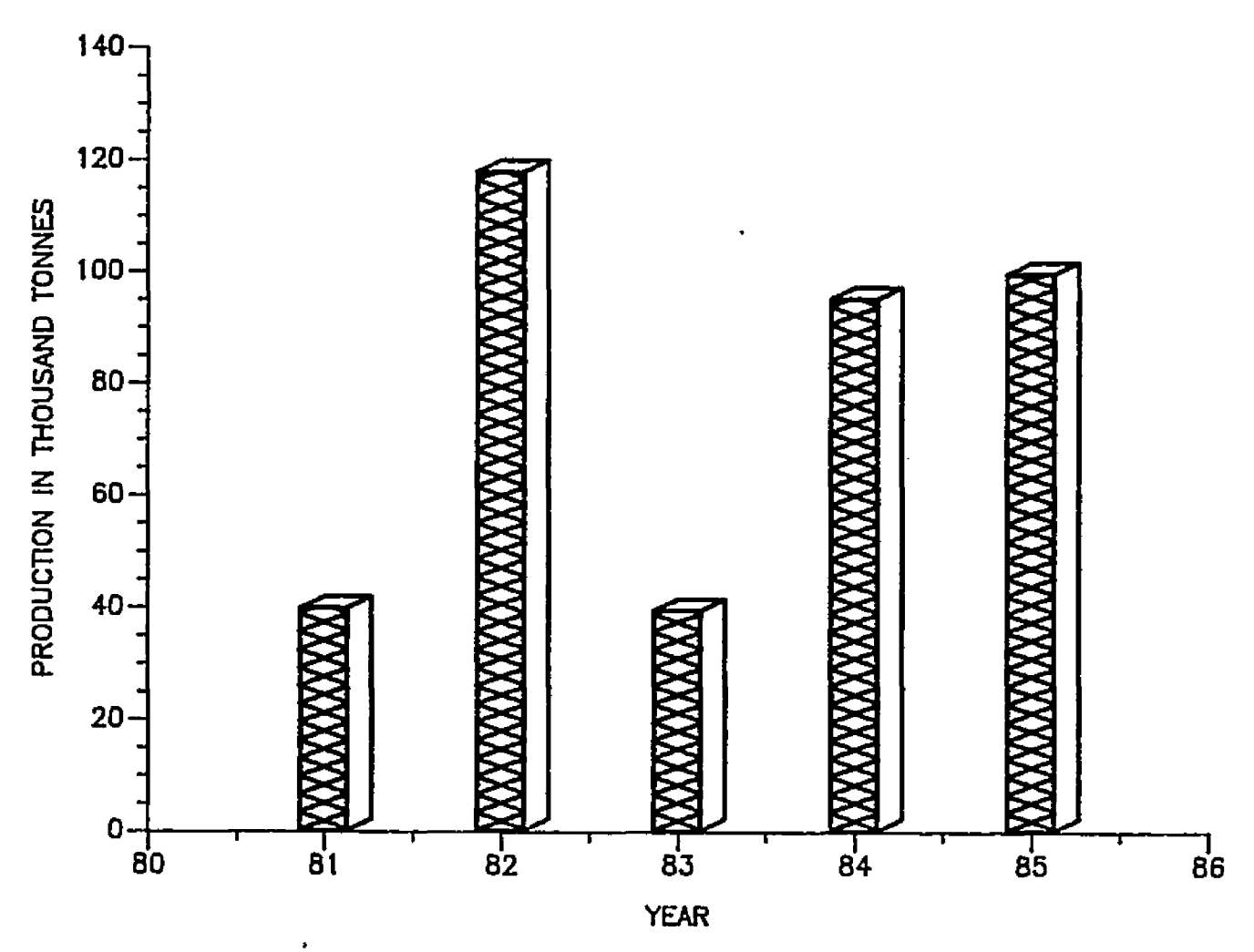


FIGURE 1.1 SOUR CHERRY PRODUCTION IN MICHIGAN BETWEEN 1981 TO 1985

Table 1.2 Michigan Sweet Cherry Production
And Utilization.

CROP	TOTAL PRODUCTION* (Tonnes)	UTILIZED PRODUCTION	
YEAR		FRESH (Tonnes)	PROCESSED (Tonnes)
1985	28,086	2,720	25,368
1984	29,900	2,720	25,368
1983	16,310	1,810	14,500
1982	28,086	1,810	21,290
1981	20,840	1,360	19,480

<sup>\*</sup> Total production defined as production available for harvest.

Source: Michigan Agricultural Production Statistics, 1985.

# SWEET CHERRY PRODUCTION IN MICHIGAN

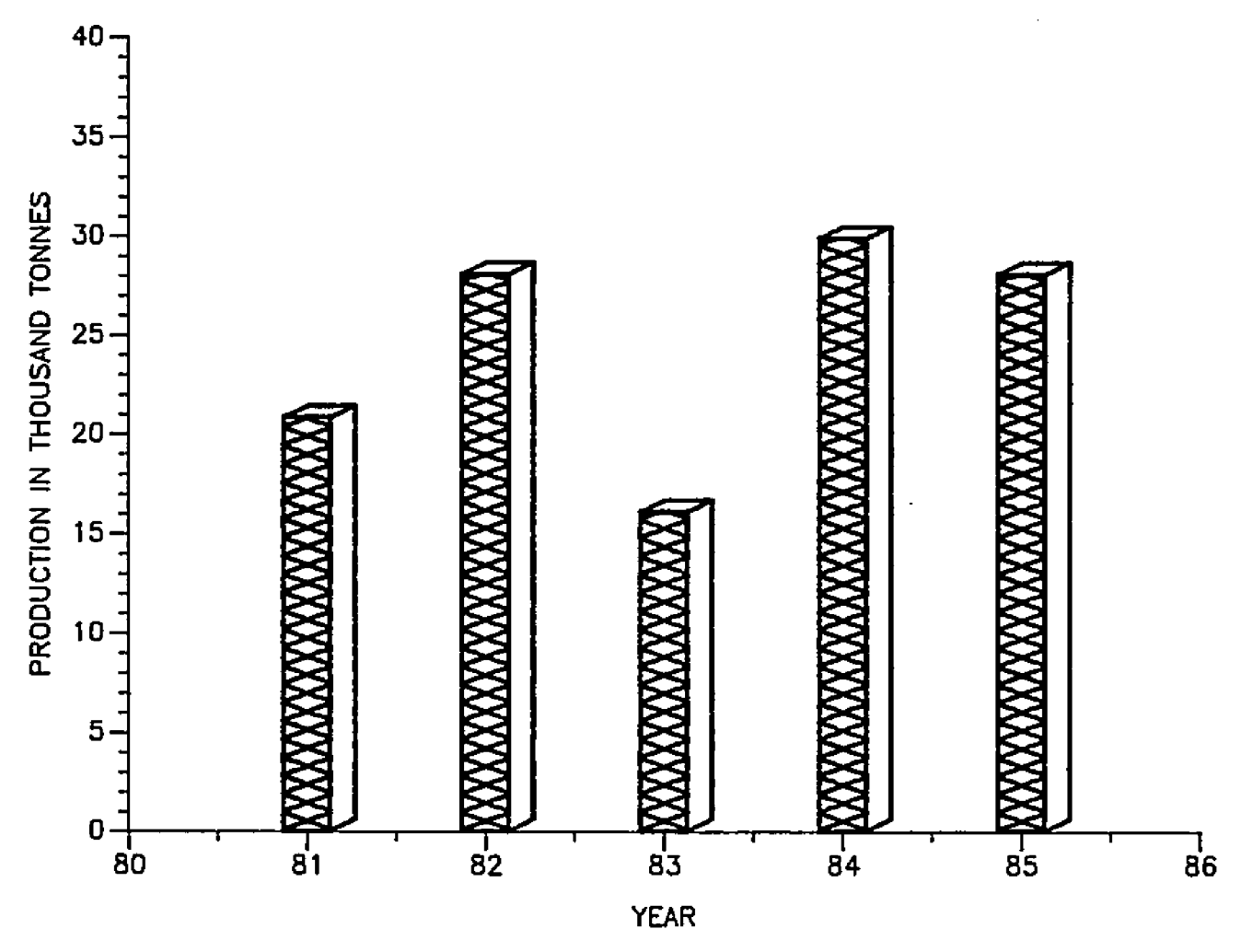


FIGURE 1.2 SWEET CHERRY PRODUCTION IN MICHIGAN BETWEEN 1981 TO 1985.

## 1.2 Mechanical Harvesting

Over the years, manual harvesting of cherries has proved to be uneconomical and inefficient. Manual harvesting the cherry crop required many migrant workers. labor during harvest reached to half the farm value the crop (Brown, 1980). With the termination of PL 78 (Bracero Program), that allowed supplementary foreign workers to enter the U.S. to meet high seasonal labor needs, had to choose between mechanical growers harvesting, switching crops or changing vocation. The growers soon recognized that a high long-term investment in mechanical harvesting equipment would permit them to supply the consumer market with cherries at an economical cost.

Shortage and cost of hand labor, labor unrest, rough handling, economic risk and other economic barriers had been the primary problems in managing a steady flow of produce from the field to the consumer in competitive markets, according to Drake (1983).

The first attempt to mechanize the shaking of cherry trees was begun by Levin et al. (1956). Hand and pole shaking methods had been studied to separate red tart cherries from the trees. Detachment was accomplished by causing the fruit to oscillate until a failure of the stem

at the spur or at the fruit occured. To overcome the worker fatique due to hand shaking, hand-carried mechanical shakers were built in 1957 which hooked to individual tree limbs. These units were heavy, transfered excessive shock to the user, caused tree damage, and worked successfully only on the smaller limbs.

Levin et al. (1958) next used a tractor-mounted, hydraulically-activated, boom shaker for harvesting tart cherries. This machine provided 95% fruit removal in seconds with little operator fatigue. The clamp was a bear-hug style covered with rubber padding to cushion tree contact. Bark damage to limbs was reported due to clamp slip, excessive clamping pressure, or deviation from a 90 degree attachment angle between the shaker and limb. Considerable bark damage also resulted when the same shaker was used for harvesting sweet cherries ( due to violent action required to remove immature fruits ) for the brining market.

The first inertia-shakers were designed by Adrian and Fridley (1965). The two mechanisms used to generate the shaking force were: (1) a pair of counter-rotating eccentric masses and; (2) a slider-crank with the slider fixed to the tree. Their clamp was a C-clamp style covered with rubber pading to cushion tree contact. Metallic fasteners were also placed permanently or semi-permanently into main scaffold limbs or trunks for shaker attachement. These were compared

to the rubber-covered clamps. The fastener permitted direct transfer of force to the structural wood rather than through the vulnerable bark and growing tissues. As a result of several experiments, they concluded that the direct clamping of a shaker to a tree through a cushioning pad was the faster and preferred method of trunk or limb attachment.

Mechanical harvesting of cherries was rapidly adopted in Michigan in the mid-1960's. The initial adoption of mechanical harvesters required drastic modification of the existing trees. The number of scaffolds were reduced to 3 or 4, low hanging branches were removed or cut back to make way for the catching frame and the willowy branches were stubbed to improve fruit removal.

Equally dramatic changes have occured in the development of harvesting equipment since the 1960's. Initially, relatively small limb shakers were used. Then, over the years, larger and more powerful trunk shakers were introduced.

Peterson and Monroe (1977) reported the development of a compact trunk shaker mounted on a catching frame that would automatically sequence, from one tree to the next, while the frame moved continuously. Compared to standard stop-and-go harvesting, harvest rate (trees/h) was increased about 50% on a time trial basis. The continous harvest rate, ranged from 210 to 284 trees/h for trees spaced 2.74 m (9)

ft) in the row and 155 to 198 trees/h for trees spaced 6.1 m (20 ft) in the row. The trunk shaker did not perform well on large trees with large limbs. Also, the tree trunk must be void of limbs to a height of 1 m (3.3 ft) to permit easy shaker attachment and good shaking action.

Limb and trunk shakers have now been used for many years for mechanized removal of fruits and nuts (Brown, 1983). In 1982, over 95% of the sweet and sour cherry trees in Michigan were harvested mechanically using shake-and-catch systems (Brown et al., 1982). The majority of these systems use trunk shakers because they provide greater speed, lower harvest cost, and minimized human effort in comparison to limb shakers.

### 1.3 The Bark Damage Problem

The area of attachment of the shaker with the tree bark has frequently been found to be damaged. Tests of the strength characteristics of bark showed that the bark injury was usually caused be excessive tangential or longitudinal stresses at the cambium under the shaker clamp (Fridley and Adrian, 1966). The stresses at which the cambium is damaged increase with tree age, decrease with turgidity, and increase from spring to fall (Fridley et al. 1970).

Excessive clamping force was found to cause crushing of the bark and cambium tissues of both tart and sweet cherry trees (Frahm, 1983). Vital nutrients cannot pass through the ruptured cells to the fruit, leaves, fruit bearing limbs, and roots.

In California, a disease-causing fungus, <u>Ceratocystis</u> <u>fimbriata</u>, can be carried by insects into the damaged area of prune or peach tree bark, where a favorable environment allows rapid spreading into healthy bark and wood (Devay et al. 1960, 1962, 1965). Fungal vectors can also be carried from tree to tree on shaker pads when continuous harvesting is conducted in a diseased orchard. The disease is potentially serious and can cause the limbs or tree to die prematuraly.

Injury to tree bark can be virtualy eliminated by using a clamp designed with adequate contact area to distribute the clamping force and the shaking force so that stress remains at safe levels. Also, the shaker must be positioned perpendicular to the limb or trunk to eliminate longitudinal stresses. Experience has shown that with a well-designed clamp, the clamping force can be set high enough to ensure adequate contact area between the clamp and the tree during shaking, but still low enough not to exceed the allowable radial stress at the cambium. Most manufacturers have minimized the transmission of stresses to the bark by installing two layers of belting over the clamp pads and lubricating the interface between the belts to create a slip surface.

### 1.4 Need For Shaker Model

In recent years, growers have reported that cherry tree decline (loss of vigor and yield, early replacement of the orchard) is an increasing problem. Tree decline has been noted in orchards of all ages throughout Michigan (Brown et al. 1982).

Research has been conducted on various aspects of the bark damage problem, to define bark strength limits ( Diener et al., 1968; Fridley et al., 1970; Brown et al., 1984) to evaluate various designs and operation methods for shaker clamps (Adrian and Fridley, 1968), and to define the static pressure applied to the bark when clamping the shaker to the tree (Brown et al., 1982; Frahm et al. 1983).

Previous research on cherry bark strength showed that contact pressures on the bark above 1035 kPa ( 150 psi) on sweet cherries and 2413 kPa (350 psi) on sour cherries were likely to initiate compressive failure in the cambium, even without the addition of shaking force (Brown et al., 1982). Studies have also shown that static clamping forces applied to tree bark do not adequately explain the bark damage problem because some damage occur may not be evident until several weeks after shaking.

Recently, the dynamic displacements of the cherry tree

trunk and the clamp area of a Friday C-clamp trunk shaker, with two independent rotating masses, were studied to estimate the relative deflections between the shaker and the tree trunk (Affeldt, 1984; Affeldt et al., 1984). Relative deflection of the trunk within the pad was found to be substantially greater during shaker startup than during steady-state operation (Affeldt et al., 1984).

Brown et al., (1984) reported that the initial clamping and shaker startup phases were the primary times when bark damage was most likely to occur, and the shaker startup on a 16.5 cm (6.5 in) diameter trunk appeared to add about 517 to 860 kPa (75 to 125 psi) of dynamic compressive stress to the recommended static clamping stress of 1136 kPa (165 psi).

With these considerations in mind, it is necessary to analyze the tree-trunk-shaker system and to study the dynamic behavior under real operation, with the goal of identifying dynamic design changes that will help reduce physical damage to the tree bark system.

To accomplish this goal, a mathematical model can be used to describe the shaker behavior as a function of time. Through this approach, possible design changes could be introduced, then evaluted for their ability to reduce conditions likely to cause bark damage.

## 1.5 Objective Of The Study

The overall objective of this study is to analyze the vibrational behavior of the Friday C-clamp trunk shaker now widely used for cherry harvesting, and to evaluate design or operational changes that may reduce the undesirable large displacements that frequently occur when the shaker is started. These large displacements are believed to lead to large shear and compression stresses being applied to the trunk bark and to be the cause of some of the bark damage. In order to meet the overall objective, the specific objectives are as follows:

- 1. Define the dimensional and main physical properties of the Friday C-clamp-trunk shaker.
- 2. Define the dimensional and main physical properties of cherry trees having different trunk diameter sizes.
- 3. Use a computer program entitled Integrated ... Mechanisms Program (IMP) as a modeling tool to study the dynamic displacement behavior of the shaker system as a function of time during the startup phase.
- 4. Evalute possible shaker design changes that may reduce the large displacements that occur when the

shaker is started. Accomplish this through a displacement sensitivity analysis of the following factors:

- a. variation of the magnitude of the shaker housing mass.
- b. variation of the magnitude of the rotating masses.
- c. variation of the rotating mass acceleration.
- d. variation of the rotating mass eccentricity.
- e. variation of the starting phase angle between the rotating masses.

#### CHAPTER 2

#### 2. LITERATURE REVIEW

### 2.1 Bark Damage And Causes

Bark damage is easily recognized by stripping, cracking or wetting of the bark in the area where the shaker was attached to the trunk or limb of the tree. A slight cracking or internal separation of the bark from the cambium is not apparent to the untrained machine operator, and thus the operator does not correct the improper procedure or machine adjustment. After the passage of time, the influence of disease, weather, insects and obstructions of nutrient flow in the damaged areas add up to a major problem of total tree decline, Figure 2.1.

Halderson (1966) suggested that damage to trees occurs in three forms: 1) physical damage by the shaker, 2) trunk damage by positioning catching frames or shakers and, 3) root damage from tree vibration. In his field experiments, all movement of the roots ceased approximately 15.2 cm (6 in.) below the soil surface and did not appear to be a major problem. Bark damage at attachment areas was minimized with good clamp design. Level ground, providing perpendicular attachment to the tree, was considered such an important factor as to necessitate leveling devices on catching frames



FIGURE 2.1 BARK DAMAGE ON A CHERRY TREE TRUNK AS A RESULT OF MECHANICAL HARVESTING.

and harvesters. Tangential clamp slip and twist were observed to cause damage problems, although they were not always immediately apparent.

Diener et al. (1968) studied bark damage problems and found that the amount of damage inflicted on a limb or trunk was determined by the bark properties, the radius of the limb or trunk, and the resistive forces of the shaken object.

Fridley and Adrian (1960) attempted to determine the power and optimum frequency of vibration in fruit removal with minimal tree damage. One possibility was to vibrate the tree at the natural frequency of the fruit stem system. Combinations of frequency and displacement that cause instability at the point of fruit suspension, however, were difficult to transmit through the branched tree system due to colliding limbs and damping by leaves. Collisions between fruit and limbs, when the shaker frequency reached the natural frequency of a limb, were observed to cause damage to tree and fruit.

The other possibility was to vibrate the tree at one of the natural frequencies of the tree or limb. The selection of the proper natural frequency was dependent on the stroke needed to remove the fruit at that frequency, the power required and the resulting tree and fruit damage. a minimum power level was needed to remove a volume of

fruit with long strokes and low frequency; increase of either stroke or frequency, however, caused an increase in tree damage, although long strokes caused the most damage. Placing the clamp at an anti-node for a given natural frequency allowed the stroke to reach a maximum for that frequency. Higher frequency with shorter strokes resulted in minimum damage. A force must be exerted perpendicular to the trunk or limb to minimize damage and power required, for as the included angle between the shaker and the trunk or limb deviated from 90 degrees, a component of force parallel to the trunk or limb induced shear and was identified as a direct cause of bark damage.

Beljakov et al. (1979) studied the effects of shaker harvest on the root system of sweet and sour cherries, peaches and plums. The exciting force was developed by an eccentric mass trunk shaker, clamped 20 cm (7.9 in.) above the earth and operated at 15 to 18 Hz with 2.4 to 3.0 cm (1.0 to 1.2 in.) strokes. The radioactive tracer P-32 was injected into the soil, and C-14 was applied to leaves, to study photosynthetic activity. Results indicated trunk shaking had no adverse effect on tree growth, and only an insignificant number of roots were severed (less than 0.05% of the roots (by weight) of diameter 0.1 cm (0.04 in.) or smaller).

Brown et al. (1982) and Cargill et al. (1982) made

direct field observations and classified 10 general causes behind the bark damage problem as follows:

- Operator error and inadequate operator training (operators, due to a lack of time or training constraints, may not follow recommended, procedures to minimize bark damage).
- 2. Improper shaker adjustment.
- 3. Improper clamp adjustment and maintenance.
- 4. Improper shaker clamp attachment.
- 5. Poor judgement in selction of a machine for young trees and/or failure to adjust existing machines for tree size.
- 6. High cambial activity at harvest due to excessive irrigation, rainfall, or physiological activity.
- 7. Immature fruit requiring an excessive force for removal (this tempts the operator to overshake for satisfactory fruit removal).
- 8. Improper machine design.
- 9. Settling or moving of the shaker due to soft soil conditions or excessive side-hill slope.
- 10. Improperly pruned trees requiring excessively long shaking cycles.

The critical concept is the transmission of proper force to a tree to remove fruit, but to do so without

harming the living tissues of the tree. This is a difficult task for, as Brown et al. (1982) noted, bark and cambium damage on cherry trees will occur at lower stress levels than on other fruit trees.

In 1982, Brown et al. expanded their general observations of bark damage in order to isolate specific operator and machine inaccuracies that may account for the observed tree damage. The list of critical points included:

- 1. Failure to center the clamp on the trunk.
- Clamping too firmly to the tree causing excessive radial stress, hence, crushing and splitting of the bark.
- Clamping too loosely during shaking where the pads tend to scuff and tear the bark (tangential shear).
- 4. Clamp pads not slipping internally due to the wrong pad design or improper lubrication of slip surfaces causing high shear forces (e.g. pads becoming heated, sticking together, including shear force and deterioration).
- Excessive eccentric setting causing excessive tree displacement and bark strain.
- 6. Excessive power applied to small trees.
- 7. Shaker "gallop" during startup and stop,

- causing torque (shear) in the bark.
- 8. Settling of the shaker carrier into the earth during shaking (causing excessive longitudinal shear).
- 9. Shaking forces not perpendicular to the trunk (causing longitudinal shear).
- 10. Clamping too low to the ground where the trunk is most rigid (causing execssive forces to be applied to the trunk).
- 11. Clamp pads too small or firm causing high stress in the bark due to small contact area.
- 12. Longitudinal shear caused by clamping to a leaning trunk.
- 13. Longitudinal shear caused if shaker is tilted when clamping to a vertical trunk.

The above list of causal factors fell into three main categories:

- 1. Operator error during shake and clamp.
- 2. Improper pad design
- 3. Improper machine design or setting.

## 2.2 Bark structure and strength

Diener et al. (1968) described the structure of cherry bark as having a thin nonliving periderm, a large spongy nonfunctioning phloem in the center, and a thin functioning The directional strength phloem next to the cambium, of cherry bark can be accounted for from properties alignment of the constituent cells. The tissues have greatest tensile strength in the direction parallel to long axis of their cells. Phloem cells have their long axis in a longitudinal (vertical on the trunk) direction, whereas periderm cells have their long axis in the tangential (horizontal on the trunk) direction. The periderm consists of thin-walled dead cells encrusted with waxes which lubricate the dead tissue and allow slippage between (Esau. 1965).

When the bark is damaged so that it separates from the wood (xylem) of the tree, the flow of fluids containing the essential life sustaining elements is interrupted in that area. Usually, hairline cracks are formed in the bark tissue, through which air enters and oxidizes the cambial tissues so that they appear brown (Adrian et al. 1965). Devay et al. (1962) notes that these damaged areas are open invitations for insects and disease, especially tree canker,

a gummosis disease caused by the fungus <u>Ceratocystis</u> fimbriata, evidenced in the fruit orchards of California. The fungus gradually spreads to healthy surrounding bark tissue, slowly causing tree death.

In the early development of tree shaker systems the design of shaker clamps, operation of shakers for minimum bark damage, and the strength of fruit tree bark in relation to the stresses applied during mechanical harvesting were studied by several investigators between 1962 and 1970. The compressive and shear strength of intact bark and cambium systems for prune trees were found to change significantly during the growing season (Fridley et al., 1970). Bark strength was lowest early in the season, when cambial activity was high. Clamping pressure above 2100 to 2400 kPa, in the absence of shear stress, was shown to cause faint browning in the bark, and above 4100 to 5200 kPa caused marked browning in the cambium and was likely to split the bark on 6-year-old prune trees at harvest time.

Adrian et al. (1963) conducted bark strength studies by applying known loads to the bark and evaluating the injury both visually and by inoculation of the test area with a pathogen. The maximum radial stress at failure was 4 to 5 times greater than the maximum tangential stress at failure.

Considering both fungus infection and visible discoloration

of the bark, an allowed radial stress (including a factor of safety for tree variability) of approximately 1700 kPa was selected.

Brown (1965) conducted a study to determine the influence of moisture and normal pressure on the shear strength between the bark and limb of fruit trees. The bark moisture was found to affect the force required to shear bark from a fruit tree limb. High moisture was associated with low shear strength and low moisture with high shear strength. Also, the shear strength could either increase or decrease with an increase in normal pressure according to some critical moisture conditions. Variety and specie differences were also found to exist in shear strength value.

Diener et al. (1968) conducted a study of the strength properties of the bark of apple, peach and cherry trees. Cherry bark was removed from the tree and placed in an environmentally controlled chamber to test its compressive, tensile, and viscoelastic strength properties. They found that the shear strength of the bark was directional, being largest in the longitudinal direction and decreasing to the lowest values in the tangential direction. Both cherry and peach ruptured at about 8300 kPa compressive stress by extruding in the tangential direction at about 45% compression.

Fridley et al. (1970) summarized their studies on the strength characteristics and magnitudes of tree bark, concluded that injury to bark and infection of these injuries by Ceratocystis canker were associated with magnitude and direction of stress applied to the bark. bark could withstand about 3 to 4 times as much stress applied radially as when stress was applied longitudinally or tangentially to the limb. The shear stress contributed about 50 to 70 % of the total tangential strength, and the tangential or longitudinal stress was a primary factor in injury compared with radial stress. Maximum radial strength was found in the range of 3450 to 6900 moisture content had a substantial affect on the required to shear bark from a fruit tree limb. High moisture associated with low shear strength, and low moisture with high shear strength.

Brown et al. (1982) conducted a study on bark damage resulting from trunk shaking of cherry trees. They found that clamping pressure above 1000 kPa caused failure (browning) on sweet cherry compared to 2400 kPa on sour cherry. At 1300 kPa radial pressure, compressive failure on sweet cherry was low and constant over the range of bark moisture observed. At 4000 kPa, compression failure increased as bark moisture increased. Sweet cherry trunk bark 9-mm thick was not aplit at 2750 kPa but had slight

splitting at 4000 kPa. Sour cherry trunk bark 9-mm thick did not split even at pressure up to 5500 kPa. They restated that clamping must be firm enough to efficiently transmit the shaking energy without the pad slipping on the bark, but not so firm that compression and splitting damage result.

### 2.3 Shaker Pads, Forces, and Pressures

Forces are transmitted from the shaker body to the tree through a pad which acts as a cushion, damper, spring. Minimum stress occurs in the bark when the required vibrational energy is transmitted over the largest possible area. Longitudinal and tangential forces from the epicyclic shaking patterns must be efficiently transmitted the tree by means of a pad that conforms well to the tree trunk. Scouring of the bark or excessive shear stress may result if pad contact area or clamping pressure are insufficient. During shaking, these inefficiencies may be observed as slipping action (tangential or longituinal) or beating action (radial). As clamping pressure is increased, pads become stiffer (smaller pad deflection per force increment) and a harder shake is imposed on the tree. Excessive torque also may arise during shaking if clamping pressure is very high, because the pad is unable to internally flex or slip. Until recently, pad design has been a trial-and-error process. The use of a poorly designed pad would likely cause bark damage regardless of attempts to control other factors during shake harvesting.

Designs for shaker pads have included a round hollow rubber tube, bags filled with sand or ground nutshells, rubber pads with small holes drilled parallel to the trec trunk axis, preformed steel clamp jaws covered by rubber pads, and other conforming materials.

Brown et al. (1982) made preliminary tests of C-clamp shaker pads for contact area and peak contact pressure at the manufacturer's recommended hydraulic circuit clamping pressures. This hydraulic pressure range was assumed to cover the unknown peak pressures between the pad and the tree during shaking. The results indicated that peak pressures between the pad and the bark were 2345 kPa (340 3450 kPa (500 psi) and 4140 kPa (600 psi) on a 114 mm (4.5 in.) diameter trunk (an instrumented steel pipe). showed that certain recommended clamping pressures were excessive and caused compressive failure of high moisture cambium for both sweet and sour cherries. Failure of the cambium from compressive stress (radial) was initiated lower clamping pressure on sweet cherry 2300 kPa (335 psi). Brown stated that "peak contact pressures higher than observed in these stationary tests certainly occur during shaking, but we have not progressed to the point of estimating dynamic pressures".

Frahm et al. (1983) continued studies on four commercial trunk shaker pads for peak bark pressure, bark contact area and pad stiffness. The results indicated that the pad pressure patterns are not uniform and differ for

each manufacturer. If a peak bark pressure of 2070 kPa (300 psi) was not exceeded, when bark contact area and pad stiffness were adequate, the pads were judged to be safe. This pressure presumably would not cause compressive failure (browning) in sour cherry tree bark, which exhibited average ultimate compressive strength of 2400 kPa (350 psi) and it would cause only minimal damage in sweet cherries, with a corresponding strength of 1030 kPa (150 psi). Reduced clamping pressure was recommended for each manufacturer's pad so as to avoid peak pressures on the bark exceeding the estimated 2070 kPa (300 psi) limit, thereby avoid compressive damage.

The Friday Tractor Co. (1982) developed a "Tri-clamp" composed of 3 pads contacting areas of a tree trunk 120 degrees apart (surrounding the trunk in a triangle). A pair of eccentric rotating masses are positioned in line on each side of the tree so their center of gravity is located within the tree trunk. This design provides a complete wrap of the pads around the tree, minimizes slip between the pad and the bark, and minimizes rotation of the shaker body about the trunk to prevent torque damage. A firmer grip on the tree was the result.

## 2.4 Dynamic Response of Trees

Years ago, farmers learned that the tree fruit could be detached by hitting the primary scaffold limbs with a mallet attached to about a 1-m long handle. The mallet was a hard rubber pad. Hitting the limbs generated a low amplitude, high frequency vibration that transmitted well in stiff trees. However, the successful application of the vibratory concept did not start until the 1960's. Since then mechanical means of detaching tree fruits have improved and enhanced both machine performance and fruit quality.

Adrian and Fridley (1958) found that fruit removal when using a boom-type shaker on the limb of prune trees was affected primarily by four variables:

- 1. The frequency of the shake.
- 2. The length of the stroke.
- The force required to remove the fruit divided by the weight of the fruit, f/w.
- 4. The number of limber fruit-bearing hangers in any given fruit tree.

They also found that limb breakage increased with increasing stroke. However, minimum limb breakage occured within a frequency range of 11 to 15 Hz.

Fridley et al. (1960) reported that the optimum frequency of operation was at a natural frequency of the system, and the natural frequency selected depended upon the following:

- The stroke required to remove fruit at the frequency.
- 2. The power required.
- 3. The resulting tree and fruit damage.

Higher frequencies and shorter strokes seemed to result in less tree and fruit damage, but required more power.

Adrian (1963) studied the amplitude and acceleration developed along the limbs as a function of exciting frequency and the position of force application. He found that increasing the frequency resulted in a general linear increase in acceleration after passing through resonance, due to an associated reduction in stroke. Also, greater power and force were evidenced when the vibrator was located closest to the fixed end of the limb.

Kronenberg (1964) studied the effects of fruit detachment forces in attempting to mechanically harvest sour cherries. He found the detachment force decreased as the fruit ripened. The difference between the force 10 days before harvest and that on the traditional picking day

varied with the equation:

$$Y = -48 X + 428$$

Where: X = 9 - Number of days before harvest

Y = Grams force for fruit detachment

Unripe cherries came off with stems, whereas ripe cherries came off without stems. With careful shaking, healthy leaves would not come off with mature fruit.

Levin et al. (1968) conducted a study to identify the suitable time to mechanically harvest cherries. They found that average pull force required to remove cherries from their stems decreased from over 9.8 N (2.20 lbs) to about 8.8 N (1.98 lbs) during the 20-day harvest period, while the force required to detach stems from branches did not decrease substantially during this period. They also found that the recovery of fruit increased, and the proportion of attached stems decreased, as the date of mechanical harvest was delayed.

Cook and Rand (1969) described a mathematical analysis of the dynamic behavior of the fruit and stem during simultaneous horizontal and vertical forcing of the fruit support structure. The analysis indicated that cherries may be harvested with stems attached if the shaking frequency was in the range of 4.16 to 5.41 Hz, and harvested without

stems if the shaking frequency was in the range of 16.66 to 28.33 Hz. They also found that the greatest dynamic instability of the fruit occurred at a shaking frequency of twice the natural frequency when the upper end of the stem undergoes small, planer, elliptic displacements.

Adrian and Fridley (1965) developed a model of inertia-type limb shakers according to the following assumptions:

- 1. The system has a single degree of freedom.
- 2. The exciting force varies sinusoidally.
- 3. The restoring force is proportional to displacement.
- 4. Damping is viscous (damping force is proportional to velocity).
- 5. Steady state vibration occurs.
- 6. Energy is conserved by the shaker.

The vibration analysis was found to be sufficiently accurate for estimating the design criteria for inertia-type tree shakers. Field tests indicated that it was possible to reliably predict the following:

- The shaker mass ratio and eccentricity required to develop a certain stroke.
- The force and torque developed and the power requirements to vibrate a limb at a certain

stroke and frequency.

Halderson (1966) studied the relationship between percentage of cherry fruit removal and elapsed shaking time. He found that a long shaking time was required for over 85% removal when fruit was immature, but only a short shaking time was required when fruit was mature. The rate of fruit removal was determined mainly by the shaking frequency. Removal was 85% in 2 s of shake, with 95% removal after 8 s, at a frequency of 16 Hz. A frequency of 13 Hz was determined to be a minimum for adequate removal. A maximum stroke of 19 mm (0.75 in.) was adequate at a frequency of 17 Hz. Using this setting, the fruit fell straight to the ground (no whipping action).

Phillips et al. (1970) developed a mathematical model to simulate the vibrations of a limb as affected by its physical properties, configuration and type of applied forces. They found that the analysis of a tree limb must have the capability of dealing with the following:

- 1. Mass distribution, which is not uniform along the length of the limb.
- 2. Enternal and external damping.
- 3. Effect of rotary inertia and shear deformation.
- 4. Variations in the rigidity of the base support.
- 5. Existence of secondary branches.

- 6. Curvature of the neutral axis.
- 7. Effect of the longitudinal forces and displacements.

They found that at lower natural frequencies, the deflection amplitudes were large when the shaker was attached the base of the limb. At higher frequencies, range of the third and fourth normal modes, the deflection amplitudes were larger when the shaker was attached closer to the base. Computed phase angle and frequency relationships for the limb showed that all points along were approximately 90 degrees out of phase with applied force when the frequency ratio (limb frequency over limb natural frequency, f/fn) was near 1.0. They also found damping factor of 0.1 for olive limbs gave a that a approximation to the steady-state response for simulated compared to experimental results.

Hoag et al. (1971) continued their experimental measurement of internal and external damping properties of tree limbs. In this experiment they used the logarithmic decrement method to investigate the damping factor and, with the aid of photography, the rate of limb vibration decay was measured. They found that the logarithmic decrement of almond wood varied from 0.0667 to 0.1015 in three samples tested when the moisture contents were above the fiber-saturating point. External damping of tree limbs due to the

limb moving through the air was non-linear in nature and seemed to be proportional to the square of the velocity. The report also indicated that the air drag on vibrating tree limbs could be a constant drag coefficient equal to about 1.5. When only branches without leaves were present, external damping forces were small enough to be neglected unless the velocities were very large.

Berlage et al. (1974) conducted experimental studies during the 1971 and 1972 harvest seasons to determine the practical value of high frequency vibrations for sweet cherry removal with minimal damage. They found that high-frequency small-displacement vibrations applied limbs did not provide any significant fruit removal. highest frequency at which fruit released from cherry limbs was 40 Hz. Lowering the frequency resulted in increasing removal. Sweeping higher frequencies did not promote additional removal. In trunk-shaker harvesting, however, a sweep of the low frequency range distributed the shake pattern through-out the variable tree structure better than fixed frequency. Nodes and anti-nodes formed on vibrating limb moved along the limb as frequencies changed, thus, preventing "dead" spots with zero displacement.

Young et al. (1975) used finite element methods to simulate the vibration of whole-tree systems. For this purpose, a complete tree system was considered as a

## combination of three portions:

- A tree structure which consists of tree trunk,
   limbs, secondary branches and hanger branches.
- 2. The fruit and stem.
- 3. The leaves and twigs.

They found that the three mathematical models developed using the finite element method were in agreement with the available answers in 1975. The natural frequencies of the system obtained by approximating the curved hanger branches by a series of straight elements resulted in very close agreement between the Ritz method and the finite element method.

In 1976, Alper et al. investigated the effect of the applied frequency and the point-of-force application on resultant amplitudes at the points of fruit suspension and at the zone of force application on orange trees. Vibrations that developed at these points were described by harmonic displacements. The tree system, when excited by a shaker, went from a transient-state to a steady-state and back to transient-state during shaking tests. The vibration amplitudes in a shaken branch at points of fruit suspension were found to increase as the force application point was moved further from the main branching point. If a constant force was applied, then the momentum transferred to nearby

branches through the joint link remained constant as the application point moved. Vibration amplitudes at points of fruit suspension remained the same with and without attached fruit.

Except at very low frequencies or very low amplitudes, changing applied frequency and amplitude had little effect on sour cherry fruit removal by limb shaking unless the combination resulted in a change in acceleration (Bruhn, 1969). Frequencies of 16 to 20 Hz with a stroke of 38 mm (1.5 in.) provided adequate fruit removal. Accelerations at the outer portions of a tree exceeded those applied to the trunk or base limb in all cases.

Khalilian et al. (1978) determined the effects of adding a spring-loading feature to a slider-crank inertiatype limb shaker on limb displacement, and maximum force and power required to shake the limbs, of an olive tree. They found that addition of this feature reduced both the required maximum force and peak power by an amount approximately equal to the product of the added spring stiffness and crank amplitude at frequencies above the second natural frequency of the system. However, the spring also caused an increase in maximum force required to start the shaker.

Upadhyaya et al. (1979) used the finite element method to investigate the dynamic response of a tree limb subjected

to an impact force. Their model was based upon a linearized theory and accounted for transverse shear as well for leaves, twigs, secondary branches and fruit. The fruit modeled as a spherical pendulum. A direct integration was used to obtain the transient response They found that the model system. predicted the experimentally observed results quite closely. Furthermore, it was found during the course of this study that use of the Timoshenko beam theory with the finite element method to ill-conditioned matrices if the shear energy associated with the problem is small. Therefore. complementary energy approach was used to provide a solution to the problem.

(1979) studied the damage sources Kirk et al. in mechanically harvested sweet cherries. The results indicated that the fruit size, stage of maturity as indicated by stem force, and maximum trunk displacement were the factors which showed a highly significant correlation with the fruit damage for both the 1975 and 1976 seasons. The results on the trunk movement during mechanical cherry indicated that the shaken tree was moving in form of an orbiting pattern, but the maximum acceleration or displacement was never constant. The motion of the often forms a daisy pattern as indicated from simultaneous X and Y recordings. Examples of patterns observed were

straight line motion, daisy pattern, circular patterns, and all combinations of these. Large unstable tree trunk displacements can result in large shear and compression forces and stresses being transmitted to the bark and can lead to bark damage.

Ortiz-Canavate et al. (1980) developed a multidirectional trunk shaker for harvesting olives. They found that shakers with two eccentric masses, each driven by a separate hydraulic motor in a series circuit produced more controlled vibration than those having the two motors in a divided-flow parallel circuit. They also reported that in olive trees better results were obtained when the two counter-rotating masses were of equal magnitude.

According to Cargill et al. (1982) the force and power required when shaking fruit trees varies with frequency, stroke, shaker design, clamp position on the tree, diameter of the tree trunk, tree species, tree yield and fruit stem detachment strength. Power for increasing trunk displacement is proportional to the square of the ratio of the increased displacement to the original displacement. Power to increase frequency varies as the cube of the frequency. The proper frequency and stroke required for adequate fruit removal depend on the type of fruit and maturity level.

#### CHAPTER 3

#### 3. COMPUTER MODELING

#### 3.1 IMP Program

The Integrated Mechanisms Program (IMP) is a computeraided design and analysis system which can be used for simulation of mechanical systems.

The IMP program is capable of simulating two-or three-dimensional rigid link mechanical systems having single or multiple degrees of freedom. The simulation can include revolute (pinned), prismatic (sliding), screw, spur gear, cylindric, universal, spheric (ball and socket), and planar joints in any open or closed-loop combination. Linear or non-linear springs and viscous dampers may also be included, either within the joint or acting between specified points on the moving links. Mass and gravity effects can be simulated. The system can be driven either by applied forces or input motions which can be specified functions of time or system geometry.

The IMP system is capable of simulation in any of three different modes: kinematic (geometric), static (equilibrium), or dynamic (time response). In any of these modes IMP can calculate the requested positions,

velocities, accelerations, static and dynamic constraint forces, natural frequencies, damping ratios and small oscillation transfer function (principal vibration modes) of the system simulated.

With these considerations in mind, the IMP program was selected to be used as a tool to study the dynamic behavior of the C-clamp trunk shaker developed by Friday Tractor Company for harvesting cherries and to help in further studies for shaker operation or design improvements.

### 3.2 Model Development

# 3.2.1 Model Assumptions

The C-clamp trunk shaker in this study was mounted on the 2250 Mount-O-Matic loader frame of a Hydro-84 International tractor. A frame was constructed on the front of the loader from which the shaker was suspended at three points. Rubber bushings (Friday standard parts) were used on the ends of the suspension bars to minimize the amount of vibration transmitted to the tractor.

In the IMP model, the C-clamp trunk shaker was assumed to be suspended on three suspension bars from three fixed points in space. The tractor was thus modeled as a large fixed mass (ground) to maintain simplicity and to focus only on the dynamic behavior of the shaker. To allow the shaker to undergo unrestricted planar motion, spherical joints were introduced at both ends of the suspension bars. The bushings used at the ends of the suspension bars were assumed to have no affect on the shaker planar motion.

In the free-shake model the shaker was assumed to run freely with no tree attached to it. In this case the rubber pads between the clamp and tree trunk would have no affect on the shaker displacements, so the shaker main frame could

be modeled as one link. However, in the shaker-tree model, the shaker was attached to a tree, as the rubber pads would be clamped to the tree trunk and expected to deflect during shaking. Field and video film observations during the shaking operation indicated that the rubber pads will deflect about 6mm to 37 mm (.25 to 1.5 in.) (depending on clamping force and tree size) under dynamic conditions. However, for simplicity, the deflection of the clamp pads was ignored in the model, assuming that the trees being shaken were small enough that the pad deflection was small compared to the shaker movement.

In field tests, Affeldt (1984) showed that the shaker rotating mass velocity passes through a critical period when velocity increases rapidly during the startup time. After about 1 s, the rotating mass velocity exceeds the steady state velocity and oscillates until it settles at the steady state.

Early test results using the IMP model show it is unrealistic to compare between the actual shaker displacement vs. time curve and the model displacement vs. time curve by feeding the actual rotating mass velocity curve into the computer model. The difficulties with this approach are:

1. The simulated rotating mass velocity curve

cannot match the actual velocity curve, so approximation is an possible. Any difference in velocity would cause a significant difference in rotating mass positions, which in would turn affect the final displacement simulation.

2. The initial positions of the rotating always different each time the shaker starts. are starting position and inability The random actual velocity curves the match makes it. impossible to match the actual and simulated displacements.

in With these considerations mind, the approach selected was to simulate the transient shaker displacements by feeding the IMP model the rotating mass velocity as a linear function with a slope equal to the mass acceleration, and to simulate the shaker steady-state displacements frequency levels of 5, 10, and 15 Hz to compare the actual with the simulated displacements at these frequencies.  $\mathbf{B}\mathbf{y}$ adopting this method, the computer time required for simulation could be reduced, and the transient as well as the steady-state displacement at different frequencies could be estimated.

During the dynamic simulation of the trunk shaker displacement, the initial positions of the shaker rotating

masses defined for IMP model were set as shown in Figure 3.1. When the shaker was started they turned counter to each other, as shown, to simulate the highest displacement that might occur during shaking operations.

#### 3.2.2 Model Development Of C-Clamp Trunk Shaker

The first phase of model development of a mechanical system using the IMP program must be the topological the system. This analysis includes analysis of the recognition of the number of links, the number and types of joints, the order in which the links and joints are and other characteristcs such arranged, as speed, acceleration, applied forces, etc. existing in the system.

The Friday trunk shaker was modeled using 8 joints connecting 6 links to describe the machine components as they are illustrated in Figures 3.1 and 3.2. The model code is presented in Appendix A. These machine components can be described as follows:

Link 1 . L1 : This link represents the shaker frame consists of the housing, beams, which bearings, motors, 2 rubber pads, hydraulic cylinder for the C-clamp mounted on the back of the shaker. The total ofthis mass link was estimated to be 465.36 kg (31.89 slug).

Joint 1 , J1: A revolute joint which connects between the inner rotating mass and the shaker

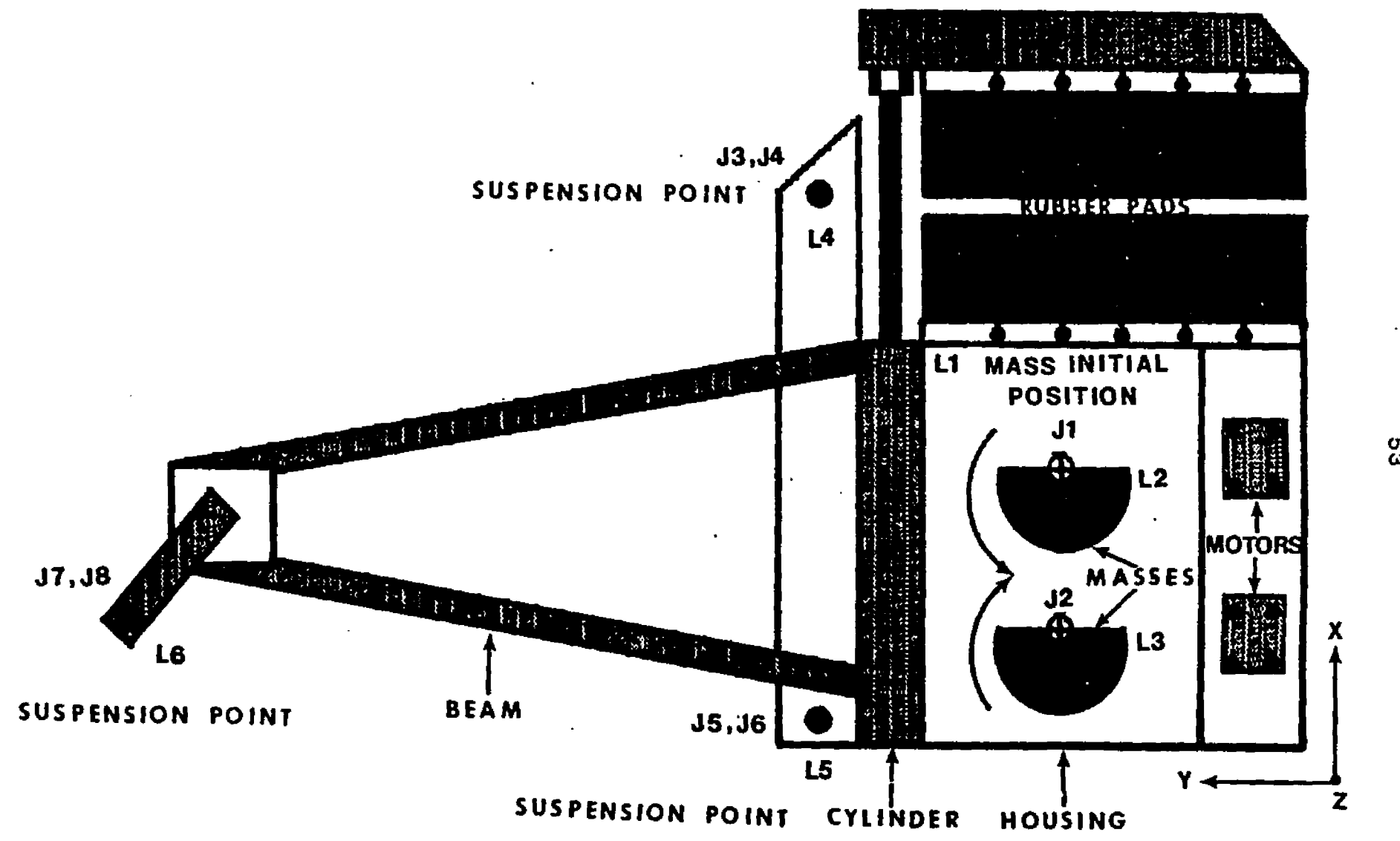


FIGURE 3.1 TOP VIEW OF FRIDAY C-CLAMP TRUNK SHAKER AS DEFINED FOR THE IMP MODEL

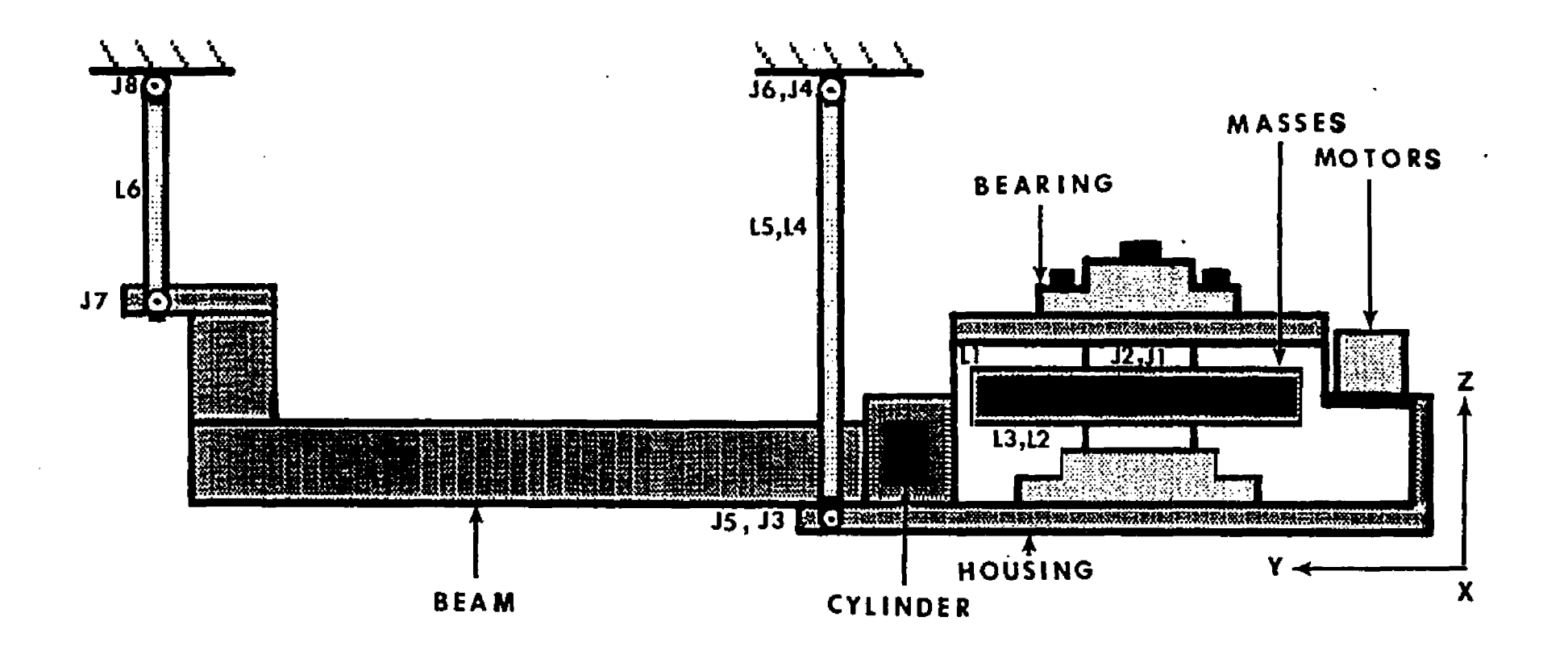


FIGURE 3.2 SIDE VIEW OF FRIDAY C-CLAMP TRUNK SHAKER AS DEFINED FOR THE IMP MODEL.

housing. This joint was set to allow the inner rotating mass to rotate and generate force enough to vibrate the shaker. The initial position of this joint was set to be 90 degrees (outer position).

- Link 2 , L2 : The inner rotating mass which is connected to the shaker housing by the revolute joint J1. The total mass was set to be 39.9 kg (2.734 slug).
- Joint 2 , J2: A revolute joint which connects between the outer rotating mass and the shaker housing. This joint was set to allow the outer rotating mass to rotate and generate force enough to vibrate the shaker. The initial position of this joint was set to be 90 degrees, (outer position).
- Link 3 , L3 : The outer rotating mass which is connected to the shaker housing by the revolute joint J2. The total mass was set at 39.9 kg (2.734 slug).
- Link 4 , L4 : The right side suspension bar which carries the shaker. This bar was set to have a total mass of 4.5 kg (0.308

slug).

Joint 3 , J3: A spherical joint which connects the shaker housing to the right side suspension bar, L4 which carries the shaker. The reason for selecting this type of joint was to allow free planar motion for the shaker during operation.

Joint 4 , J4: A spherical joint which connects the right side suspension bar to the tractor frame (ground).

Link 5 , L5 : The left side suspension bar which connects between the tractor frame (ground) and the shaker housing. The total mass of the bar was set at 4.5 kg (0.308 slug).

Joint 5 , J5: A spherical joint which connects the left side suspension bar to the shaker housing.

Joint 6 , J6: A spherical joint which connects the left side suspension bar to the tractor frame (ground).

Link 6 , L6 : The rear suspension bar which connects between the tractor frame (ground) and the shaker beam. The total mass of the bar was set at 4.5 kg

(0.308 slug).

Joint 7, J7: A spherical joint which connects the rear suspension bar to the shaker beam.

Joint 8 , J8: A spherical joint which connects the rear suspension bar to the tractor frame (ground).

The second phase of model development was to specify link mass moments of inertia. These are calulated in Chapter 4 and summarized in Table 4.5.

# 3.2.3 Model Development Of C-Clamp Trunk Shaker-Tree System

The Friday trunk shaker-tree system was modeled by adding a tree to the previous free-shake model. A sweet Cherry tree with a 63 mm (2.5 in.) trunk diameter and a total mass of 9.345 kg (0.6404 slug) was selected to be used in the IMP model. The tree mass moment of inertia relative to the tree center was calculated by assuming the tree had a cylindrical shape and applying the following equations:

$$Ix = Iy = m.r^2/4 + m.L^2/12$$
  
 $Iz = m.r^2/2$ 

Where:

Ix, Iy, Iz: The mass moment of inertia of the tree
in x, y, and z direction.

m : The tree mass (9.345 kg (0.64 slug)).

r: The trunk radius (31 mm (1.25 in.)).

L : The tree height (3.25 m (128 in.)).

The calculated results of mass moments of inertia (Ix, Iy, and Iz) of the selected tree were found to be 8.233, 2 2 8.233, 0.0047 kg.m (73, 73, 0.0417 lbm.in ), respectively.

The Friday trunk shaker clamped to a tree was modeled

using 9 joints connecting 7 links. Six of these links and 8 of the joints were already described for the free-shake model. The other joint and link are:

Link 7 , L7 : This link represents the tree trunk which is connected to the pads by a revolute joint. The link is connected in both the x and directions by a spring and a damper. The spring stiffness and damping factor were set at 12.69 N/mm (71 lb/in.) and 0.31 N/mm per 8 (1.8 lb/in. per s), respectively. The total free spring length was set equal to 51 mm (2 in.) (the maximum expected trunk displacement). springs and damper connect between the tree link L7 and the ground, as shown in Figure 3.3.

Joint 9 , J9: A revolute joint which connects between the shaker housing L1 and the tree link L7. This joint was selected to allow for the translation of linear motion from the shaker to the tree link.

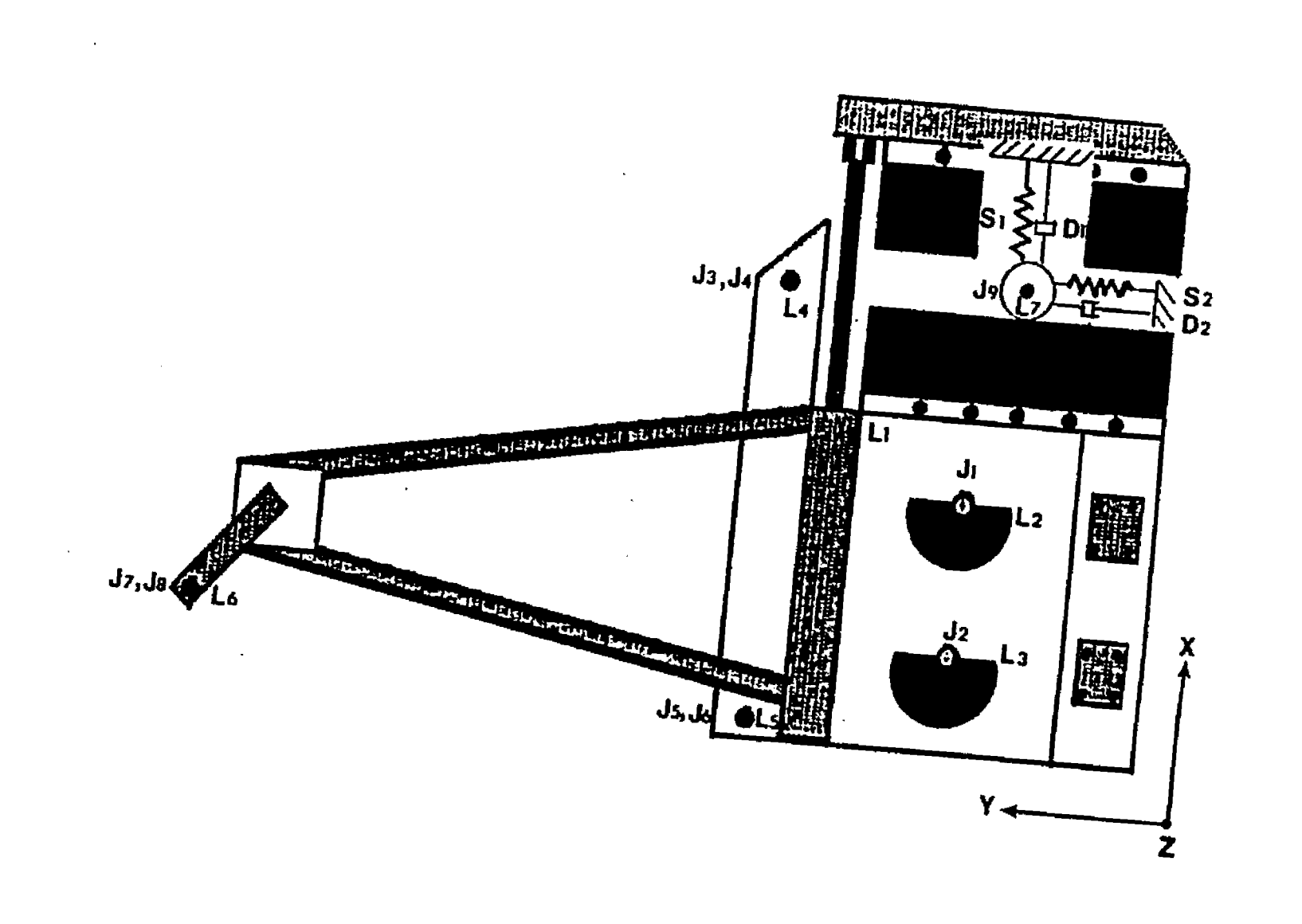


FIGURE 3.3 TOP VIEW OF FRIDAY C-CLAMP TRUNK SHAKER-TREE SYSTEM AS DEFINED FOR THE IMP MODEL

#### CHAPTER 4

#### 4. EXPERIMENTAL MEASUREMENTS

#### 4.1 Tree Measurments

Experiments have shown that tree physical properties have important affects on trunk-shaker behavior, fruit detachment efficiency, and the amount of trunk bark damage caused during the harvesting operation. This suggests that a meaningful modeling analysis of trunk shaker behavior has to take into account the tree physical properties that contribute significantly in a displacement simulation study.

To achieve this goal, selected physical properties for both sweet and tart cherry trees were investigated during the 1985 cherry harvesting season. The purpose of the study was to determine the following cherry tree properties:

- 1- Height, center of gravity, and mass above ground.
- 2- Linear and torsional stiffness of the trunk.
- 3- Linear and torsional damping coefficient effective at the shaker attachment height.

# 4.1.1 Cherry Tree Height, Center Of Gravity And Mass Measurments

During the 1985 cherry harvesting season, 65 sweet and 45 sour cherry trees that were about 10 years old were cut to determine tree height, center of gravity. and mass for different tree trunk diameter sizes. Each tree trunk diameter was measured 228 mm (9 in.) above the ground level. The sweet cherry tree trunk diameters ranged from 58 to 97 mm (2.3 to 3.8 in.) with an average value of 79 mm (3.1 in.) and standard deviation of 9.5 mm (0.38 in.). The sour cherry tree trunk diameters ranged from 61 to 89 mm (2.4 to 3.5 in.) with an average value of 76 mm (3.04 in.) and standard deviation of 7 mm (0.284 in.).

The sweet cherry tree heights ranged from 2.90 to 4.67 m (114 to 184 in.) with an average value of 3.80 mm (149.7 in.) and standard deviation of 0.62 m (24.56 in.). The sour cherry tree heights ranged from 2.94 to 4.49 m (116 to 176.8 in.) with an average value of 3.50 m (137.9 in.) and standard deviation of 0.33 m (13 in.). Thus, the average tree height was 0.30 m (12 in.) less for sour cherry than sweet cherry. Although the tree heights were linearly distributed when plotted against tree trunk diameter, Figures 4.1 and 4.2, the correlation factors between height and diameter were very small (r = 0.2 for sweet cherry, and

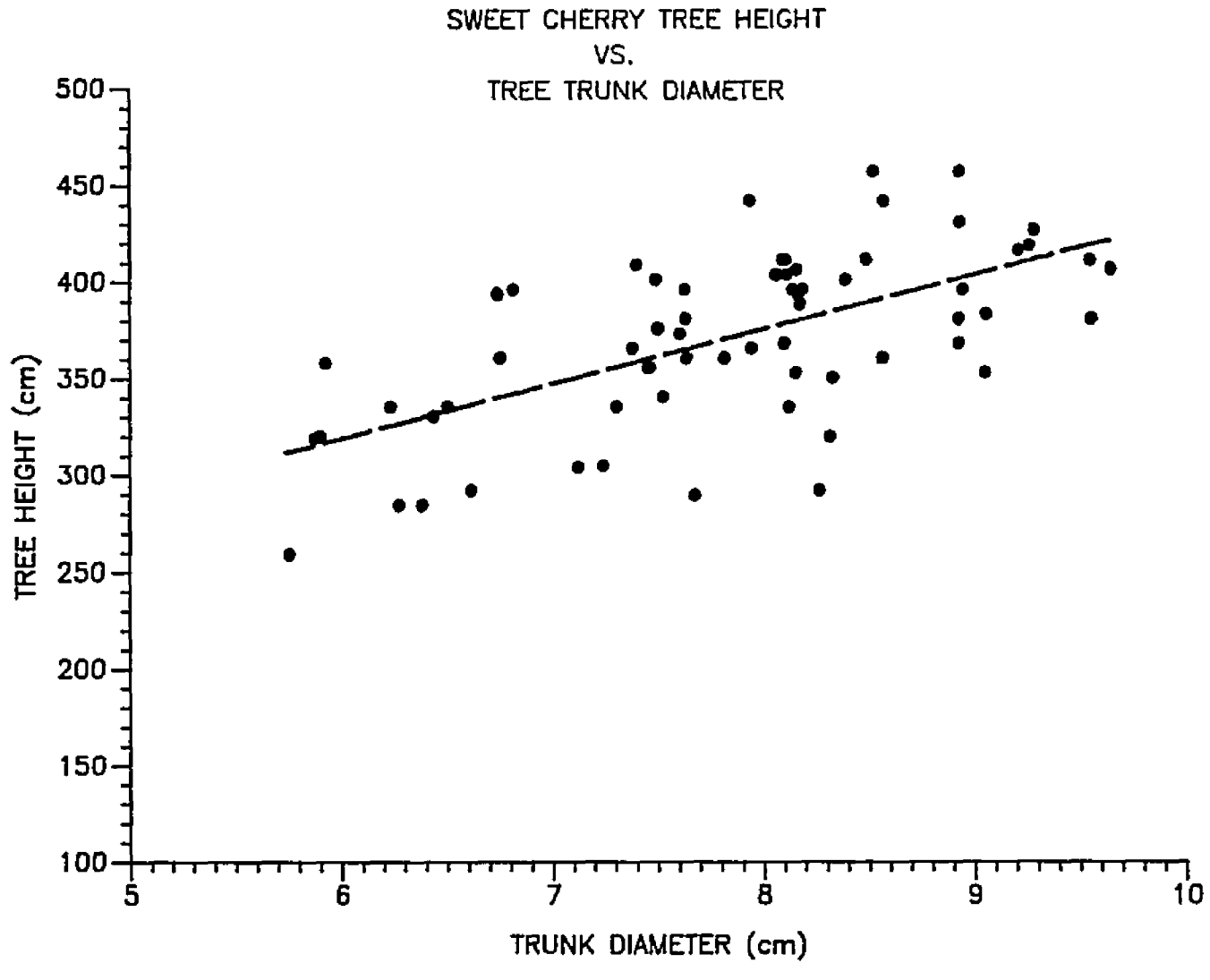


FIGURE 4.1 SWEET CHERRY TREE HEIGHT VS. TREE TRUNK DIAMETER.

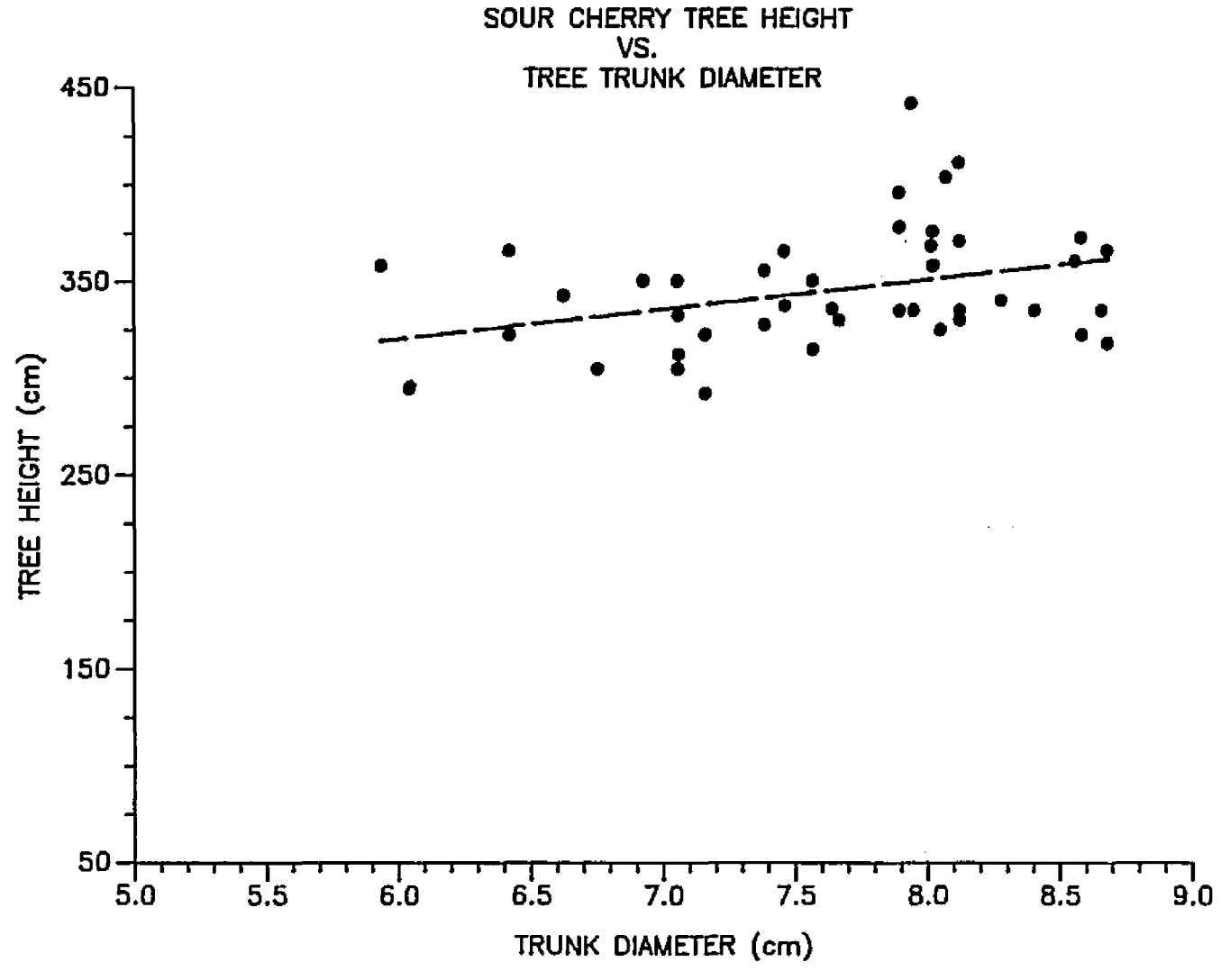


FIGURE 4.2 SOUR CHERRY TREE HEIGHT VS. TREE TRUNK DIAMETER.

#### 0.28 for sour cherry).

The center of gravity above ground of each cherry tree was determined after the tree was cut, balanced on a knife edge beam, and measured. The center of gravity of the sweet cherry trees ranged from 1.07 to 1.78 m (42 to 70 in.) with an average value of 1.53 m (60.3 in.) and standard deviation of 0.13 m (5 in.). The center of gravity of the sour cherry trees ranged from 1.25 to 1.85 m (50 to 74 in.) with an average value of 1.85 m (59.4 in.) and standard deviation of 0.12 m (4.8 in.). Although the relationship between the tree mass center of gravity and the trunk diameter for both sweet and sour cherry trees was also linear, as illustrated in Figures 4.3 and 4.4, the correlation factors were again found to be small (r = 0.20 for both sweet and sour cherry).

The mass of each cherry tree was determined by weighing the tree after it had been cut. The mass of sweet cherry trees ranged from 8 to 37.1 kg (17.6 to 81.8 lb) with an average of 19.9 kg (43.9 lb) and standard deviation of 6.2 kg (13.67 lb). Sour cherry tree mass ranged from 10.2 to 30.9 kg (22.5 to 68.1 lb) with an average of 20.5 kg (45.2 lb) and standard deviation of 5.37 kg (11.84 lb). When the relationship between tree mass and trunk diameter was fitted with a power curve, a high correlation was found (r = 0.83) for sweet cherry and 0.84 for sour cherry), Figures 4.5 and 4.6.

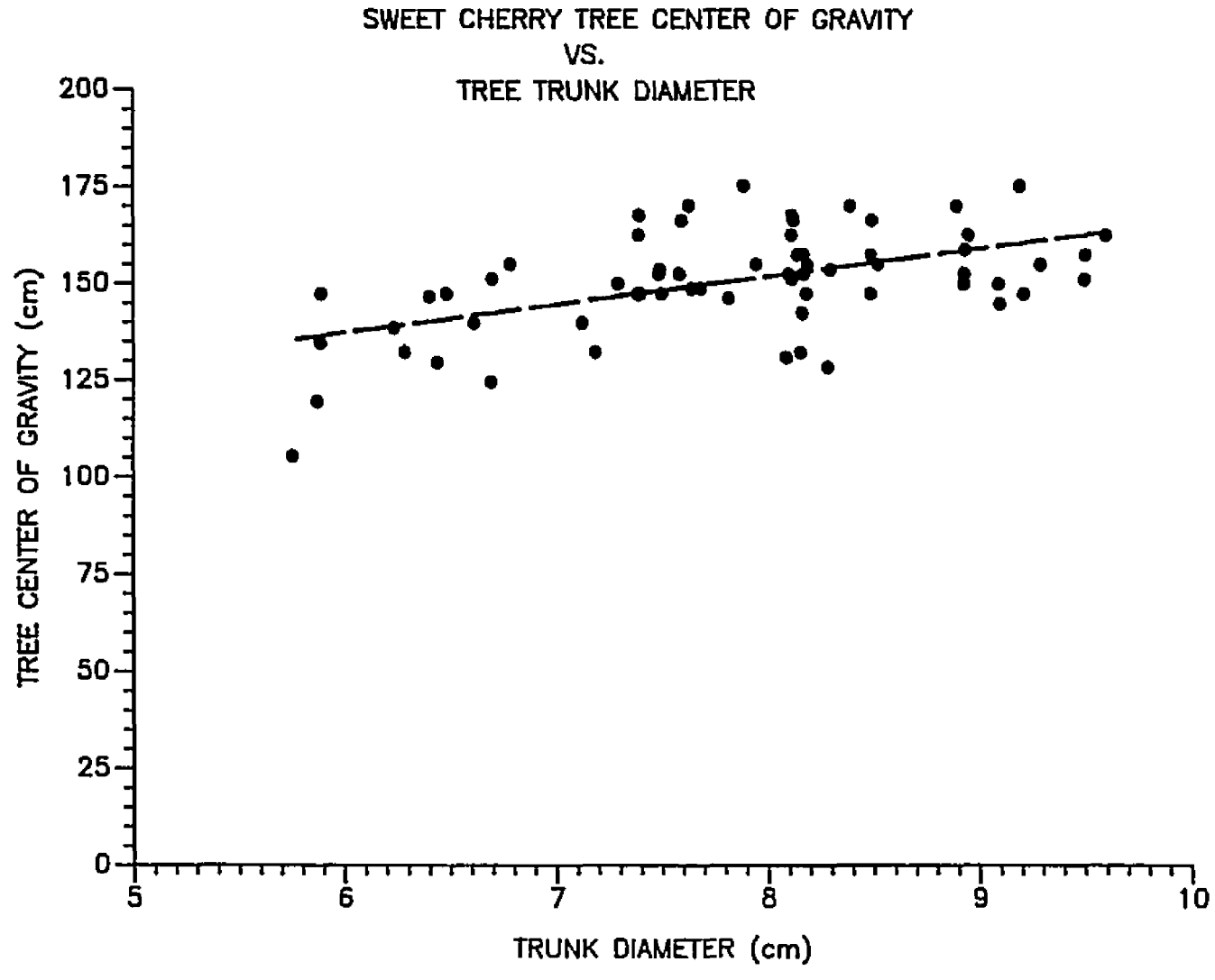


FIGURE 4.3 SWEET CHERRY TREE CENTER OF GRAVITY VS. TREE TRUNK DIAMETER.

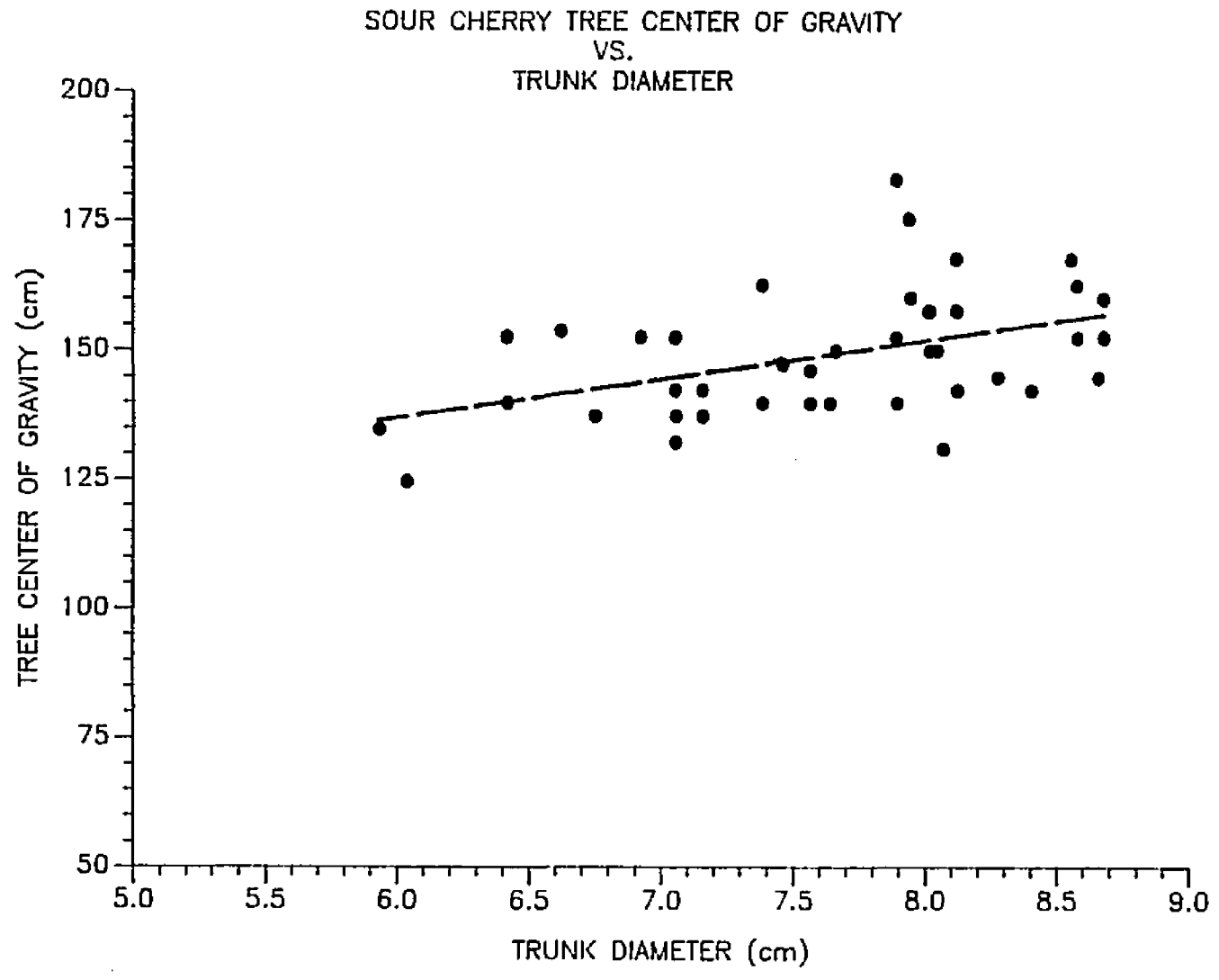


FIGURE 4.4 SOUR CHERRY TREE CENTER OF GRAVITY VS. TREE TRUNK DIAMETER.

# SWEET CHERRY TREE MASS VS. TRUNK DIAMETER

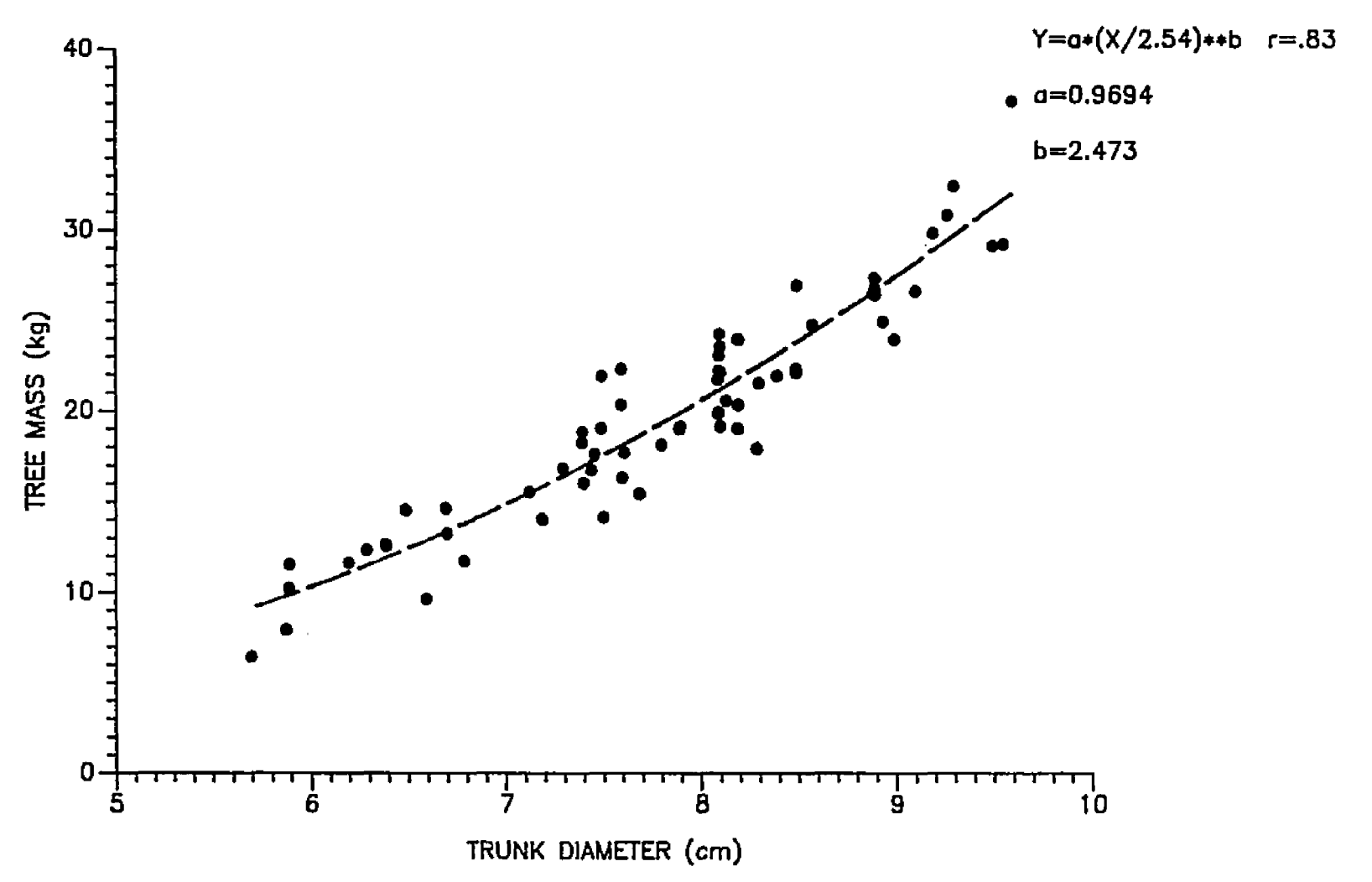


FIGURE 4.5 SWEET CHERRY TREE MASS VS. TREE TRUNK DIAMETER.

### SOUR CHERRY TREE MASS VS. TREE TRUNK DIAMETER

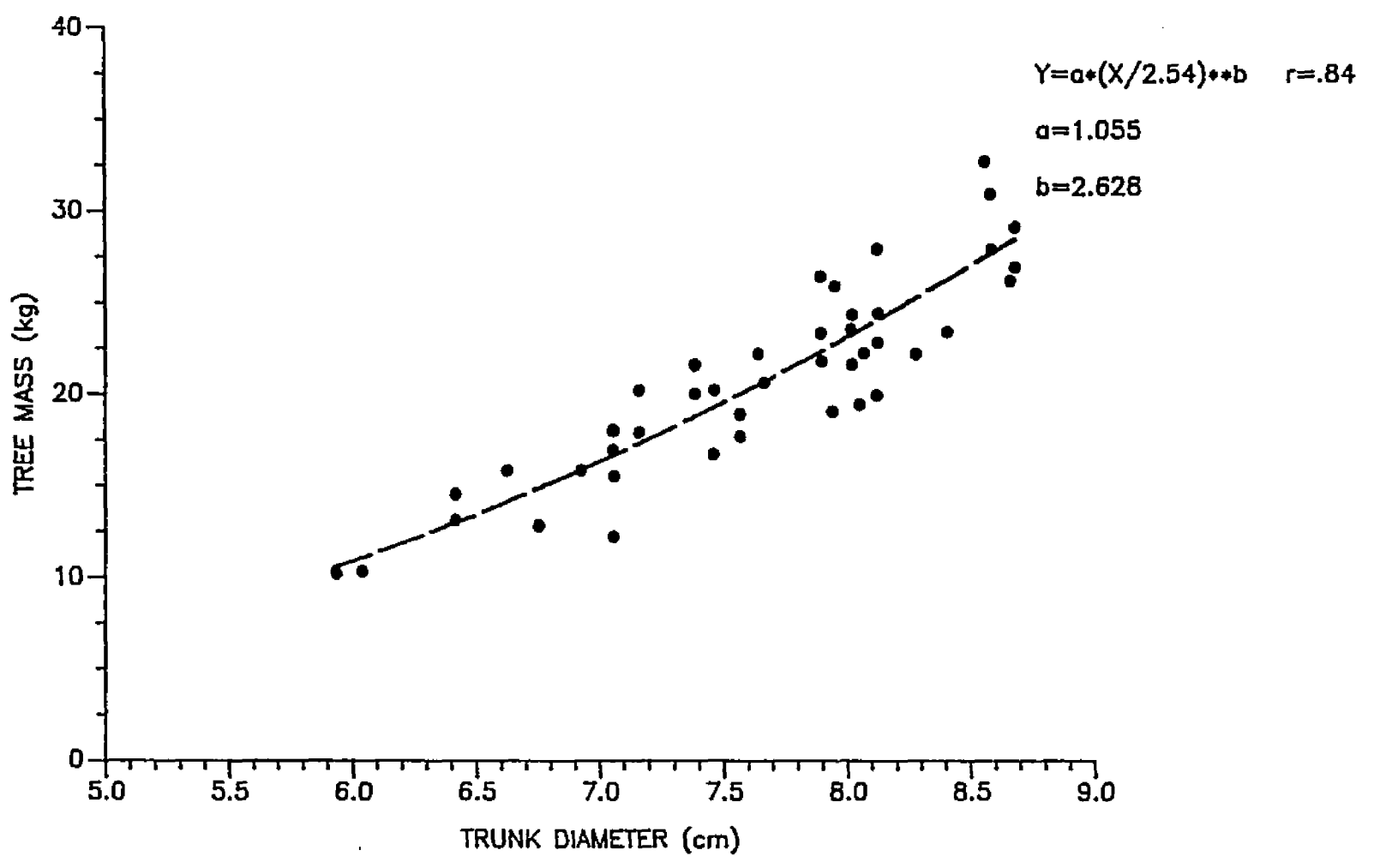


FIGURE 4.6 SOUR CHERRY TREE MASS VS. TREE TRUNK DIAMETER

#### 4.1.2 Stiffness And Damping Measurements

The dynamic displacements of a cherry tree trunk during the shaking operation have been the main concern of many studies related to bark damage, bark strength, and trunk displacement modeling. This dynamic behavior of the tree trunk during harvesting can be simulated using the IMP program, if the the stiffness and the damping of cherry tree trunks are determined.

During the 1985 cherry harvesting season, a study was conducted to measure both linear and torsional sour cherry (Montmorency variety) tree trunk stiffness and damping factors corresponding to three different tree trunk diameters (small, medium, and large). These diameters were selected to be 63 mm (2.5 in.) for small, 114 mm (4.5 in.) for medium, and 165 mm (6.5 in.) for large tree trunks. Three trunks of each size were analyzed.

Force for the linear stiffness and damping tests was applied to the cherry tree trunks using two sizes of hydraulic cylinders. A 63 mm (2.5 in.) inside diameter (ID) hydraulic cylinder, with a 25.4 mm (1 in.) diameter rod was used to pull the small trunks. A 89 mm (3.5 in.) ID hydraulic cylinder with a 38 mm (1.5 in.) diameter rod was used to pull the medium and large trunks.

The pressure developing the pulling force in the hydraulic cylinders was monitored by two strain gage pressure transducers (San-Sym LX0540A for up to 6894 kPa (1000 psi), model LX0560A for up to 20680 kPa (3000 psi)). Each pressure transducer was calibrated by recording its electrical output for incremental changes in pressure input that was developed by a 41360 kPa (6000 psi) hydraulic press. The press cylinder was equipped with a precision pressure gage. Figure 4.7 shows the tree pull test setup as it was used in the field.

The hydraulic cylinder used in trunk stiffness and damping experiments was fastened to a beam extending from a tractor drawbar. The cylinder rod was connected to an arm ended with a lock mechanism. This arm was connected to a chain about 2 m (80 in.) long circling around the cherry tree trunk to transmit the pulling force from the hydraulic cylinder rod and the arm mechanism to the tree trunk. During operation the cylinder rod moved backward pulling the arm mechanism with it and causing the chain to pull the tree trunk to a new position. The arm mechanism lock then released causing the tree trunk to oscillate to rest.

A linear voltage differential transformer (LVDT) was calibrated and connected to the cherry trunk to detect the trunk horizontal displacement resulting from application of the pulling force. The LVDT was mounted in a holder and

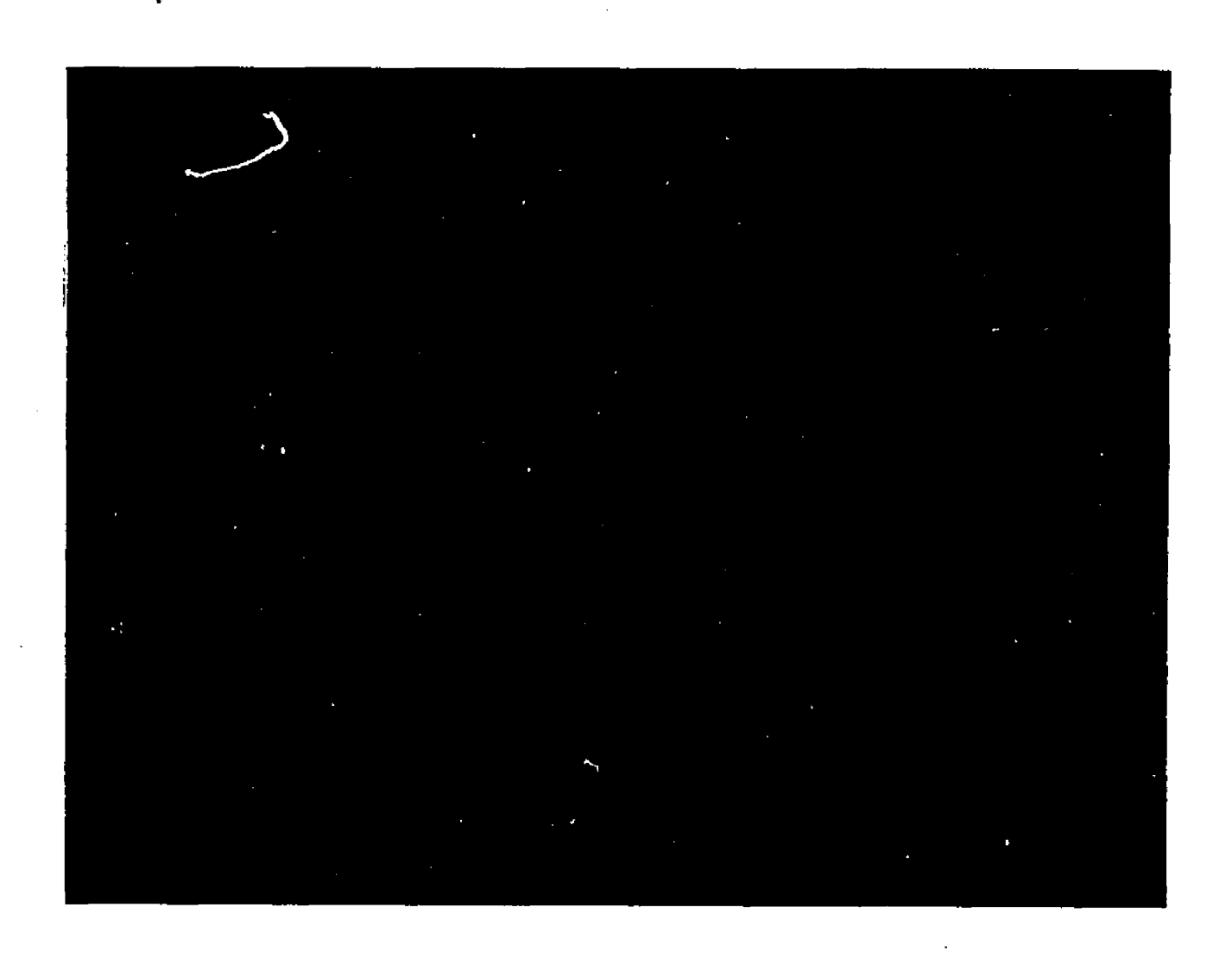


FIGURE 4.7 TREE PULL TEST SETUP FOR LINEAR STIFFNESS.

positioned horizontal at about 255 mm (10 in.) above the ground. The LVDT rod was attached to the tree trunk by a screw. Undesired lateral and vertical movements during the test were eliminated with the use of a spring absorber mounted in-line between the tree attachement point and the LVDT rod.

The signals from the pressure transducers and LVDT were recorded on a Racal 4DS four-channel analog instrumentation tape recorder (Racal Recorders Inc., Covina, CA) a tape speed of 190.5 mm/s ( 7.5 in./s ). at A data 6000 spectral waveform analyzer (Analogic Data Precision, Danvers, MA) was used to digitize the analog signals to 6000 points over a period of 20 s. Each digitized signal was recorded on a floppy disk. Calibration factors were then used to convert the signal values into either force values or displacement values. A HP 7475A plotter was used to plot the results as graphs of force and displacement versus time, as shown in Figure 4.8 and 4.9. The stiffness factors (K) were determined from the force and displacement appropriate time along the curves was selected curves. An and the corresponding force and displacement ratio were calculated. In Figures 4.8 and 4.9 the selected time was 5.5 s and the corresponding force and displacement were 328 N and 30.2 mm, respectively, giving a stiffness factor of 10.86 N/mm. The damping ratios were approximated by using

### LINEAR DISPLACEMENTS MEASUREMENTS VERSUS TIME

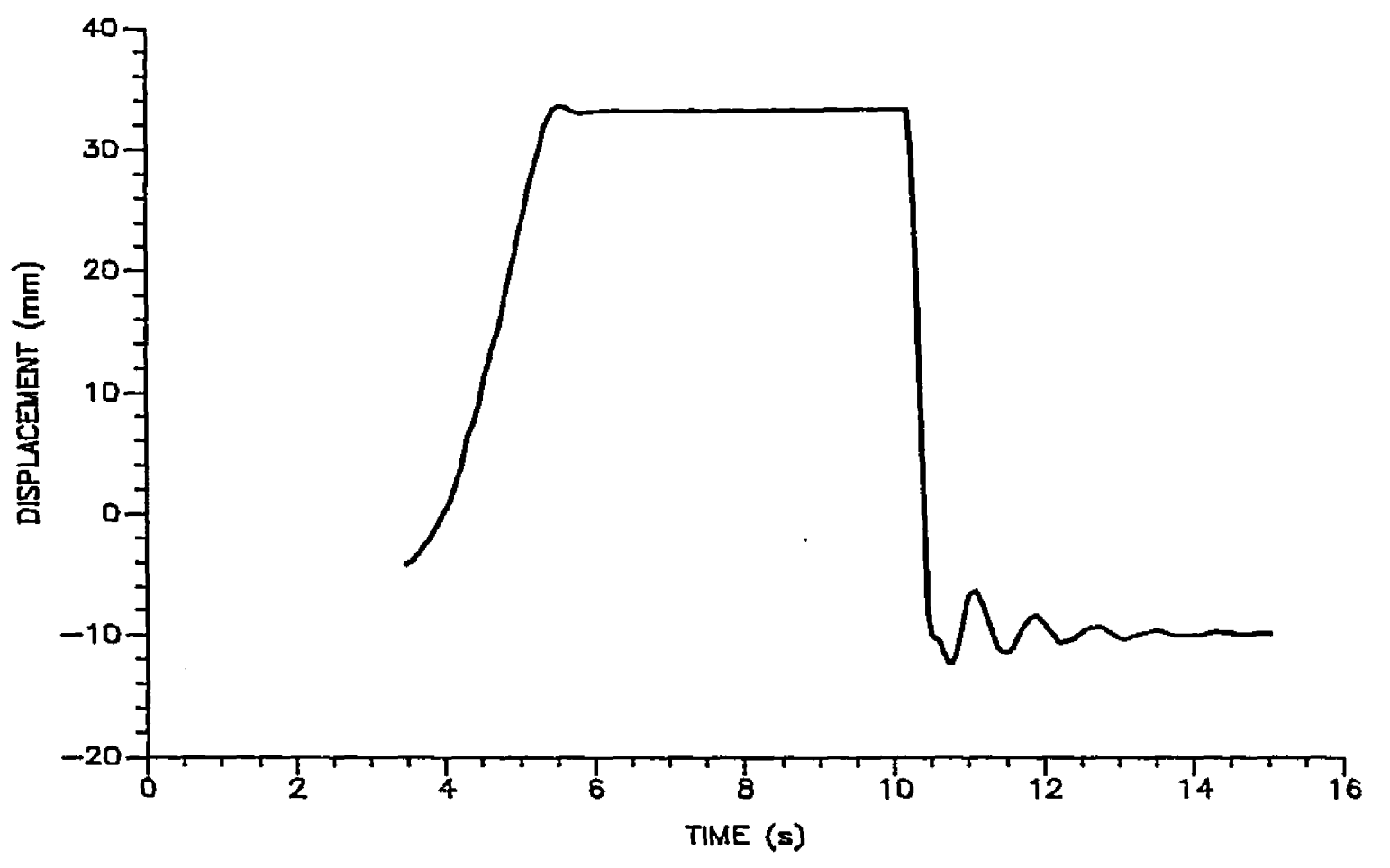


FIGURE 4.8 LINEAR DISPLACEMENTS MEASUREMENTS OF A 63 mm DIAMETER CHERRY TREE TRUNK.

# LINEAR FORCE MEASUREMENTS VS. TIME (s)

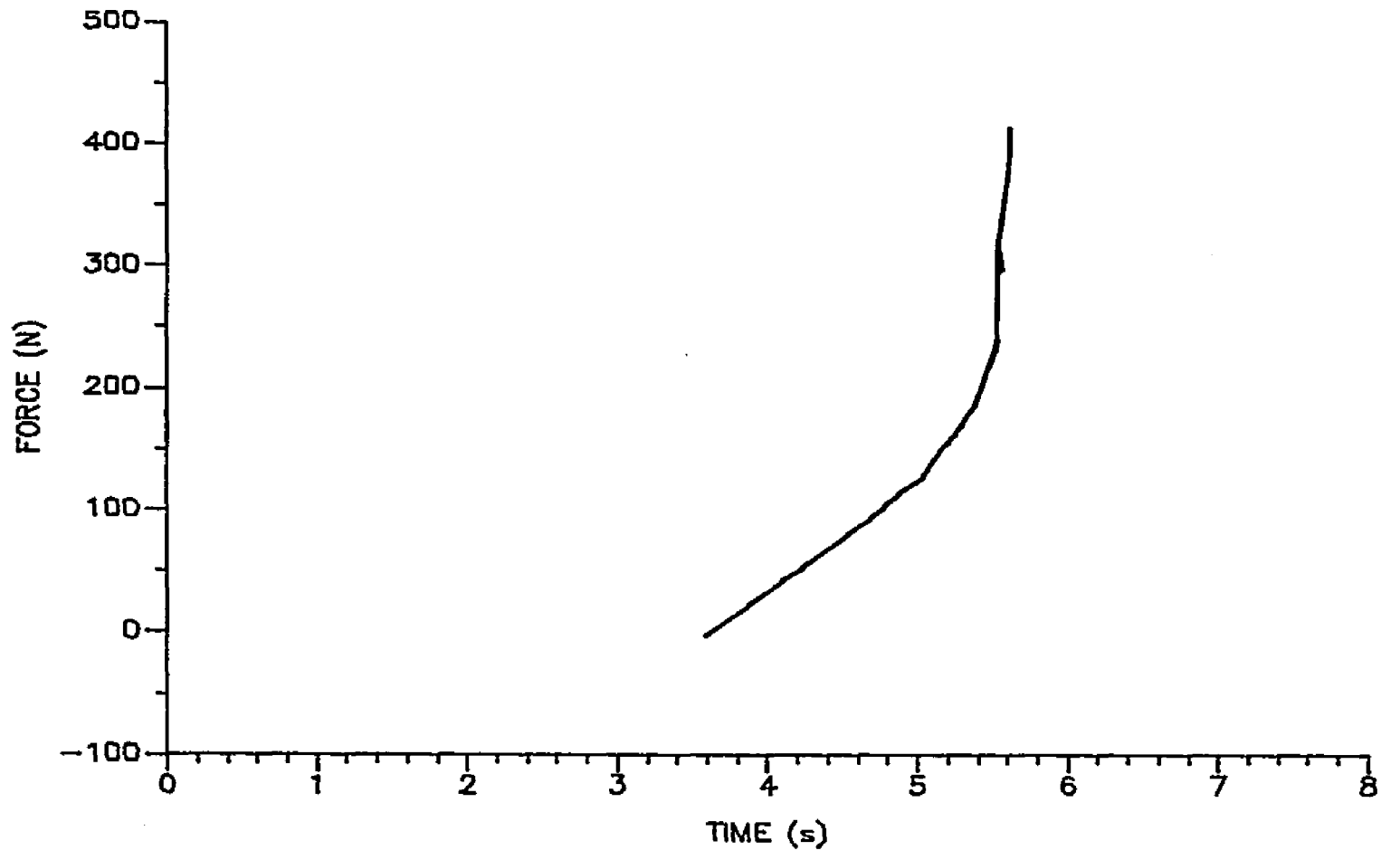


FIGURE (4.9) LINEAR FORCE MEASUREMENTS OF A 63 mm DIAMETER CHERRY TREE TRUNK.

Table 4.1 Linear Stiffness And Damping
Properties Of The Sour Cherry Tree.

Tree ID	Trunk Dia.	Pull Velocity (mm/s)	Stiffness K (N/mm)	Damping Ratio
10	63	76.0	11.84	0.135
10	63	48.8	14.10	0.148
11	63	44.0	16.62	0.138
11	63	100.0	10.86	0.110
11	63	56.8	12.12	0.118
12	63	38.0		
12	63	44.2		
Average S.dev.	63	58.25 22.21	12.69 2.31	0.1290 0.0124
A	114	6.15	137.1	
В	114	3.76	148.6	
С	114	5.38	145.7	
Average S.dev.	114	5.09 1.22	144.5 6.4	
3 Stripe	165	3.32	867.0	
Nancy's	165	3.57	440.0	
2 Stripe	165	1.60	666.6	
Average S.dev.	165	2.83	657.86 213.63	

the following equation:

Damping ratio = 
$$\frac{\text{Ln } (X1/Xn)}{2 \pi n}$$

#### Where:

X1: The amplitude of the first cycle.

Xn: The amplitude of the n'th cycle.

n : The number of cycles from X1 to Xn.

Ln: Natural logarithm.

In Figure 4.8 the first and second cycle amplitude were 6 mm and 3 mm, respectively, and the calculated damping ratio was 0.110. Table 4.1 presents the linear stiffness and damping results for three different tree trunk diameter sizes.

Torque for the torsional stiffness and damping tests was applied using a tree twister, Figure 4.10. Force for these tests was applied using a 63 mm (2.5 in.) inside diameter hydraulic cylinder, with a 25.4 mm (1 in.) diameter rod. The hydraulic cylinder was fastened to a frame which was connected to a tractor drawbar. The cylinder rod was pinned to the tree trunk twister to convert the linear force to a torque applied at the clamping position of the tree trunk. The tree twister mechanism consisted of four arms pinned together as a 4-bar linkage provided with a lock

# TREE TWISTER

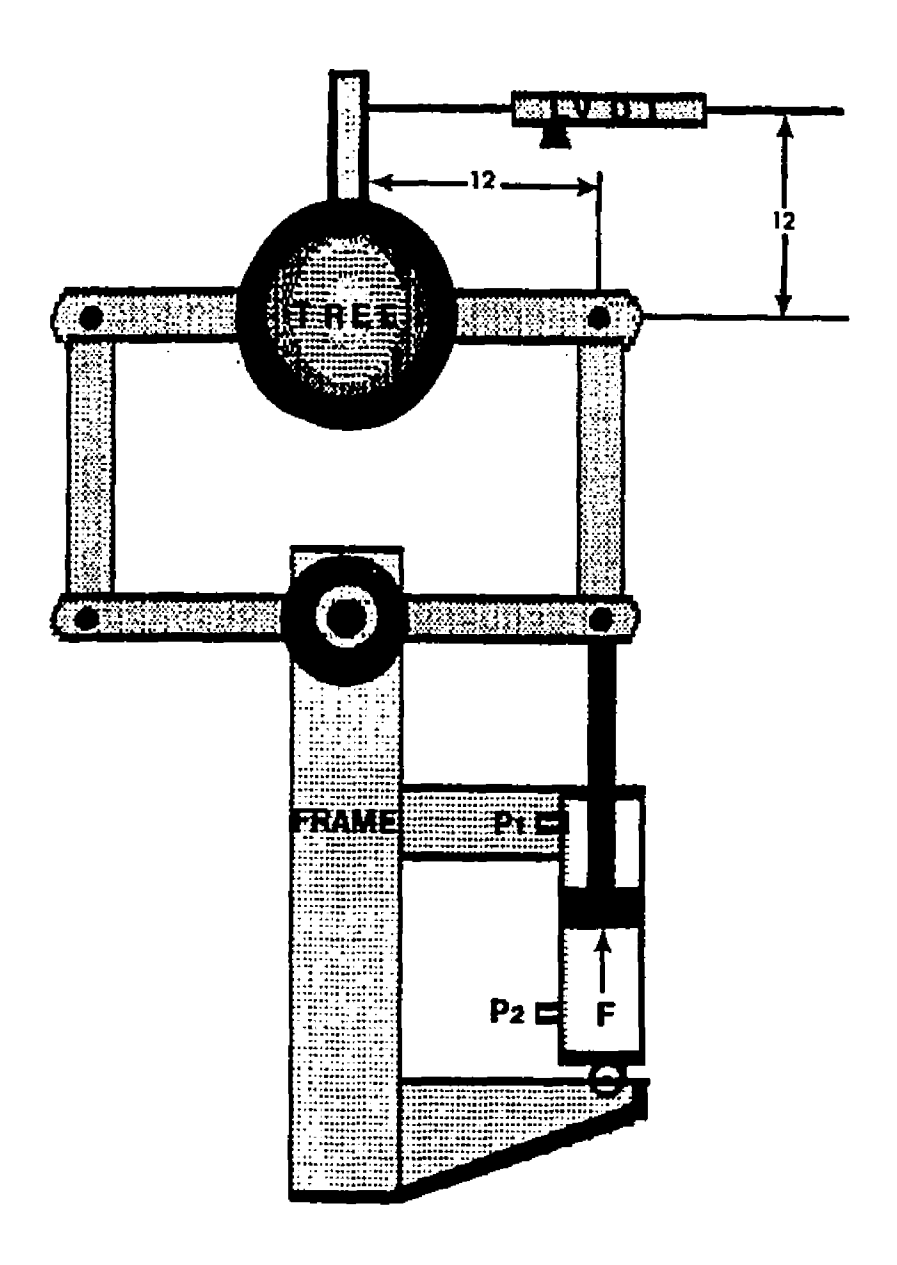


FIGURE 4.10 TREE TWISTER SETUP FOR ROTARY STIFFNESS.

mechanism to release the energy stored by the tree trunk.

The linkage was fastened to the tree trunk by four bolts through each of two metal semi-circular pads.

The same LVDT used in the tree pull test was calibrated and connected to a 305 mm (12 in.) arm bolted to the tree trunk to detect the rotational displacement resulting from both the applied torque and the energy stored in the trunk. The LVDT was carried by a holder and positioned at 255 to 305 mm (10 to 12 in.) above the ground level.

The same two pressure transducers used in the tree pull test were also used to measure the pressure required to twist the cherry tree trunk. During operation the cylinder rod extended forward, causing the frame to rotate and twist the cherry tree trunk. With the tree in the twisted position the lock mechanism was released and the tree trunk oscillated to its rest position.

The analog signals from the transducers were recorded on the instrumentation tape recorder, digitized, then recorded on a floppy disk, calibrated and plotted as previously described. The graphs of forces and rotational displacements versus time are shown in Figures 4.11 and 4.12. Using both curves, the rotational displacement and torque were estimated to be 9.34 degrees and 152,242 N.m, respectively, at 8.25 s, resulting in a stiffness of 16,300

# ANGULAR DISPLACEMENT MEASUREMENTS VS. TIME

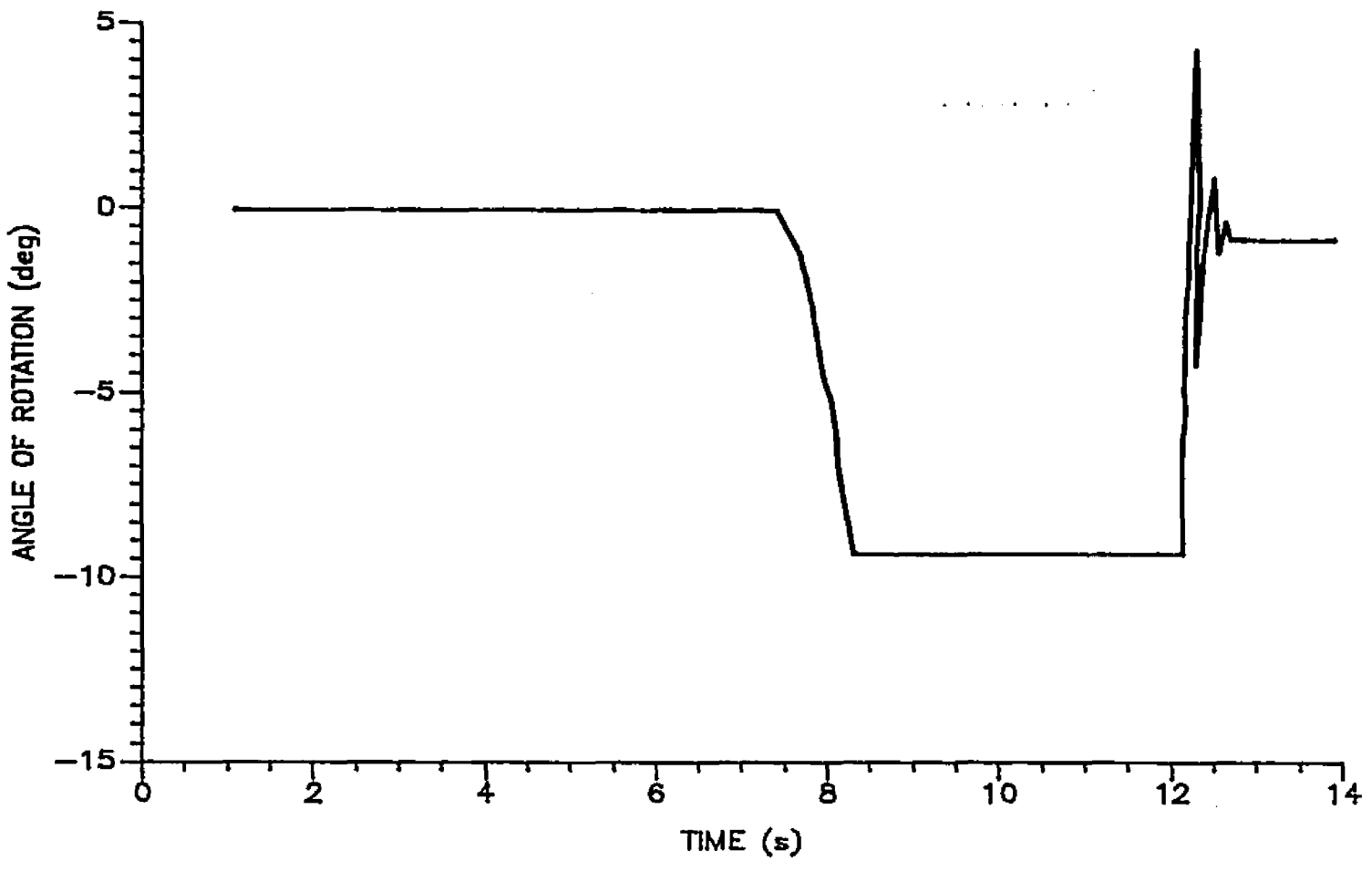


FIGURE 4.11 ANGULAR DISPLACEMENT VERSUS TIME OF A 63 mm DIAMETER CHERRY TREE TRUNK.

# EXPERIMENTAL TORQUE MEASUREMENTS VS. TIME

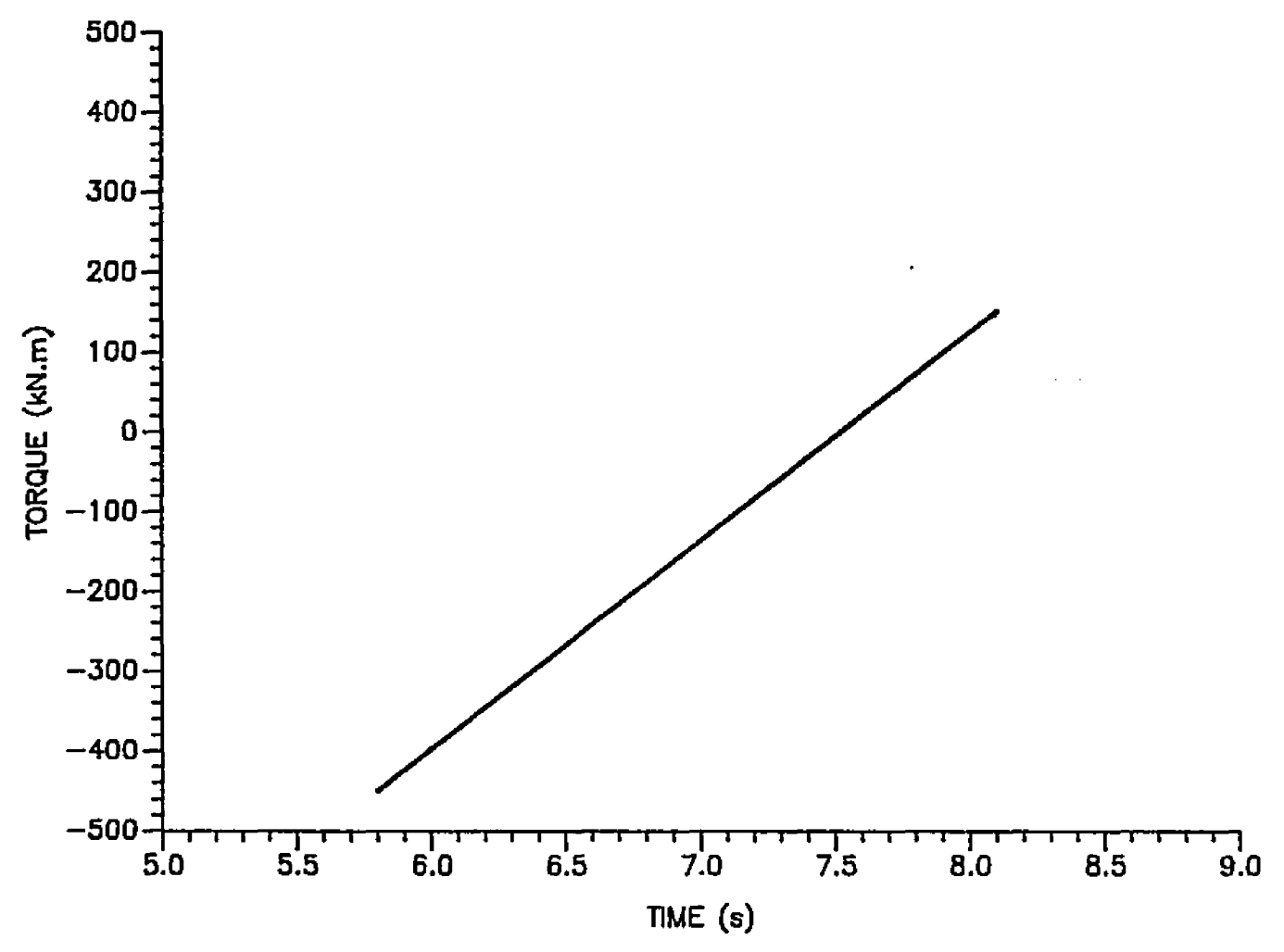


FIGURE 4.12 EXPERIMENTAL TORQUE MEASUREMENTS OF A 63 mm DIAMETER CHERRY TREE TRUNK.

N.m/degree. The damping ratio was calculated as previously described in Section 4.1.2. The first and second cycle amplitudes were estimated to be 17.6 and 4.2 mm, respectively, and the calculated damping ratio was 0.227. Table 4.2 presents the rotational stiffness and damping results for the three different cherry tree trunk diameters.

Table 4.2 Rotary Stiffness And Damping
Properties Of The Sour Cherry Tree.

Tree ID	Trunk Dia.	Max. Disp. (deg.)	Stiffness Kt (N.m/deg.)	Damping Ratio
10	63	9.10	16600	0.274
10	63	9.34	16300	0.227
11	63	8.78	15500	0.258
11	63	8.42	13500	0.215
12	63	4.28	18100	0.251
12	63	4.14	17700	0.238
Average S.dev.	63	7.33 2.44	16,280 1,660	0.244 0.021
A	114	9.50	60400	
A	114	9.95	73300	
С	114	9.94	65800	0.134
С	114	9.74	70400	0.239
Average S.dev.	114	9.78	67,470 5,637	0.189 0.052

Table 4.2 Continued

Tree ID	Trunk Dia.	Max. Disp. (deg.)	Stiffness Kt (N.m/deg.)	Damping Ratio
Nancy's	165	0.541	2,250,000	0.156
Nancy's	165	0.564	2,170,000	0.195
2 Stripe	165	0.293	3,150,000	
2 Stripe	165	0.316	3,370,000	
3 Stripe	165	0.339	4,150,000	0.160
3 stripe	165	0.338	3,590,000	0.121
Average S.dev.	165	0.398 0.12	3,110,000 775,000	0.158 0.030

#### 4.2 Trunk Shaker Description

The total mass of the C-clamp Friday trunk shaker was 544 kg (37.3 slug), including two 350 mm (14 in.) diameter semicircular unbalanced rotating masses of about 38 kg (2.6 slug) each. The eccentricity of each mass was 76 mm (3 in.). Each mass was attached to a separate shaft, and each shaft was chain driven by individual 2.8 L/s (44 gpm) and 10340 kPa (1500 psi) counter-rotating vickers hydraulic vane motors, Figure 4.13.

The shaker was mounted on a 2250 Mount-O-Matic loader frame of a Hydro-84 International tractor. A frame was attached to the loader to suspend the shaker at three points as recommended by the manufacturer. Rubber bushings supplied with the shaker were used on both ends of the suspension bars to minimize the amount of vibration transmitted to the tractor. The tilt mechanism of the loader frame was used to level the shaker during attachment to the tree trunk.

A separate hydraulic system, mounted on the rear 550 PTO of the tractor, powered the shaker drive motors. A 150 L (40 gal) reservoir, equipped with a master shut-off valve and return-line oil filter, was mounted above the PTO shaft. The hoses used to distribute the flow were at least 19 mm

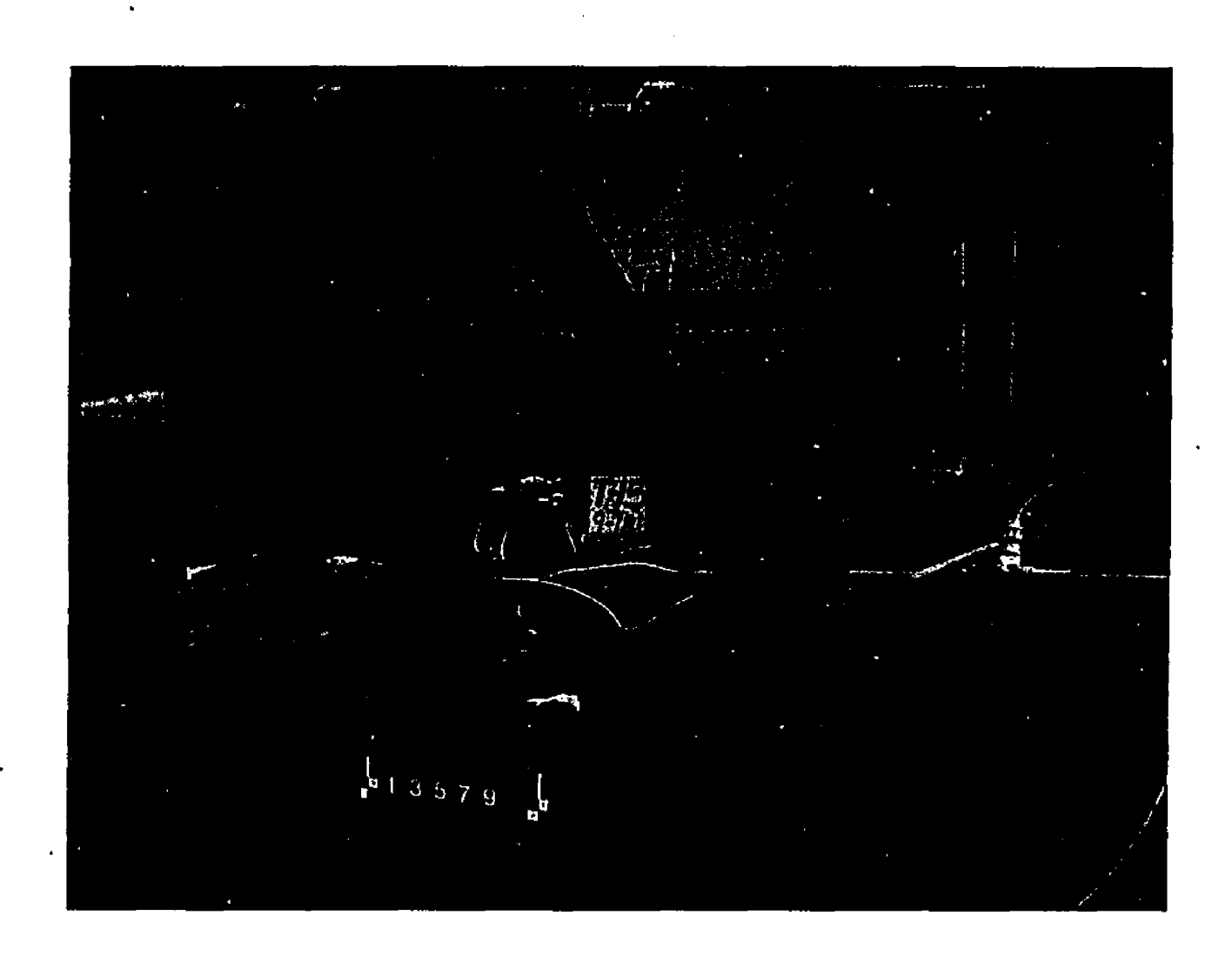


FIGURE 4.13 FRIDAY C-CLAMP TRUNK SHAKER.

(0.75 in.) ID. A 50-50 flow divider allocated equal volume to two separate continuously variable flow control valves that controlled each shaker drive motor. The speed of each motor could be independently selected. Each shaker drive motor then transmitted power from a 18-tooth sprocket to a 45-tooth sprocket mounted on the shaft of the eccentric mass.

A double-acting 80 mm ID X 610 mm stroke (3 in. X 24 in.) hydraulic cylinder, mounted on the back of the shaker activated the opening and closing of the C-clamp. This hydraulic cylinder was connected directly to the tractor's hydraulic system which operated at 0.7 L/s (11 gpm) and 12410 kPa (1800 psi) at 2200 engine r/min.

Two rubber pads were fastened in support slings (rubber covered belting) within the clamping jaw. The interface between the belting sling and a covering flap was coated with a lubricant (grease). This followed the manufacturer's recommended practice for reducing shear force on the tree bark by allowing low-friction slip to occur between the pad sling and the flap.

The location of the center of gravity of the trunk shaker was obtained by balancing the machine with respect to its orthognal axes, on the tip of a 50 mm X 50 mm (2 in.X 2 in.) piece of angle iron. The eccentric masses were not removed due to difficulties involved in disassembly.

Instead, the center of gravity was corrected for the presence of the masses by taking measurements on the appropriate axis with both masses inward, then outward, and calculating an average. This provided an accurate measurement of the location of the center of gravity of the shaker without the masses. The shaker physical dimensions and the location of the center of gravity are presented in Figure 4.14.

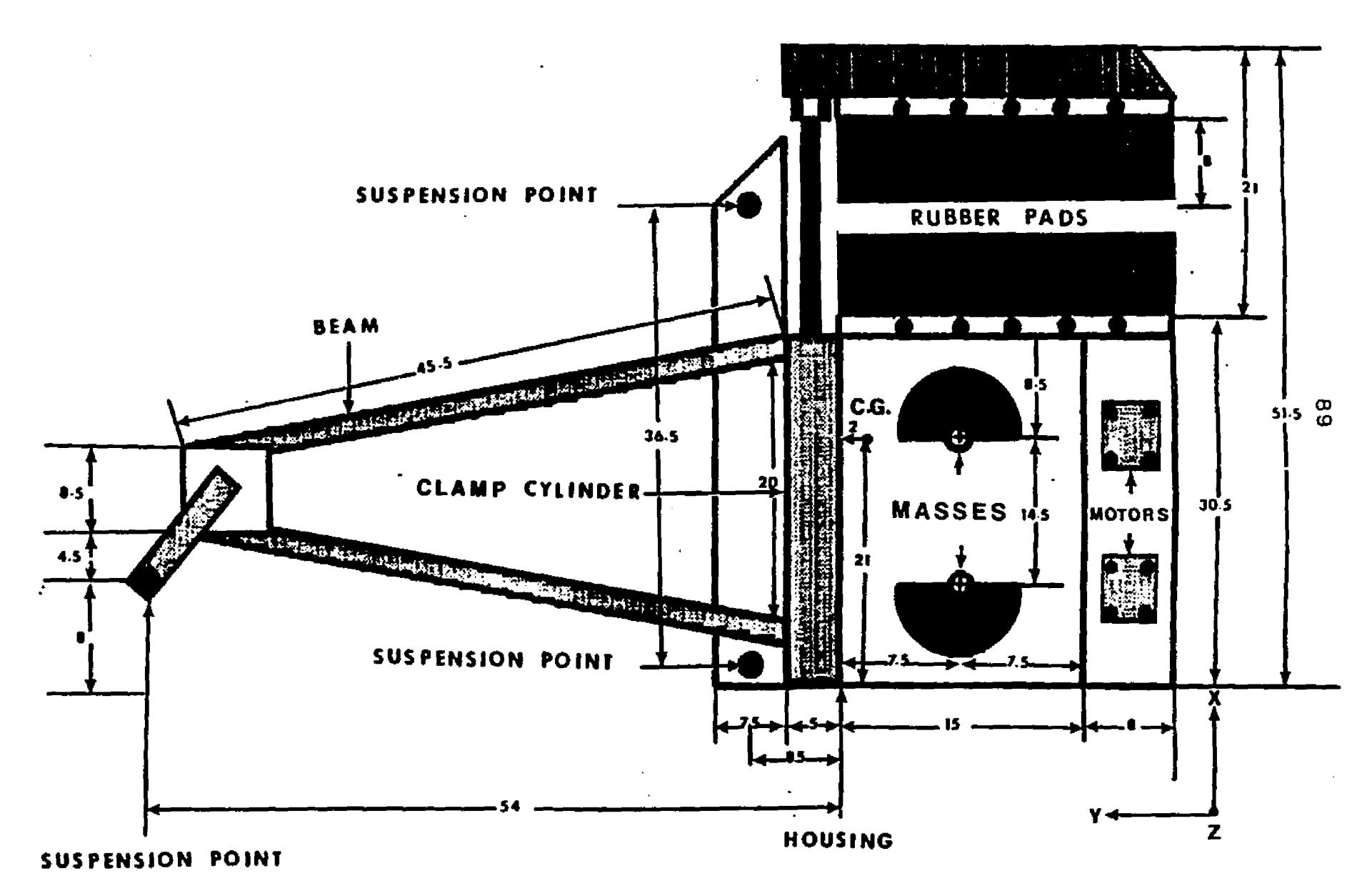


FIGURE 4.14 SHAKER PHYSICAL DIMENSIONS (ALL DIMENSIONS ARE IN INCHES)

#### 4.3 Trunk Shaker Physical Properties

The physical dynamic properties of any trunk shaker play an important role in determining the shaker dynamic behavior during operation. These physical properties, which must be considered in any shaker mathematical model, can be defined as:

- 1- Mass moments of inertia.
- 2- Stiffness and damping factors.

To obtain the mass moments of inertia of the shaker, the shaker was suspended and swung from two different points. At a point located 140 mm (5.5 in.) directly above the shaker center of gravity (CG) in the z direction, the shaker was swung to determine its mass moments of inertia in the x and y directions (Ix, and Iy). The mass moment of inertia in the z direction (Iz) was obtained by swinging the shaker from the rear suspension point, located 1420 mm (56 in.) from the shaker center of gravity. The number of swing cycles about each point and the total swing time were recorded. The mass moments of inertia (Ix, Iy, and Iz) were calculated using the compound pendulum theory for a rigid body of mass (M) pivoted at a point a distance (d) from its center of gravity (CG) and free to rotate under its own

gravitational force. The following equation is :

$$I = \frac{MG \cdot d}{(wn)^2}$$

Where:

M : Total mass.

d: Distance between the suspension point and CG.

G : Gravitational constant.

wn : Natural frequency of the shaker.

The experimental results of shaker mass moments of inertia are presented in Table 4.3. It is required that when using the IMP program to model the shaker, mass moments of inertia (Ix, Iy, and Iz) must be specified according to one of the shaker joints. The rear suspension point (spherical joint J7), Figure 4.2, which connects the rear suspension hanger with the shaker was chosen as this reference point. Then the mass moments of inertia in the x and y directions (Ix, and Iy) were transferred to joint J7 by applying the parallel axis theorem using the following equations:

$$Ix = Ix' + M (Y'^2 + Z'^2)$$

$$Iy = Iy' + M (Z'^2 + X'^2)$$

Where:

Ix: Shaker mass moment of inertia in the x direction

Table 4.3 Shaker Moment Of Inertia Determined

By Swinging.

Axis Trial	Mass Location	Cycles	Time (s)	Average Frequency (Hz)	Moment Of Inertia (I lbm.in2
X1	* Front	31	60.2	0.515	683.279
X2	Front	31	60.4	0.513	683.355
хз	Front	31	60.8	0.510	683.515
Averag S.dev.	е				683.383
Y 1	Front	33	60.4	0.546	603.038
Y2	Front	33	60.8	0.542	603.165
Υ3	Front	33	59.0	0.559	582.978
Average S.dev.				596.393 11.610	
Y1	** F.E.O.		60.9	0.509	683.540
		31	61.4	0.505	706.326
	F.E.O.	31	61.1		706.216
 Averag S.dev.	e				698.694 13.124

Table 4.3 Continued

Axis Trial	Mass Location	Cycles	Time (s)	Average Frequency (Hz)	Moment Of Inertia (I) lbm.in?
Y1	F.E.O.	33	60.3	0.547	603.012
Y2	F.E.O.	33	59.7	0.552	583.207
У.3	F.E.O.	33	59.1	0.558	582.998
Average S.dev.					589.739 11.495
X1	*** F.A.				706.326
X 2	F.A.	31	61.4	0.505	706.326
х 3	F.A.	31	61.2	0.505	706.242
Average S.dev.					706.298 0.047
Y 1	F.A.	33	60.5	0.545	603.678
Y2	F.A.	33	60.3	0.547	602.998
73	F.A.	33	60.1	0.549	602.945
Average S.dev.					603.007

Table 4-3 Continued

Axis Trial	Mass Location	Cycles	Time (s)	Average Frequency (Hz)	Moment Of Inertia (I) lbm.in2.
Z 1	F.A.	24	60.9	0.394	10644.01
<b>Z2</b>	F.A.	24	61.9	0.387	10996.42
23	F.A.	24	60.7	0.395	10642.99
Average S.dev.					10761.14 0.05
21	*** Back	24	60.0	0.400	10638.76
<b>Z</b> 2	Back	24	60.0	0.400	10638.76
<b>Z3</b>	Back	24	60.0	0.400	11096.25
Average S.dev.					10791.25 0.05

\* Front : Masses in the front Position.

\*\* F.E.O. : Masses facing each other.

\*\*\* F.A. : Masses facing away from each other.

\*\*\*\* Back : Masses in the back position.

relative to joint J7.

- Iy: Shaker mass moment of inertia in the y direction relative to joint J7.
- Ix': Shaker mass moment of inertia in the x direction relative to the CG.
- Iy': Shaker mass moment of inertia in the y direction relative to the CG.
- M : Shaker mass (543.6 kg (37.3 slug)).
- X': The distance from CG to the rear vertical hanger joint J7 in the x direction (406.4 mm (16 in.)).
- Y': The distance from CG to the rear vertical hanger joint J7 in the y direction (1422 mm (56 in.)).
- Z': The distance from CG to joint J7 in the z direction (14 mm (5.5 in.)).

The calculated results of the shaker mass moments of inertia relative to the rear vertical hanger joint J7 were found to be as follows:

The mass moments of inertia of the shaker rotating

masses , relative to the rotating mass shaft center, were found by assuming the rotating masses have a semicylindrical shape and applying the following equations:

$$Ix = Iy = m \cdot r / 4 + m \cdot L / 12$$

$$Iz = mr / 2$$

Where:

Ix, Iy, Iz: The mass moments of inertia of the shaker rotating masses in the x, y, and z directions, respectively.

m: The amount of rotating mass (39.8 kg (2.75 slug)).

L: The rotating mass height (3.87 in.).

r: The rotating mass radius (178 mm (7 in.)).

The calculated results of mass moments of inertia (Ix, Iy, and Iz) of the shaker rotating masses were found to be 0.347, 0.347, and 0.63 kg.m ( 3.076, 3.076, 5.584 lbm.in. ), respectively.

The linear stiffness and damping of the shaker, as suspended on the rubber bushings, were determined by applying a force and measuring the resulting shaker displacements, and by releasing the displaced shaker and letting it oscillate to its rest position.

A hydraulic cylinder having 22 mm ID and 76 mm stroke

(0.875 in. X 3 in.) was selected to apply the tension force required to displace the shaker, and a pair of LVDT's (previously described ) were used to measure the displacement. The cylinder rod was connected, through a lock mechanism, to a thin chain about 2 m (6.5 ft) long attached to a specified position along the x or y direction on the shaker. Pressures in the hydraulic cylinders and displacements of the shaker were monitored by the pressure transducers and LVDT's as previously described.

Stiffness and damping of the shaker in the x direction were measured by applying the cylinder force at different positions along the y side of the shaker until a point was found that resulted in pure translation in the x direction. The lock mechanism was then released and the force, displacement, and oscillation data were recorded on a tape, and analyzed as previously described. Stiffness and damping of the shaker in the y direction were determined in the same manner as in the x direction.

Rotational stiffness and damping of the shaker were obtained by applying the cylinder force at different positions along the y axis and monitoring the LVDT displacement at both that location and at the rear shaker hanger. The measurements were recorded when displacements were not detected at the rear hanger LVDT. That was an indication of pure rotation about the rear hanger by the

shaker as a result of force application. Figure 4.15 shows the LVDT locations for stiffness and damping measurements in x, y, and directions. Stiffness factors (K) and damping ratios were determined as described in Section 4.1.2. Table 4.4 Lists the experimental results of the shaker stiffness and damping tests in the x, y, and  $\theta$  directions.

### MOUNT PROPERTIES TEST

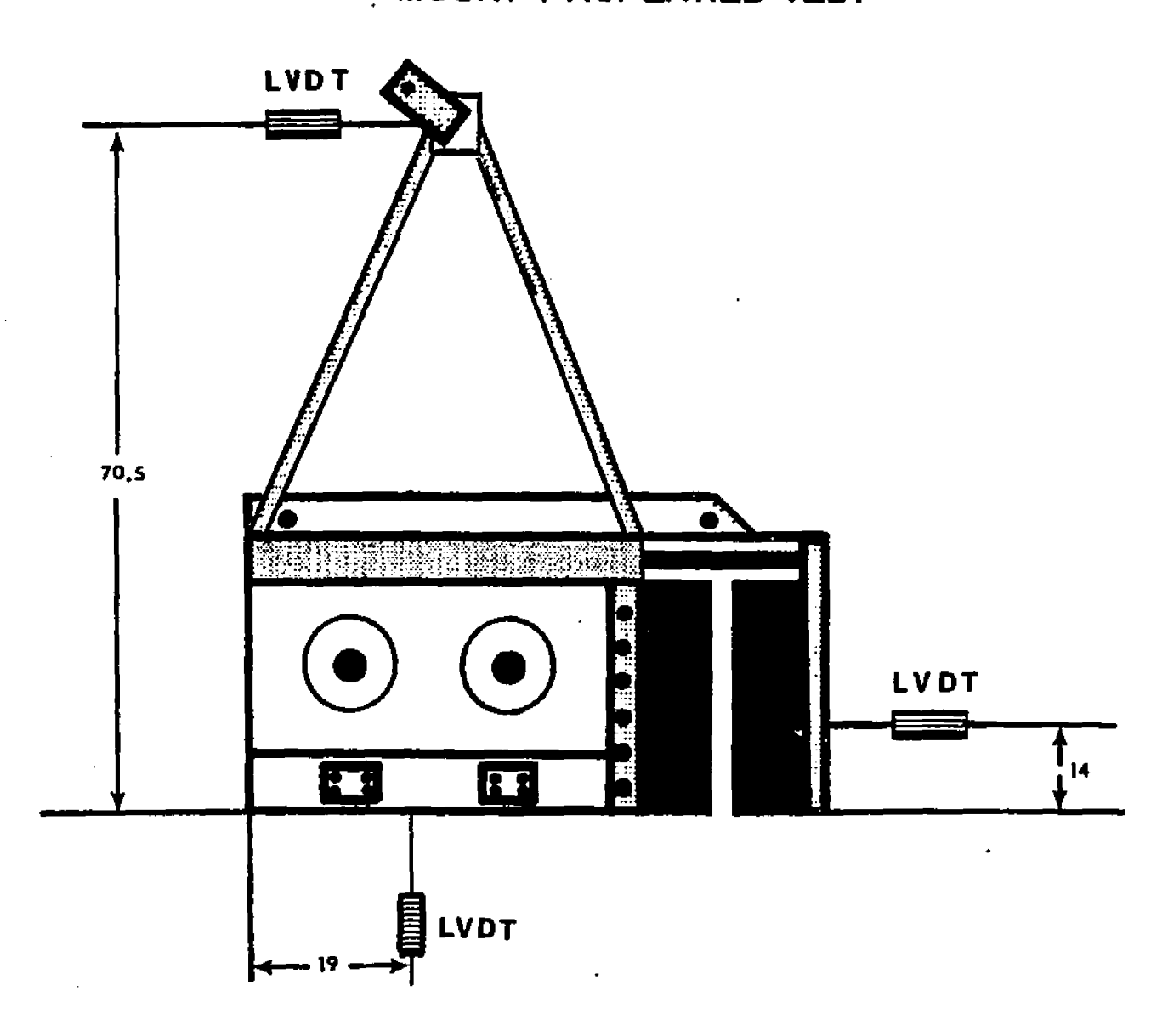


FIGURE 4.15 LVDT LOCATIONS FOR STIFNESS AND DAMPING MEASUREMENTS OF THE TRUNK SHAKER (ALL DIMENSIONS ARE IN INCHES).

Table 4.4 Stiffness And Damping Constants
For Shaker Mounts.

Test	Direction Monitor	Stiffness K (N/mm)	Damping ratio	
Т1	Y	160.0	0.154	
T2	Y	137.2	0.145	
Т3	Y	159.4	0.167	
T 4 Y		156.0	0.158	
Average S.dev.		153.15 10.78	0.156 0.009	
Т5	x	85.4	0.180	
Т6	x	92.6	0.177	
Т7	x	78.4	0.184	
Т8	x	87.5	0.192	
 Average S.dev.		85.9 5.9	0.183 0.006	

#### 4.4 Rotating Mass Velocity Measurements

Affeldt, (1986) conducted an experiment to determine the shaker rotating mass velocity and angular position the center mass as a function of time. An electromagnetic inductive type sensor was mounted in proximity to each of rotating mass shafts to determine the angular position rotational velocity of the masses at all times during a tree shaking test. His results were presented as voltage pulses in a voltage vs. time plot. Each pulse indicated that the mass center passed the sensor location. The time between pulses indicated the average velocity for each rotation. digitized these velocity plots using the Prime computer digitizer and plotted the frequency vs. time results using the PLOTIT software package. Figures 4.16 to 4.19 show frequency curve samples for the inside and outside rotating masses when the shaker is not clamped to a tree (free-shake condition) or is clamped to tree having a 63 mm (2.5 diameter trunk (shaker-tree condition).

In order to use the rotating mass velocity in the IMP model, the rotating mass frequency curves for the free-shake and shaker-tree condition were divided into two stages. The first stage represented the transient velocity and was approximated by a line having a slope equal to the rotating

2

mass acceleration (278 rad/s). The second stage was the steady state velocity and was approximated by a line having a slope of 0 and a fixed frequency of 15 Hz.

A summary of the physical properties of the C-clamp trunk shaker and a 63 mm diameter sweet cherry trunk used in the IMP model are presented in Table 4.5.

### INSIDE ROTATING MASS FREQUENCY VS. TIME (3)

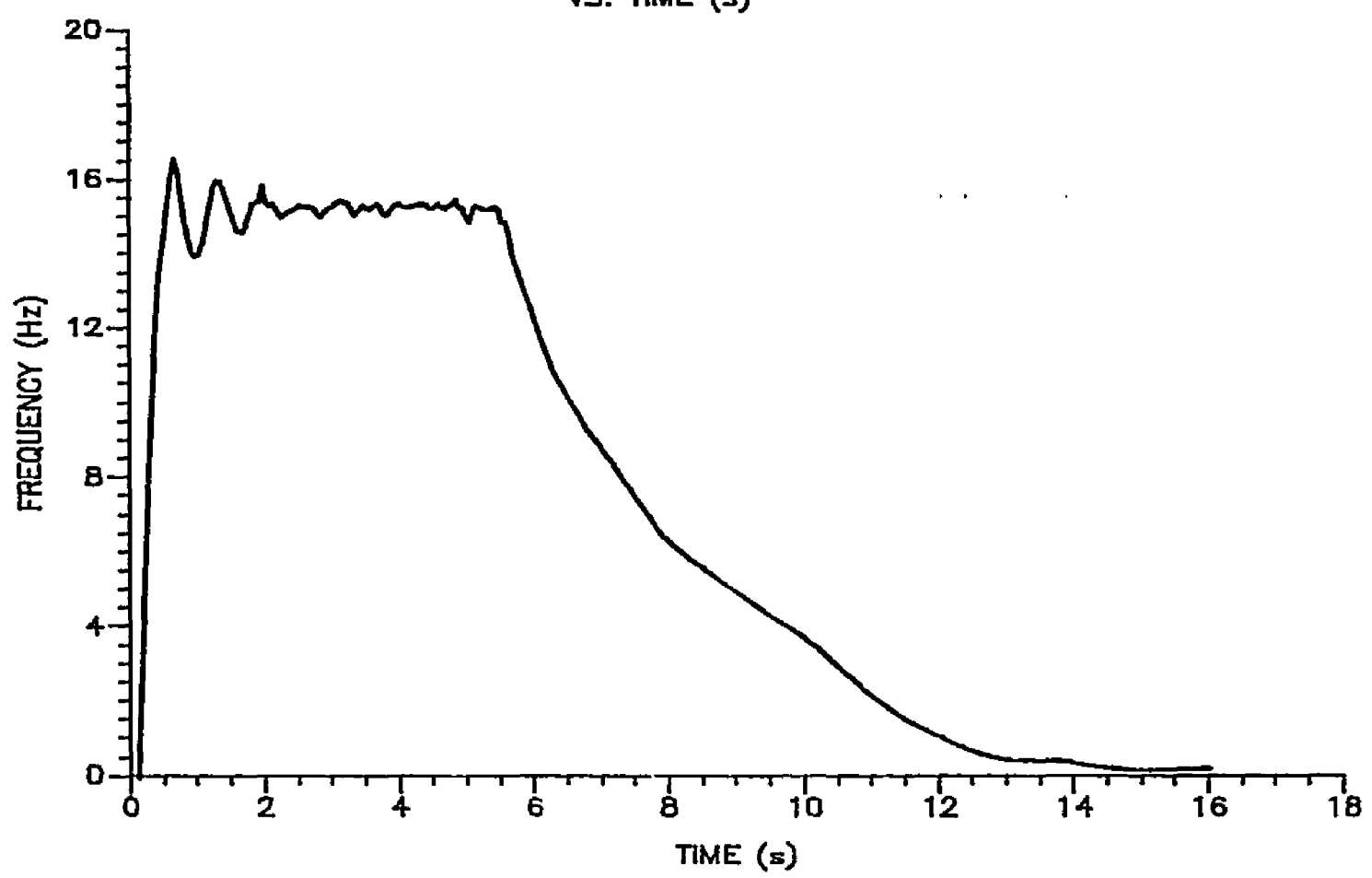


FIGURE 4.16 INSIDE ROTATING MASS FREQUENCY OF A FREE SHAKER.

# OUTSIDE ROTATING MASS FREQUENCY VS. TIME (3)

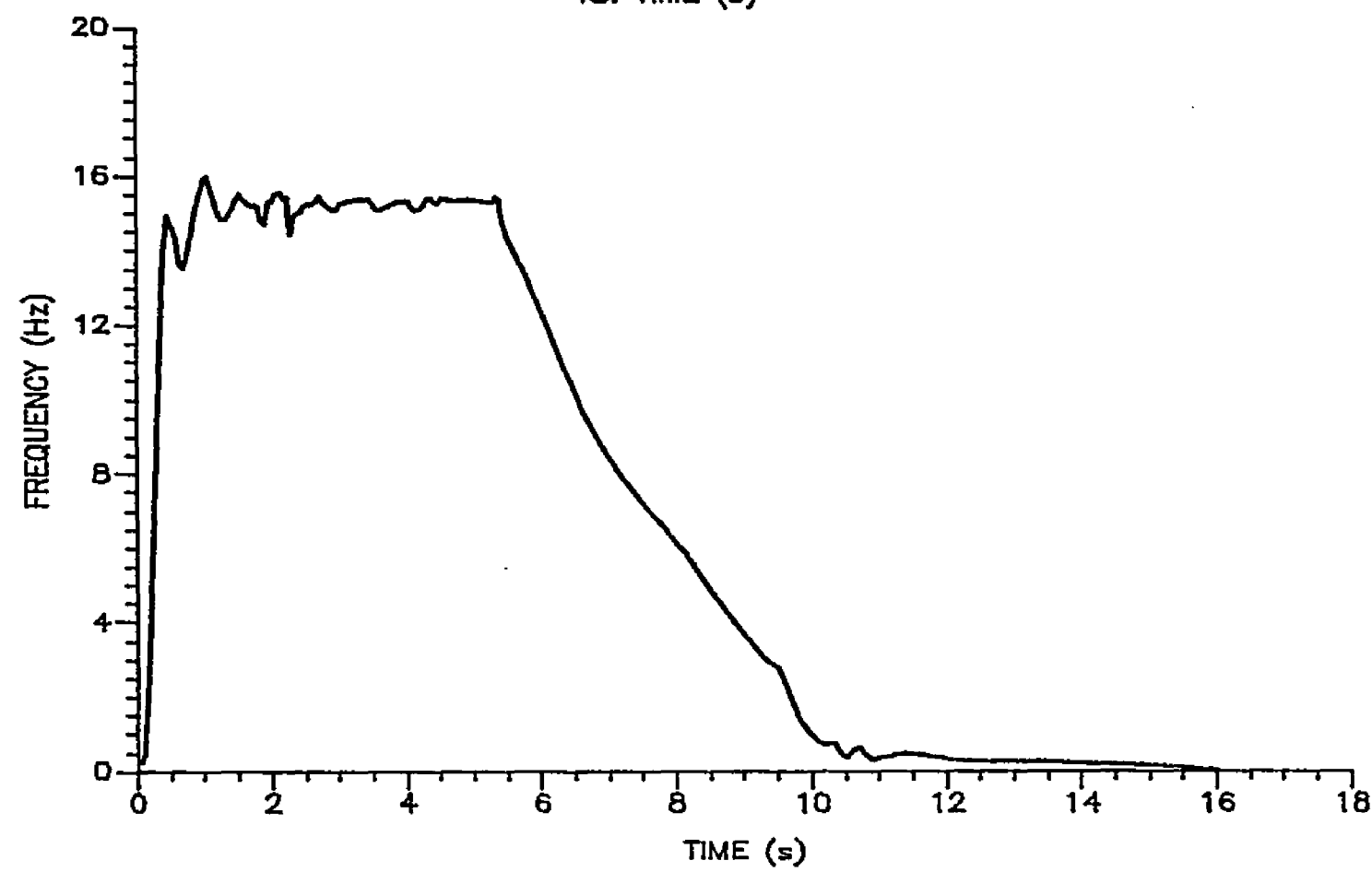


FIGURE 4.17 OUTSIDE ROTATING MASS FREQUENCY OF A FREE SHAKER.

# INSIDE ROTATING MASS FREQUENCY VS. TIME (5)

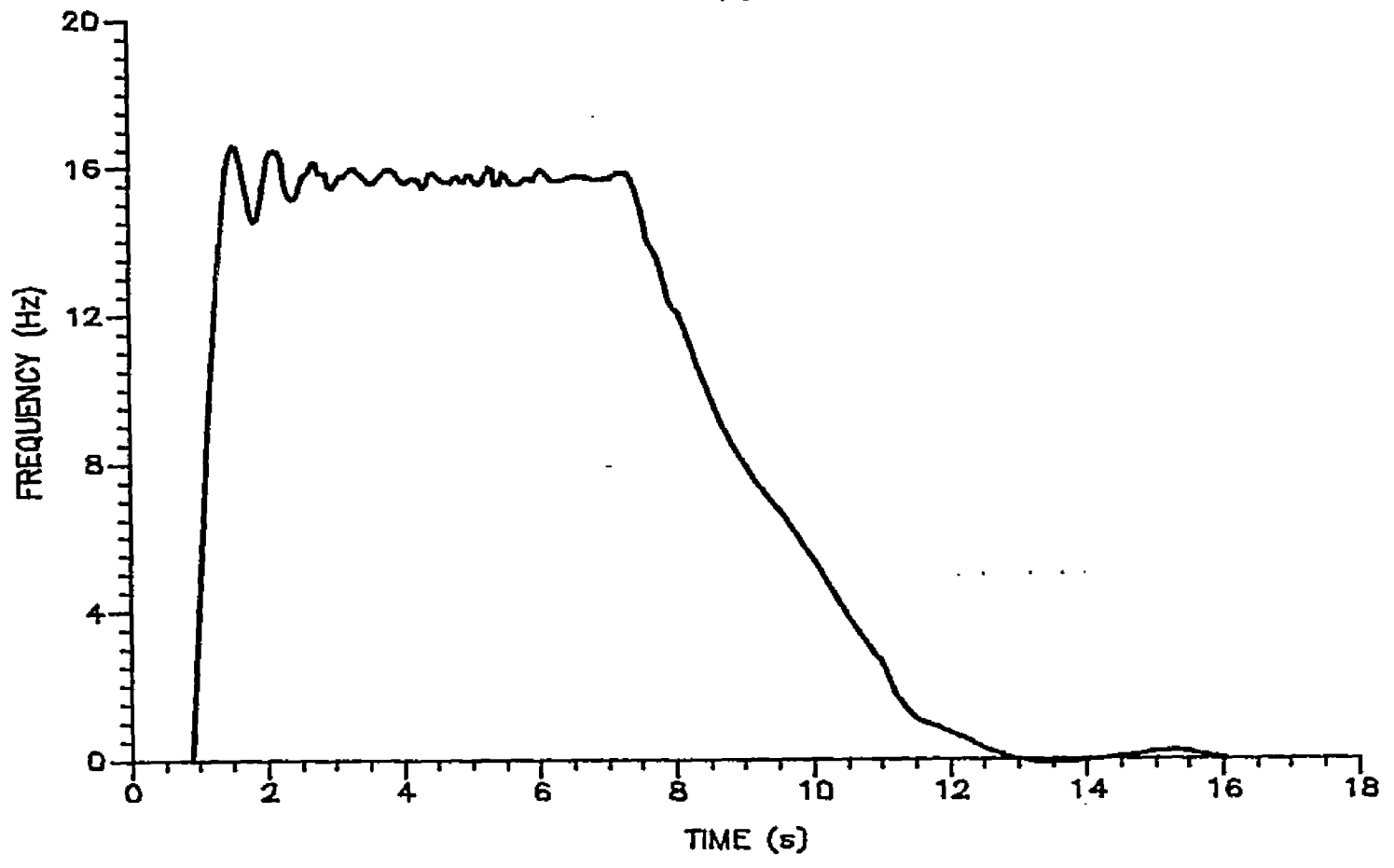


FIGURE 4.18 INSIDE ROTATING MASS FREQUENCY OF A SHAKER ATTACHED TO A 63 mm DIAMETER CHERRY TREE TRUNK.

### OUTSIDE ROTATING MASS FREQUENCY VS. TIME (5)

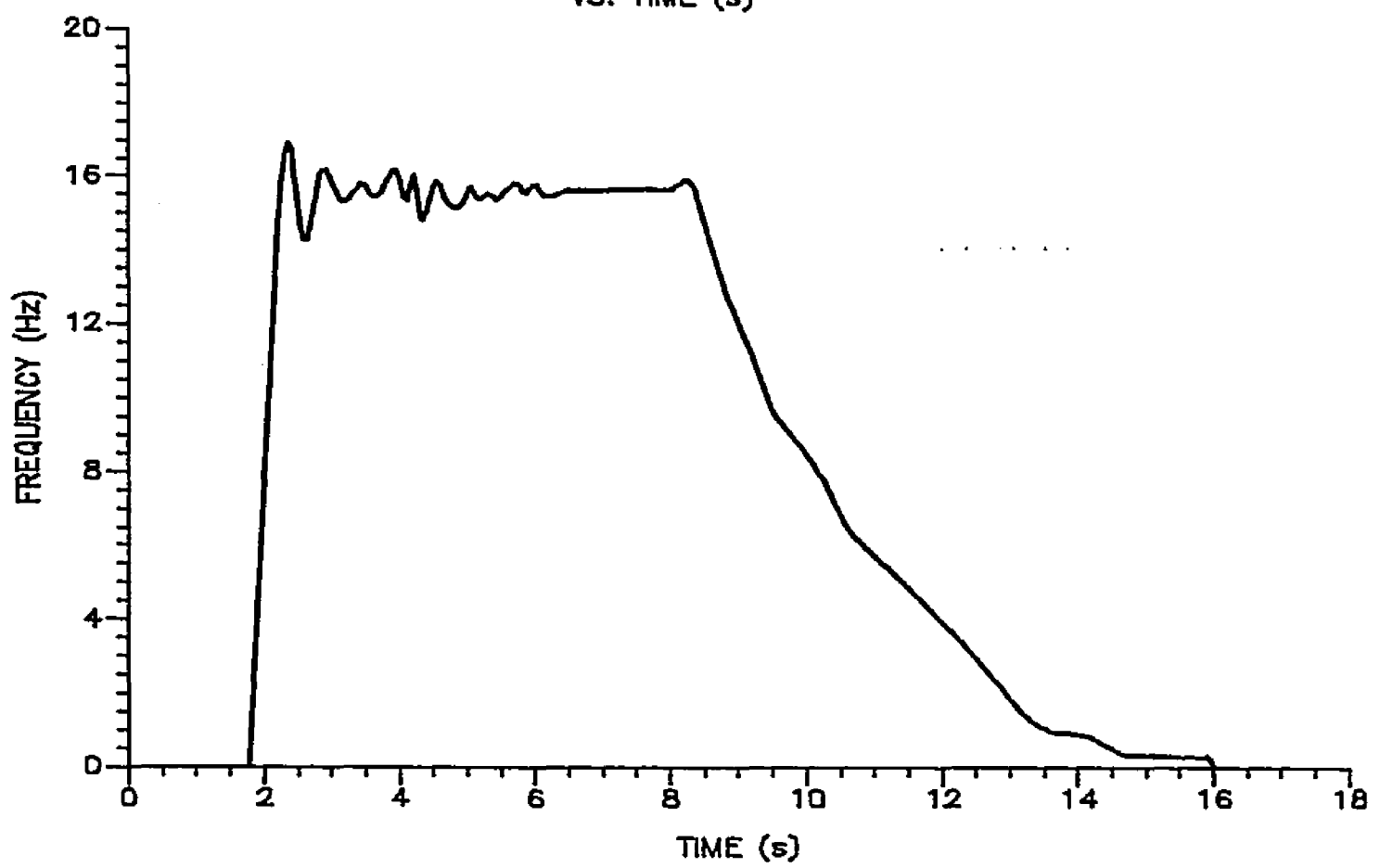


FIGURE 4.19 OUTSIDE ROTATING MASS FREQUENCY OF A SHAKER ATTACHED TO A 63 mm DIAMETER CHERRY TREE TRUNK.

Table 4.5 Summary Of The Physical Properties
Of Friday C-Clamp Trunk Shaker And A 63 mm
Sour Cherry Tree Used In IMP Model.

Description	Value	SIU Unit	Value	Customary Unit	Value	IMP Unit*
Shaker					· -	
Housing mass	464.32	kg	31.810	slug	2.6548	1 bm
rotating "	39.86	kg	2.7313	slug	0.2279	1 bm
Hanger "	4.53	kg	0.3104	slug	0.259	1bm
Tree						
Tree mass	9.34	kg	0.6404	slug	0.0534	1 bm
Mass moment of	inert	<u>ia</u>				
Shaker Housing						
Ix	1187	$kg.m^2$	10524	lbm.in <sup>2</sup>	10524	lbm.in <sup>2</sup>
Iy	167	$kg.m^2$	1486	lbm.in <sup>2</sup>	1486	16m.in <sup>2</sup> .
Ιz	1213	kg.m <sup>2</sup>	10761	lbm.in <sup>2</sup>	10761	lbm.in <sup>2</sup> .
Rotating mass						
Ix	0.347	kg.m <sup>2</sup>	3.076	1bm.in <sup>2</sup> .	3.076	Ibm.in <sup>2</sup> .

Table 4.5 Continued

Describtion	Value	SIU Unit	Value	Customary Unit	Value	IMP Unit
Iy	0.317	kg.m <sup>2</sup>	3.076	lbm.in <sup>2</sup>	3.076	1bm.in <sup>2</sup> .
Ιz	0.630	kg.m <sup>2</sup>	5.584	$1bm.in^2$	5.584	1bm.in <sup>2</sup>
Tree						
Ix	8.233	kg.m <sup>2</sup>	73.0	lbm.in <sup>2</sup>	73.0	lbm.in <sup>2</sup> .
ly	8.233	kg.m <sup>2</sup>	73.0	lbm.in <sup>2</sup>	73.0	lbm.in <sup>2</sup> .
Ιz	0.005	kg.m <sup>2</sup>	0.042	lbm.in <sup>2</sup>	0.042	lbm.in <sup>2</sup>
Stiffness (K	12690	N/m	71.0	lb/in.	71.0	lb/in.
Damping (C	0.31	**	1.8	***	1.8	***

<sup>\* 1</sup> lbm = lb.s /386.1 in.

<sup>\*\*</sup> N.s/mm.

<sup>\*\*\*</sup> Ib.s/in.

#### CHAPTER 5

#### 5. SHAKER DISPLACEMENT RESULTS

#### 5.1 Free-Shake Vibration

A point located at the center of the clamp was selected for studying the shaker displacements using the IMP program. The shaker rotating masses were assumed to run counter to each other starting at zero phase angle between them (mass initial starting position as defined in Figure 3.1). The shaker displacements were simulated for the rotating mass motion in two stages:

- 1- Steady state displacement, and
- 2- Transient state displacement.

The steady state displacements were simulated by feeding the IMP model the rotating mass angular positions as a linear function of time corresponding to three frequency levels (5, 10, and 15 Hz), as illustrated in the following equation:

 $\Theta = C * Time$ 

Where:

O: Rotating mass displacement.

C: Constant velocity in rad/s (for rotational joints J1 and J2 only).

The IMP program can only accept the motion of a joint in terms of position. The steady state frequency was computed from the curves given in Figures 4.16 and 4.17. The transient shaker displacements were simulated by feeding the IMP program the rotating mass angular position as a second-order function of time after the rotational acceleration was integrated twice as follows:

$$\dot{\Theta} = \alpha * time$$

$$\theta = 1/2 * a * (time)$$

The mass acceleration was determined by taking the slope of the experimental rotating mass frequency curves presented in Figures 4.16 and 4.17. The rotating mass frequency curves indicated that the masses reached their maximum frequency of 15.66 Hz (98.4 rad/s) in 0.353 s with a constant acceleration of 278.7 rad/s.

The IMP model results, when the rotating masses were running at a constant frequency of 5 Hz (31.42 rad/s), indicated that the average shaker displacement in the x direction was about a constant 26 mm (1.02 in.) with a shaker shift of 14 mm (0.55 in.) throughout the simulation

time (0.5 s), Figure 5.1. The shaker shift was defined as follows:

Shift = 
$$1/2$$
 (D1 - d1)

where:

D1: Maximum simulated shaker displacement at the first cycle.

d1: Minimum simulated shaker displacement at the first cycle.

By increasing the rotating mass frequency from 5 to 10 Hz, the shaker displacement decreased slightly from 26 to about a constant 24 mm (1.02 to 0.94 in.) and the shaker shift decreased from 14 mm to 12 mm (0.55 to 0.47 in.) over the IMP simulation time (0.5 s), Figure 5.2.

At the highest frequency of 15 Hz (94.24 rad/s) the shaker displacement decreased further to about a constant 23 mm (0.90 in.), and the shaker shift decreased also to about 10 mm (0.39 in.) Figure 5.3. During this simulation, the shaker experienced instability and tended to drift. The shaker drift was defined as follows:

Drift = 
$$1/2$$
 (Dn - dn) - Shift

Where:

Dn: Maximum simulated shaker displacement at n'th cycle.

dn: Minimum simulated shaker displacement at n'th

cycle.

n: The last cycle in a simulated shaker curve displacement.

The total shaker drift was about 25 mm (1 in.) from the rest position. The shaker drift was achieved almost uniformly over the first 4 or 5 cycles.

The transient shaker displacements were simulated by accelerating the rotating masses counter to each other at 2 278 rad/s from rest to reach the maximum frequency of 15.66 Hz in 0.353 s. The model results indicate that the shaker displacements were almost stable at an average of 23 mm (0.90 in.), but initially the shaker shifted to the left about 11 mm (0.43 in.), then gradually drifted to the right about 15 mm (0.59 in.), Figure 5.4. Further study conducted to evaluate the affect of the starting phase angle between the rotating masses on the shaker displacements indicated a high correlation between the starting phase angle and the shaker shift and drift (Section 6.5). Using different starting phase angles resulted in different shaker shift and drift behaviors.

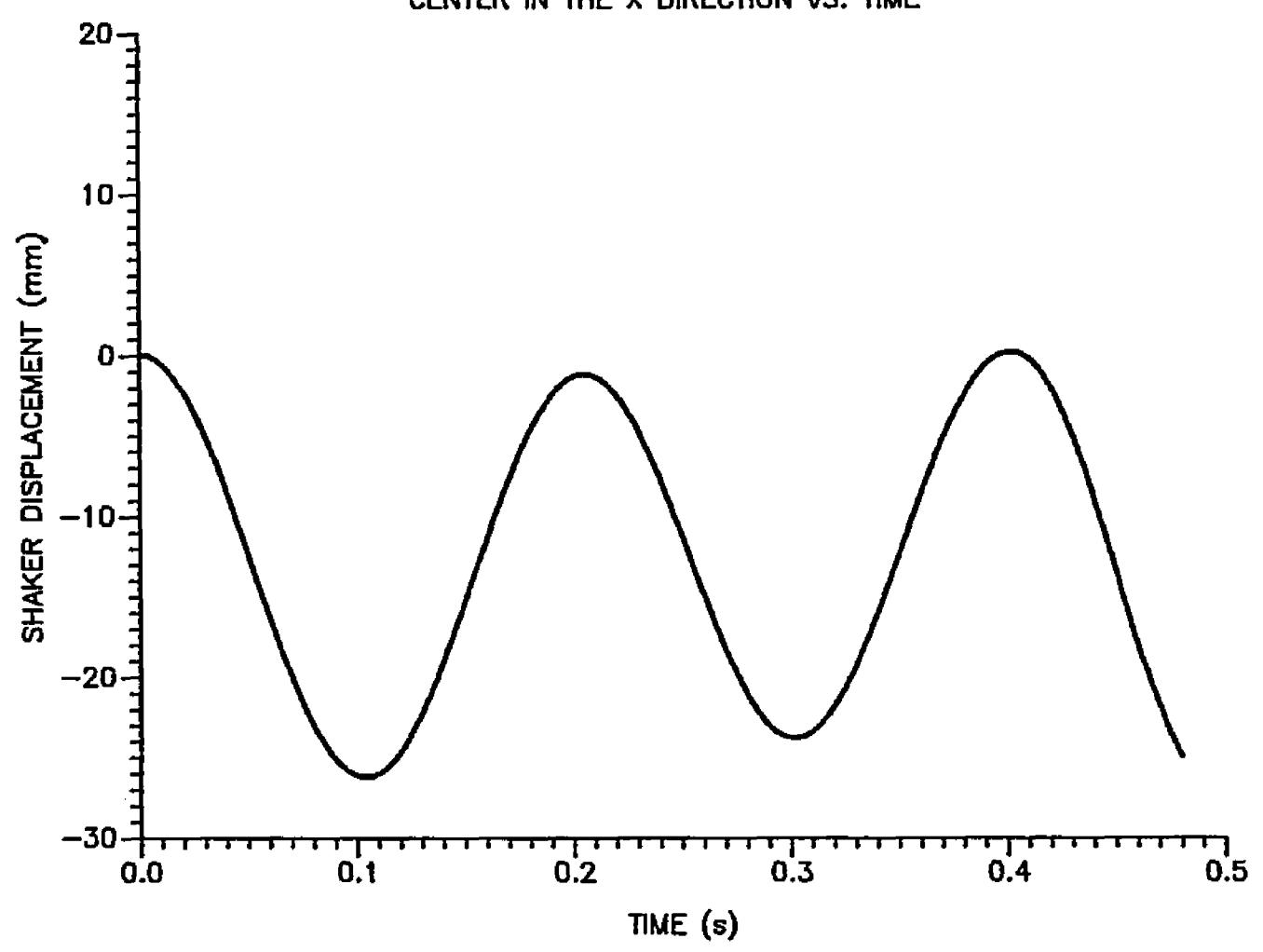


FIGURE 5.1 FREE SHAKING DISPLACEMENT VS. TIME AT A MASS ROTATING FREQUENCY OF 5 HZ.

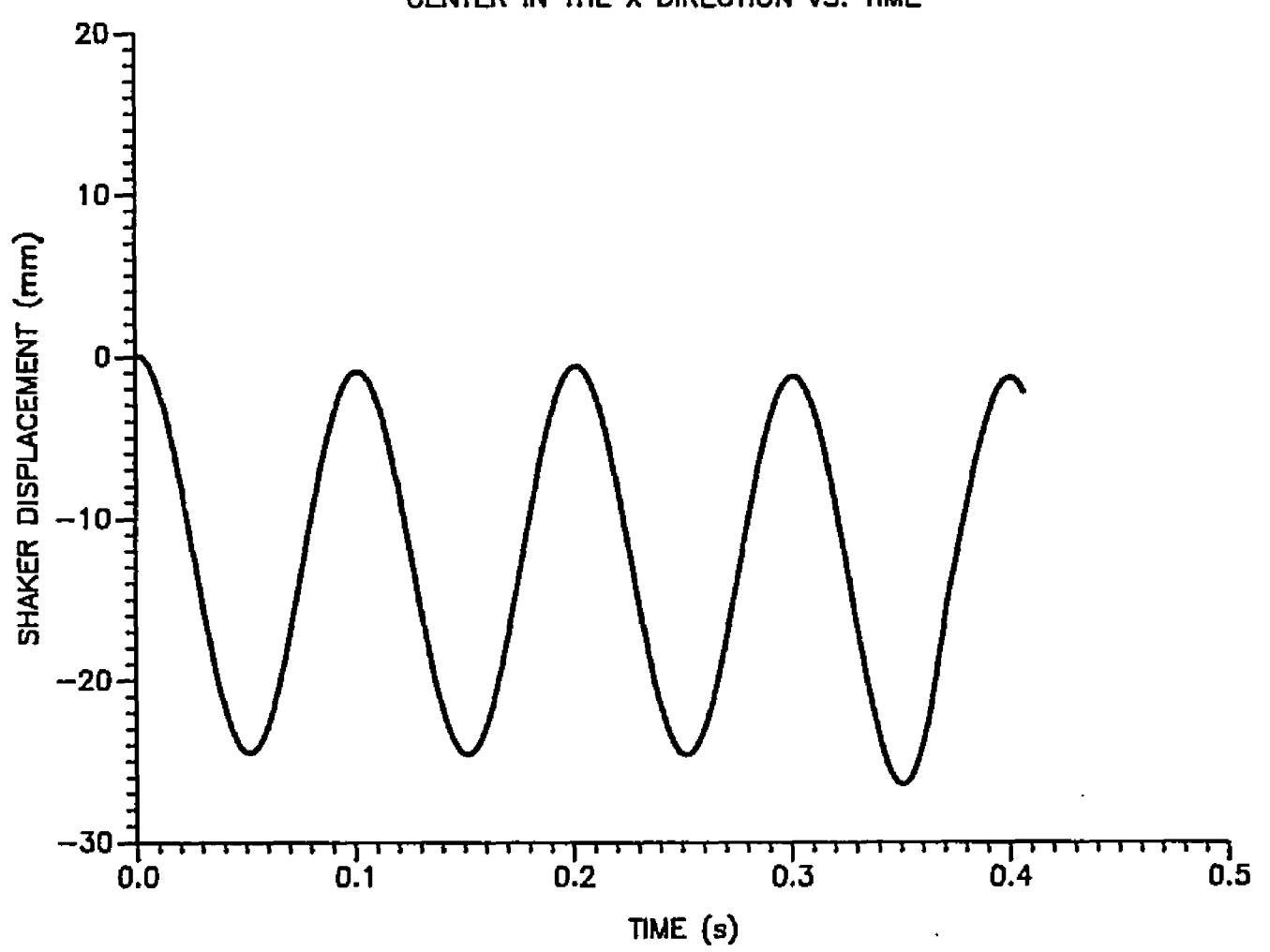


FIGURE 5.2 FREE SHAKING DISPLACEMENT VS. TIME AT A MASS ROTATING FREQUENCY OF 10 HZ.

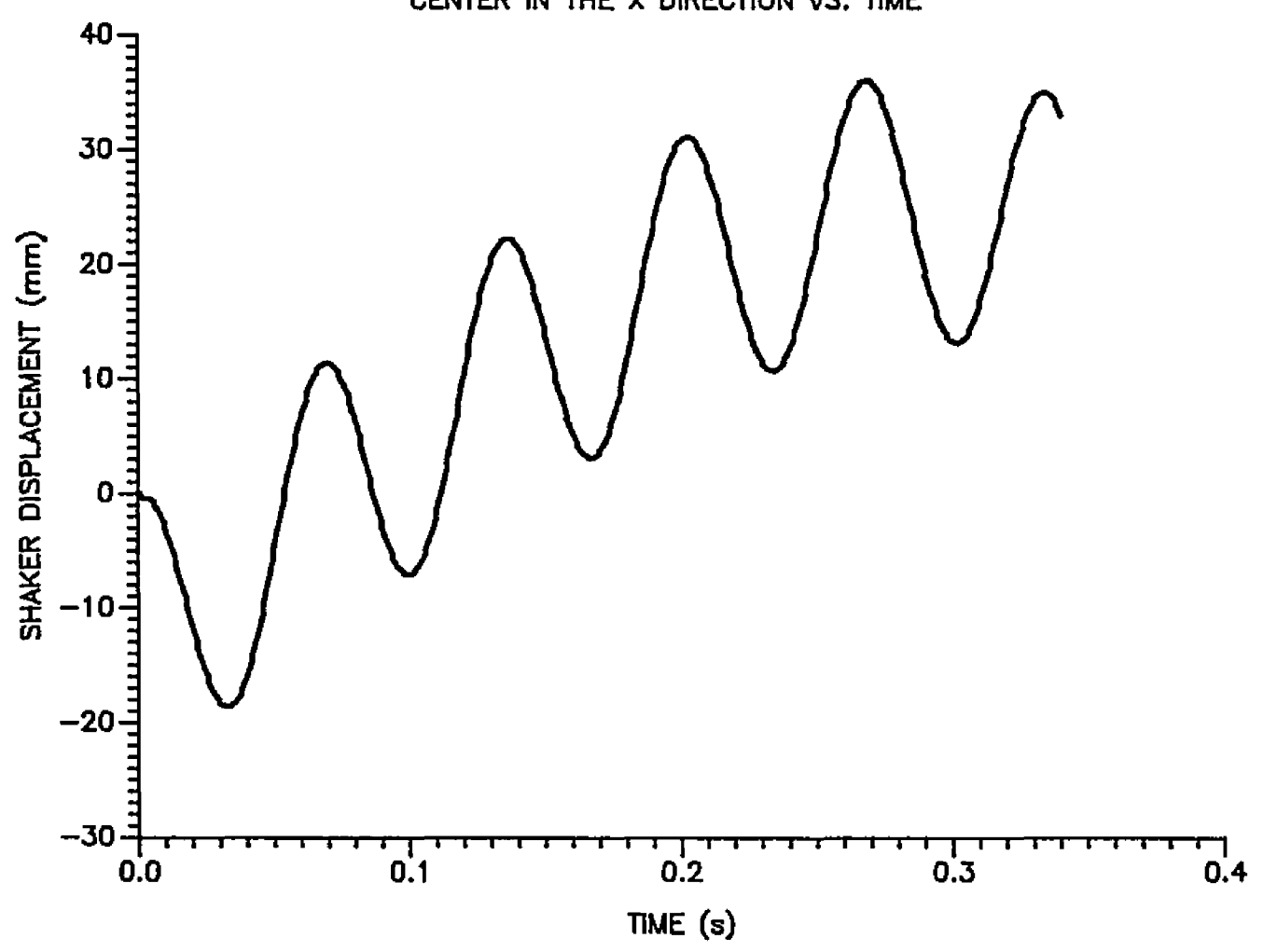


FIGURE 5.3 FREE SHAKING DISPLACEMENT VS. TIME AT A MASS ROTATING FREQUENCY OF 15 HZ.

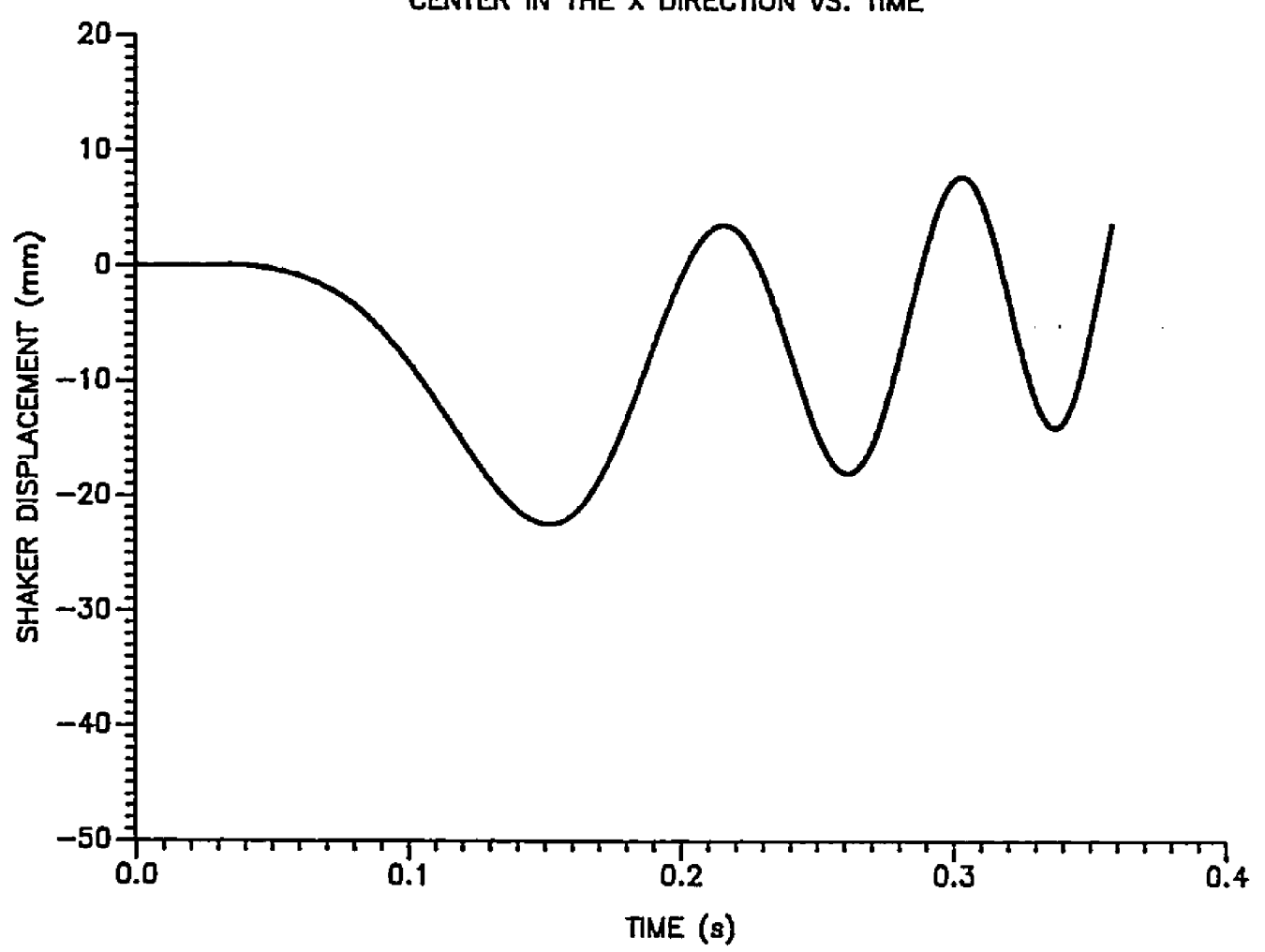


FIGURE 5.4 ROTATING MASSES ARE RUNNING ACCORDING TO SIMULATED TRANSIENT VELOCITY FUNCTION.

#### 5.2 Shaker-Tree Vibration System

The tree trunk displacement simulation was performed by adding the tree mass, stiffness and damping properties to the shaker model previously described for the IMP program. The tree trunk displacements were obtained by simulating the displacement of a point located at the tree trunk center when the tree was clamped between the shaker pads. The displacement simulation was performed in two stages:

- 1- Steady state displacements of the tree trunk at three shaker rotating mass frequency levels (5, 10, and 15 Hz). The mass and inertia properties of a 63 mm (2.5 in.) diameter tree trunk were introduced in the IMP model. No tree stiffness or damping were introduced in this first simulation.
- 2- Steady state displacements of a 63 mm (2.5 in.) diameter tree trunk at a shaker rotating mass frequency of 15 Hz. The tree physical properties of stiffness and damping were added to those of mass and mass moment of inertia.

The simulation results for a rotating mass frequency

of 5 Hz (31.42 rad/s) indicate that the tree trunk displacement in the x direction was about 26 mm (1.02 in.). The displacement was stable throughout the simulation time with a 13 mm (0.5 in.) shift from the shaker rest position and no drift was noticed, Figure 5.5.

Increasing the rotating mass frequency to 10 Hz (62.83 rad/s) resulted in tree displacement of 25 mm (1 in.). The displacement did not experience any drift, however, the shaker shifted about 12.5 mm (0.5 in.) during the simulation, Figure 5.6.

At a rotating mass frequency of 15 Hz (94.24 rad/s) the tree trunk displacement was about 22 mm (0.86 in.). Although uniform displacement occured throughout the simulation, the shaker shifted 10 mm (0.39 in.) to the left and drifted 25 mm (1 in.) to the right during the simulation, Figure 5.7.

The results presented in Figures 5.5, 5.6, and 5.7 show that displacement behavior at the three steady frequency levels was very much in agreement with the displacement behavior during free vibration, Figures 5.1, 5.2, and 5.3. Thus, the tree mass and mass moment of inertia affects on the displacements simulated by the shaker-tree model were very minimum.

Tree stiffness and damping properties were then introduced to the shaker-tree model. Linear springs and

### SIMULATED TREE DISPLACEMENT IN THE X DIRECTION VS. TIME

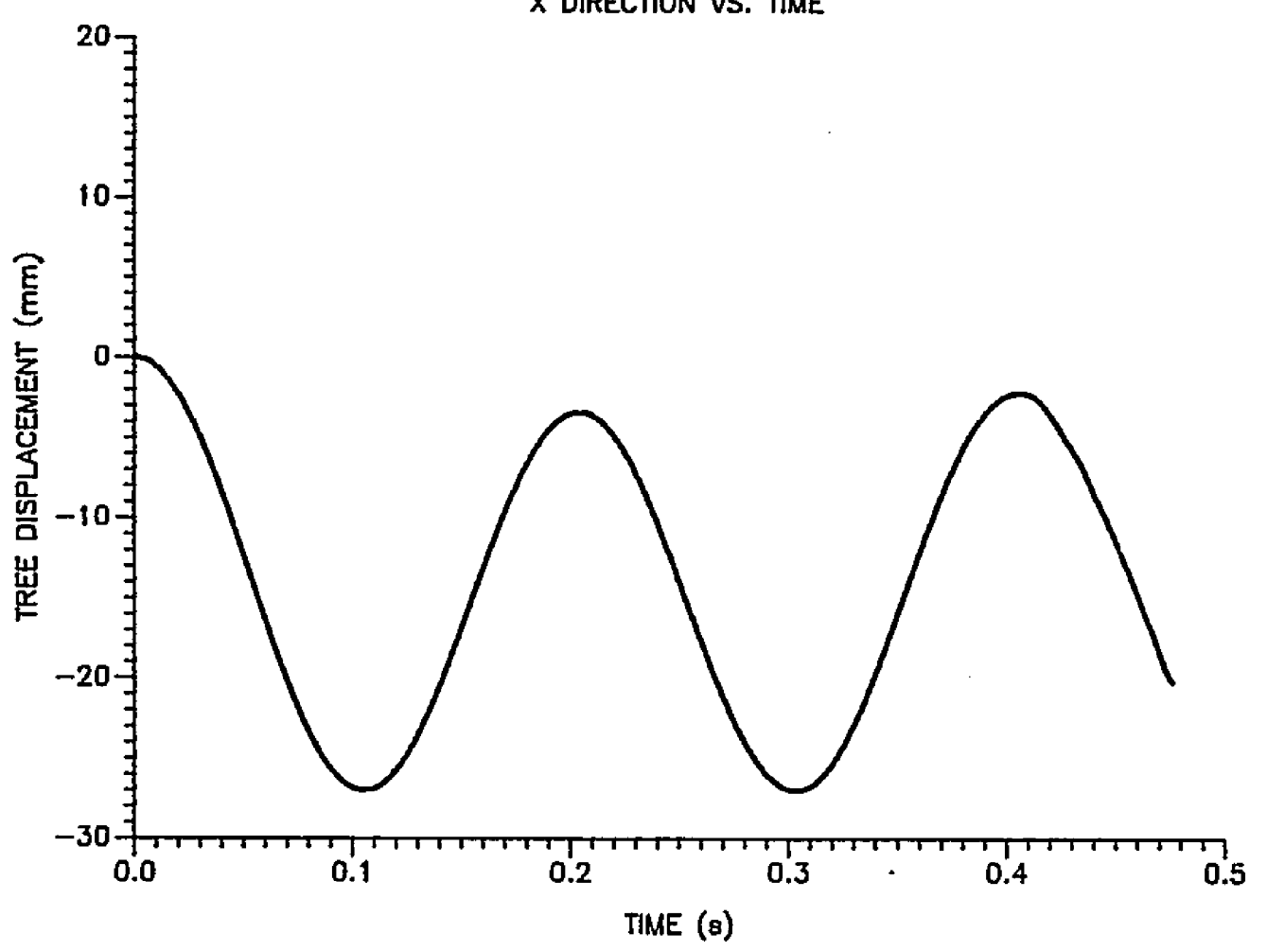


FIGURE 5.5 TREE DISPLACEMENT AT A MASS ROTATING FREQUENCY OF 5 HZ, WITH NO TREE STIFFNESS OR DAMPING.

### SIMULATED TREE DISPLACEMENT IN THE

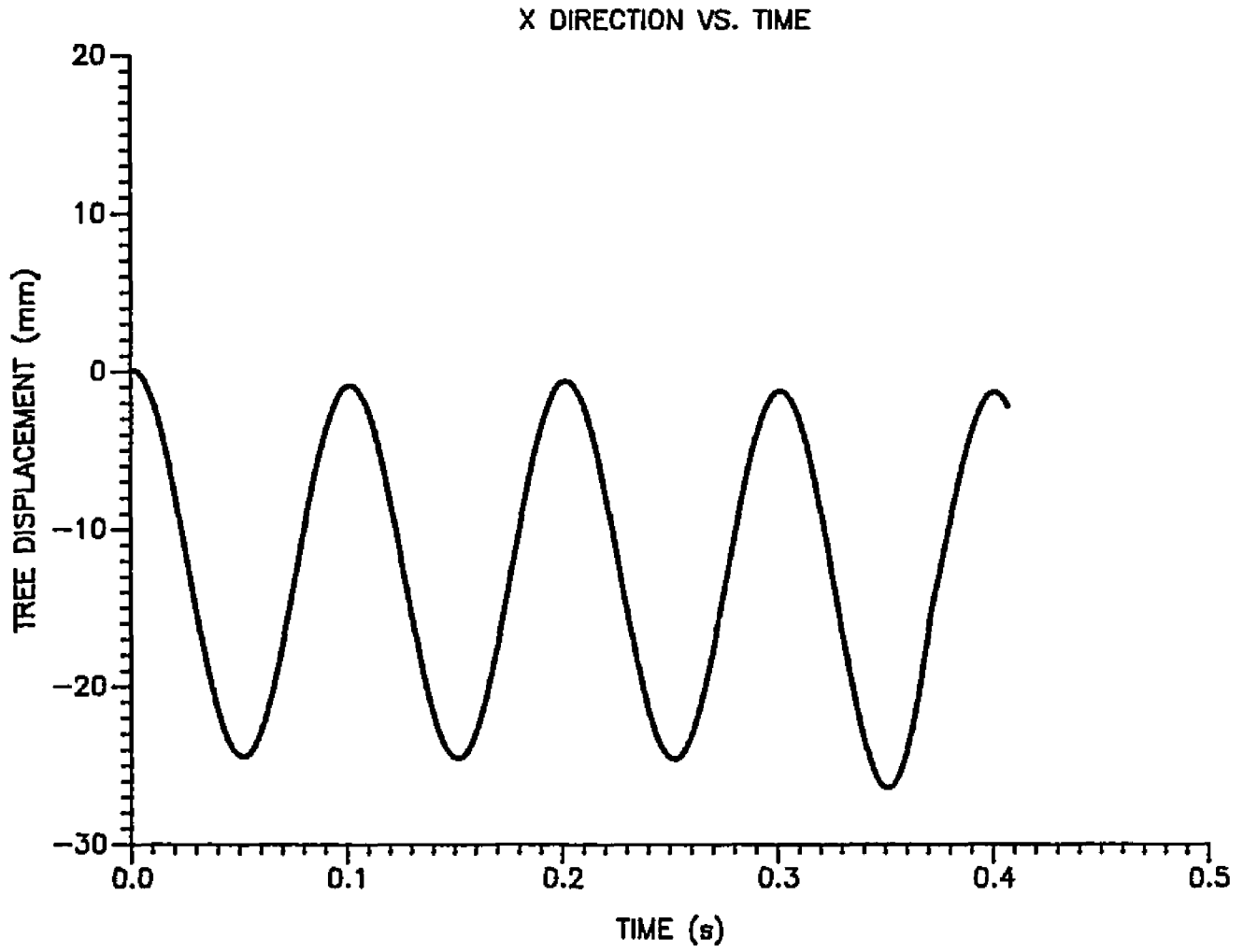


FIGURE 5.6 TREE DISPLACEMENT AT A MASS ROTATING FREQUENCY OF 10 HZ WITH NO TREE STIFFNESS OR DAMPING.

### SIMULATED TREE DISPLACEMENT IN THE X DIRECTION VS. TIME

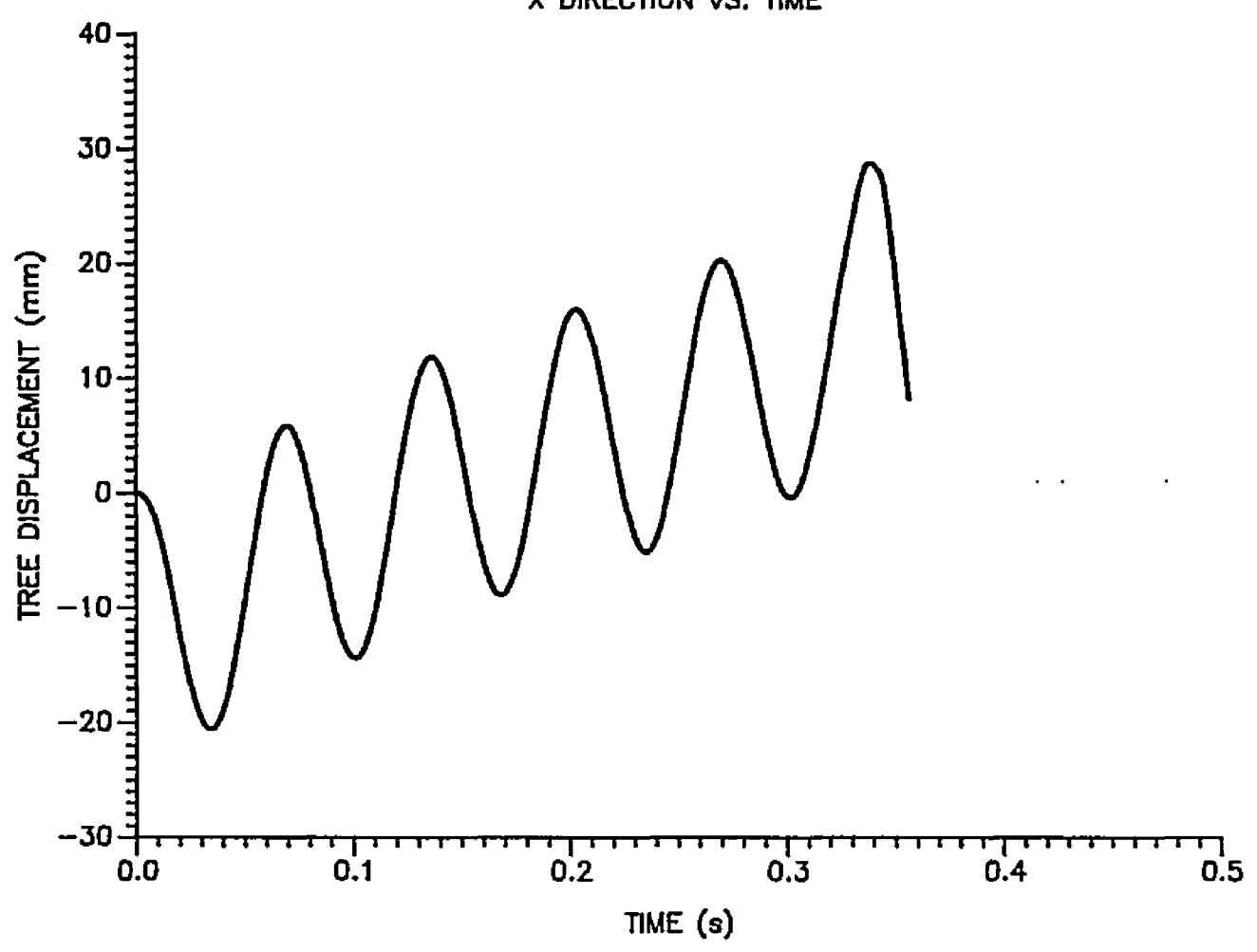


FIGURE 5.7 TREE DISPLACEMENT AT A MASS ROTATING FREQUENCY OF 15 HZ WITH NO TREE STIFFNESS OR DAMPING.

dampers were attached to the tree trunk in the x and y directions, shown in Figure 3.3. The rotating mass frequency was set at 15 Hz (94.24 rad/s). With stiffness and damping added to the IMP model the displacement results were much different, and unrealistic.

The program simulation stopped (after 50 to 100 simulation time steps) before it reached the specified simulation time, Figure 5.8. Many attempts were tried to get the program working by changing the spring length, location, direction, and stiffness value, but all produced the same results. The tree trunk was also modeled as a spherical joint at the ground having spring stiffness and damping equal to that at the trunk clamping point, but that attempt did not help either.

To determine whether the problem was caused by tree stiffness or tree damping, the stiffness matrix was set to zero. As a result the program ran with no problems. This raised questions about the algorithm accuracy involved in the IMP program stiffness matrix. The problem was reported to the software company and their response was that the program had never been tried on mechanical systems having more than 5 degrees of freedom. The shaker-tree model was a 9 degrees of freedom system.

At this point in time the IMP model can not simulate the tree and shaker displacement behavior when tree

# SIMULATED TREE DISPLACEMENT IN THE X DIRECTION VS. TIME

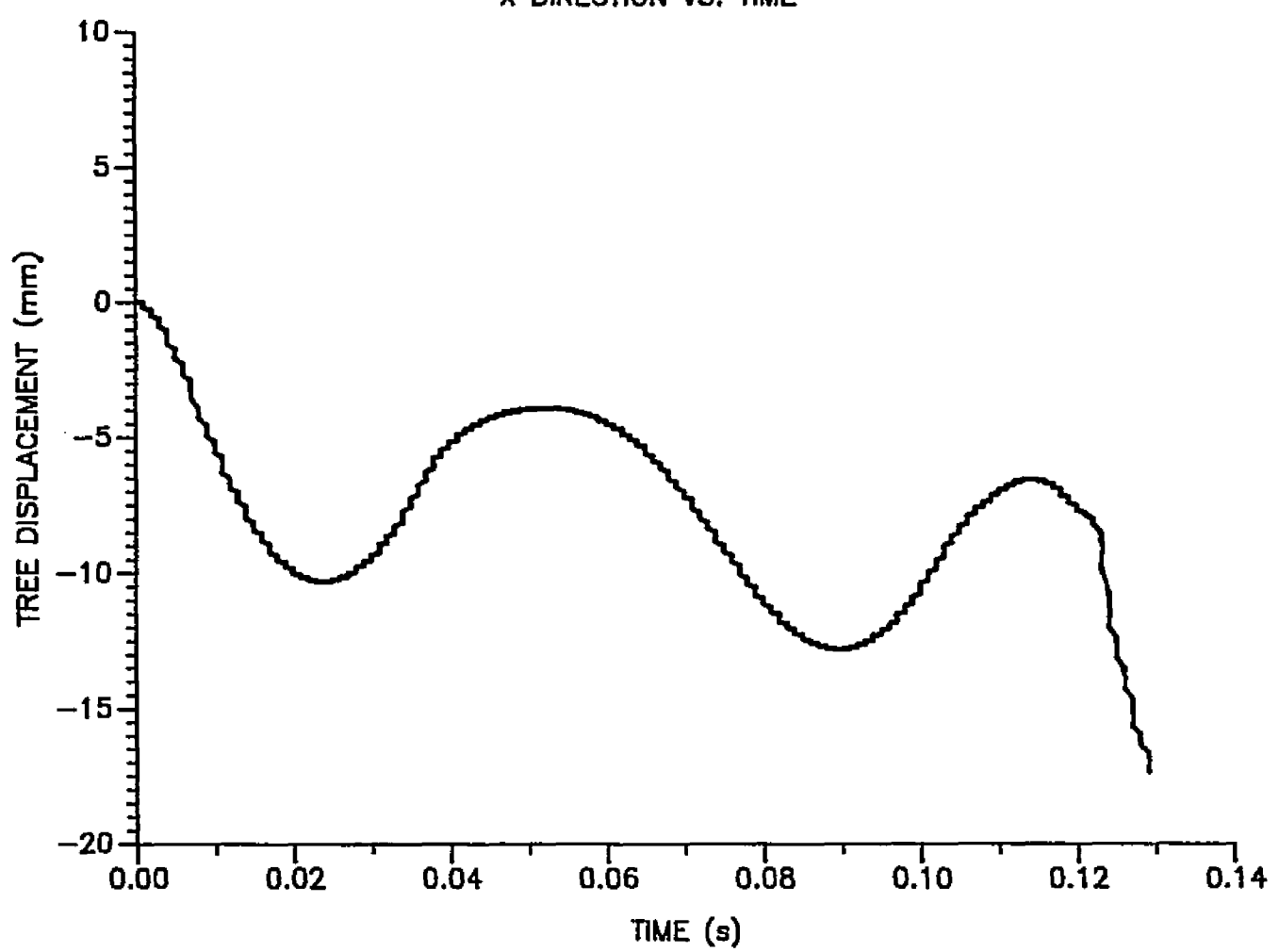


FIGURE 5.8 TREE DISPLACEMENT AT A SHAKER ROTATING MASS FREQUENCY OF 15 HZ.

stiffness is included in the model. Because of this limitation, further studies of the displacement behavior of the shaker when attached to various sizes of trees were terminated.

### 5.3 Model Verification

Marshall (1986) used high-speed photography optically record the free-shake displacements of several selected points located on the shaker and on a post clamped between the shaker pads. The resulting displacement graph free-shake (FS), Appendix C, indicates that the maximum displacement of the post in the x direction during the transient stage was about 25 mm (1 in.). Shaker drift in the first eight cycles was very small, the maximum shaker drift of 20 mm (0.78 in.) occured at the ninth cycle with a shaker displacement of 25 mm (1 in.). The shaker continued to oscillate about the same system center during the steady state, with a displacement ranging from 25 to 10 mm (1 to 0.39 in.). The displacement variation during shaking was caused by the changing phase angle between the rotating masses, which were rotating at different frequencies.

The results obtained from the free-shake model during the transient stage show a maximum displacement amplitude of 23 mm (0.90 in.) only 2 mm (0.07 in.) less than determined using the photographic method. The total shaker drift simulated by the shaker model was 15 mm (0.59 in.) 5 mm (0.19 in.) less than determined in the photographic method. It should be indicated, that the shaker drift during simulation did not happen suddenly, as recorded using the

photographic method. Instead, the drift occured gradually over the first 6 cycles of simulation time. The simulated shaker shift during the transient stage was 11 mm (0.43 in.) to the left, due to the starting phase angle specified in the IMP model.

During steady state simulation at a rotating mass frequency of 15 Hz the displacement was 23 mm (0.90 in.), almost the same displacement obtained from the experiment. The shaker drift according to the experimental results was about 20 mm (0.78 in.), while the model simulated result was 25 mm (0.98 in.), off by 5 mm (0.20 in.).

During high-speed photography tests (Marshall 1986) on a 63 mm (2.5 in.) diameter tree trunk, Appendix D (T20), the trunk displacement during shaking ranged from 20 mm (0.78 in.) to 25 mm (1 in.). Some higher displacements were observed in the first 2 cycles, however, the remaining displacements were almost uniform. A 5 mm (0.20 in.) drift occured during steady state shaking.

Tree trunk displacements simulated using the shaker-tree model, with no tree stiffness or damping, were about 20 to 25 mm (0.78 to 1 in.) at the three steady state frequencies of 5, 10, and 15 Hz.

Comparing the high-speed photography tests with the simulated displacement results indicated that the shaker model was able to predict the shaker displacements and

drift very closely over the simulated period, for both transient and steady state frequencies.

#### CHAPTER 6

### 6. SENSITIVITY ANALYSIS STUDY

### OF DISPLACEMENT

The sensitivity analysis study was conducted on the free vibration shaker model. The purpose of the study was to impose some changes on the shaker properties and to evaluate the model simulated shaker displacements, at a point located at the center of the clamp, corresponding to these changes. Most of the changes introduced in the model were studied at two rotating mass frequencies:

- 1- Steady state rotating mass frequency of 15 Hz.
- 2- Transient state rotating mass frequency ranging from 0 to 15.66 Hz with an acceleration rate of  $\frac{2}{278}$  rad/s .

The changes imposed on the shaker IMP model were:

- 1- Variation of the magnitude of the shaker housing mass.
- 2- Variation of the magnitude of the rotating masses.
- 3- Variation of the rotating mass acceleration.
- 4- Variation of the eccentricity of the rotating masses.
- 5- Variation of the starting phase angle between the

rotating masses.

# 6.1 Variation Of The Magnitude Of The Shaker Housing Mass

The impact of changing the shaker housing mass, on the shaker displacement behavior, were investigated by testing two smaller housing mass values using either a steady rotating mass frequency of 15 Hz or a transient frequency of 0 to 15.66 Hz, over a simulation period of 0.353 s.

A shaker housing mass of 317 kg (21.75 slug) and mass 2 moment of inertia equal to 724.6, 125.8, and 1213.84 kg.m in the x, y, and z directions, respectively, were introduced in the shaker model. The shaker rotating masses were assumed to run counter to each other, to start at a zero phase angle between them (mass initial starting position), and to accelerate from rest at 278 rad/s until they reached a frequency of 15.66 Hz. The shaker simulated displacement in the x direction was 30 mm (1.18 in.), 7 mm (0.27 in.) greater than the displacement obtained from using the original shaker with a housing mass of 464.32 kg (31.856 slug). The shaker shifted 15 mm (0.59 in.) and drifted about 10 mm (0.39 in.) over the first 0.353 s during the transient stage, Figure 6.1.

At a constant rotating mass frequency of 15 Hz (94.2 rad/s), assuming that the shaker rotating masses were

still at a zero phase angle, the shaker displacement in the x direction was about 30 mm (1.18 in.), the same value obtained from the transient test, Figure 6.2. The shaker shifted 17 mm (0.67 in.) and drifted about 15 mm (0.59 in.) before it became stable. The shaker shift and drift was due to starting the rotating masses from rest position during the model simulation.

Decreasing the shaker housing mass again to 226.5 kg (15.54 slug) with mass moment of inertia equal to 539.6, 2 109, and 1213.84 kg.m in the x, y, and z direction respectively, and simulating the shaker displacements using the same transient velocity function resulted in a 40 mm (1.57 in.) displacement in the x direction, 10 mm (0.39 in.) greater than the displacement of a shaker housing mass of 317 kg. The shaker shifted about 19 mm (0.75 in.) and drifted 15 mm (0.59 in.) during the simulation period of 0.353 s before it reached the steady state, Figure 6.3.

At a steady state frequency of 15 Hz, the simulated shaker displacement in the x direction was again 40 mm (1.57 in.) with a shaker shift of 20 mm (0.75 in.) and drift of 20 mm (0.78 in.), Figure 6.4.

The results obtained from testing the two lighter shaker housing masses for their affect on the shaker displacement behavior allow the following conclusions to be drawn:

- 1- The average ratio of the shaker displacement increase to the shaker housing mass decrease was 11 mm/100 kg (0.19 in./100 lbs).
- 2- The average ratio of the shaker shift or drift increase to the shaker housing decrease, during the transient frequency stage, was 4.4 mm/100 kg (0.07 in./100 lbs).

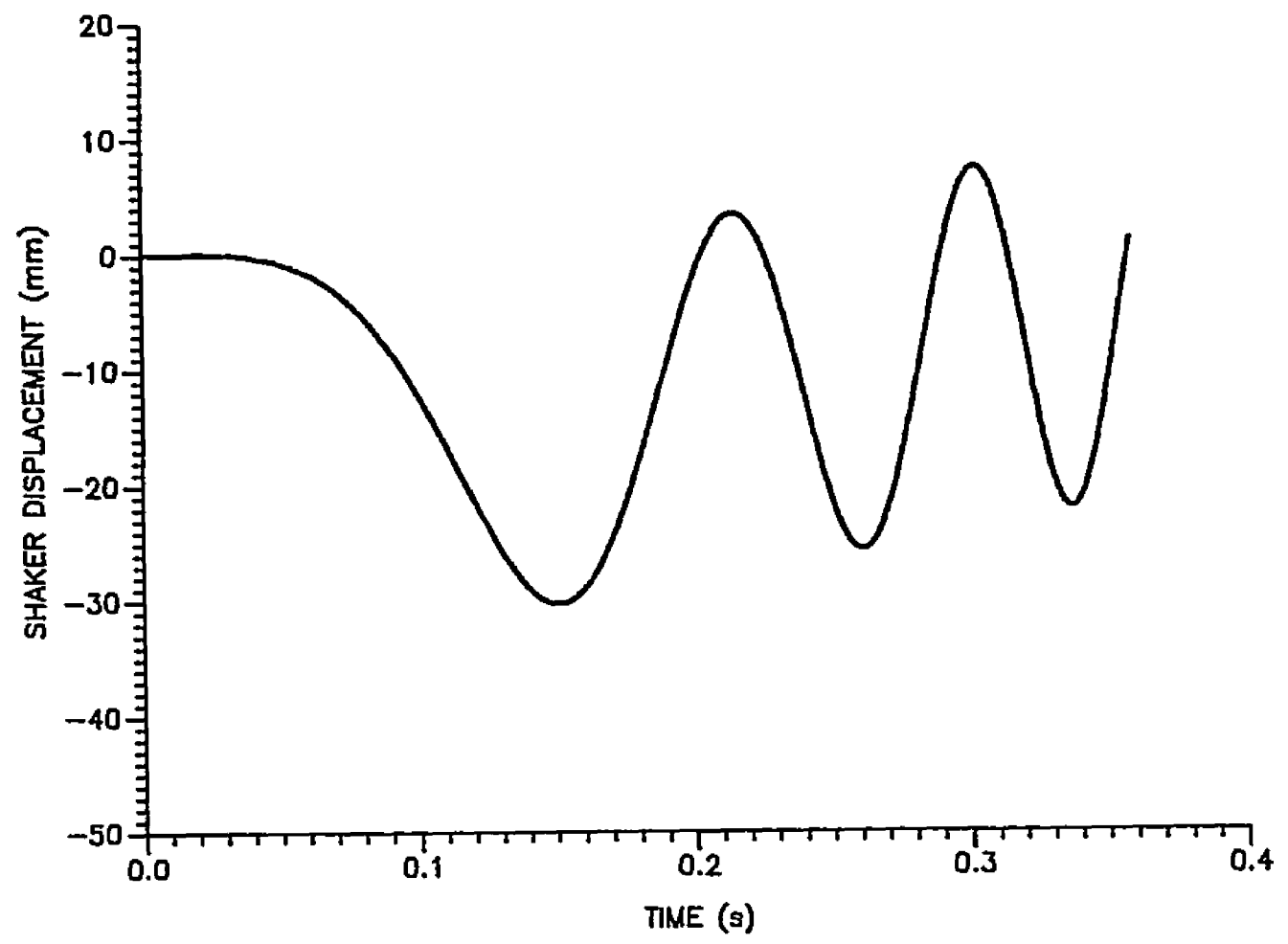


FIGURE 6.1 ROTATING MASSES ARE RUNNING ACCORDING TO SIMULATED TRANSIENT VELOCITY FUNCTION FOR A SHAKER HOUSING MASS OF 317 kg.

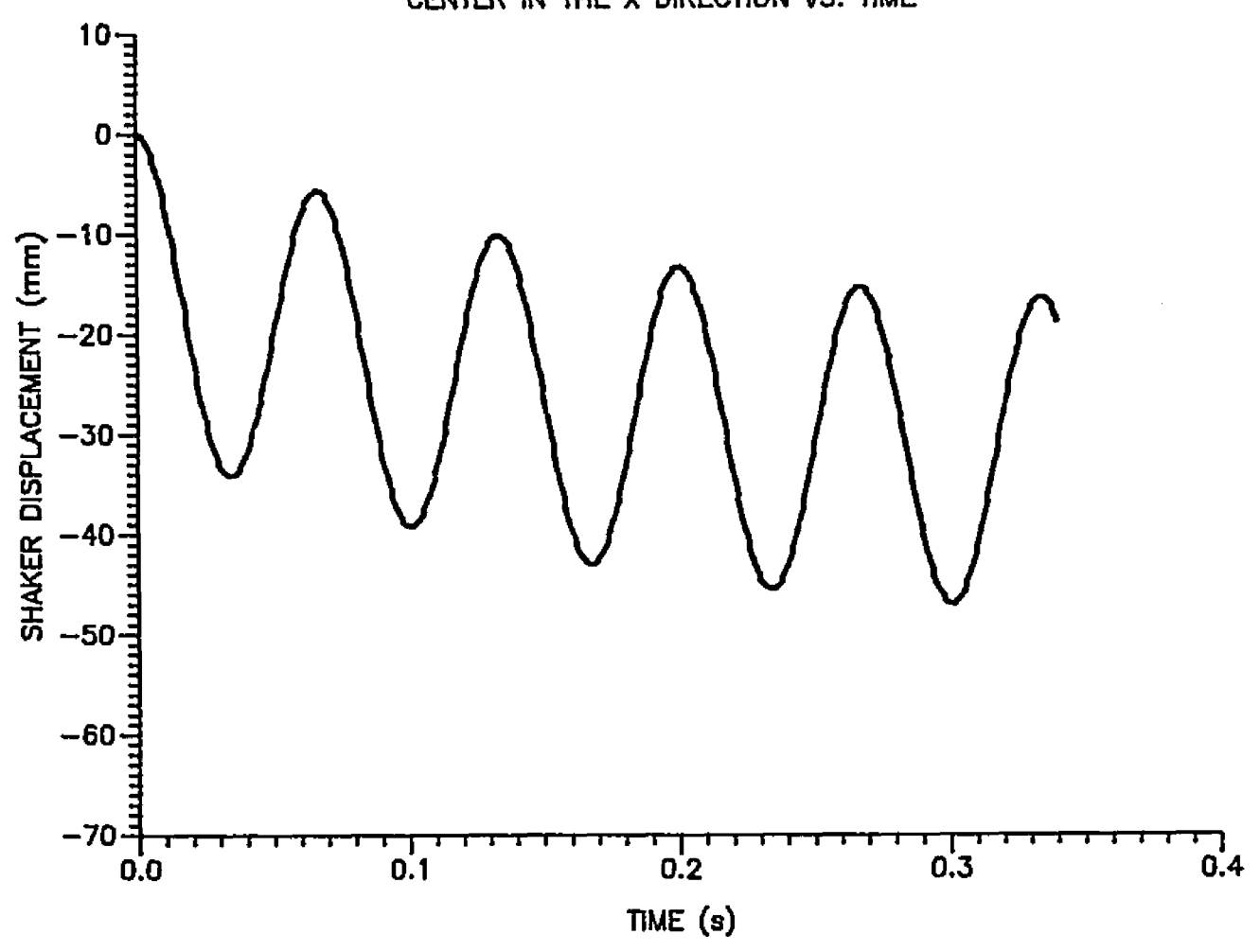


FIGURE 6.2 FREE SHAKING DISPLACEMENT VS. TIME AT A MASS ROTATING FREQUENCY OF 15 HZ, AND SHAKER HOUSING MASS OF 317 kg.

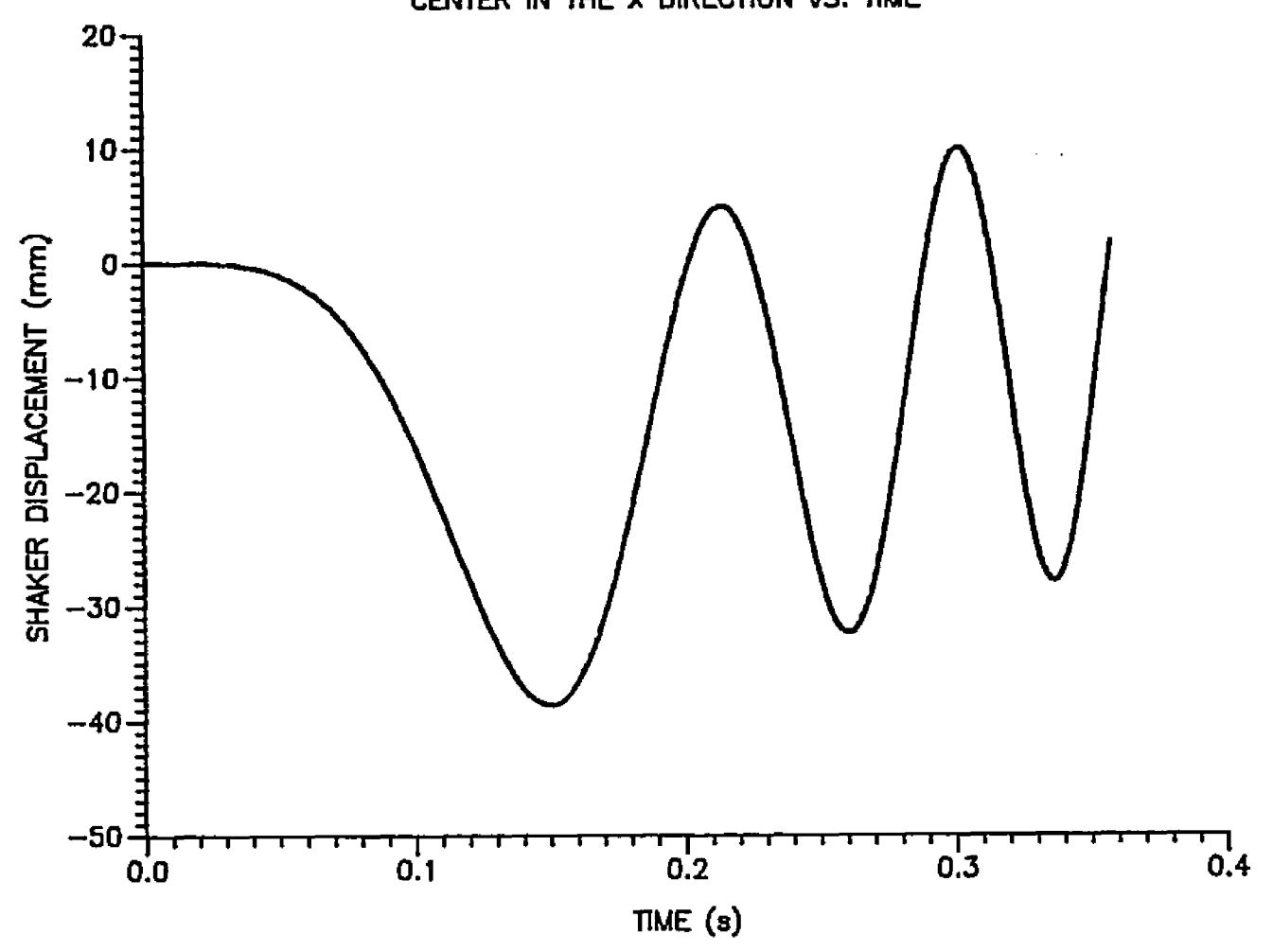


FIGURE 6.3 ROTATING MASSES ARE RUNNING ACCORDING TO SIMULATED TRANSIENT VELOCITY FUNCTION FOR A SHAKER HOUSING MASS OF 226.5 kg.

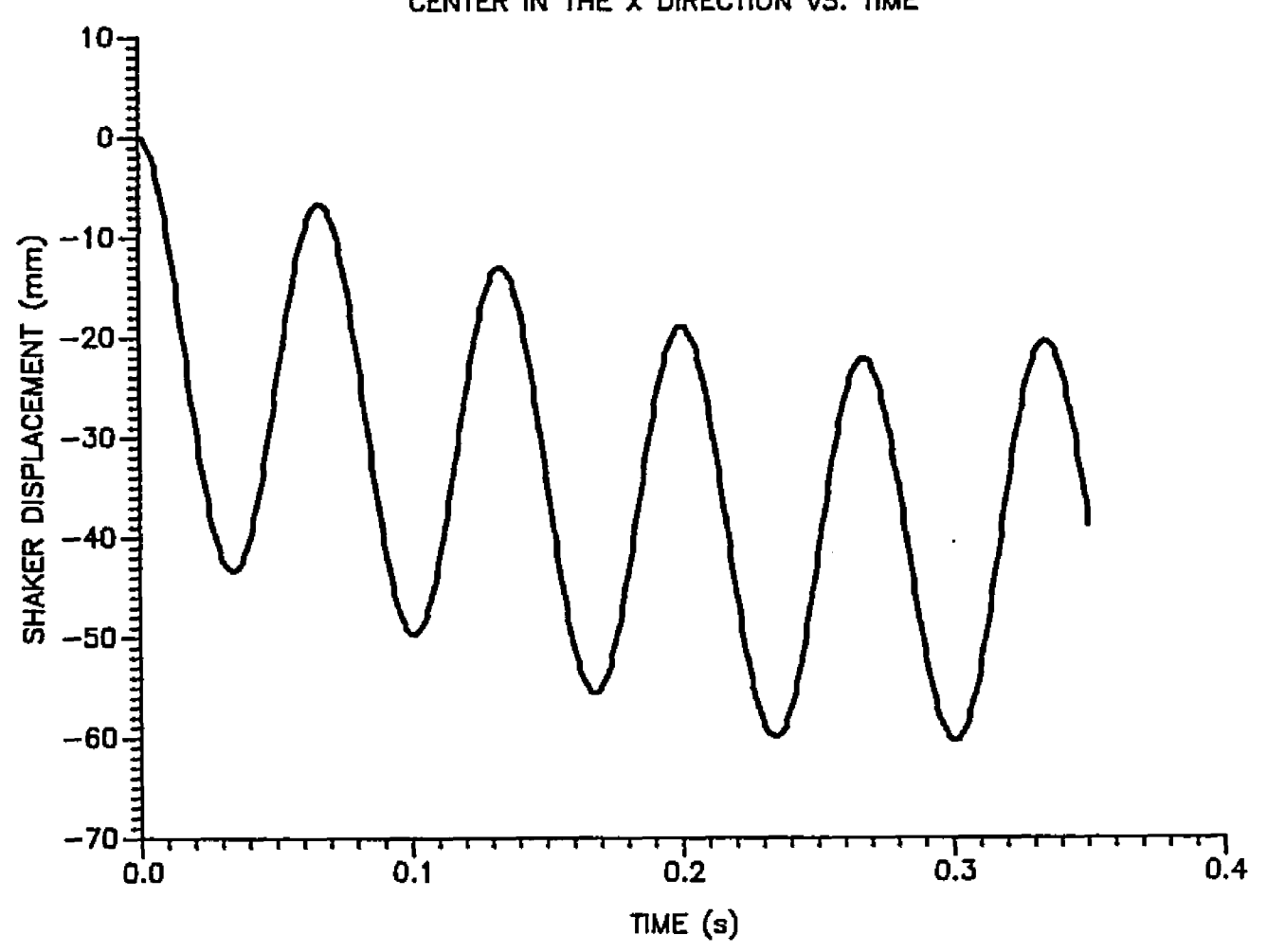


FIGURE 6.4 FREE SHAKING DISPLACEMENT VS. TIME AT MASS ROTATING FREQUENCY OF 15 HZ, AND SHAKER HOUSING MASS OF 226.5 kg.

# 6.2 Variation Of The Magnitude Of The Rotating Masses

Two smaller rotating mass values were tested to evaluate their affect on shaker displacements. A simulation period of 0.353 s was again used, and the rotating masses were assumed to run counter to each other after starting at a phase angle of zero degrees (mass initial starting position).

The two rotating masses where first reduced to 31.75 kg (2.17 slug) each with mass moment of inertia equal to 20.137, 0.137, and 0.2756 kg.m in the x, y, and z directions, respectively. The transient frequency function again ranged from 0 to 15.66 Hz with an acceleration of 278 2 rad/s. The simulated shaker displacement in the x direction was about 20 mm (0.78 in.), 3 mm (0.12 in.) less than the displacement using the original masses, Figure 6.5. During this simulation the shaker shifted 9 mm (0.35 in.) to the left and drifted 8 mm (0.31 in.) to the right from the rest position.

At a steady state rotating mass frequency of 15 Hz (94.24 rad/s) the simulated shaker displacement was 20 mm (0.78 in.) with a shaker shift of 11 mm (0.43 in.) and drift of 22 mm (0.86 in.), Figure 6.6.

Decreasing the rotating masses further to 18.12 kg (1.24 slug) each with mass moment of inertia equal to 0.07, 2 0.07, and 0.14 kg.m in the x, y, and z directions, respectively, and the transient frequency function, resulted in a simulated shaker displacement in the x direction of about 14 mm (0.55 in.) with a shaker shift of 8 mm (0.31 in.) and drift of 7 mm (0.27 in.), Figure 6.7.

At a steady rotating mass frequency of 15 Hz (94.24 rad/s), the simulated shaker displacement was 14 mm (0.55 in.) with a total shaker shift of 8 mm (0.31 in.) and drift of 17 mm (0.67 in.), Figure 6.8. From these displacement results the conclusions are:

- 1- The average ratio of the shaker displacement decrease to the rotating mass decrease was 4.4 mm/10 kg (0.78 in./10 lbs).
- 2- The average shaker shift or drift decrease to the shaker rotating mass decrease was 1.5 mm/10 kg (0.027 in./10 lbs).

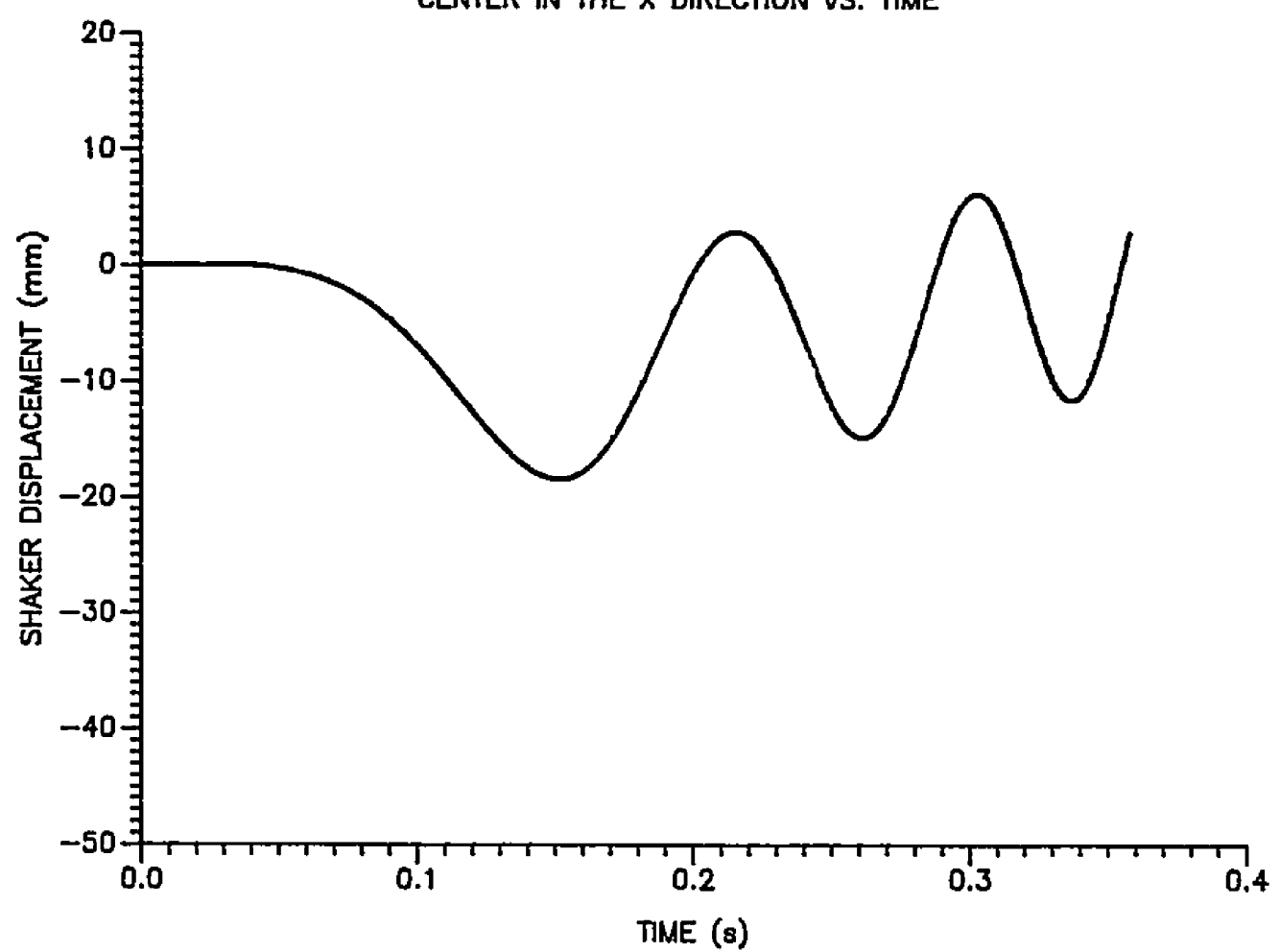


FIGURE 6.5 ROTATING MASSES ARE RUNNING ACCORDING TO SIMULATED TRANSIENT VELOCITY FUNCTION FOR A MASS OF 31.7 kg.

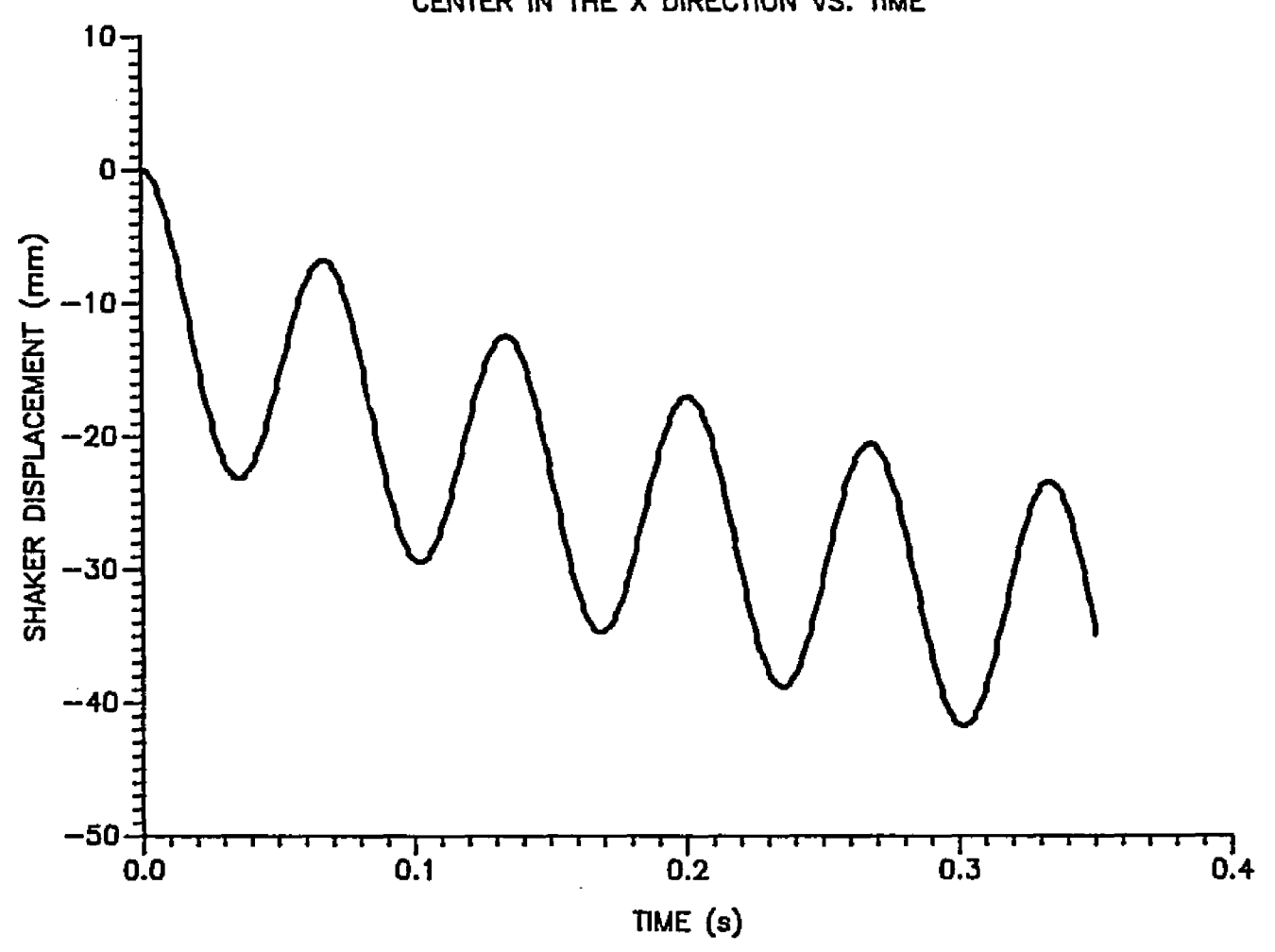


FIGURE 6.6 FREE SHAKING DISPLACEMENT VS. TIME AT FREQUENCY OF 15 HZ, AND SHAKER ROTATING MASS OF 31.7 kg.

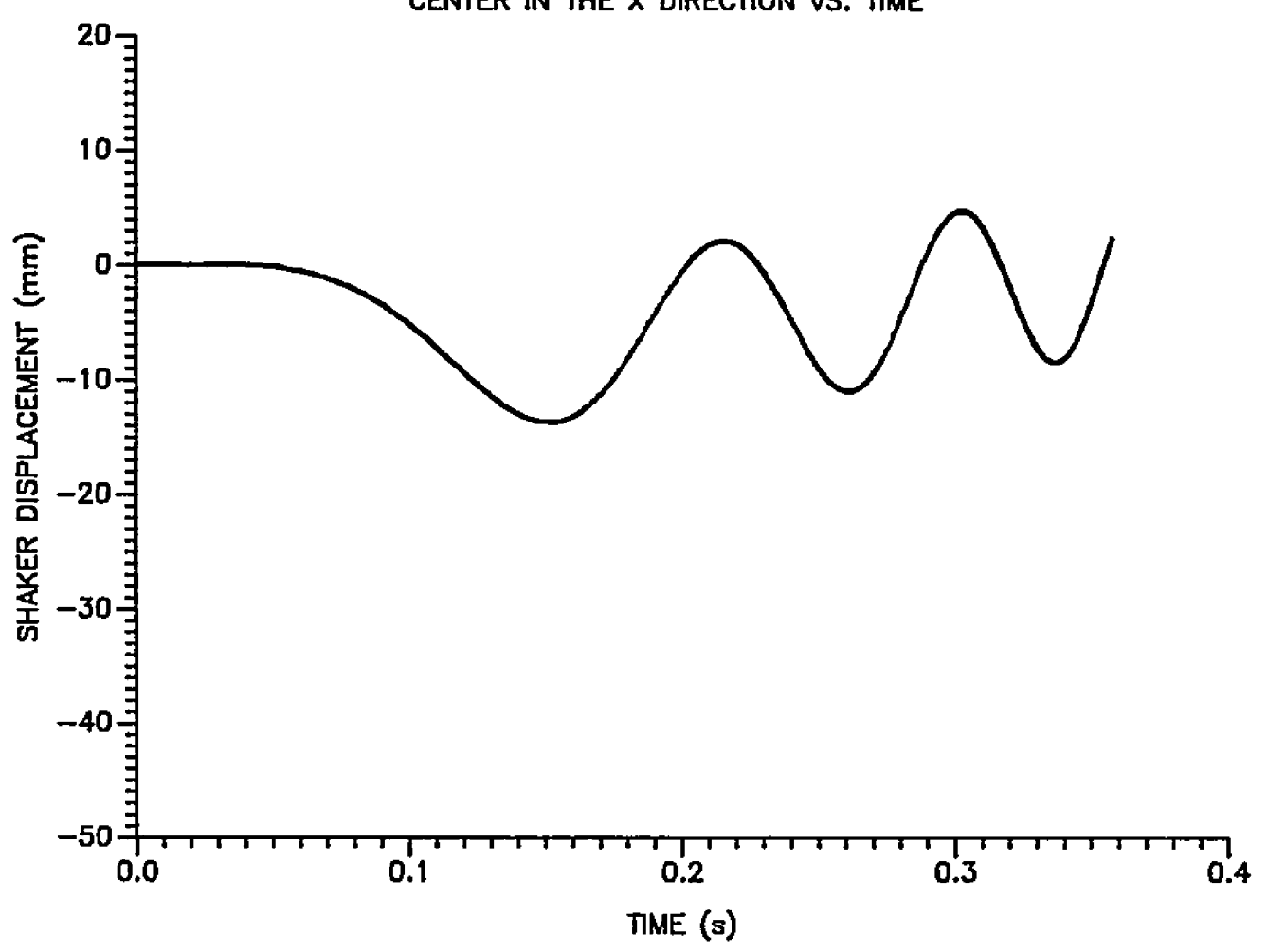


FIGURE 6.7 ROTATING MASSES ARE RUNNING ACCORDING TO SIMULATED TRANSIENT VELOCITY FUNCTION FOR A MASS OF 18.12 kg.

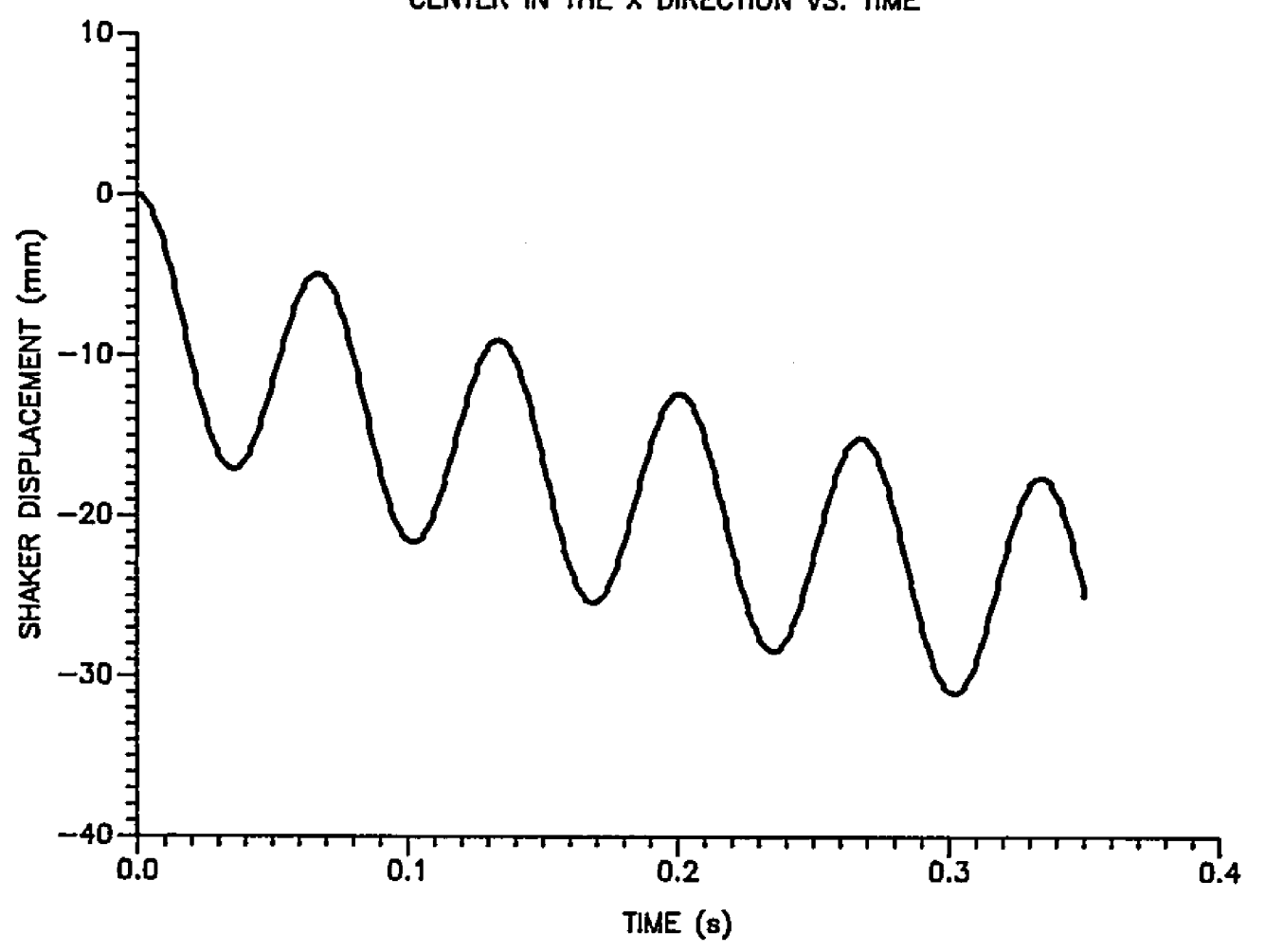


FIGURE 6.8 FREE SHAKING DISPLACEMENT VS. TIME AT FREQUENCY OF 15 HZ, AND SHAKER ROTATING MASS OF 18.12 kg.

### 6.3 Variation Of The Rotating Mass Acceleration

During these tests, three different rotating mass acceleration combinations were chosen to study their affect on the shaker displacement behavior during the transient stage. The rotating masses were assumed to start from the rest position at an initial phase angle of zero degrees (mass initial starting position). The selected combinations of rotating mass accelerations were:

- 2 1- 280 and 270 rad/s .
- 2- 280 and 260 rad/s .
  - 2
- 3- 328 and 246 rad/s .

The results of these tests indicated that rotating 2 mass accelerations of 280 and 270 rad/s for the inside and outside rotating masses, respectively, decreased the simulated shaker maximum displacement slightly from 25 mm (1 in.) to 22 mm (0.86 in.). The total shaker shifted 15 mm (0.59 in.) to the left in the first cycle then drifted 24 mm (0.94 in.) to the right by the fifth cycle, Figure 6.9.

At 280 and 260 rad/s acceleration levels for the inside and outside rotating masses, respectively, the shaker maximum displacements decreased from 25 mm (1 in.) to 15 mm (0.59 in.). The shaker shift and drift were the same as

previously observed, Figure 6.10.

The greatest difference in acceleration levels of 2 328 and 246 rad/s resulted in a marked difference in displacement behavior. The largest shaker displacement was 25 mm (1 in.), and occured when both rotating masses were in phase. The smallest displacement was 4 mm (0.15 in.), when the phase angle between masses was nearly 180 degrees. The shaker shift and drift were the same as previously observed, Figure 6.11. From these results the following conclusions can be made:

- 1- Changing the acceleration levels of the inside and outside rotating masses changes the phase angle between the masses during startup and results in displacement gallop (large displacement followed by small displacement in two following cycles) during startup. The most noticeable gallop occured for the acceleration combination of 328 and 246 rad/s .
- 2- Changing the rotating mass accelerations, within the range of 328 to 246 rad/s, does not affect the shaker shift or drift.

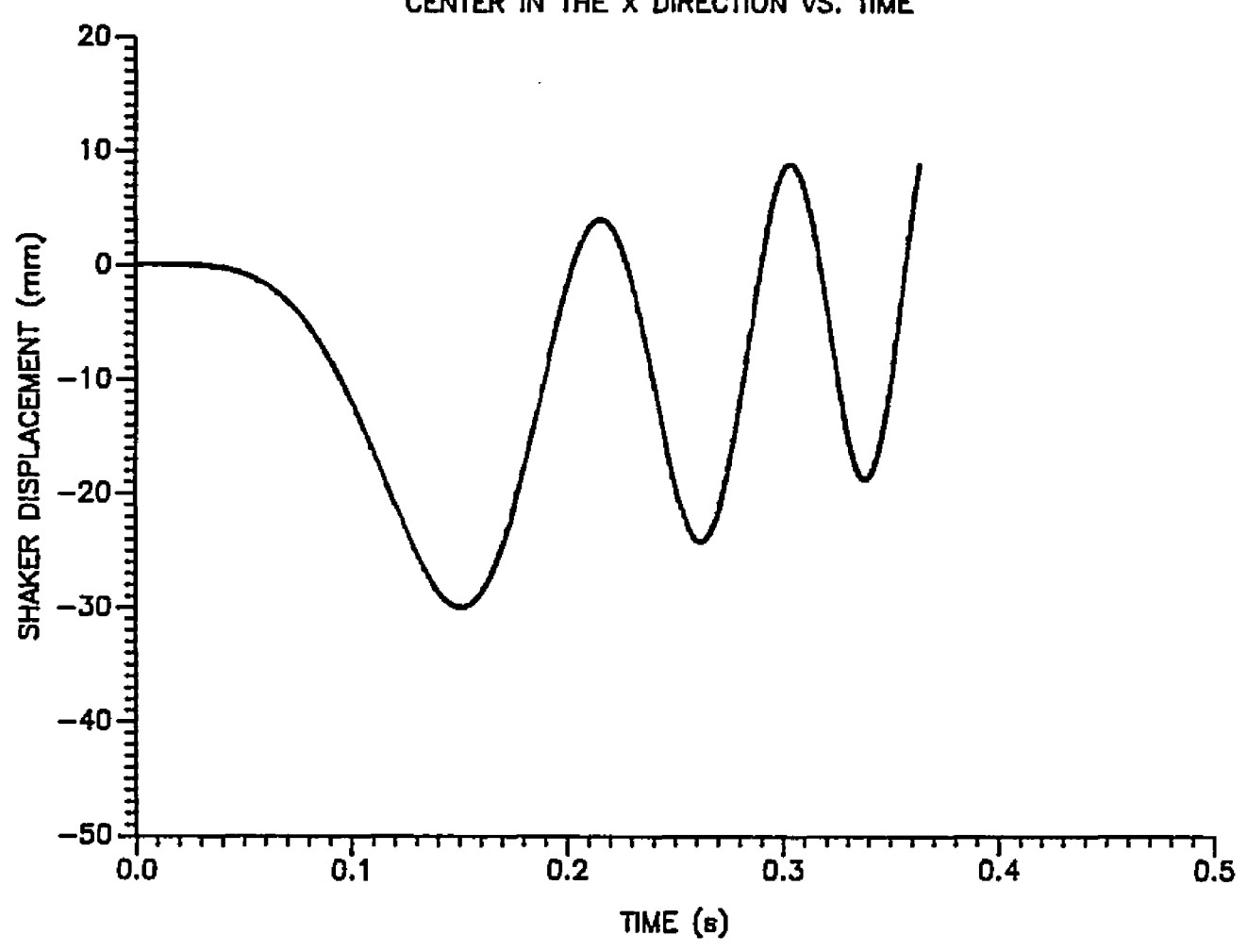


FIGURE 6.9 ROTATING MASSES ARE RUNNING ACCORDING TO SIMULATED TRANSIENT VELOCITY FUNCTION FOR TWO DIFFERENT ACCELERATION LEVELS, 280 AND 270 rad/s.s.

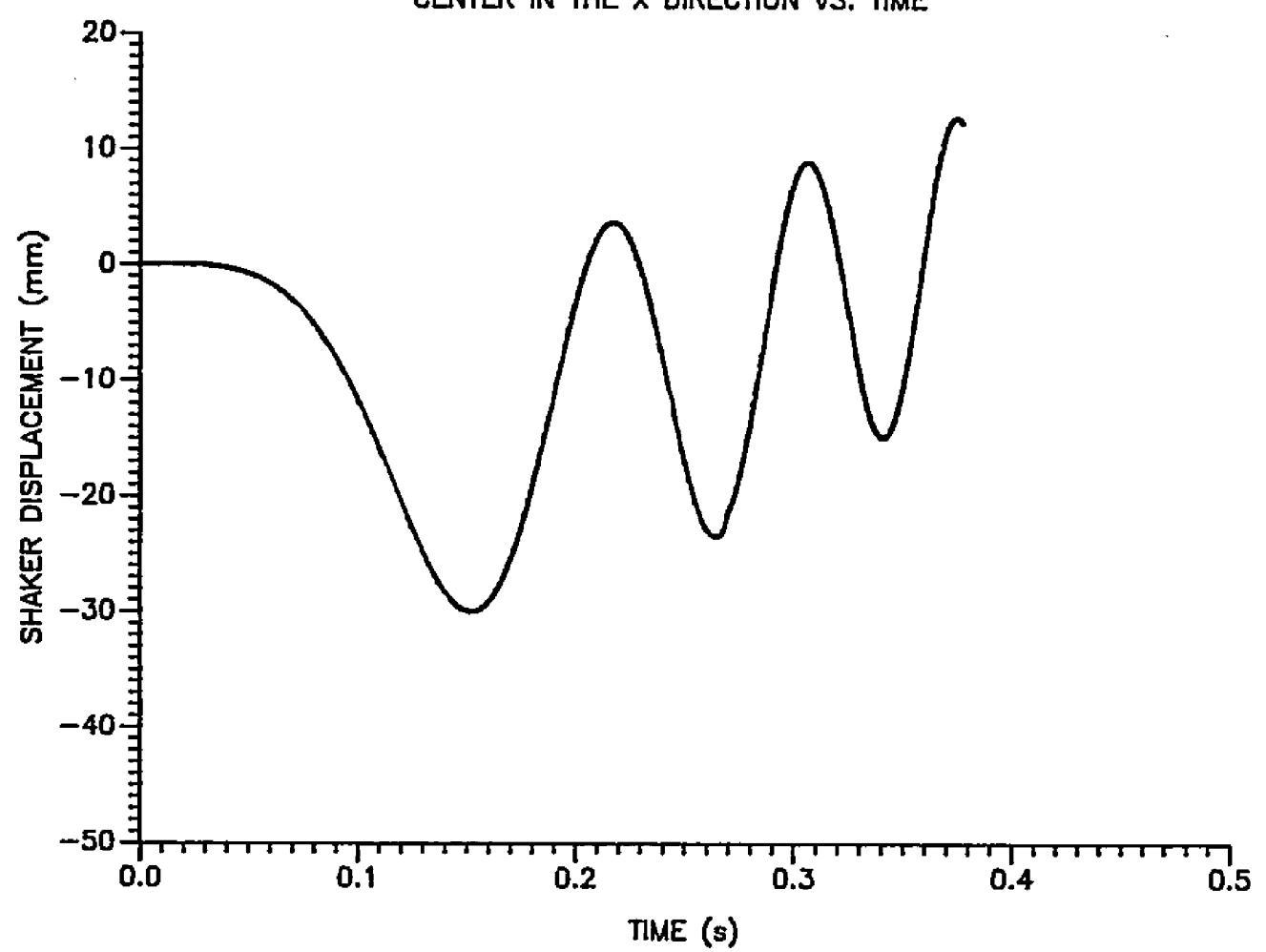


FIGURE 6.10 ROTATING MASSES ARE RUNNING ACCORDING TO SIMULATED TRANSIENT VELOCITY FUNCTION FOR TWO DIFFERENT ACCELERATION LEVELS, 280 AND 260 rad/s.s.

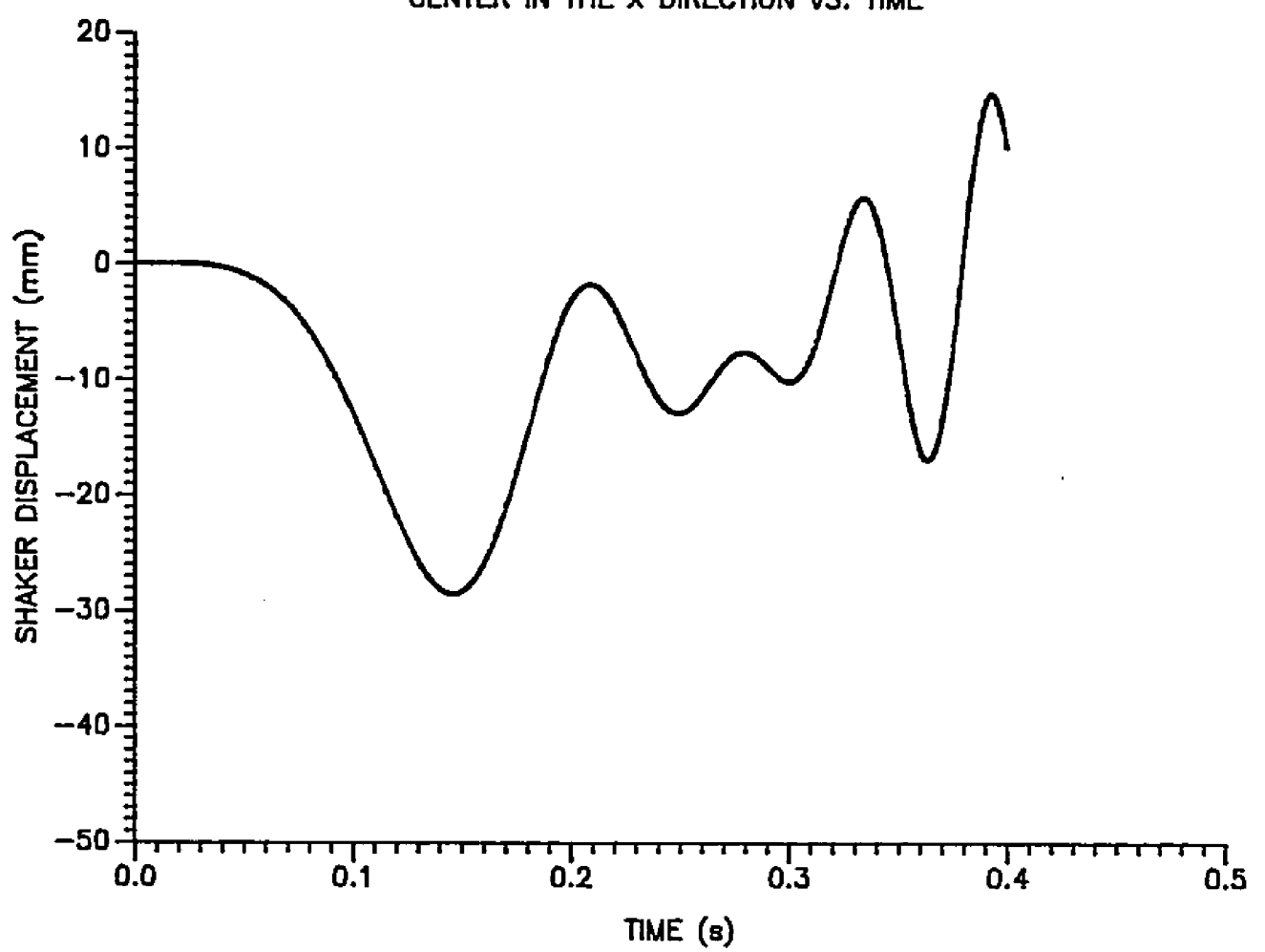
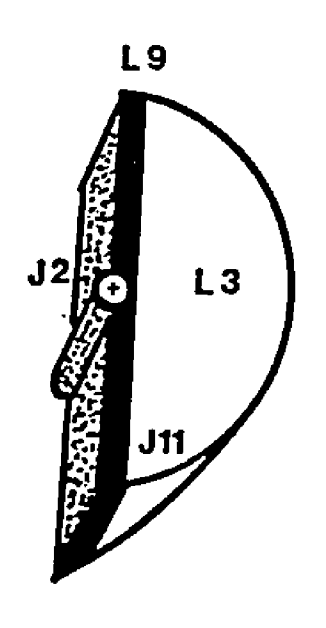


FIGURE 6.11 ROTATING MASSES ARE RUNNING ACCORDING TO SIMULATED TRANSIENT VELOCITY FUNCTION FOR TWO DIFFERENT ACCELERATION LEVELS, 328 AND 246 rad/s.s.

# 6.4 Variation Of Eccentricity Of The Rotating Masses

To vary the shaker rotating mass eccentricity, the free-shake IMP model was modified by introducing a slider joint between the axis of rotation and the center of mass for each rotating mass, Figure 6.12. The center of gravity of each rotating mass was assumed to be initially located 0.0025 mm (0.001 in.) away from the mass axis of rotation. The motion of each rotating mass slider joint was controlled by a slider position command inside the IMP model. opening the slider joints at a specified rate the mass center of gravity of each rotating mass would move outward, causing larger forces to be produced as a result of the mass eccentricity product. Three different slider opening rates were tested (217, 190, and 165 mm/s) during the shaker displacement simulation using the transient rotating mass frequency function. The starting phase angle between the rotating masses was zero.

The model results indicated that by using two rotating masses opening at a rate of 217 mm/s (their center of gravity can reach 76 mm (3 in.) eccentricity in 0.353 s) the simulated shaker displacement started from zero and increased uniformly to a maximum displacement of 25 mm (1



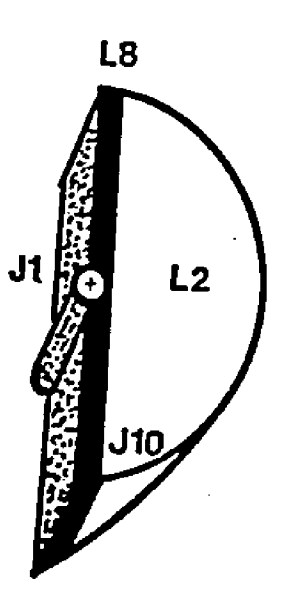


FIGURE 6.12 SLIDING ROTATING MASS MODEL

in.) as the frequency of 15.66 Hz was reached following the transient function. The shaker drift during the similation was 7 mm (0.27 in.) and no shaker shift was observed, Figure 6.13.

By decreasing the mass opening rate to 190 mm/s the simulated shaker displacements again increased uniformly from zero, but at a slower rate. The maximum displacement would have equalled the same 25 mm (1 in.) after 0.4 s. The shaker drift was stable at the same previous value of 7 mm (0.27 in.) and again no shaker shift, Figure 6.14.

At the lowest mass opening rate of 165 mm/s, the simulated shaker displacements still increased uniformlly from zero, but at the slowest rate. Final maximum displacement would again have been 25 mm (1 in.) after 0.46 s because of the final eccentricity and frequency. The shaker drift was again 5 mm (0.19 in.) and no shaker shift was observed over the simulated period, Figure 6.15.

The affects of using three different constant rotating mass frequencies (5, 10, and 15 Hz) and a mass opening rate of 217 mm/s were studied to determine if the shaker displacement would increase uniformly if the masses were always rotating but shaking was initiated by moving the masses outward.

The model results indicated that at steady rotating mass frequencies of 5, 10, or 15 Hz, the simulated shaker

displacement increased uniformly from zero to a maximum. The shaker drift was 5 mm (0.19 in.) at a frequency of 5 Hz and 9 mm (0.35 in.) at 10 and 15 Hz, Figures 6.16, 6.17, and 6.18. These test results lead to the following conclusions:

- 1- No shaker gallop or shift occured during the startup period of the transient frequency function when the rotating mass eccentricity was increased from zero at different rates.
- 2- Shaker drift was minimized during the transient frequency function by increasing the mass eccentricity from zero to 76 mm (3 in.) at different rates.
- 3- Full shaker displacement was reached in about the same time (0.353 s) by increasing the mass eccentricity at 217 mm/s while running at 15 Hz or by following the transient function to reach 15 Hz, although about twice as many shaking cycles were developed at the 15 Hz constant frequency.
- 4- These simulation results indicate that the shaker gallop, shift, drift and displacements during shaking operations might be controlled by increasing the rotating mass eccentricity from zero to the desirable position during either a transient frequency startup or a steady state frequency startup.

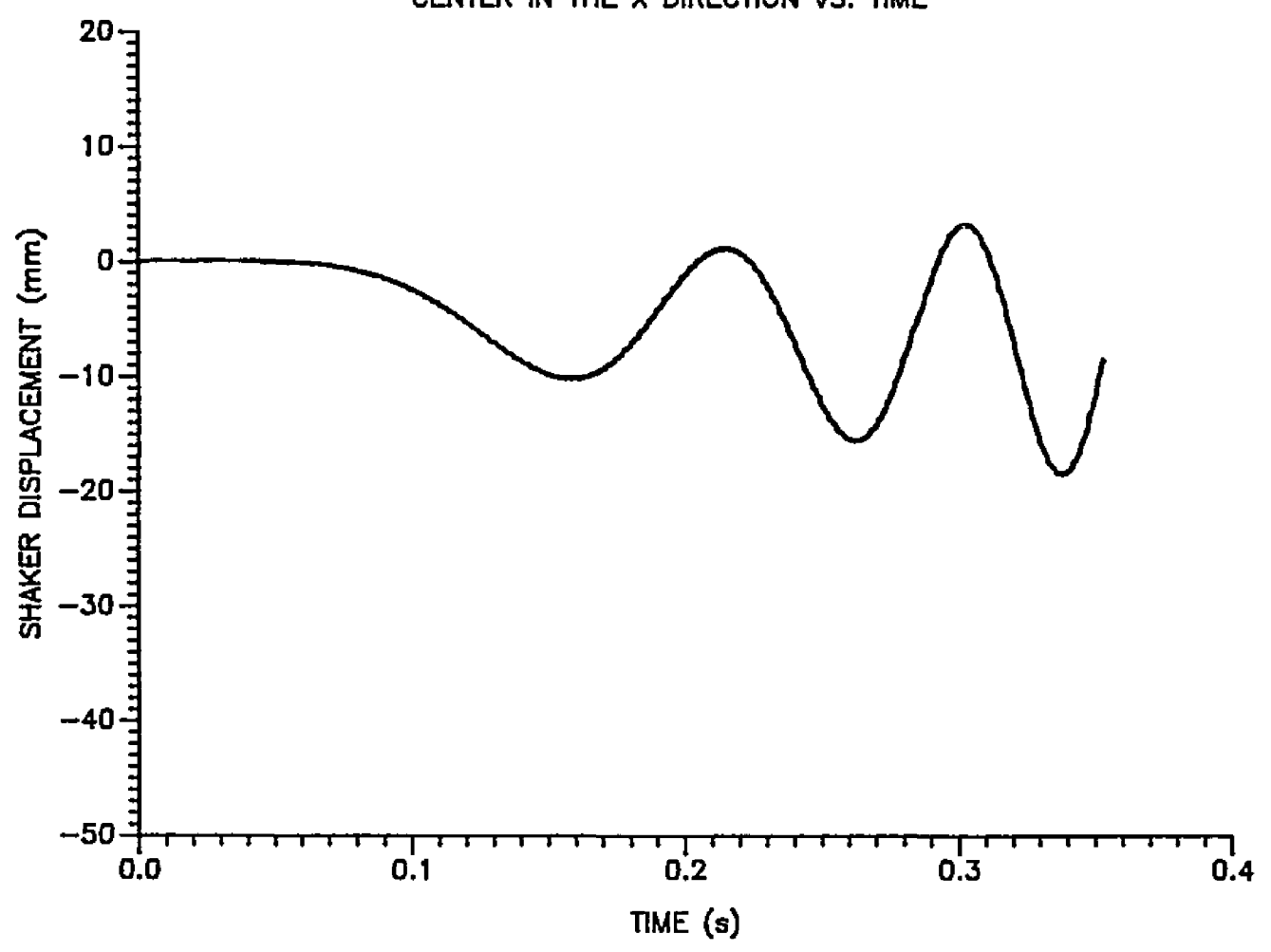


FIGURE 6.13 ROTATING MASSES ARE RUNNING ACCORDING TO SIMULATED TRANSIENT VELOCITY FUNCTION WITH MOVING ECCENTRICITY AT RATE OF 217 mm/s.

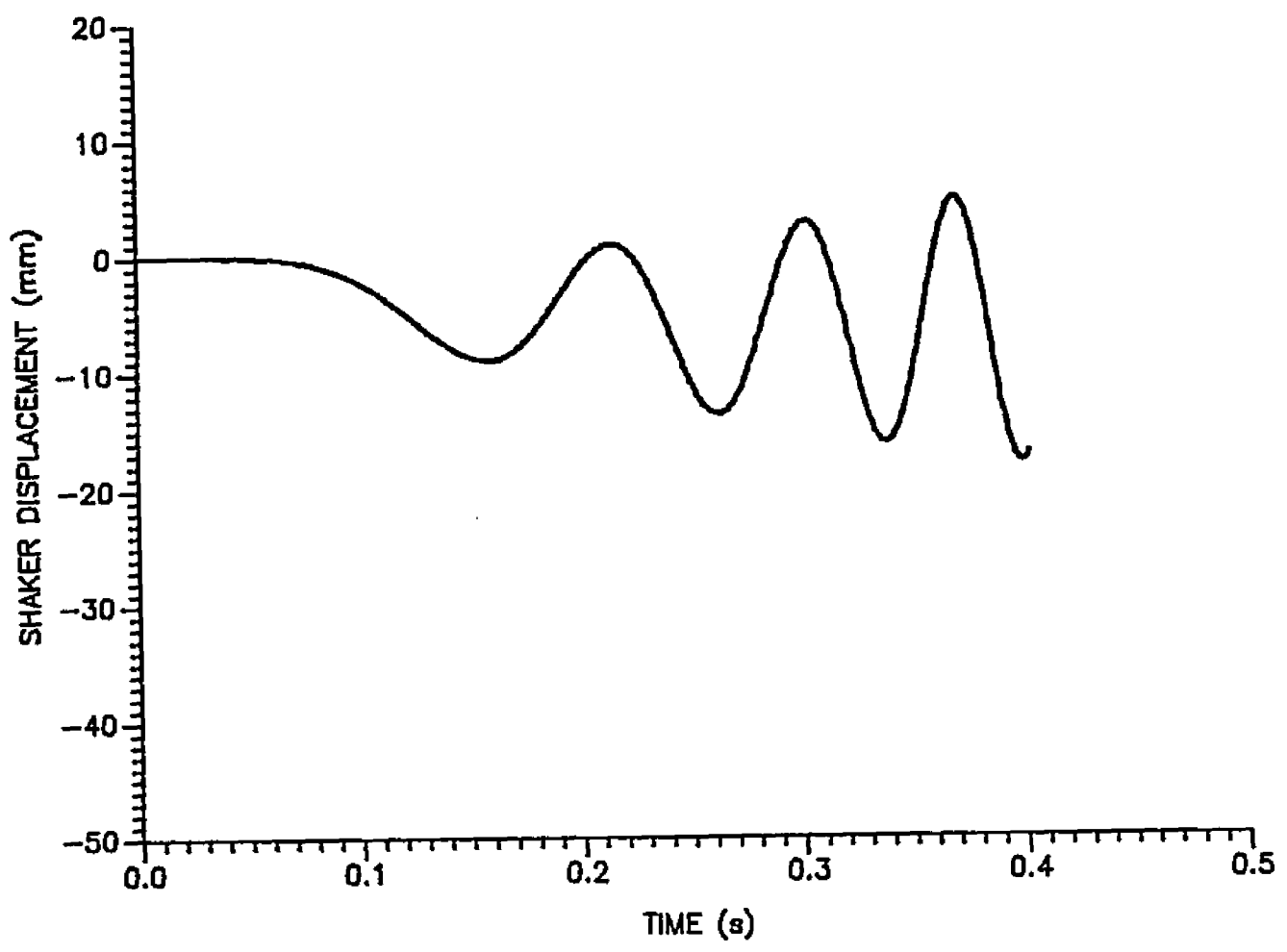


FIGURE 6.14 ROTATING MASSES ARE RUNNING ACCORDING TO SIMULATED TRANSIENT VELOCITY FUNCTION WITH MOVING ECCENTRICITY AT RATE OF 190 mm/s.

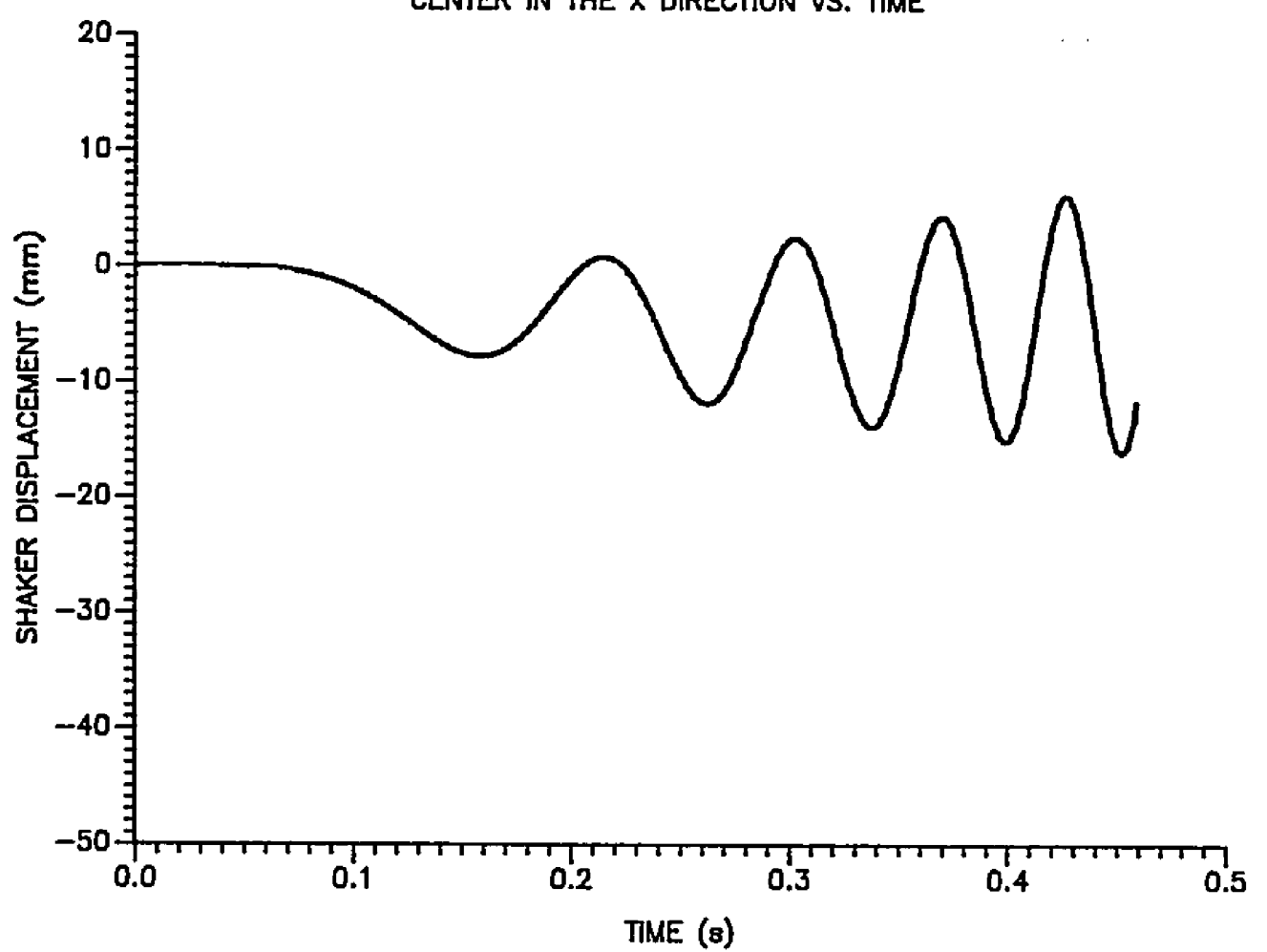


FIGURE 6.15 ROTATING MASSES ARE RUNNING ACCORDING TO SIMULATED TRANSIENT VELOCITY FUNCTION WITH MOVING ECCENTRICITY AT RATE OF 165 mm/s.

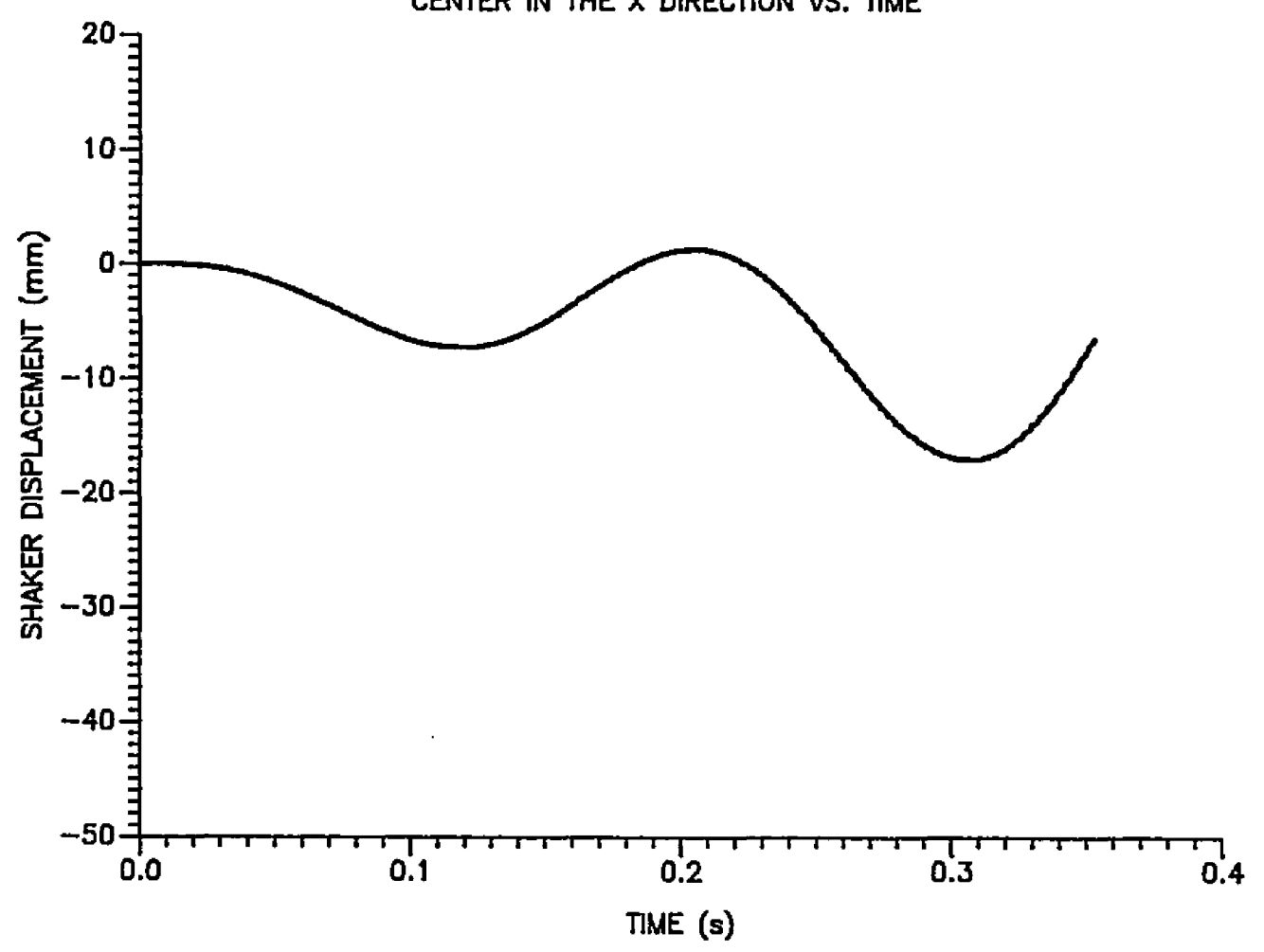


FIGURE 6.16 ROTATING MASSES ARE RUNNING AT STEADY FREQUENCY OF 5 HZ WITH MOVING ECCENTRICITY AT RATE OF 217 mm/s.

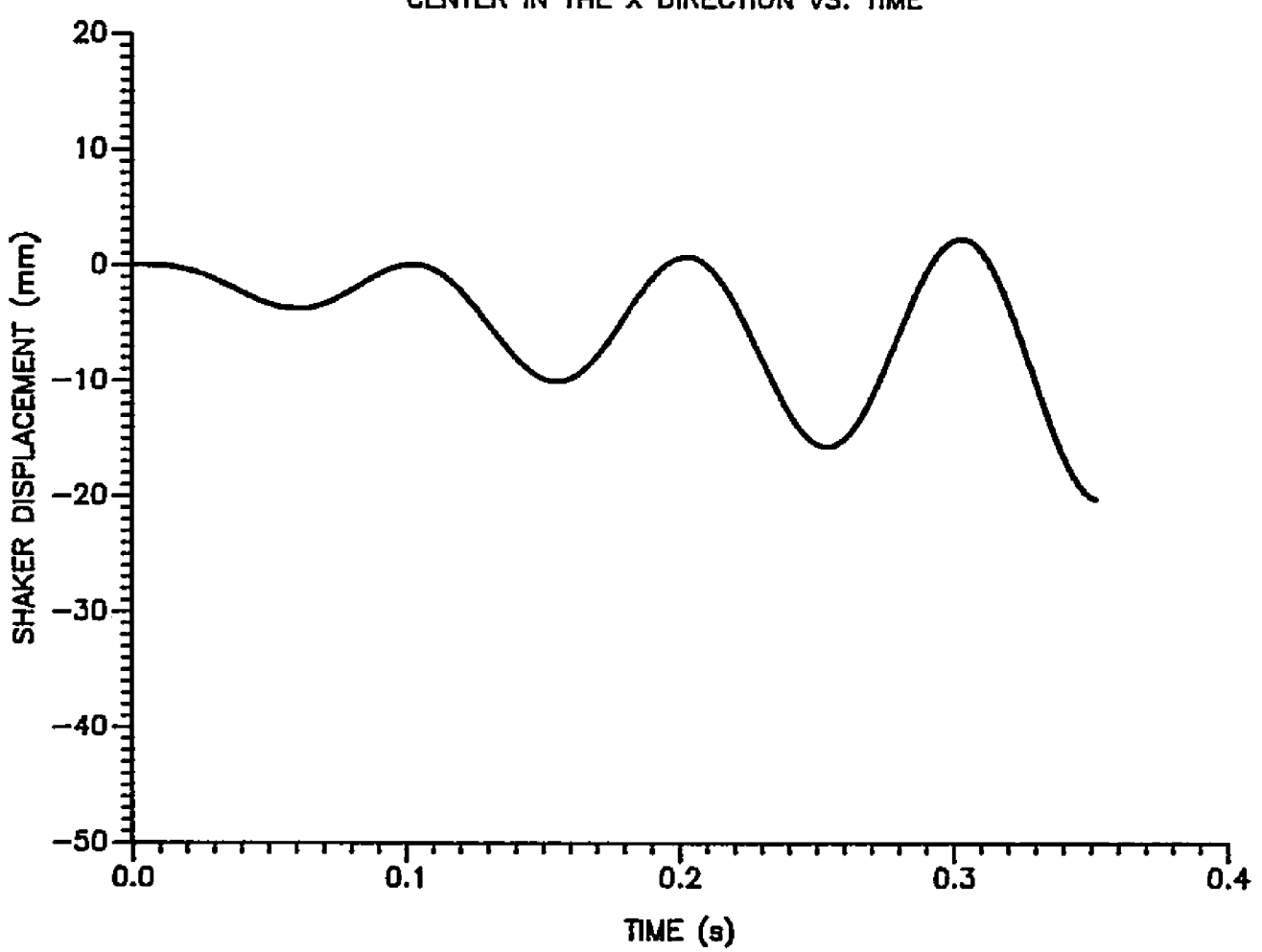


FIGURE 6.17 ROTATING MASSES ARE RUNNING AT STEADY FREQUENCY OF 10 HZ WITH MOVING ECCENTRICITY AT RATE OF 217 mm/s.

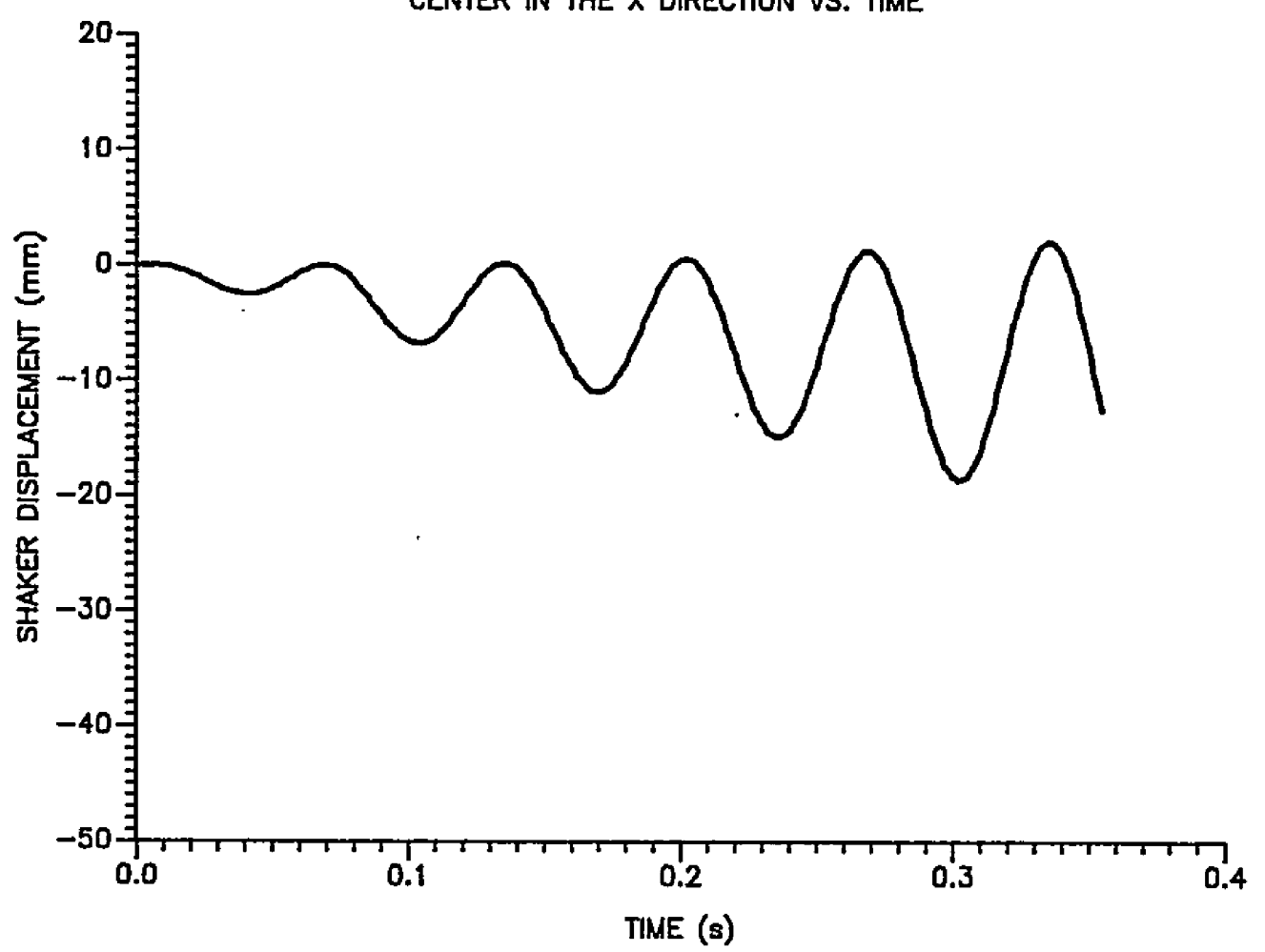


FIGURE 6.18 ROTATING MASSES ARE RUNNING AT STEADY FREQUENCY OF 15 HZ WITH MOVING ECCENTRICITY AT RATE OF 217 mm/s.

# 6.5 Variation Of The Starting Phase Angle Between The Masses

This study was conducted to examine the affect of the starting phase angle between the rotating masses on the shaker displacements. During these shaker simulations the rotating masses followed the transient frequency function between zero and 15.66 Hz at accelerations of 328 and 246 2 rad/s for the inside and outside rotating mass, respectively. The inside and the outside mass would reach the maximum frequency in 0.3 and 0.4 s, respectively.

The shaker displacements were tested for starting phase angles ranging from 0 to 360 degrees, by keeping the inside rotating mass at its original starting position and reseting the outside rotating mass at increments of 45 degrees counterclockwise from its original position. The resulting shaker displacements in the x, y, and x-y plane directions were then plotted, and are presented in Figures 6.19 to 6.42.

The simulation displacement results indicated that by using starting phase angles ranging from zero to 360 degrees between the rotating masses, the shaker displacements in the x and y directions fluctuated between a maximum value of 25 mm (1 in.), when both masses were in

phase, and a minimum value of 4 mm (0.15 in.), when the masses were out of phase by 180 degrees. However, the shaker shift and drift were unstable at different phase angles.

At a starting phase angle of zero degrees, the shaker planar motion was unstable during the simulation. The shaker shifted about 14 mm (0.55 in.) and drifted 14 mm (0.55 in.) in the x direction, and shifted 2 mm (0.07 in.) and drifted only 5 mm (0.19 in.) in the y direction. The shaker gallop in the x direction was grater than in y direction. It displaced 42 mm (1.65 in.) in the x direction and 30 mm (1.18 in.) in the y direction, respectively, resulting in large shaker drift, Figures 6.19, 6.20, and 6.21.

At a starting mass phase angle of 45 degrees, the shaker was also unstable. The shaker shift was 11 mm (0.43 in.) and 6 mm (0.23 in.) in the x and y directions, respectively. The shaker drift in the y direction increased to 10 mm (0.39 in.) while it was only 12 mm (0.47 in.) in the x direction. The shaker gallop was observed in both the x and y directions, Figures 6.22, 6.23, and 6.24.

At a 90 degree starting mass phase angle, the shaker shifted 5 mm (0.19 in.) and 9 mm (0.35 in.) in the x and y directions, respectively. The drift in the x direction decreased to 5 mm (0.19 in.) while it increased to 15 mm (0.59 in.) in the y direction. The shaker gallop in the x direction was observed to be smaller than in the y

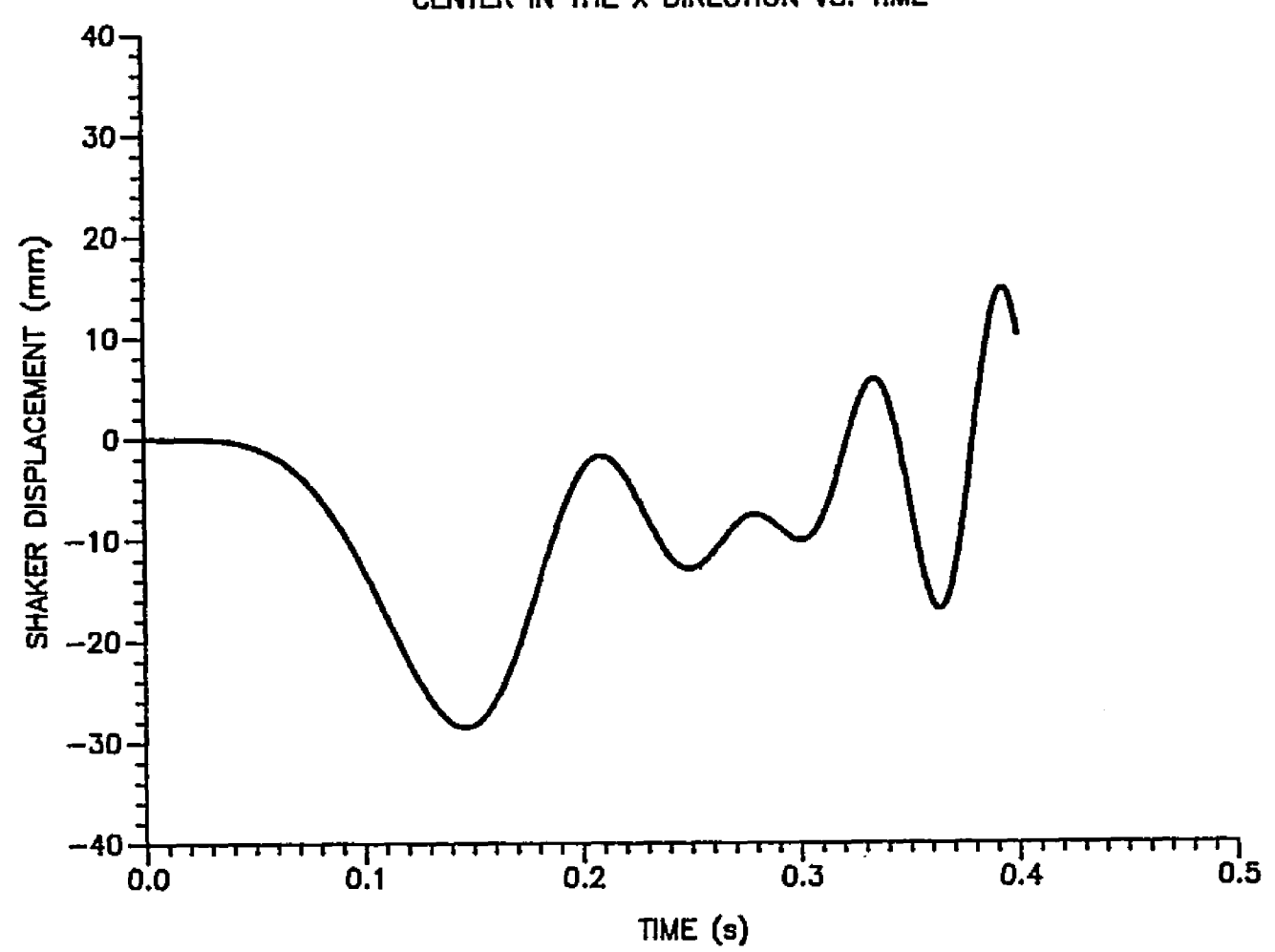


FIGURE 6.19 SHAKER DISPLACEMENT IN THE X DIRECTION. MASSES ARE RUNNING AT ACCELERATIONS OF 328 AND 246 rad/s.s. At a starting phase angle of 0 degrees.

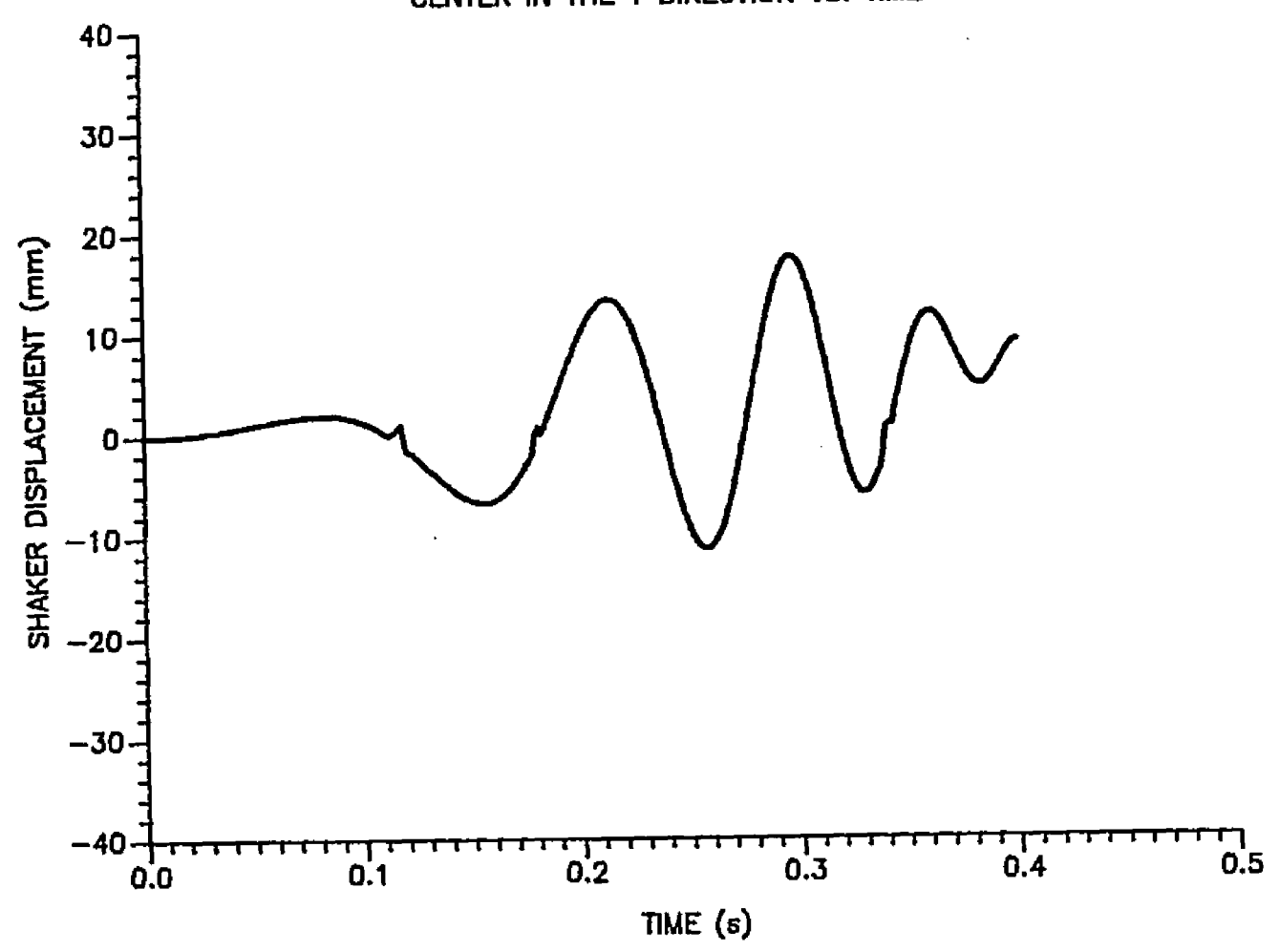


FIGURE 6.20 SHAKER DISPLACEMENT IN THE Y DIRECTION.
MASSES ARE RUNNING AT ACCELERATIONS OF 328 AND 246
rad/s.s. AT A STARTING PHASE ANGLE OF 0 DEGREES.

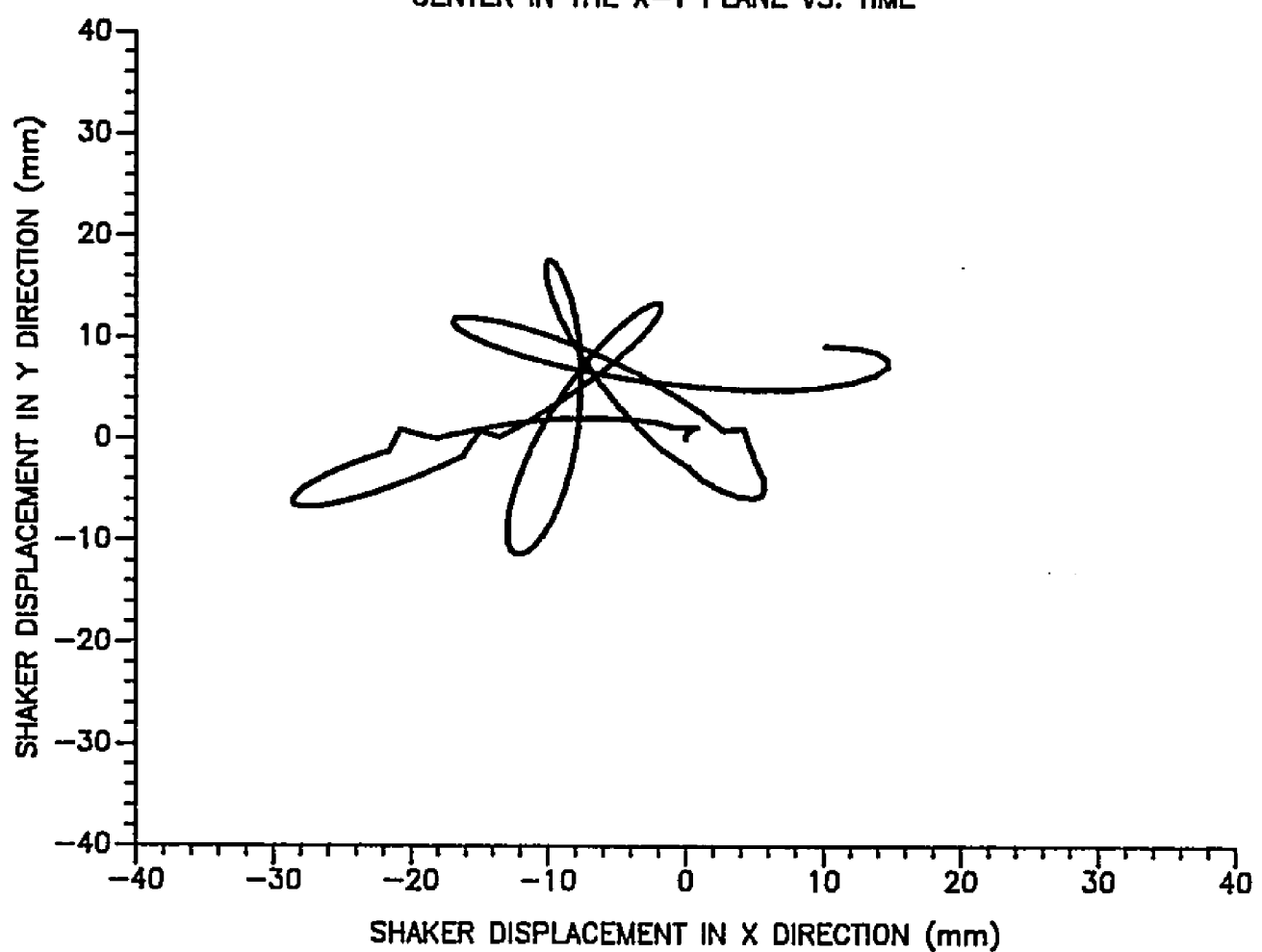


FIGURE 6.21 SHAKER DISPLACEMENT IN THE X-Y PLANE.
MASSES ARE RUNNING AT ACCELERATIONS OF 328 AND 246 rad/s.s. AT A STARTING PHASE ANGLE OF O DEGREES.

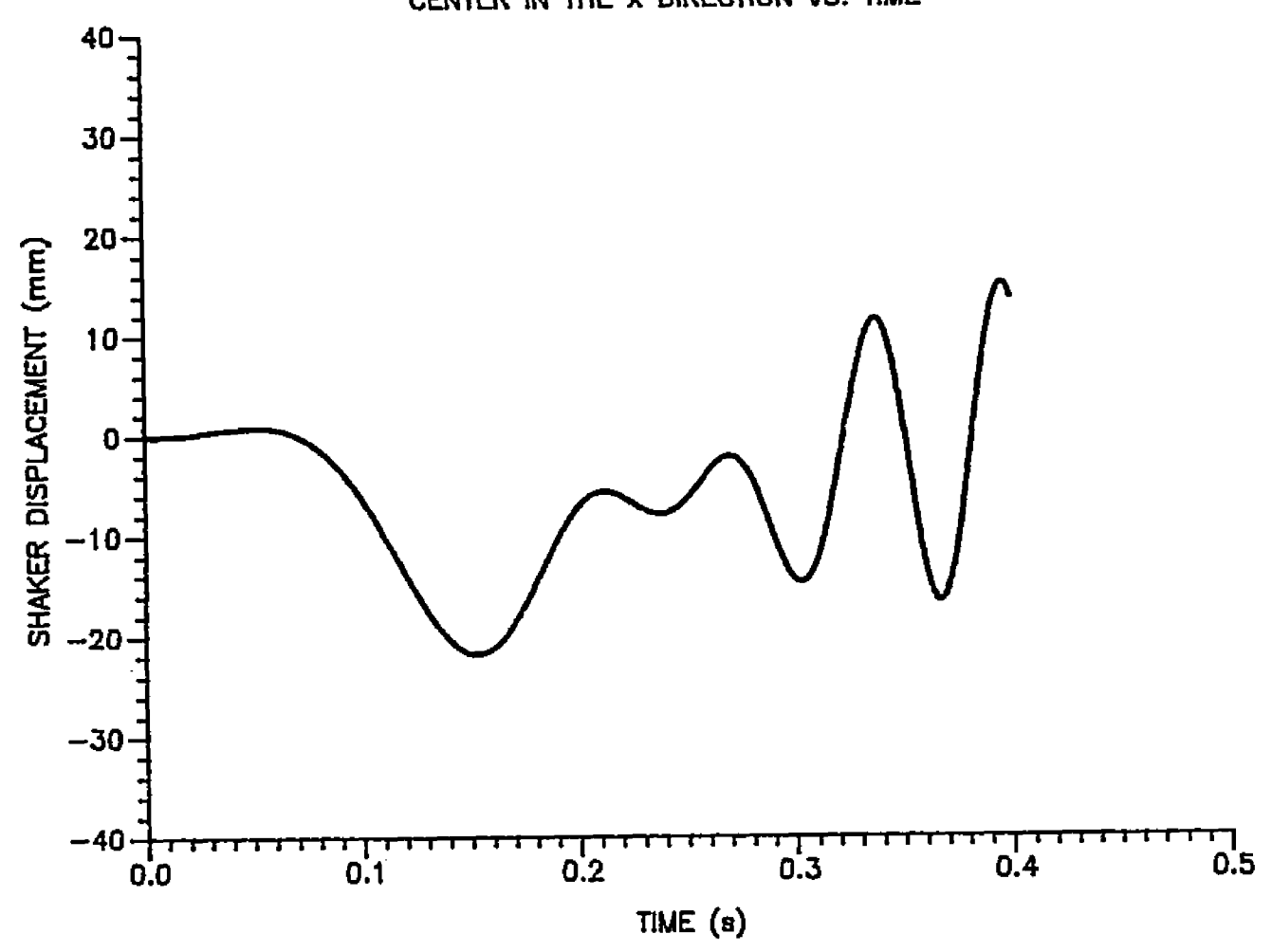


FIGURE 6.22 SHAKER DISPLACEMENT IN THE X DIRECTION. MASSES ARE RUNNING AT ACCELERATIONS OF 328 AND 246 rad/s.s. At a starting phase angle of 45 degrees.

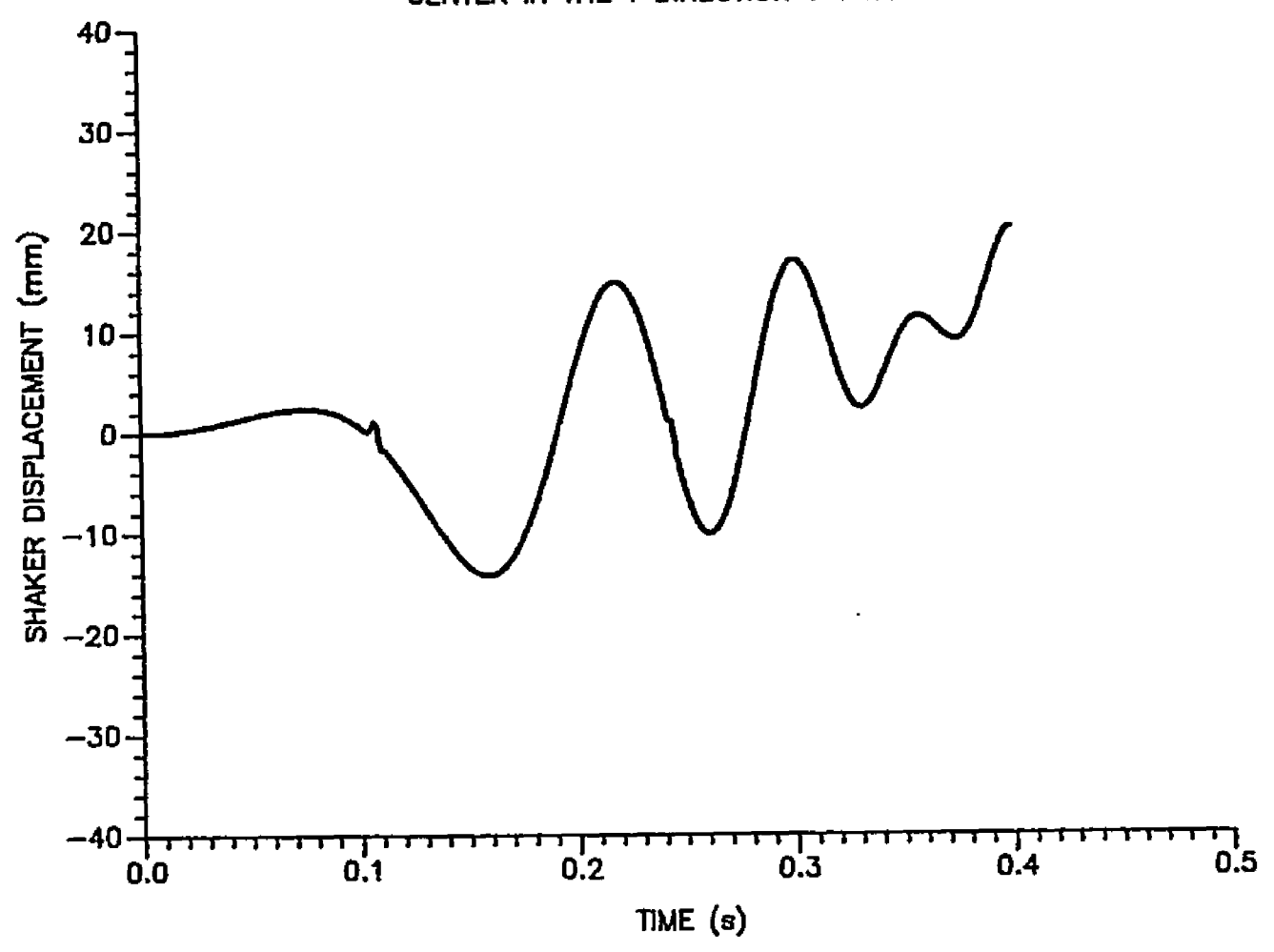


FIGURE 6.23 SHAKER DISPLACEMENT IN THE Y DIRECTION. MASSES ARE RUNNING AT ACCELERATIONS OF 328 AND 246 rod/s.s. AT A STARTING PHASE ANGLE OF 45 DEGREES.

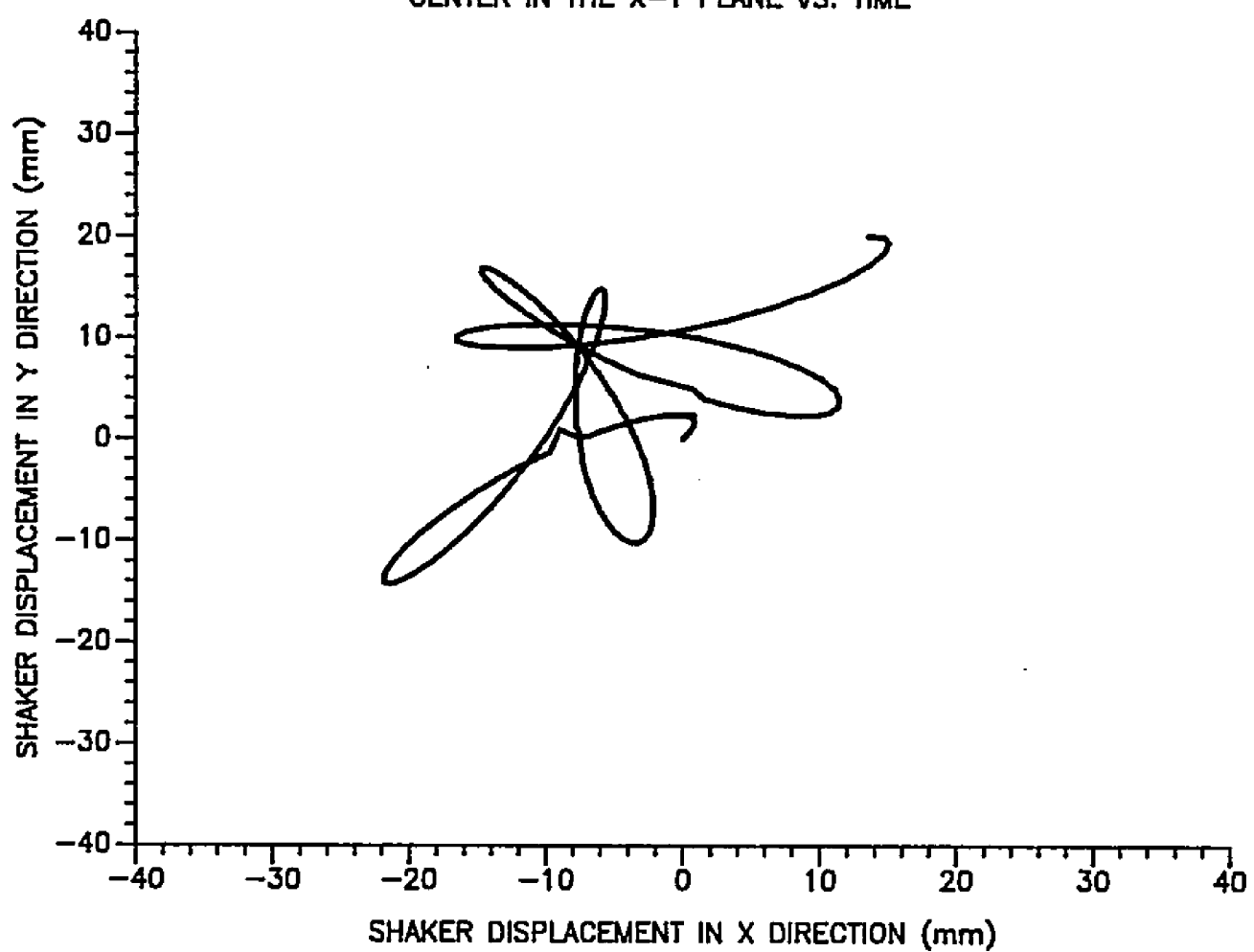


FIGURE 6.24 SHAKER DISPLACEMENT IN THE X-Y PLANE. MASSES ARE RUNNING AT ACCELERATIONS OF 328 AND 246 rad/s.s. AT A STARTING PHASE ANGLE OF 45 DEGREES.

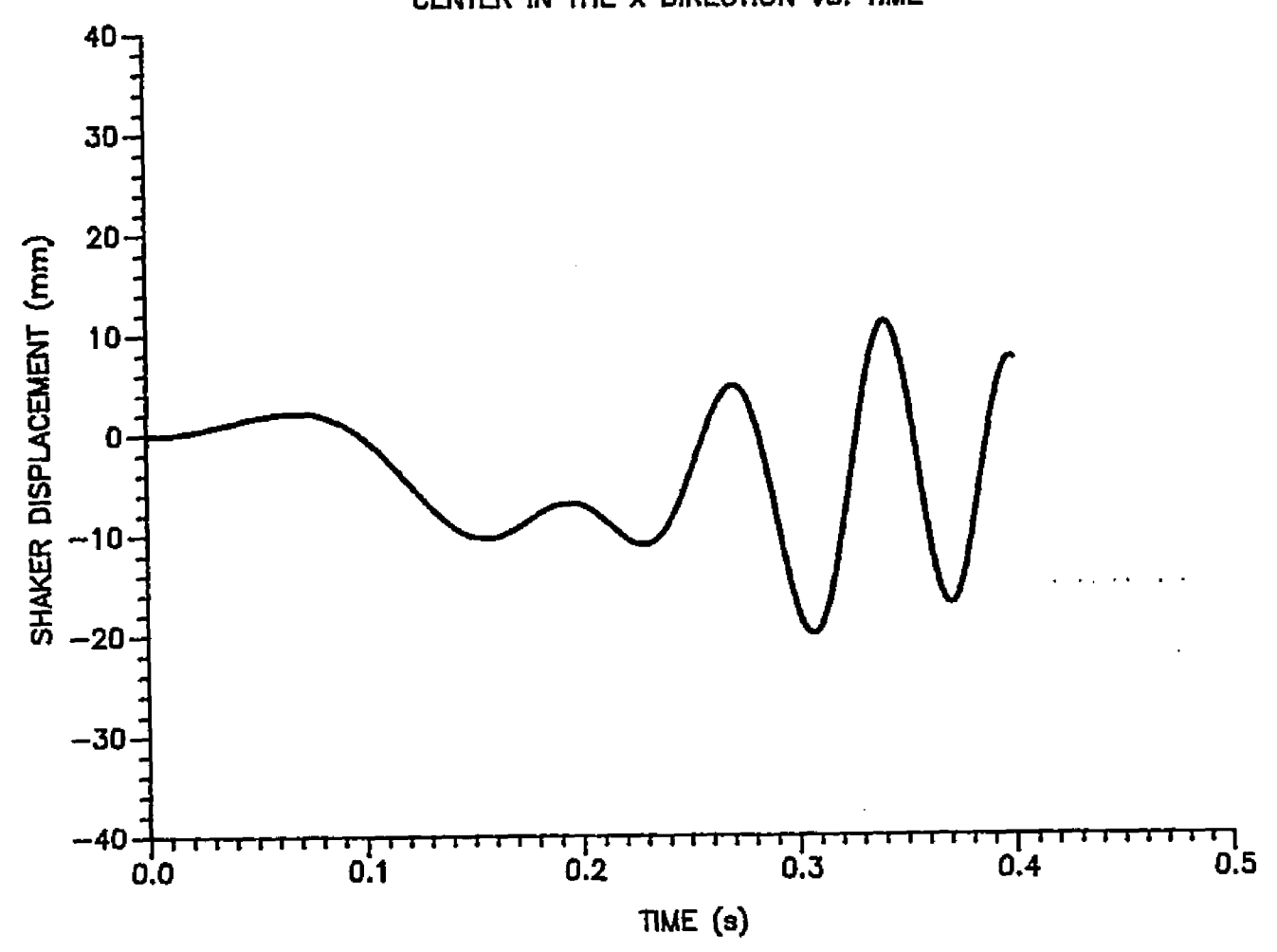


FIGURE 6.25 SHAKER DISPLACEMENT IN THE X DIRECTION.
MASSES ARE RUNNING AT ACCELERATIONS OF 328 AND 246 rod/s.s. AT A STARTING PHASE ANGLE OF 90 DEGREES.

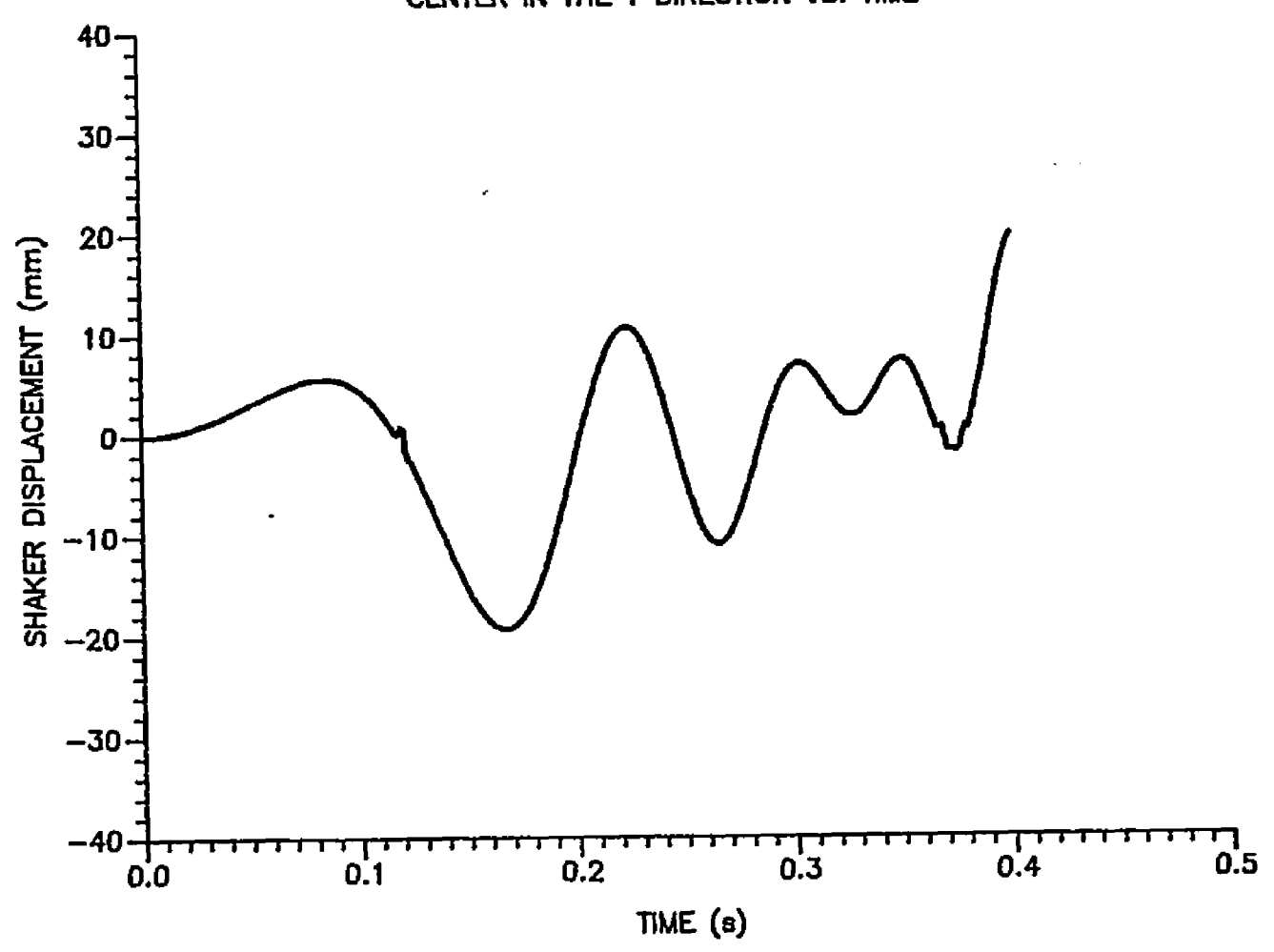


FIGURE 6.26 SHAKER DISPLACEMENT IN THE Y DIRECTION.
MASSES ARE RUNNING AT ACCELERATIONS OF 328 AND 246 rad/s.s. AT A STARTING PHASE ANGLE OF 90 DEGREES.

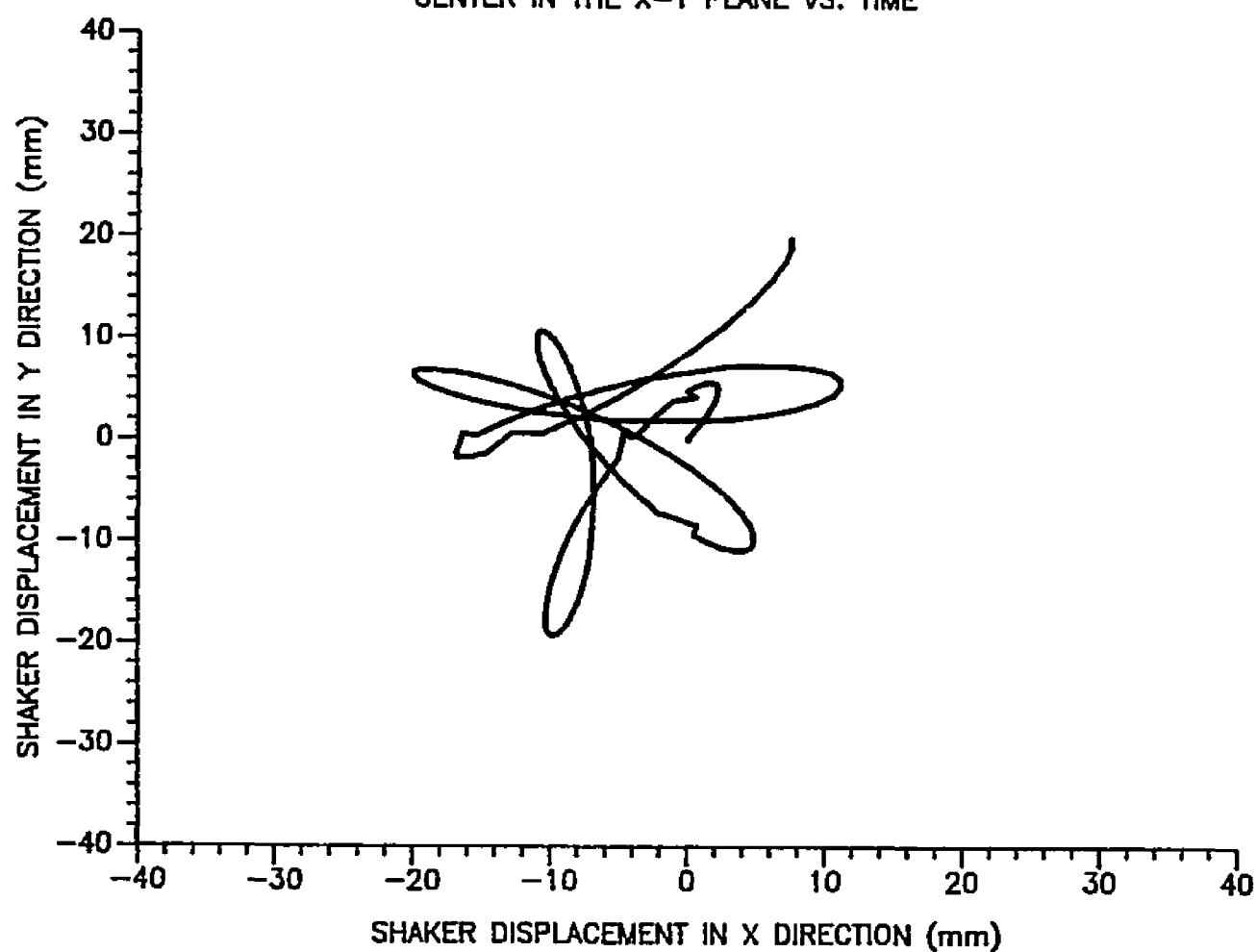


FIGURE 6.27 SHAKER DISPLACEMENT IN THE X-Y PLANE.
MASSES ARE RUNNING AT ACCELERATIONS OF 328 AND 246 rad/s.s. AT A STARTING PHASE ANGLE OF 90 DEGREES.

direction, Figures 6.25, 6.26, and 6.27.

At a starting phase angle of 135 degrees, the shaker drift in the x direction declined to the lowest value of 5 mm (0.19 in.) and decreased to 11 mm (0.43 in.) in the y direction. No shaker shift was observed in the x direction while only 2 mm (0.07 in.) shift occured in the y direction. The shaker gallop decreased also in both the x an y directions, Figures 6.28, 6.29, and 6.30.

Better shaker stability was obtained at a starting phase angle of 180 degrees. The shaker drifted 5 mm (0.19 in.) and 2 mm (0.07 in.) in the x and y directions, respectively. No shaker shift occurred in either the x or y directions. The shaker gallop was minimum in both the x and y directions, Figures 6.31, 6.32, and 6.33.

The best shaker stability was obtained at a starting phase angle of 225 degrees. The shaker shifted only 3 mm (0.11 in.) in the y direction with no shaker shift in the x direction. The shaker drift was only 2 mm (0.07 in.) and 3 mm (0.11 in.) in the x and y directions, respectively. No shaker gallop was observed during the simulations, Figures 6.34, 6.35, and 6.36.

By increasing the starting phase angle to 270 degrees, the shaker shift increased in both the x and y direction to 6 mm (0.23 in.). The shaker drift in the x direction increased to 8 mm (0.31 in.) while it reached the lowest

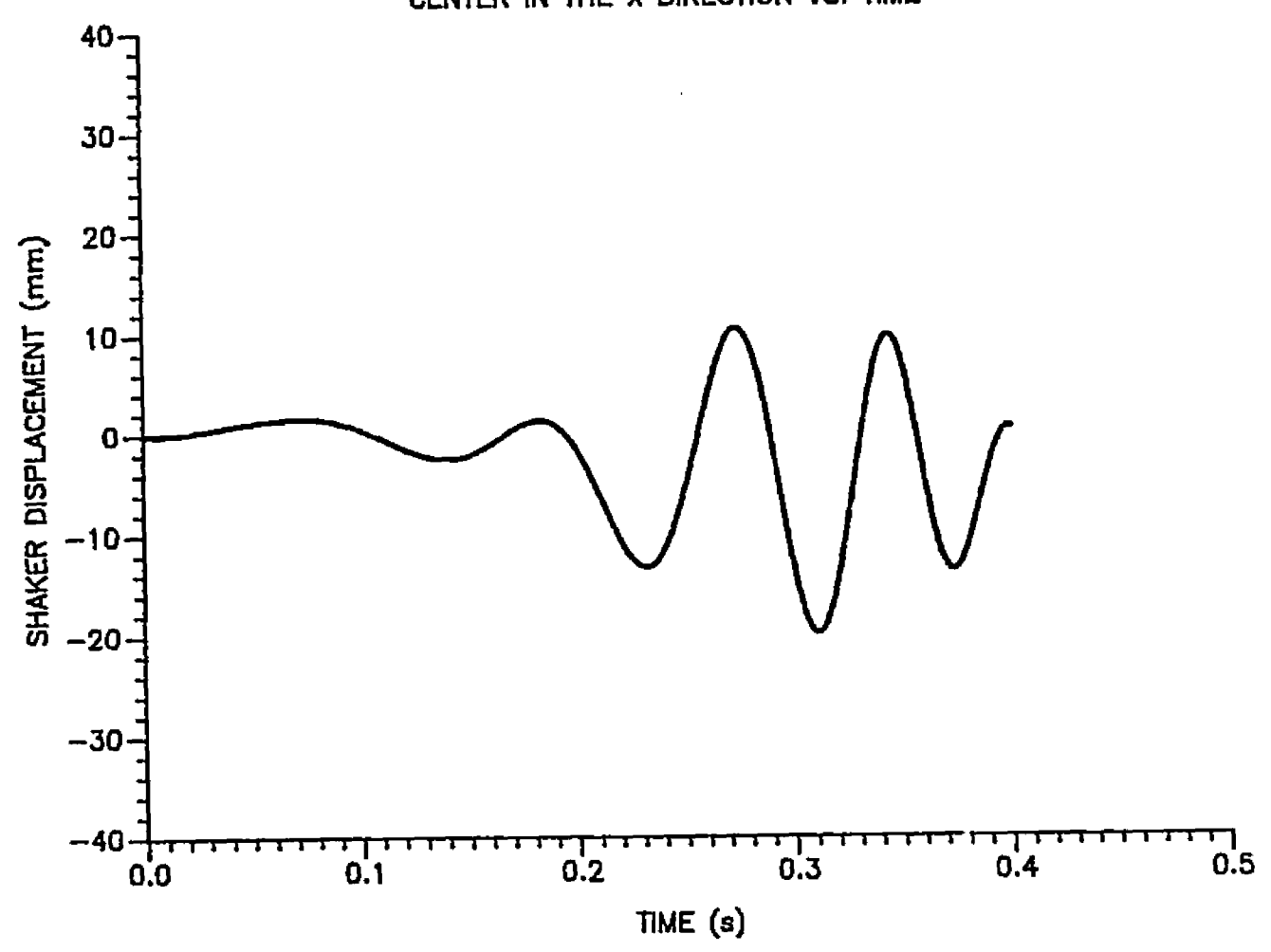


FIGURE 6.28 SHAKER DISPLACEMENT IN THE X DIRECTION. MASSES ARE RUNNING AT ACCELERATIONS OF 328 AND 246 rad/s.s. AT A STARTING PHASE ANGLE OF 135 DEGREES.

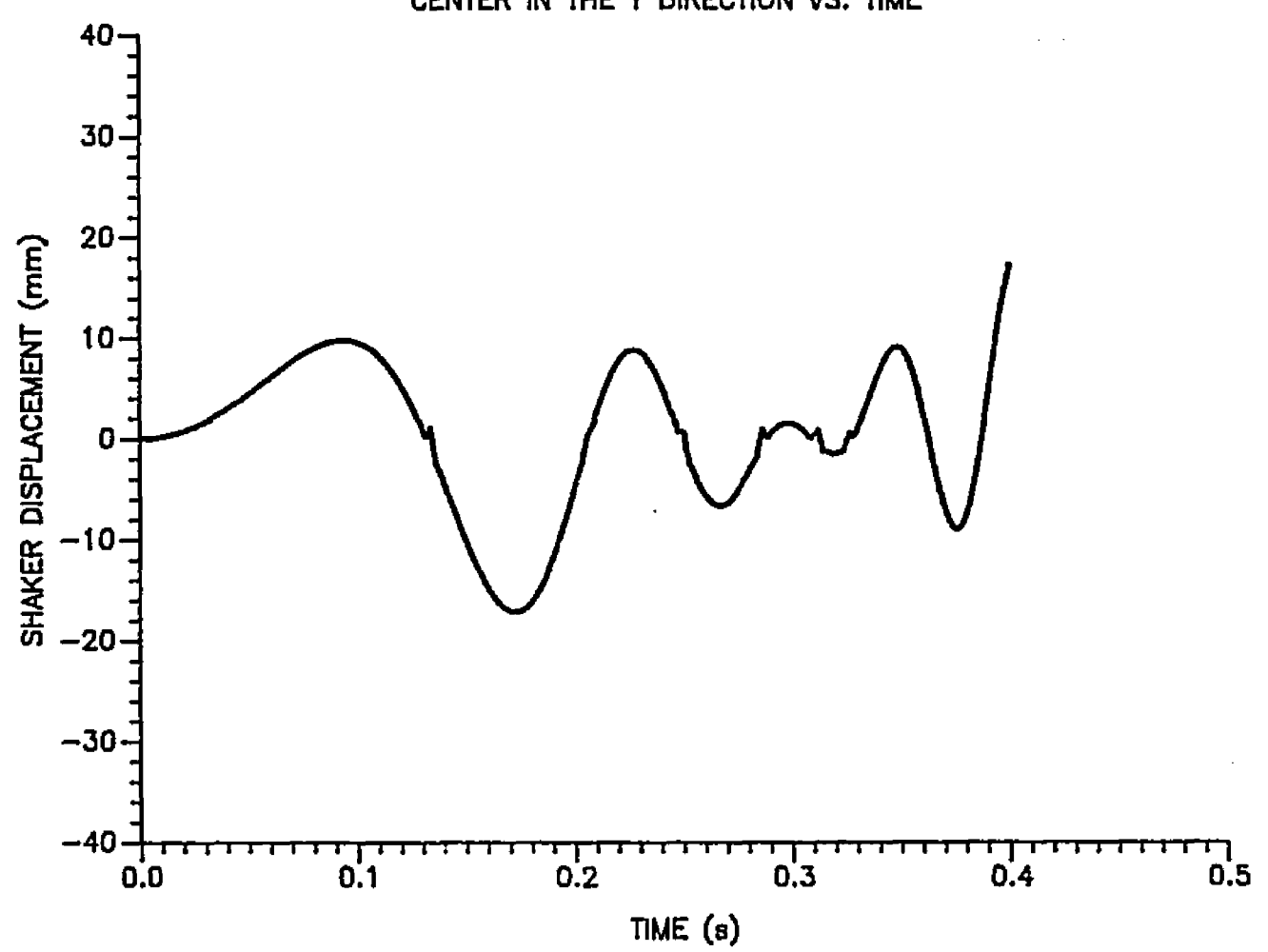


FIGURE 6.29 SHAKER DISPLACEMENT IN THE Y DIRECTION. MASSES ARE RUNNING AT ACCELERATIONS OF 328 AND 246 rad/s.s. AT A STARTING PHASE ANGLE OF 135 DEGREES.

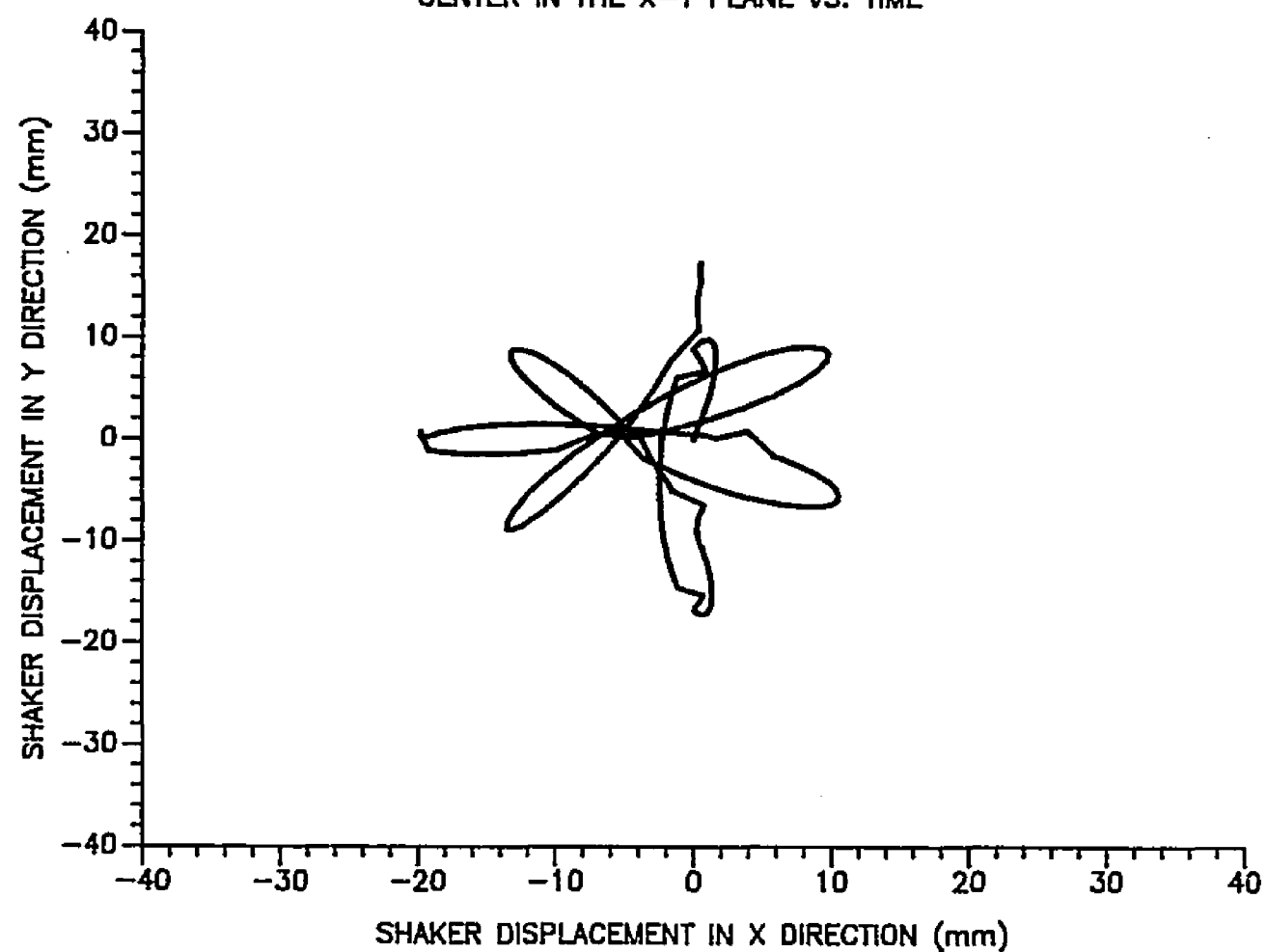


FIGURE 6.30 SHAKER DISPLACEMENT IN THE X-Y PLANE. MASSES ARE RUNNING AT ACCELERATIONS OF 328 AND 246 rad/s.s. At a starting phase angle of 135 degrees.

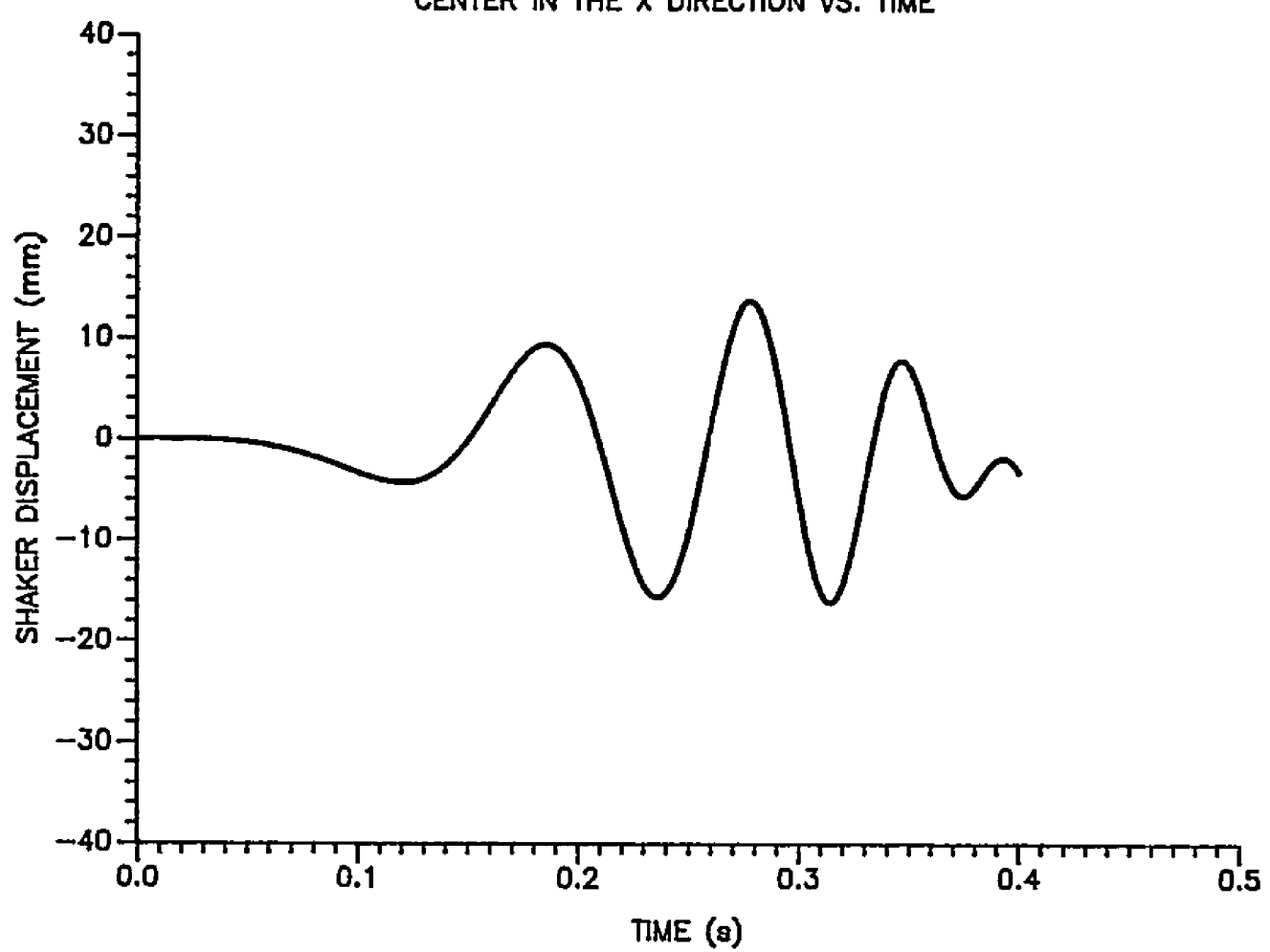


FIGURE 6.31 SHAKER DISPLACEMENT IN THE X DIRECTION. MASSES ARE RUNNING AT ACCELERATIONS OF 328 AND 246 rad/s.s. AT A STARTING PHASE ANGLE OF 180 DEGREES.

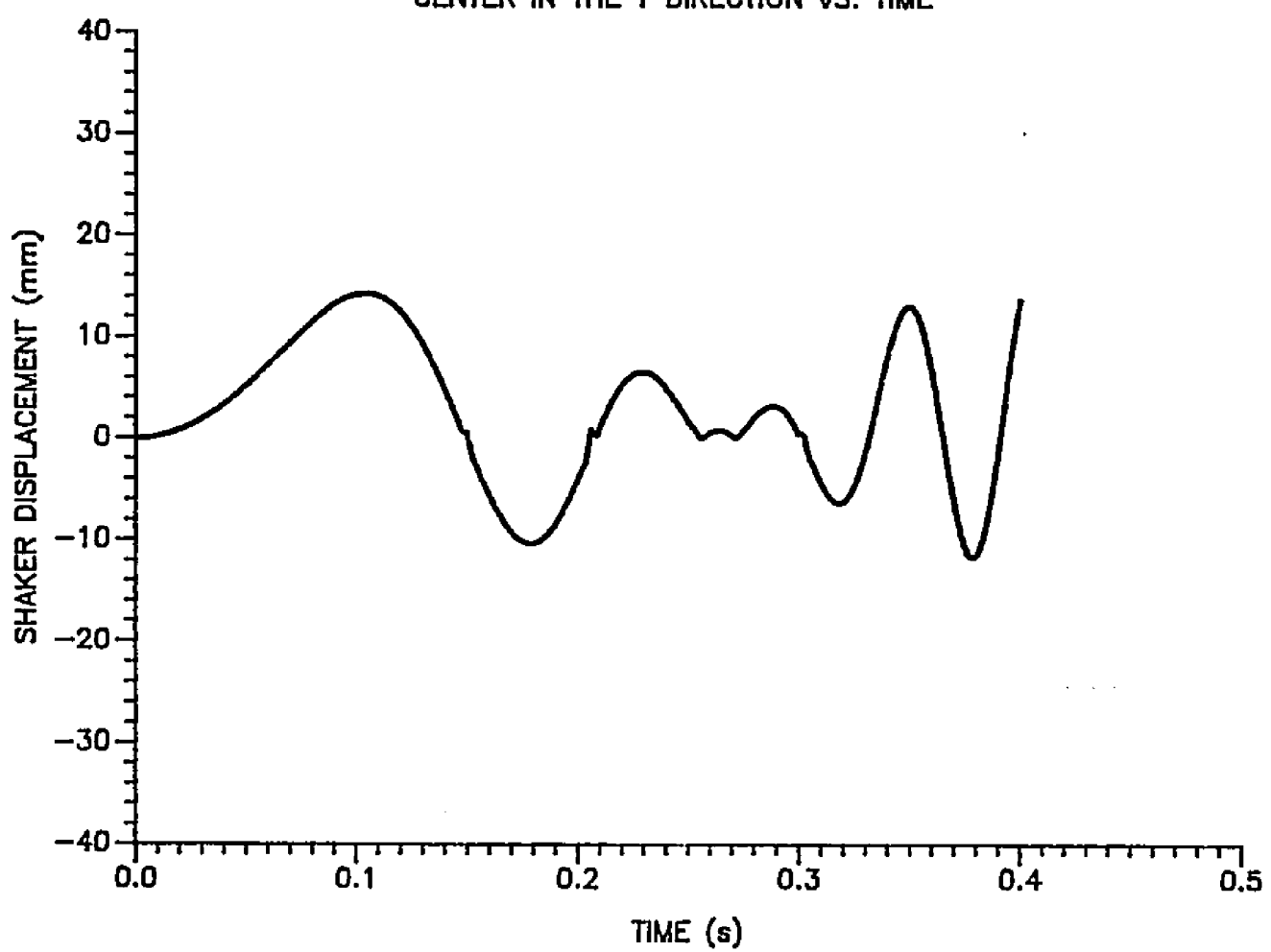


FIGURE 6.32 SHAKER DISPLACEMENT IN THE Y DIRECTION. MASSES ARE RUNNING AT ACCELERATIONS OF 328 AND 246 rad/s.s. AT A STARTING PHASE ANGLE OF 180 DEGREES.

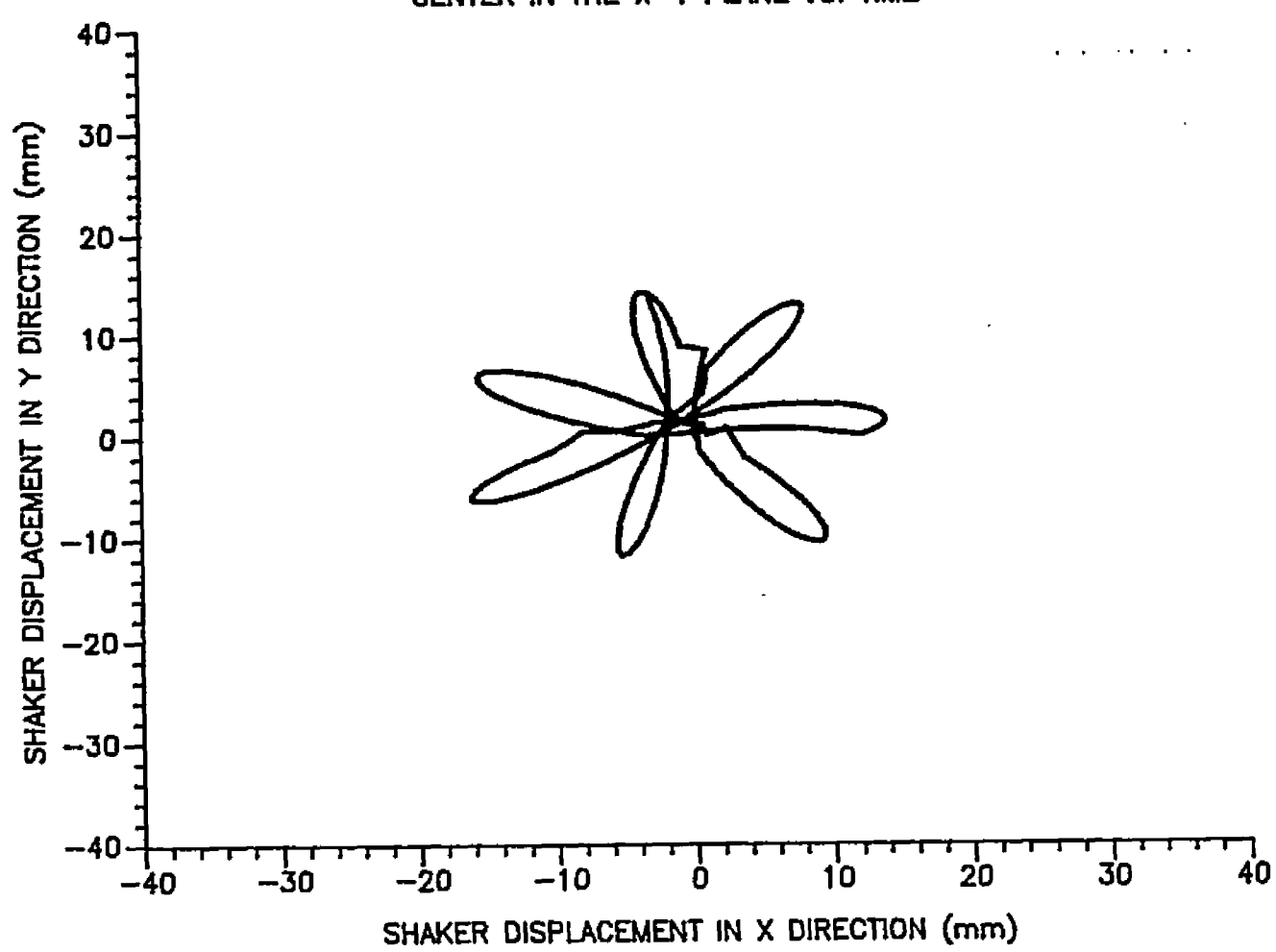


FIGURE 6.33 SHAKER DISPLACEMENT IN THE X-Y PLANE.
MASSES ARE RUNNING AT ACCELERATIONS OF 328 AND 246 rad/s.s. AT A STARTING PHASE ANGLE OF 180 DEGREES.

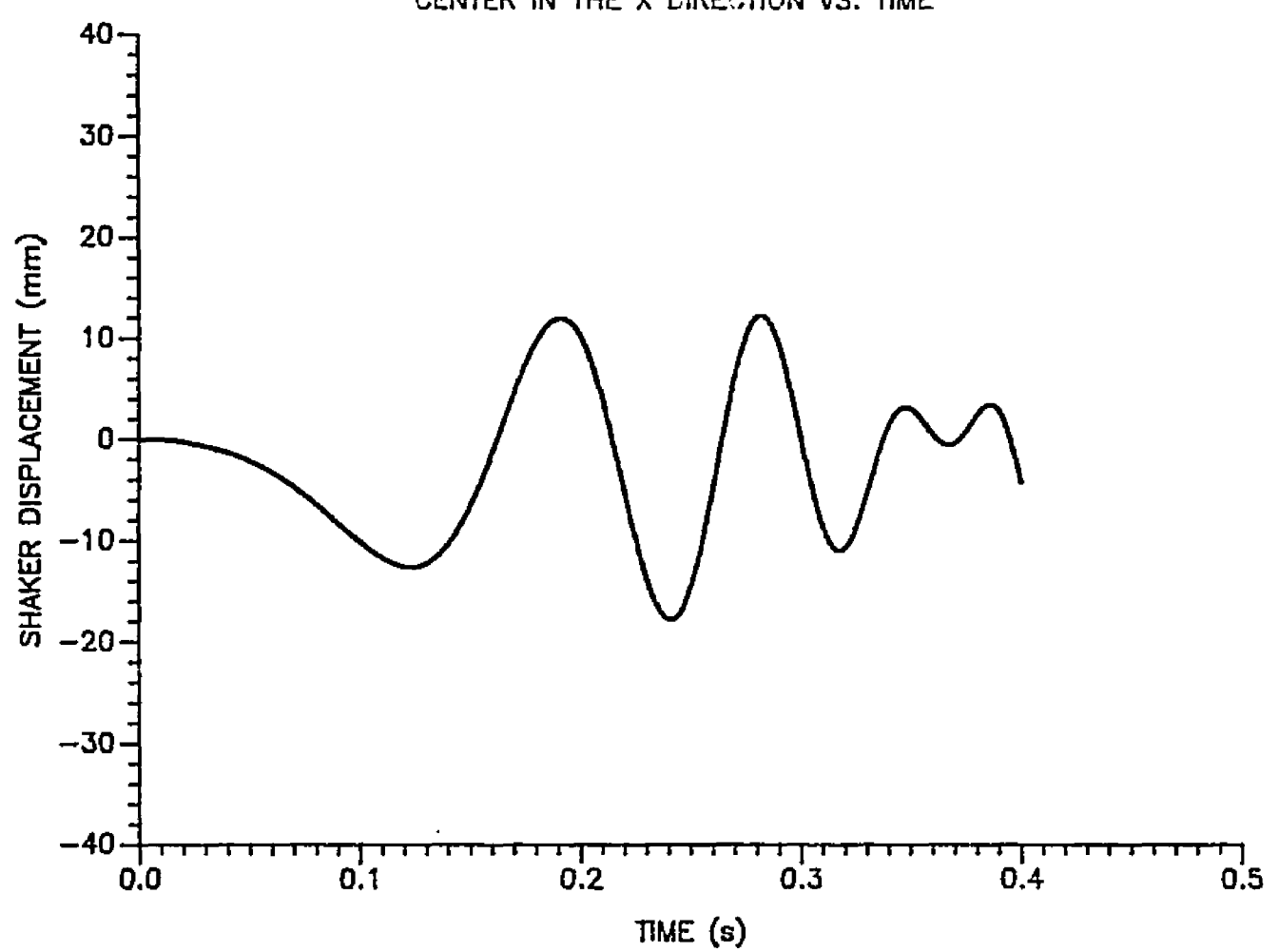


FIGURE 6.34 SHAKER DISPLACEMENT IN THE X DIRECTION. MASSES ARE RUNNING AT ACCELERATIONS OF 328 AND 246 rad/s.s. AT A STARTING PHASE ANGLE OF 225 DEGREES.

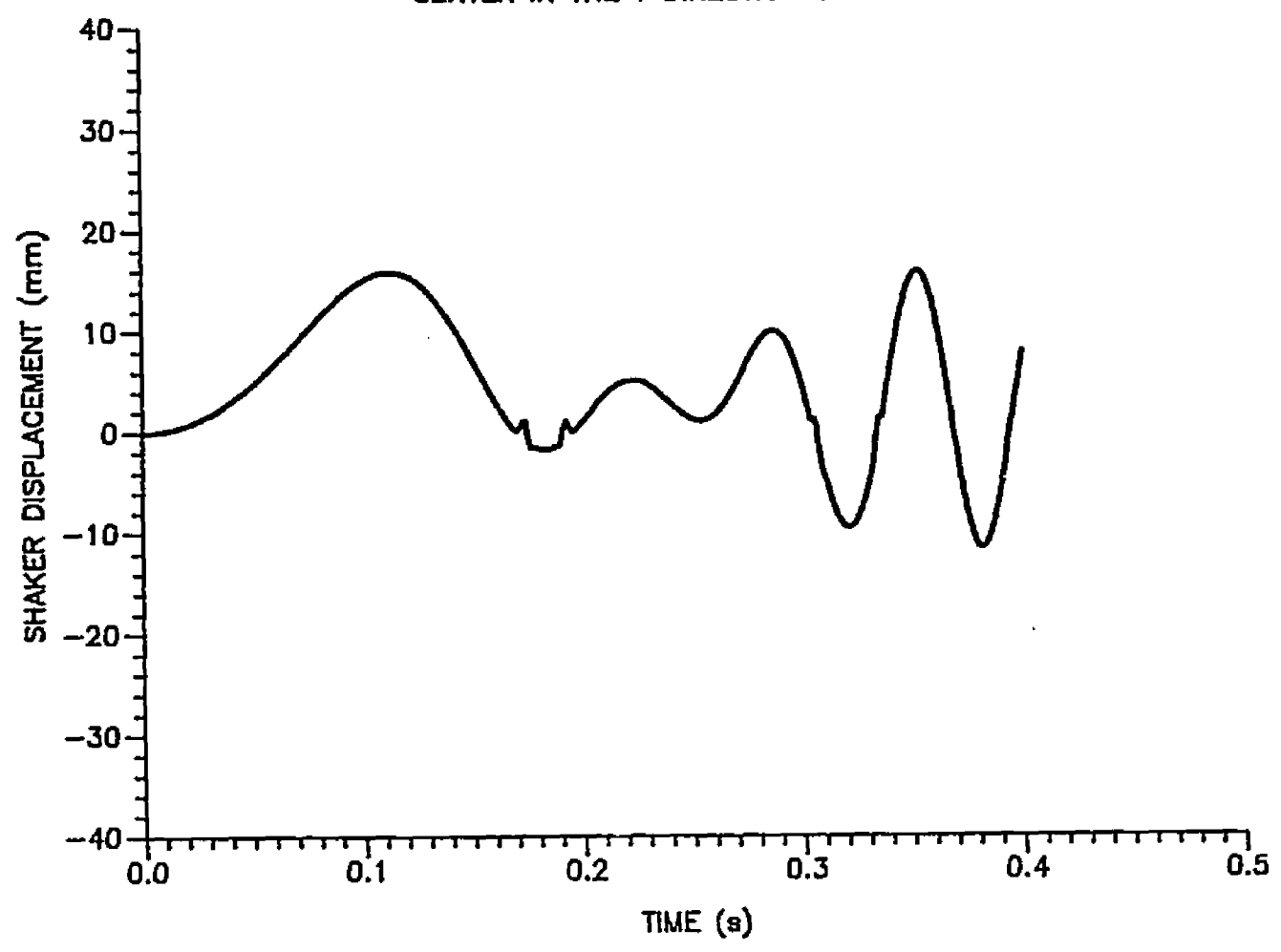


FIGURE 6.35 SHAKER DISPLACEMENT IN THE Y DIRECTION. MASSES ARE RUNNING AT ACCELERATIONS OF 328 AND 246 rdd/s.s. At a starting phase angle of 225 degrees.

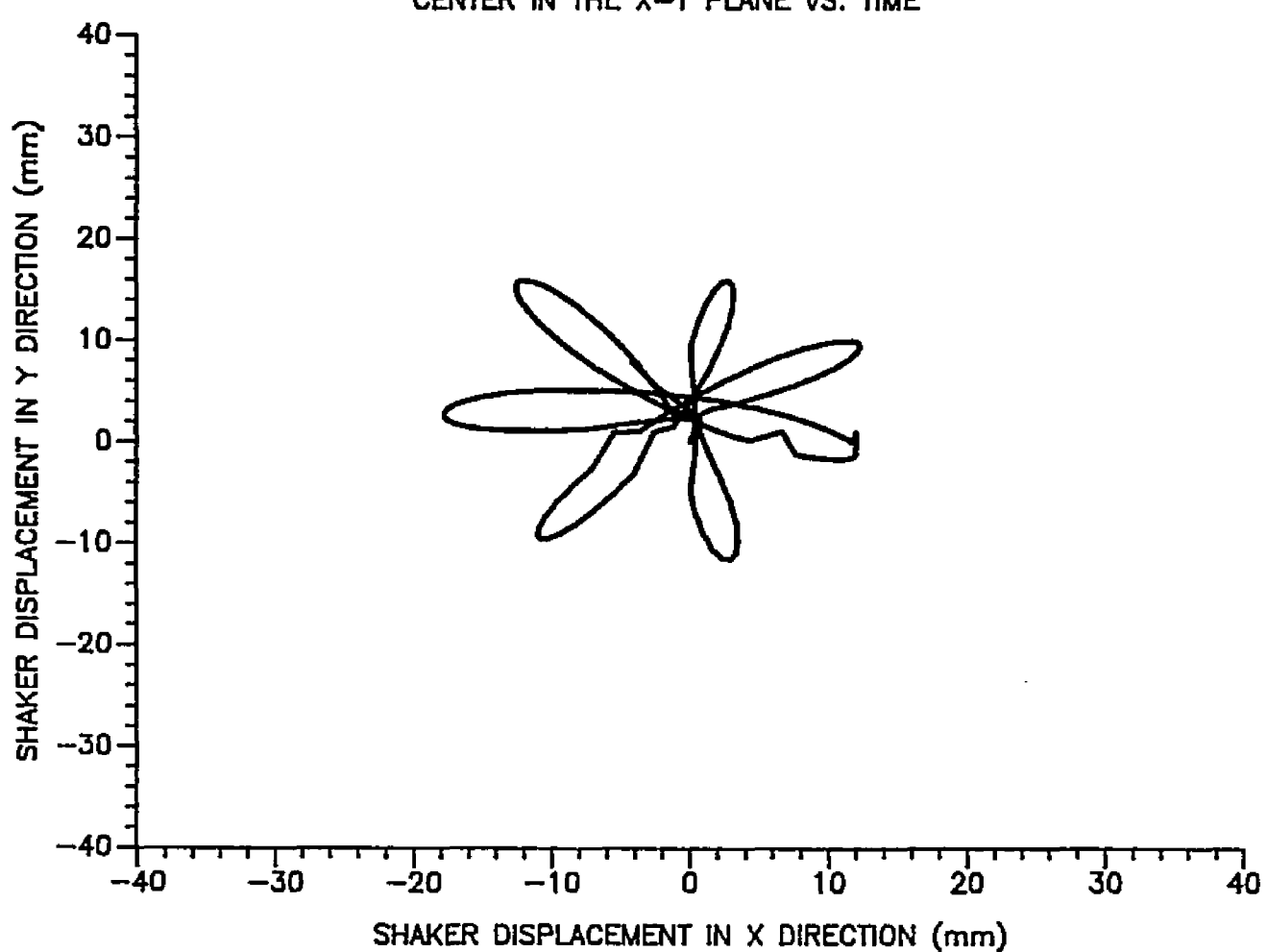


FIGURE 6.36 SHAKER DISPLACEMENT IN THE X-Y PLANE. MASSES ARE RUNNING AT ACCELERATIONS OF 328 AND 246 rad/s.s. At a starting phase angle of 225 degrees.

value of 2 mm (0.07 in.) in the y direction. The shaker gallop in the x direction was also increased, however, no gallop in the y direction was observed; Figures 6.37, 6.38, and 6.39.

When a 315 degree starting phase angle was tested, the shaker shift in the x direction jumped to 15 mm (0.59 in.) with shaker drift of 17 mm (0.67 in.) while the shift and drift maintained a minimum value of 3 mm (0.11 in.) in the y direction. Some signs of shaker instability were observed. The shaker gallop in the x direction was obvious, but no gallop in the y direction was observed, Figures 6.40, 6.41, and 6.42.

A summary of the simulated shaker displacement results at different starting phase angles between the rotating masses is presented in Table 6.1. The results obtained from testing these different starting phase angles at acceleration levels of 328 and 246 rad/s for their affect on the shaker displacement behavior lead to the following conclusions:

- 1- The largest shift, drift and gallop in shaker displacement in the x direction occured at starting phase angles of 0, 45, and 270 degrees, while they occured at 90 and 135 degrees in the y direction.
- 2- The smallest shift, drift and gallop in shaker displacement occured at starting phase angles of

Table 6.1 Summary Of The Simulated Displacement
Results At Different Rotating Mass Starting
Phase Angles.

Direction	Angle (deg.)	Shift (mm)	Drift (mm)	Max. Disp. (mm)	Total Disp.
X	O	14	17	25	42
Z	0	2	5	25	30
X	45	11	12	25	37
Υ.	45	6	10	25	35
X	90	5	5	25	30
γ.	90	9	15	25	40
X	135	0	5	25	30
Υ	135	2	11	25	36
X	180	0	5	25	30
Y	180	0	2	25	27
X	225	0	2	25	27
Y	225	3	3	25	28
X	270	6	8	25	33
Y	270	6	2	25	27
x	315	15	17	25	42
Y	315	3	3	25	28

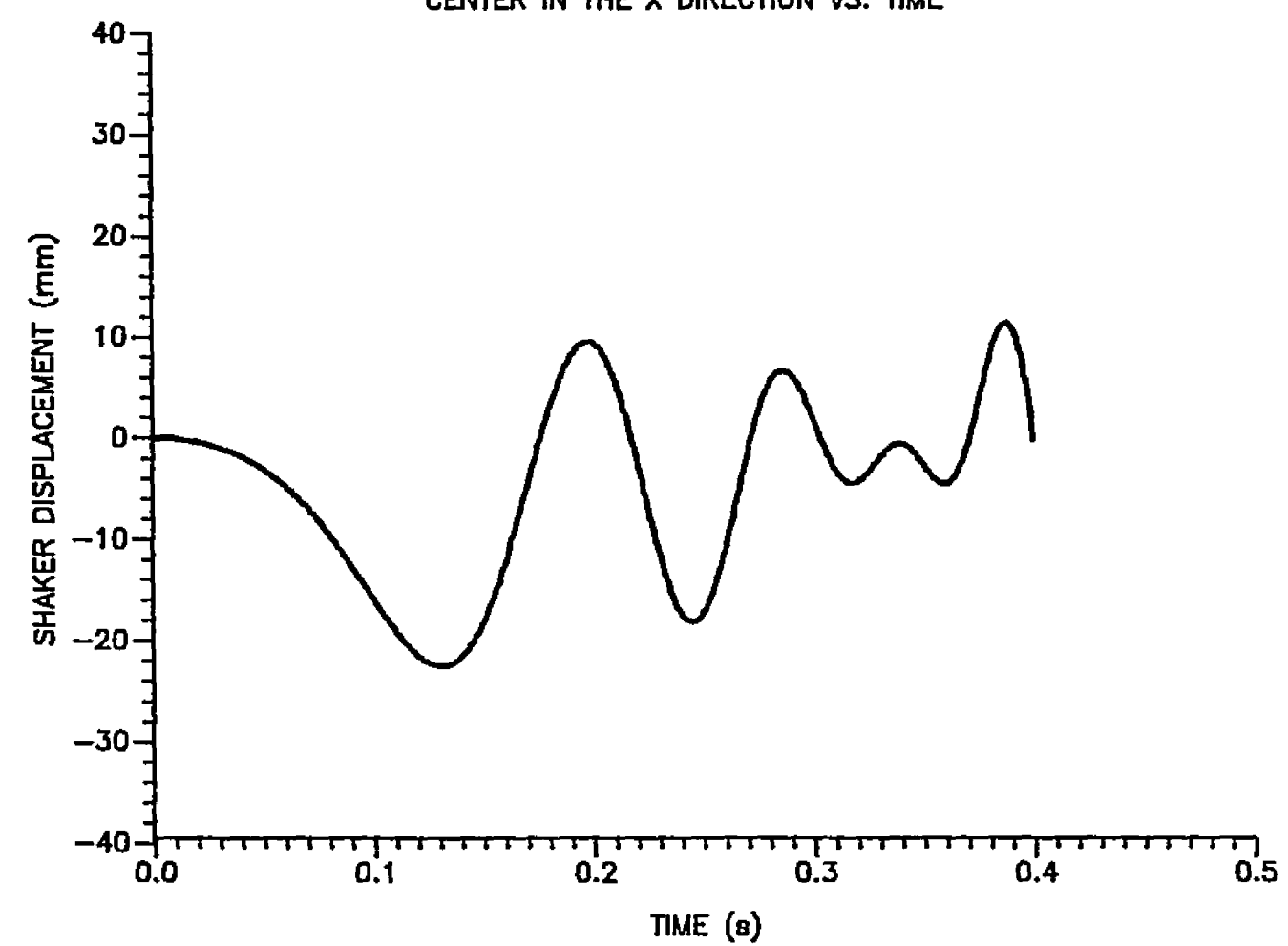


FIGURE 6.37 SHAKER DISPLACEMENT IN THE X DIRECTION. MASSES ARE RUNNING AT ACCELERATIONS OF 328 AND 246 rad/s.s. AT A STARTING PHASE ANGLE OF 270 DEGREES.

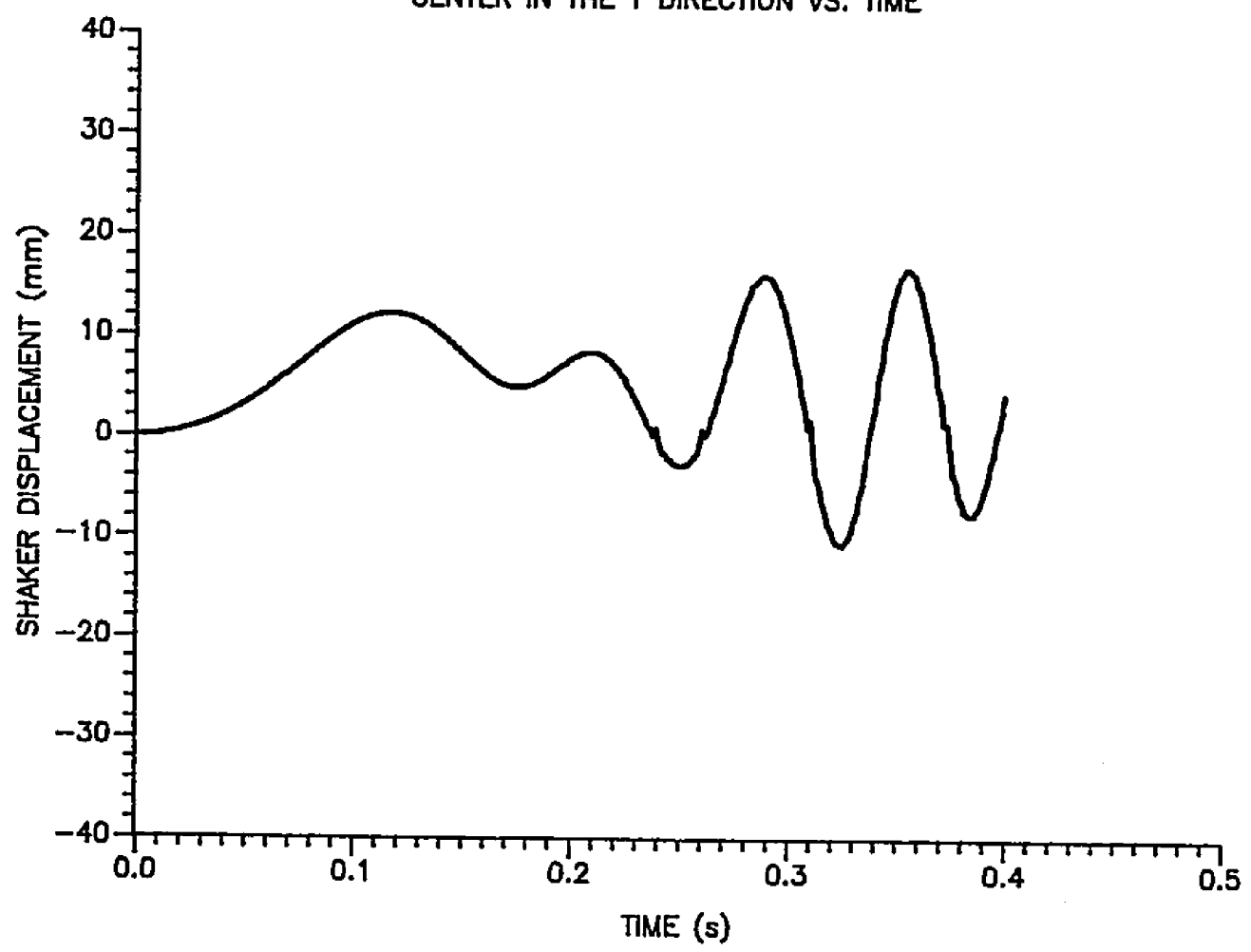


FIGURE 6.38 SHAKER DISPLACEMENT IN THE Y DIRECTION. MASSES ARE RUNNING AT ACCELERATIONS OF 328 AND 246 rad/s.s. At a starting phase angle of 270 degrees.

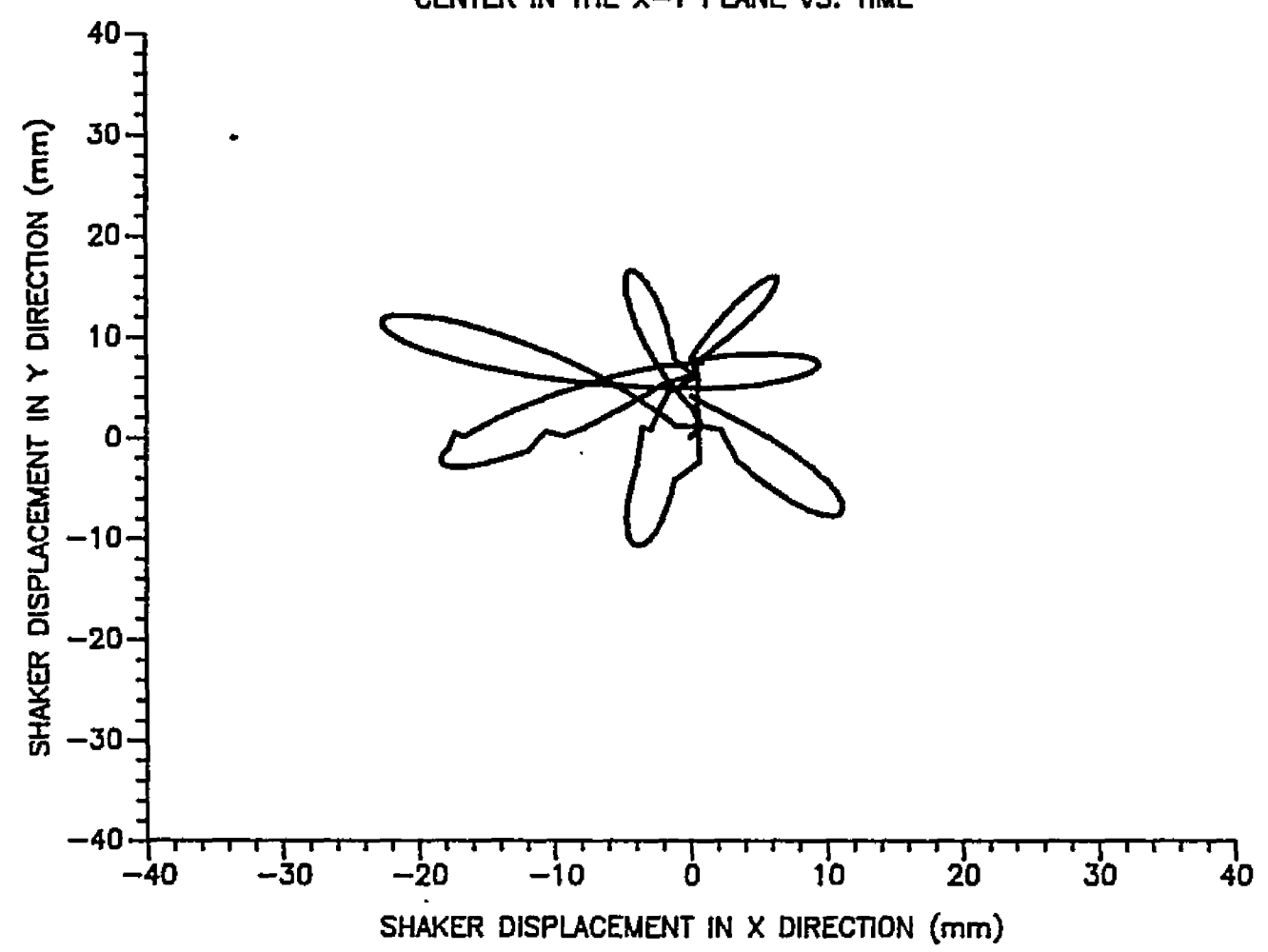


FIGURE 6.39 SHAKER DISPLACEMENT IN THE X-Y PLANE. MASSES ARE RUNNING AT ACCELERATIONS OF 328 AND 246 rad/s.s. AT A STARTING PHASE ANGLE OF 270 DEGREES.

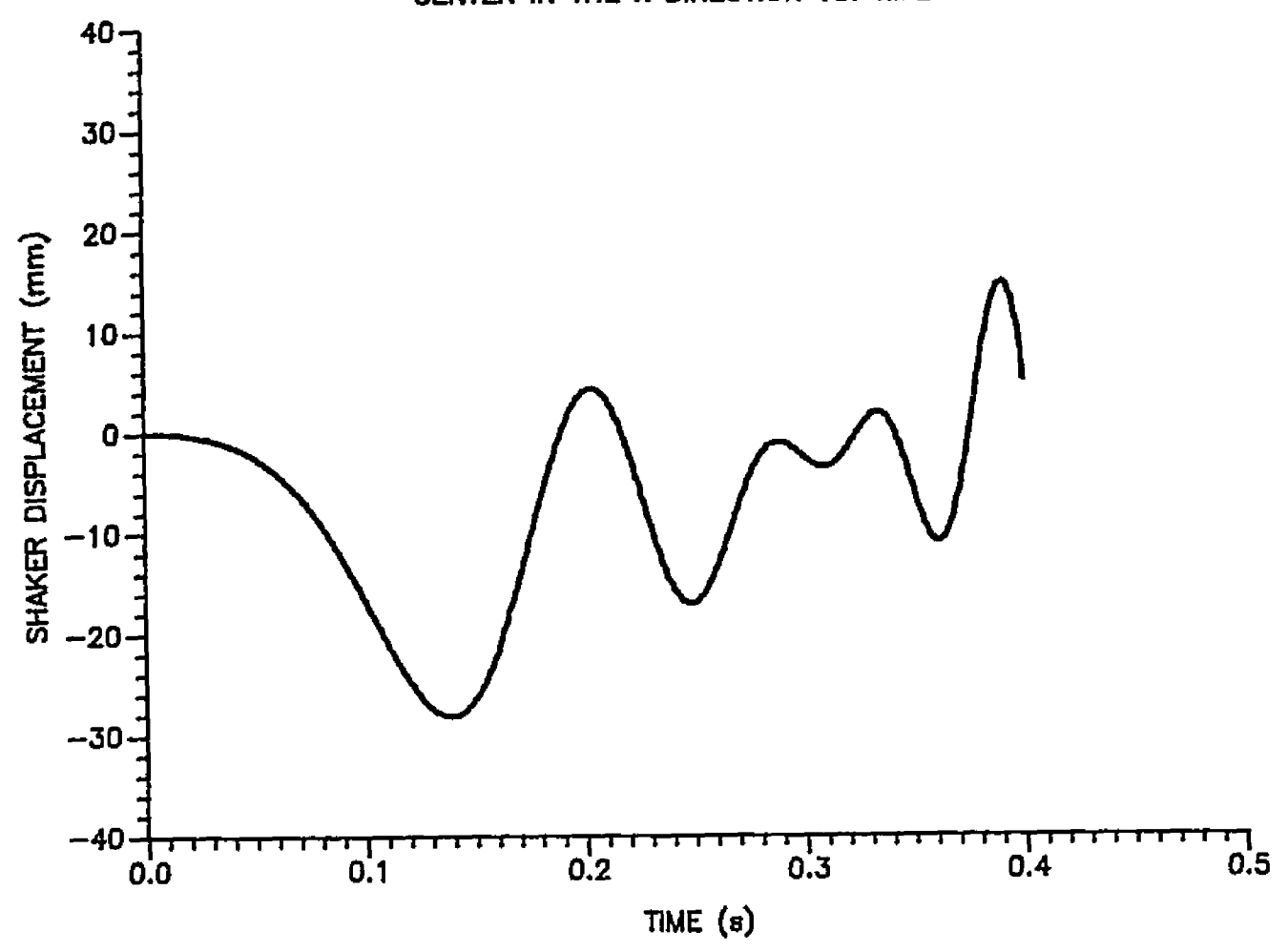


FIGURE 6.40 SHAKER DISPLACEMENT IN THE X DIRECTION. MASSES ARE RUNNING AT ACCELERATIONS OF 328 AND 246 rad/8.8. AT A STARTING PHASE ANGLE OF 315 DEGREES.

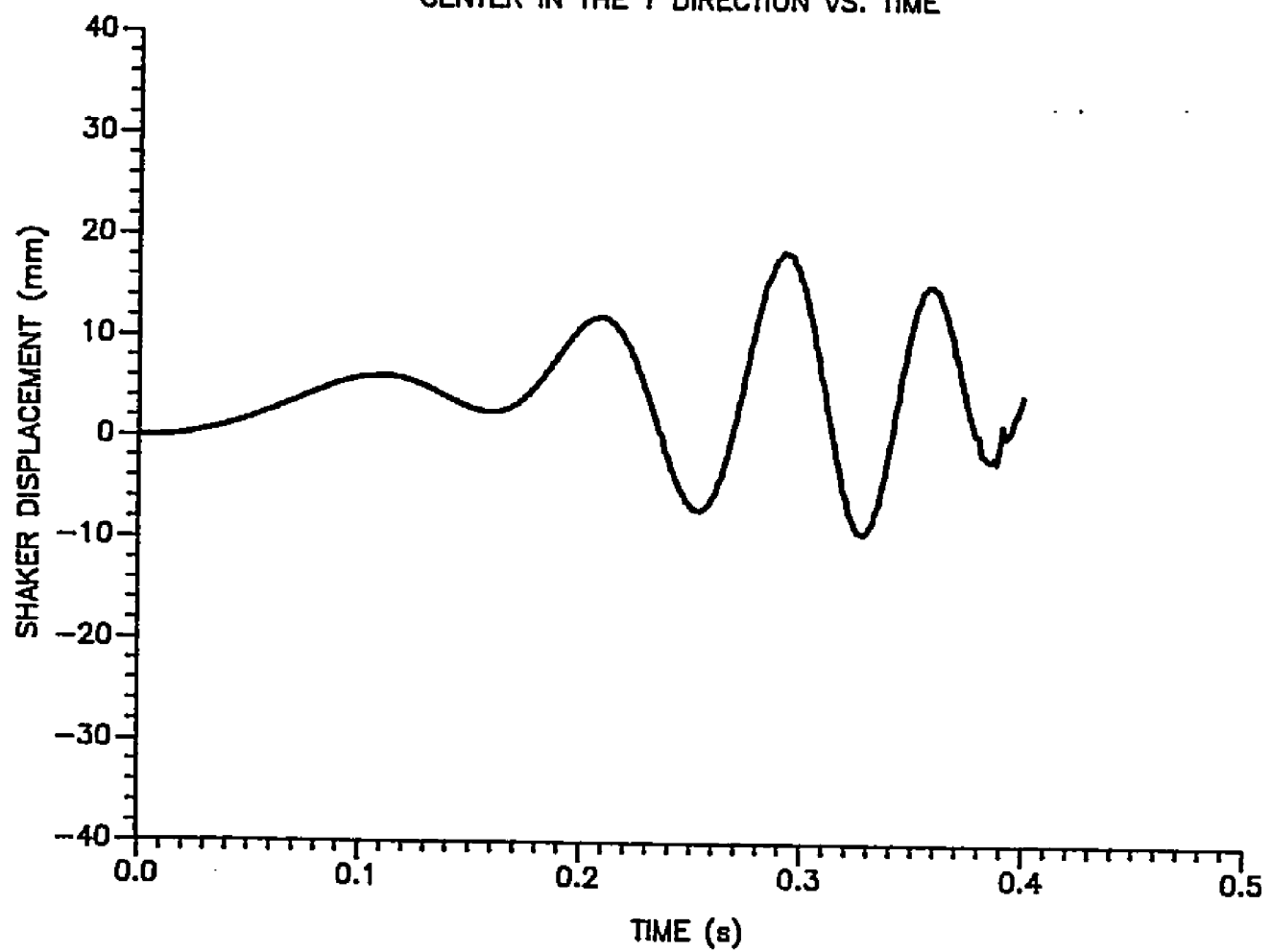


FIGURE 6.41 SHAKER DISPLACEMENT IN THE Y DIRECTION. MASSES ARE RUNNING AT ACCELERATIONS OF 328 AND 246 rad/8.s. At a starting phase angle of 315 degrees.

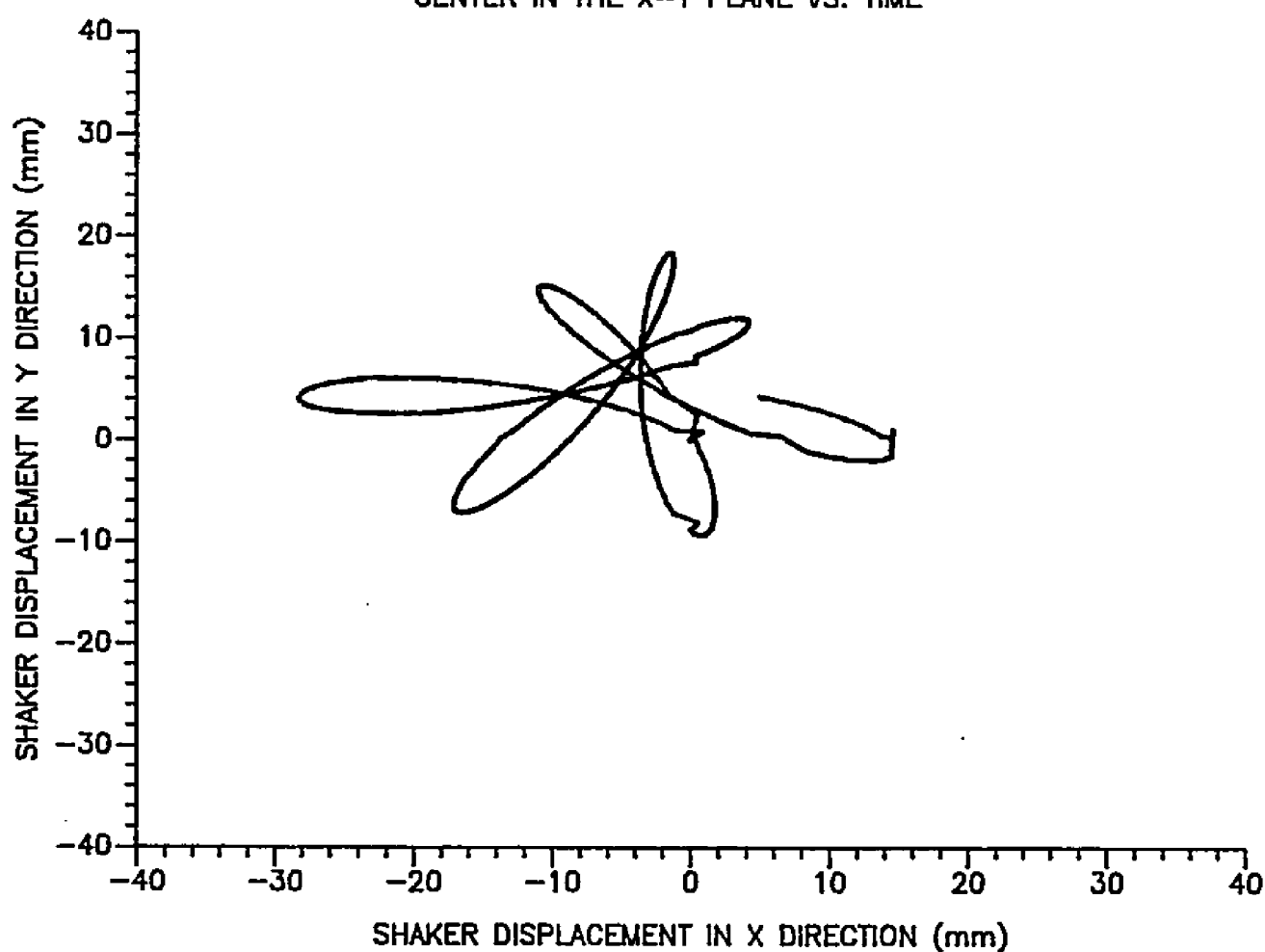


FIGURE 6.42 SHAKER DISPLACEMENT IN THE X-Y PLANE. MASSES ARE RUNNING AT ACCELERATIONS OF 328 AND 246 rad/s.s. AT A STARTING PHASE ANGLE OF 315 DEGREES.

180 and 225 degrees.

3- The shaker shift, drift and gallop problem can be essentially eliminated by using a starting phase of 225 degrees.

The above shaker displacement results for different starting phase angles between the rotating masses raised the question whether the shaker drift was related to the rotating mass acceleration, or to the starting phase angle between them. To answer this question, two starting phase angles that resulted in large drift (zero degrees, Figure 6.21) and small drift (225 degrees, Figure 6.36) were selected for tests at both higher and lower accelerations.

The higher accelerations were 358 and 276 rad/s, and the lower were 298 and 216 rad/s, for the inside and outside masses, respectively.

The model results indicated that by using a starting phase angle of 225 degrees between the masses and two accelerations of 358 and 276 rad/s, the simulated shaker displacement was observed to be stable. Drift was only 5 mm (0.19 in.) and 3 mm (0.11 in.), with no shift, in the x and y directions, respectively, Figures 6.43, 6.44, and 6.45.

Changing the starting phase angle to zero degrees and 2 using the same acceleration values (358 and 276 rad/s ) resulted in unstable shaker displacements. The shaker shift

was 14 mm (0.55 in.) and 2 mm (0.07 in.) in the x and y direction, respectively. The shaker drifted 17 mm (0.66 in.) and 7 mm (0.27 in.) in the x and y directions, respectively, Figures 6.46, 6.47, and 6.48.

These results reflect the same displacement results obtained at the same starting phase angles (zero and 225 degrees, Figures 6.21 and 6.36) but at two different acceleration levels (328 and 246 rad/s ).

The same shaker displacement results were also obtained using lower acceleration levels of 298 and 216 2 rad/s, compared with the original acceleration levels (328 and 246 rad/s) at starting phase angles of zero and 225 degrees, Figures 6.49 to 6.54.

The results regarding shaker displacement behavior using high and low acceleration levels at two starting phase angles of zero and 225 degrees indicated that shaker drift was not affected by using different unequal rotating mass accelerations. Shaker drift seems only related to the starting phase angle between the rotating masses.

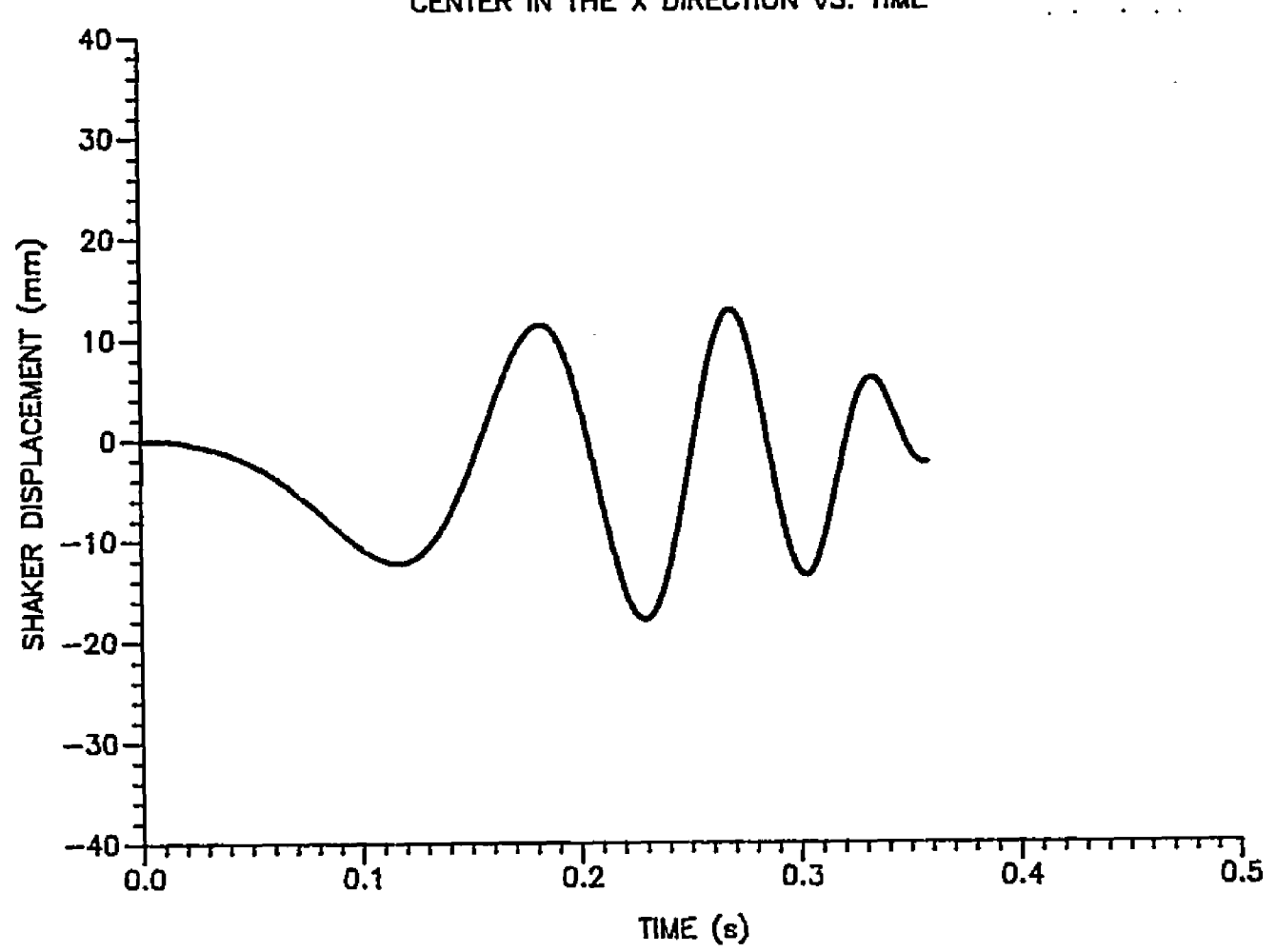


FIGURE 6.43 SHAKER DISPLACEMENT IN THE X DIRECTION. MASSES ARE RUNNING AT ACCELERATIONS OF 358 AND 276 rad/s.s. AT A STARTING PHASE ANGLE OF 225 DEGREES.

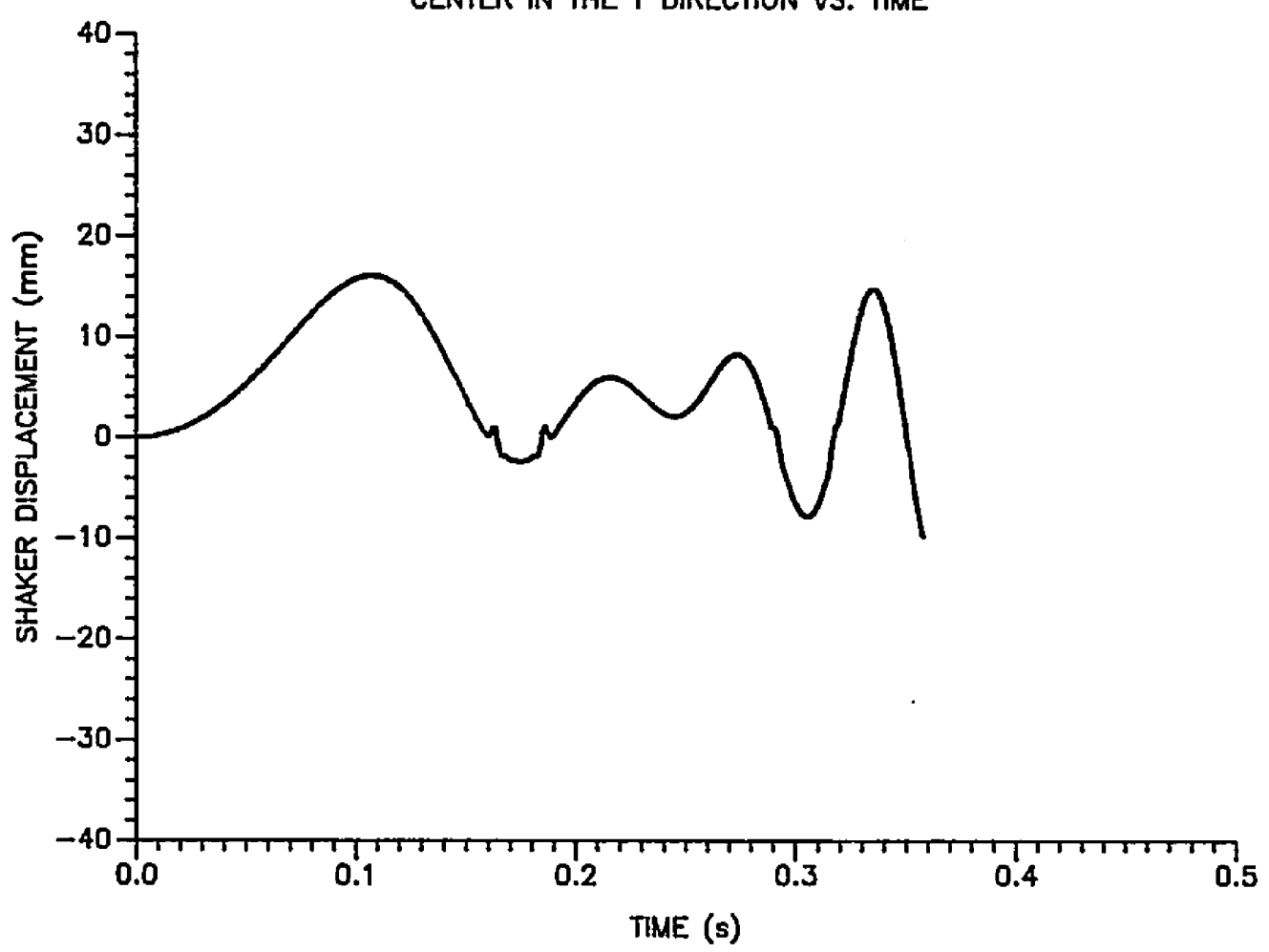


FIGURE 6.44 SHAKER DISPLACEMENT IN THE Y DIRECTION. MASSES ARE RUNNING AT ACCELERATIONS OF 358 AND 276 rad/s.s. AT A STARTING PHASE ANGLE OF 225 DEGREES.

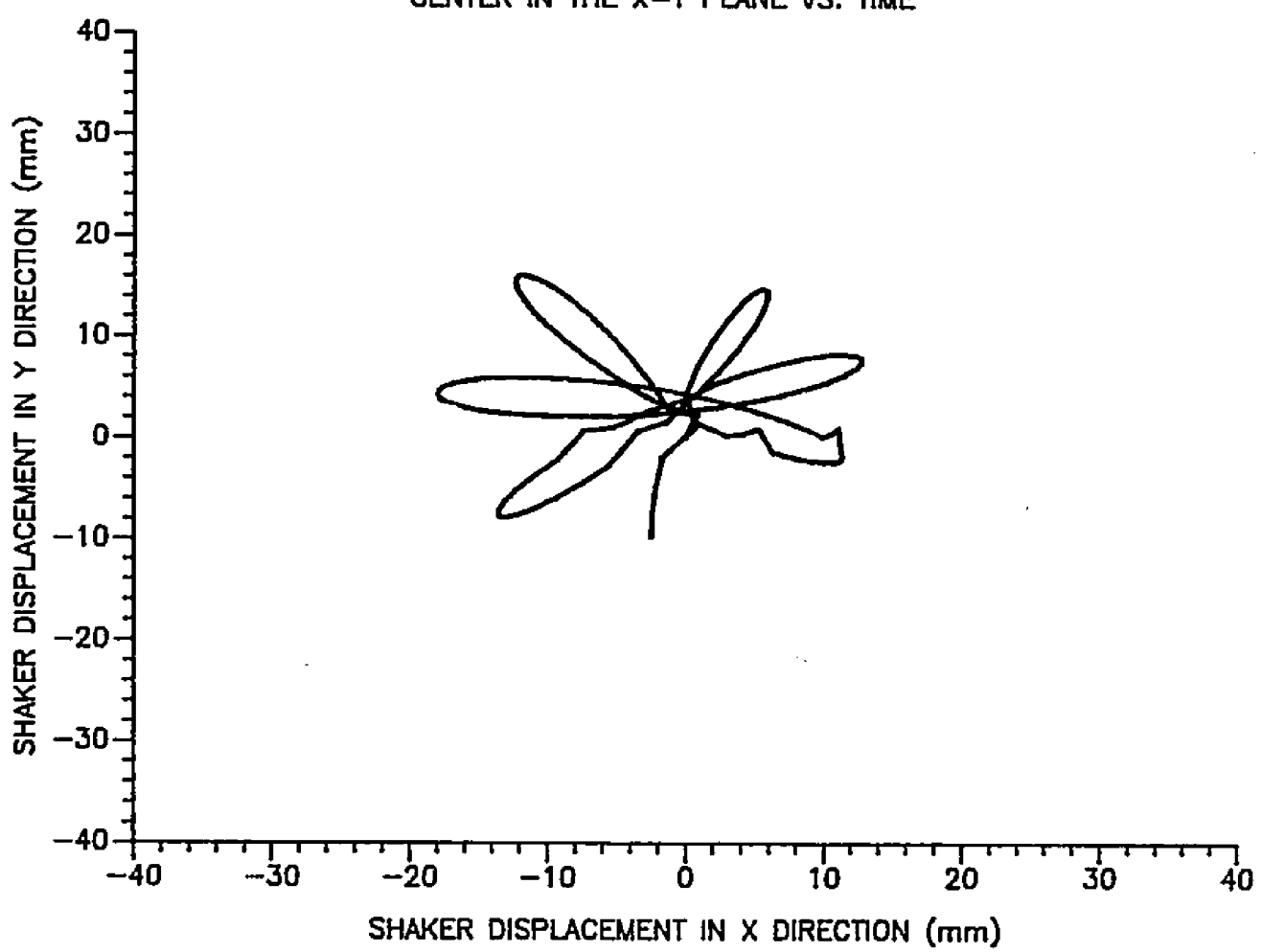


FIGURE 6.45 SHAKER DISPLACEMENT IN THE X-Y PLANE. MASSES ARE RUNNING AT ACCELERATIONS OF 358 AND 276 rad/s.s. AT A STARTING PHASE ANGLE OF 225 DEGREES.

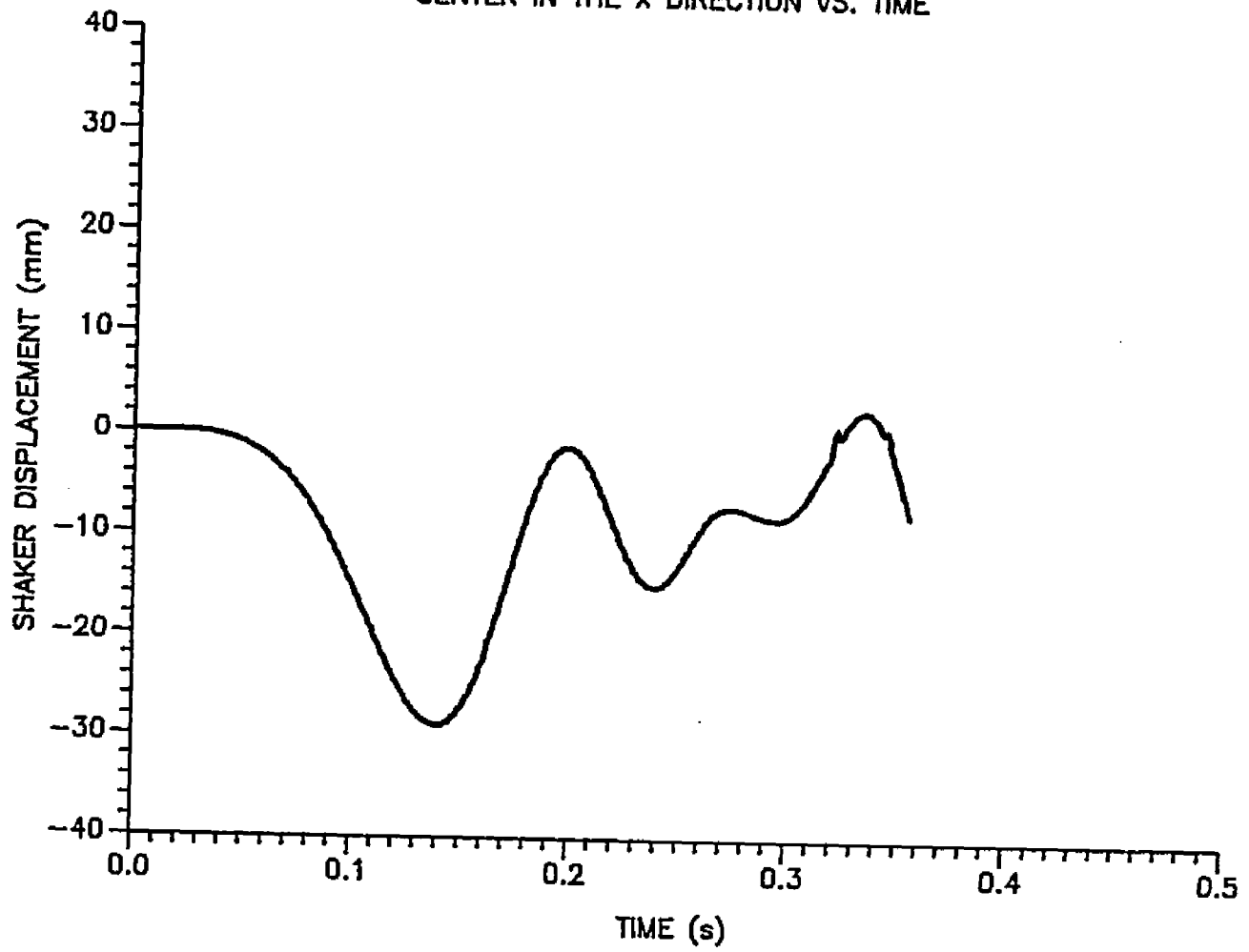


FIGURE 6.46 SHAKER DISPLACEMENT IN THE X DIRECTION MASSES ARE RUNNING AT ACCELERATIONS OF 358 AND 276 rad/s.s. At a starting phase angle of 0 degrees.

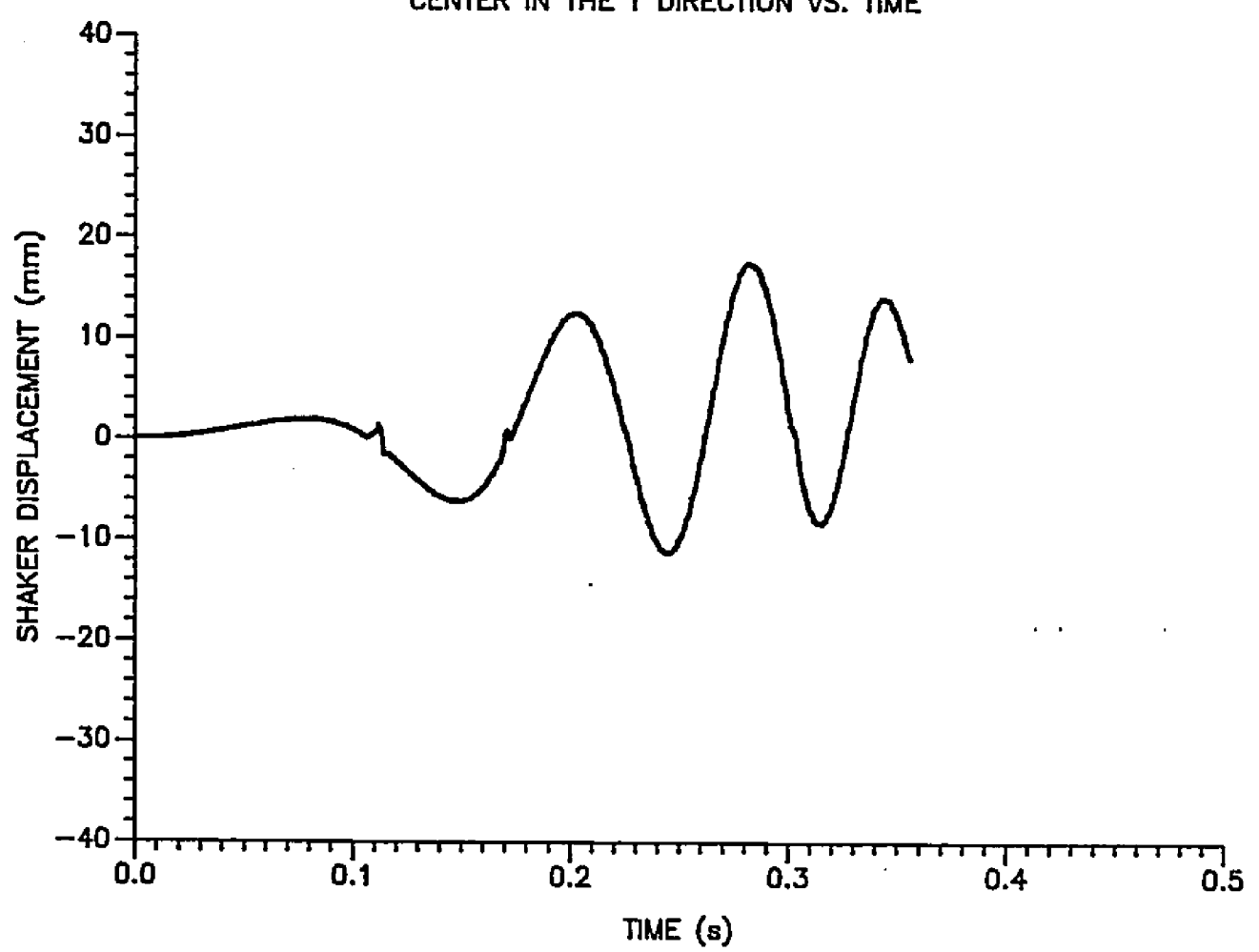
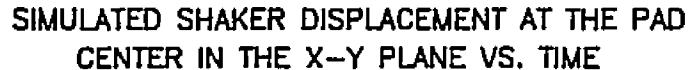


FIGURE 6.47 SHAKER DISPLACEMENT IN THE Y DIRECTION. MASSES ARE RUNNING AT ACCELERATIONS OF 358 AND 276 rad/s.s. AT A STARTING PHASE ANGLE OF 0 DEGREES.



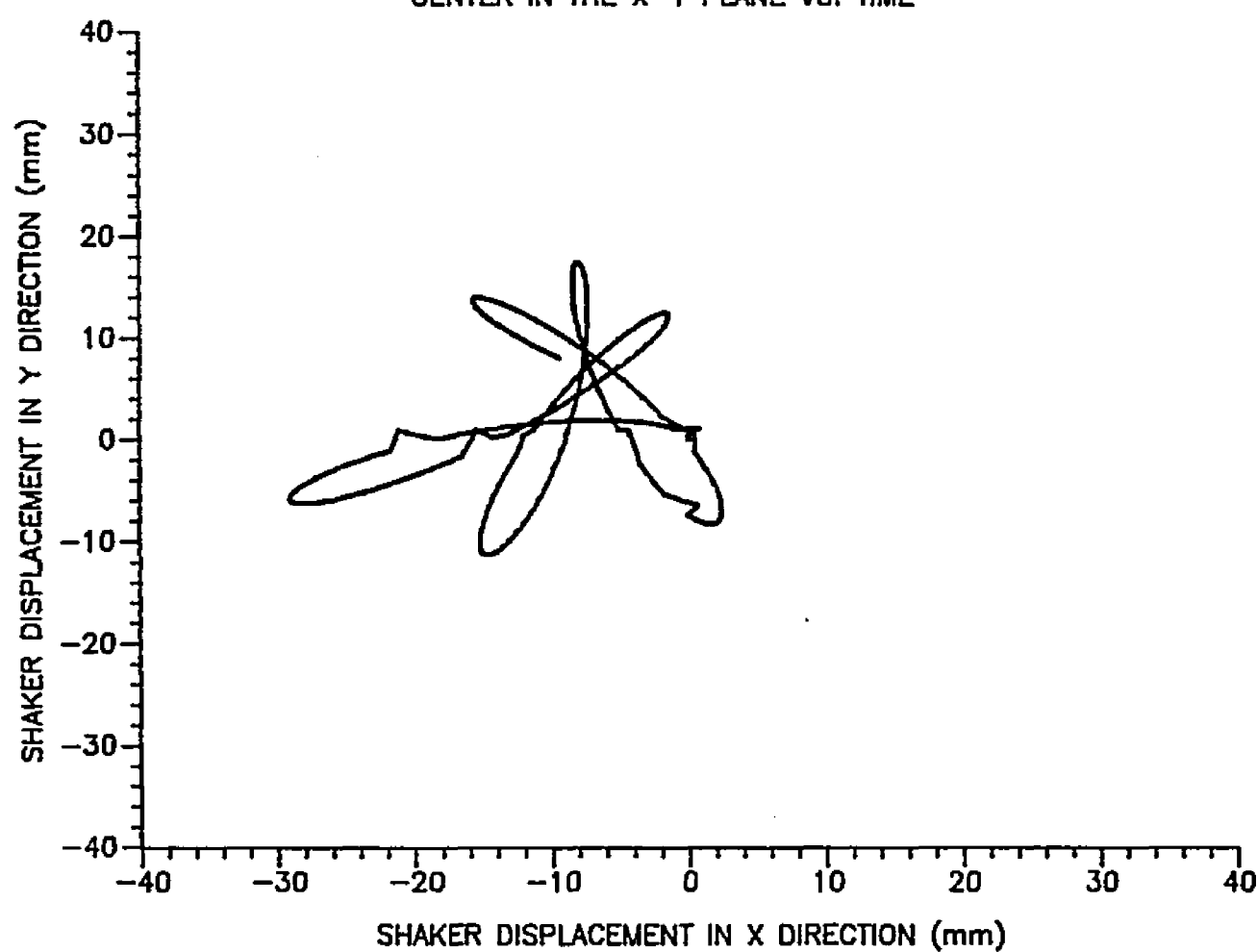


FIGURE 6.48 SHAKER DISPLACEMENT IN THE X-Y PLANE. MASSES ARE RUNNING AT ACCELERATIONS OF 358 AND 276 rad/s.s. AT A STARTING PHASE ANGLE OF 0 DEGREES.

# SIMULATED SHAKER DISPLACEMENT AT THE PAD CENTER IN THE X DIRECTION VS. TIME

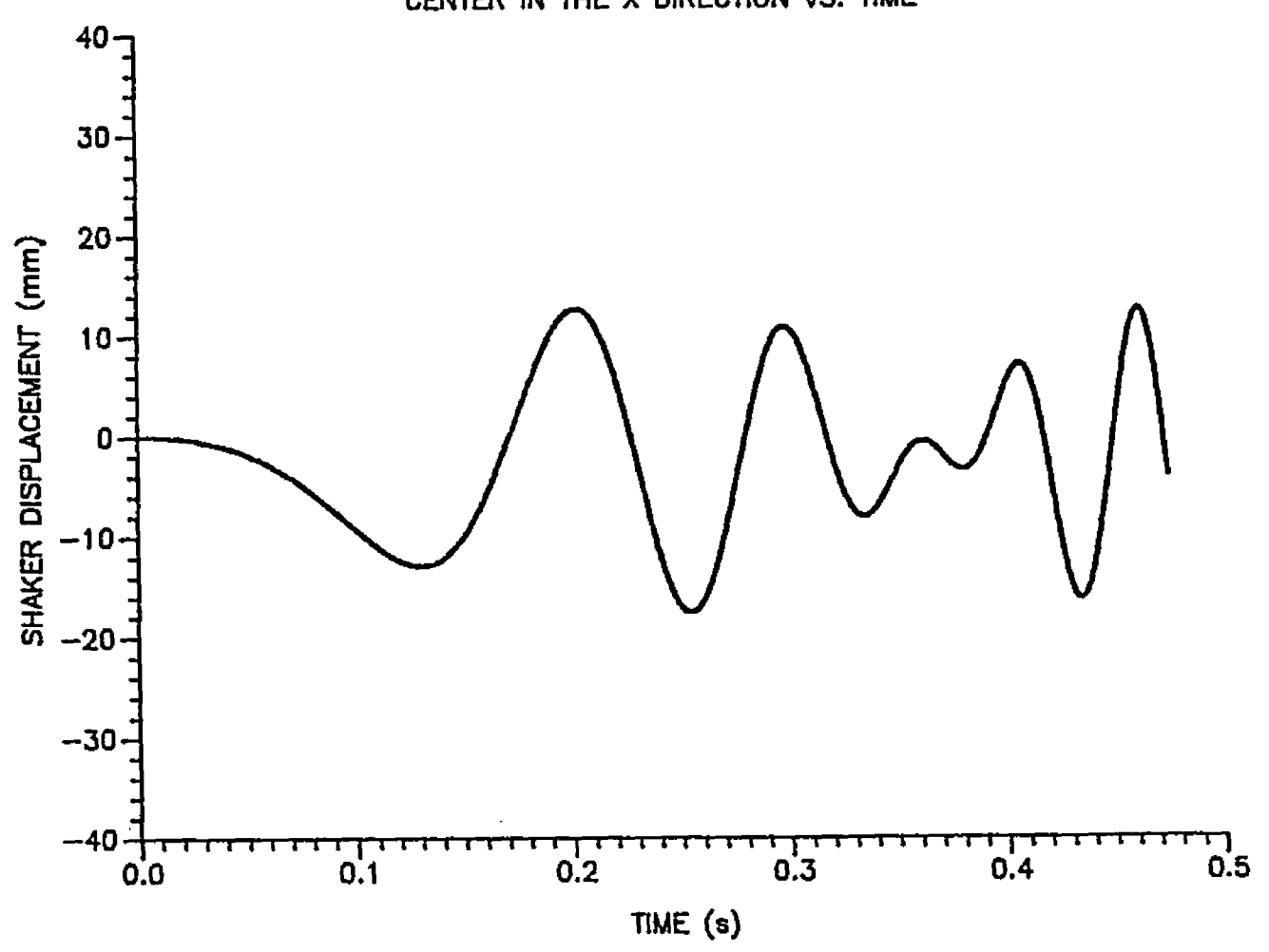


FIGURE 6.49 SHAKER DISPLACEMENT IN THE X DIRECTION.
MASSES ARE RUNNING AT ACCELERATIONS OF 298 AND 216
rad/s.s. AT A STARTING PHASE ANGLE OF 225 DEGREES.

# SIMULATED SHAKER DISPLACEMENT AT THE PAD CENTER IN THE Y DIRECTION VS. TIME

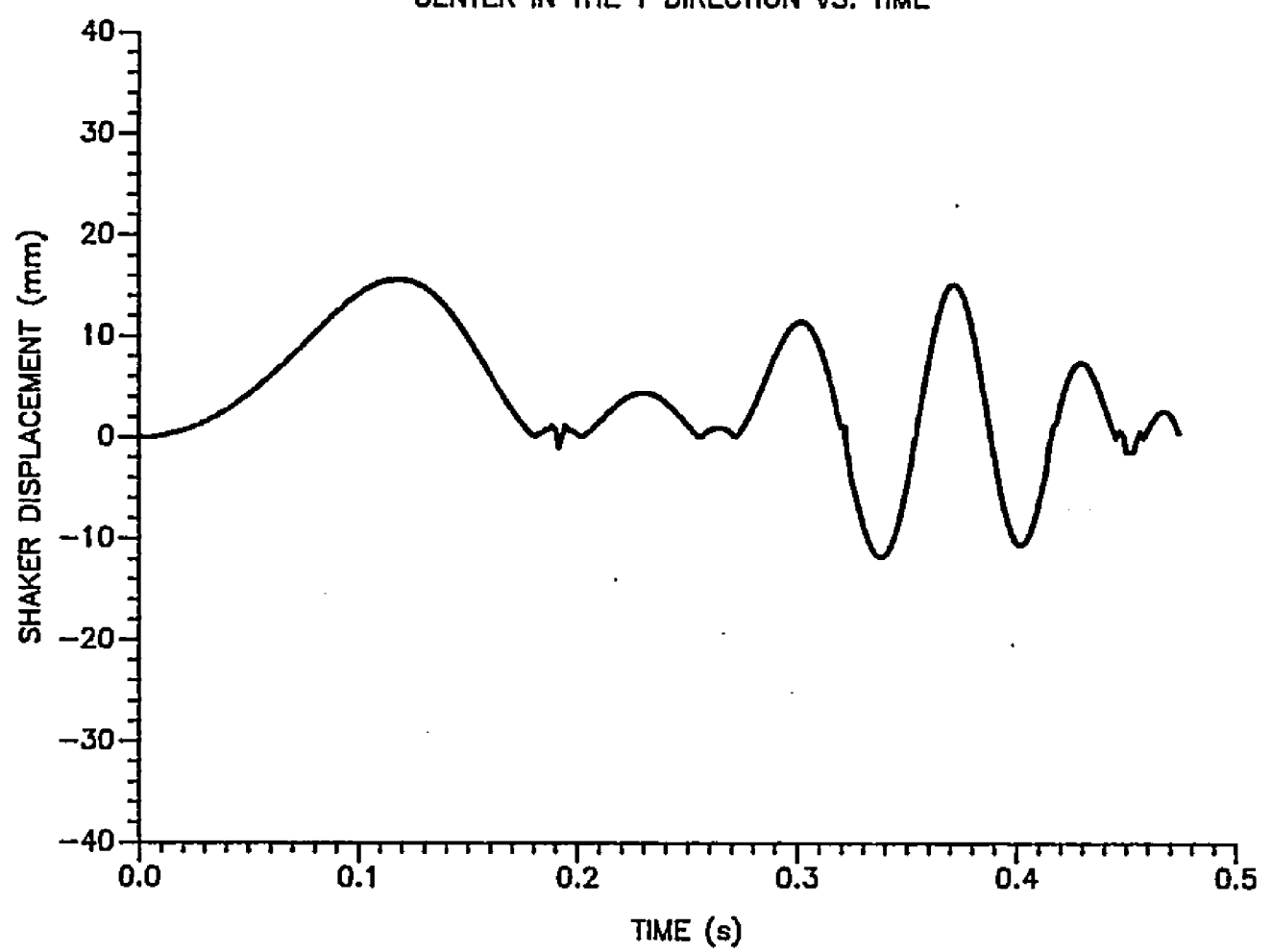


FIGURE 6.50 SHAKER DISPLACEMENT IN THE Y DIRECTION. MASSES ARE RUNNING AT ACCELERATIONS OF 298 AND 216 rad/s.s. AT A STARTING PHASE ANGLE OF 225 DEGREES.

# SIMULATED SHAKER DISPLACEMENT AT THE PAD CENTER IN THE X-Y PLANE VS. TIME

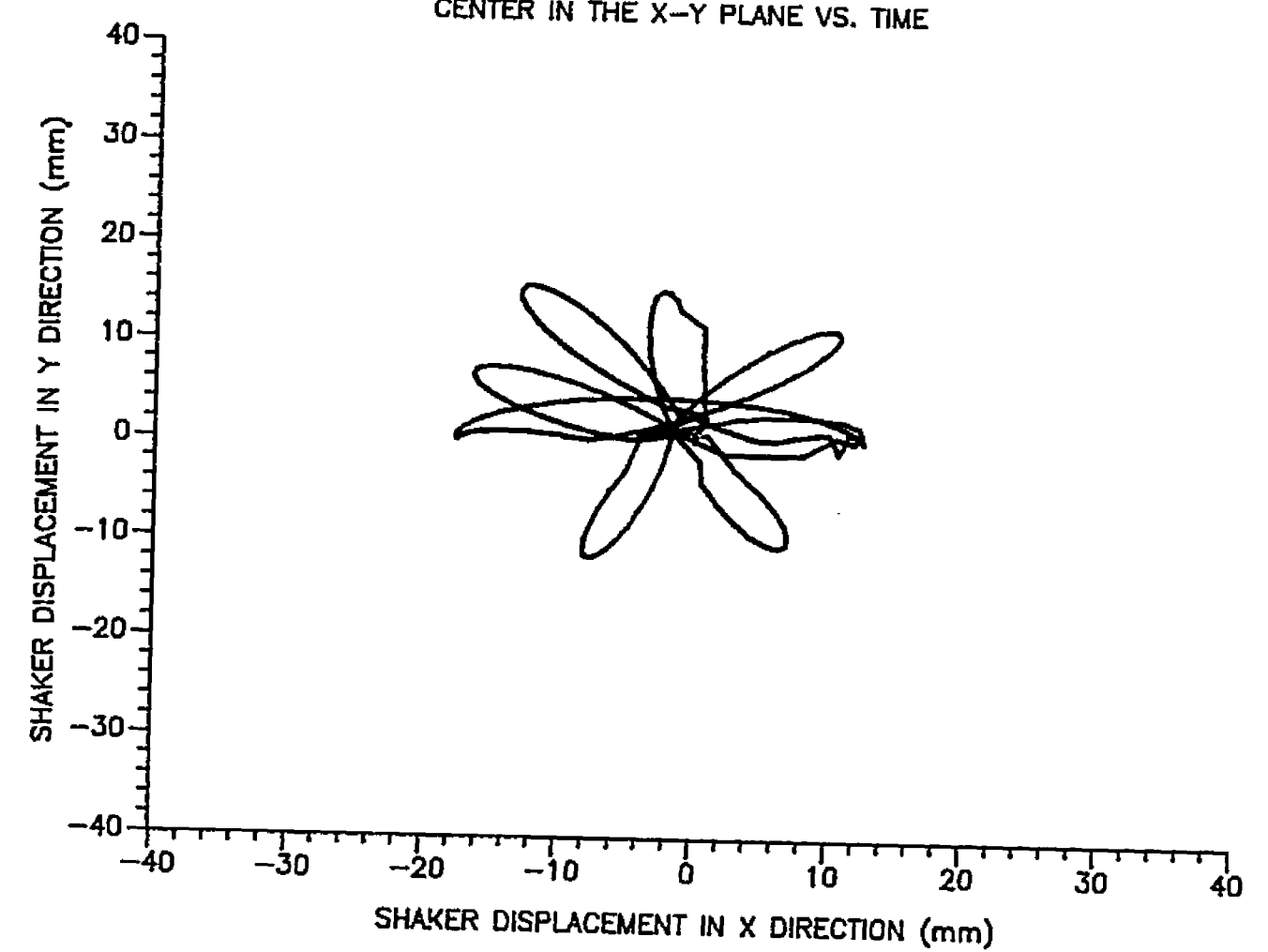


FIGURE 6.51 SHAKER DISPLACEMENT IN THE X-Y PLANE. MASSES ARE RUNNING AT ACCELERATIONS OF 298 AND 216 rad/s.s. AT A STARTING PHASE ANGLE OF 225 DEGREES.

## SIMULATED SHAKER DISPLACEMENT AT THE PAD CENTER IN THE X DIRECTION VS. TIME

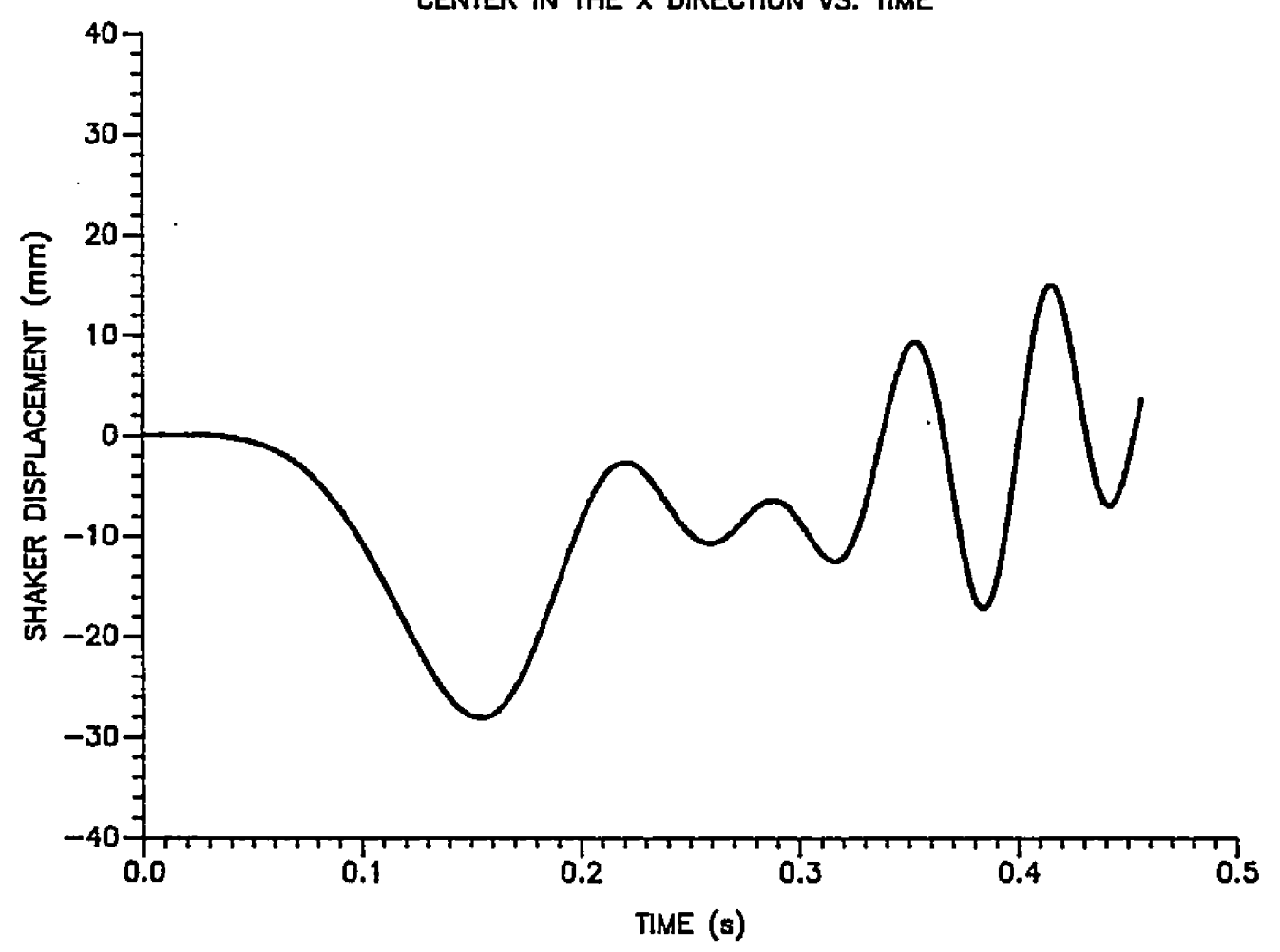


FIGURE 6.52 SHAKER DISPLACEMENT IN THE X DIRECTION MASSES ARE RUNNING AT ACCELERATIONS OF 298 AND 216 rad/s.s. AT A STARTING PHASE ANGLE OF 0 DEGREES.

# SIMULATED SHAKER DISPLACEMENT AT THE PAD CENTER IN THE Y DIRECTION VS. TIME

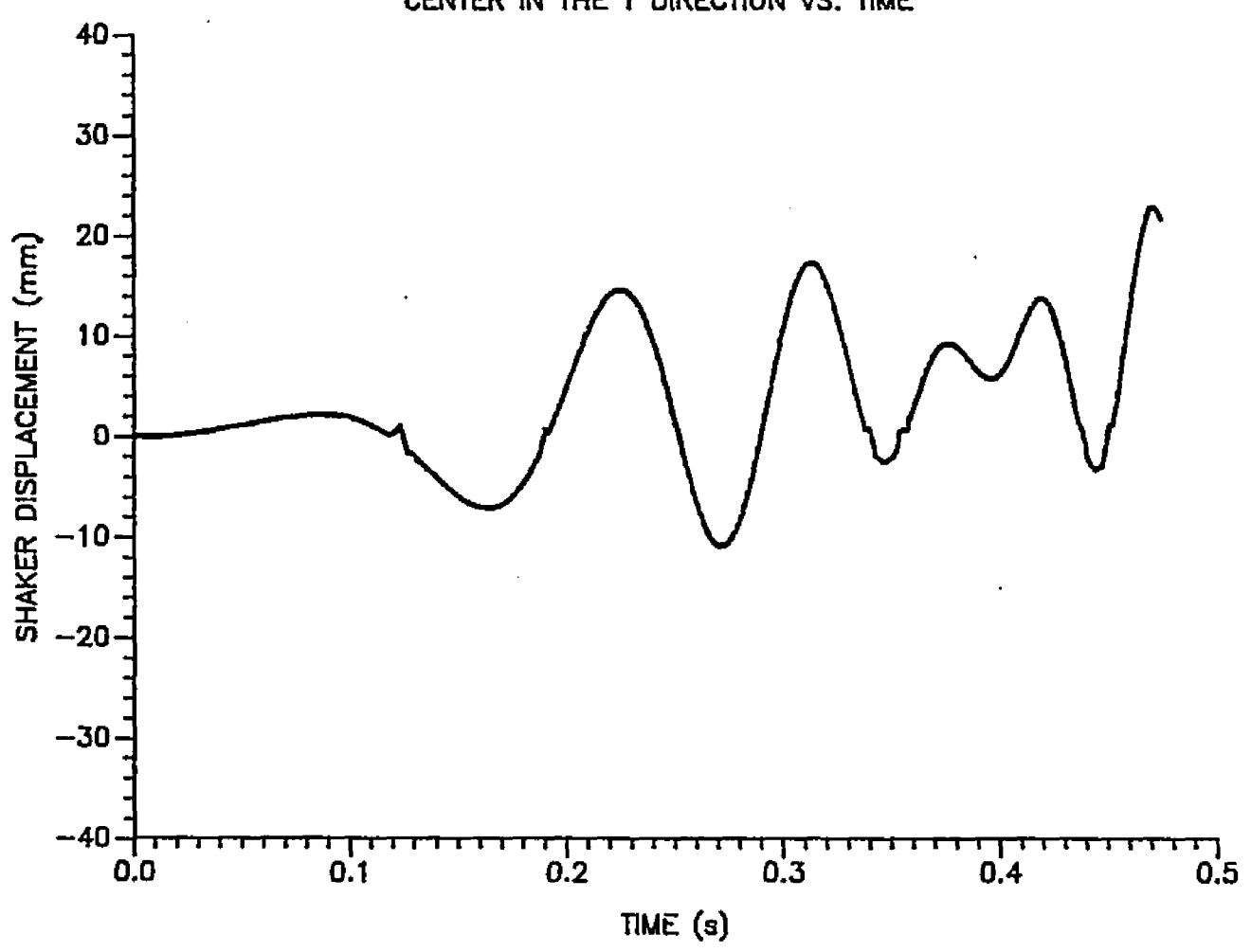


FIGURE 6.53 SHAKER DISPLACEMENT IN THE Y DIRECTION.
MASSES ARE RUNNING AT ACCELERATIONS OF 298 AND 216 rad/s.s. AT A STARTING PHASE ANGLE OF 0 DEGREES.

### SIMULATED SHAKER DISPLACEMENT AT THE PAD CENTER IN THE X-Y PLANE VS. TIME

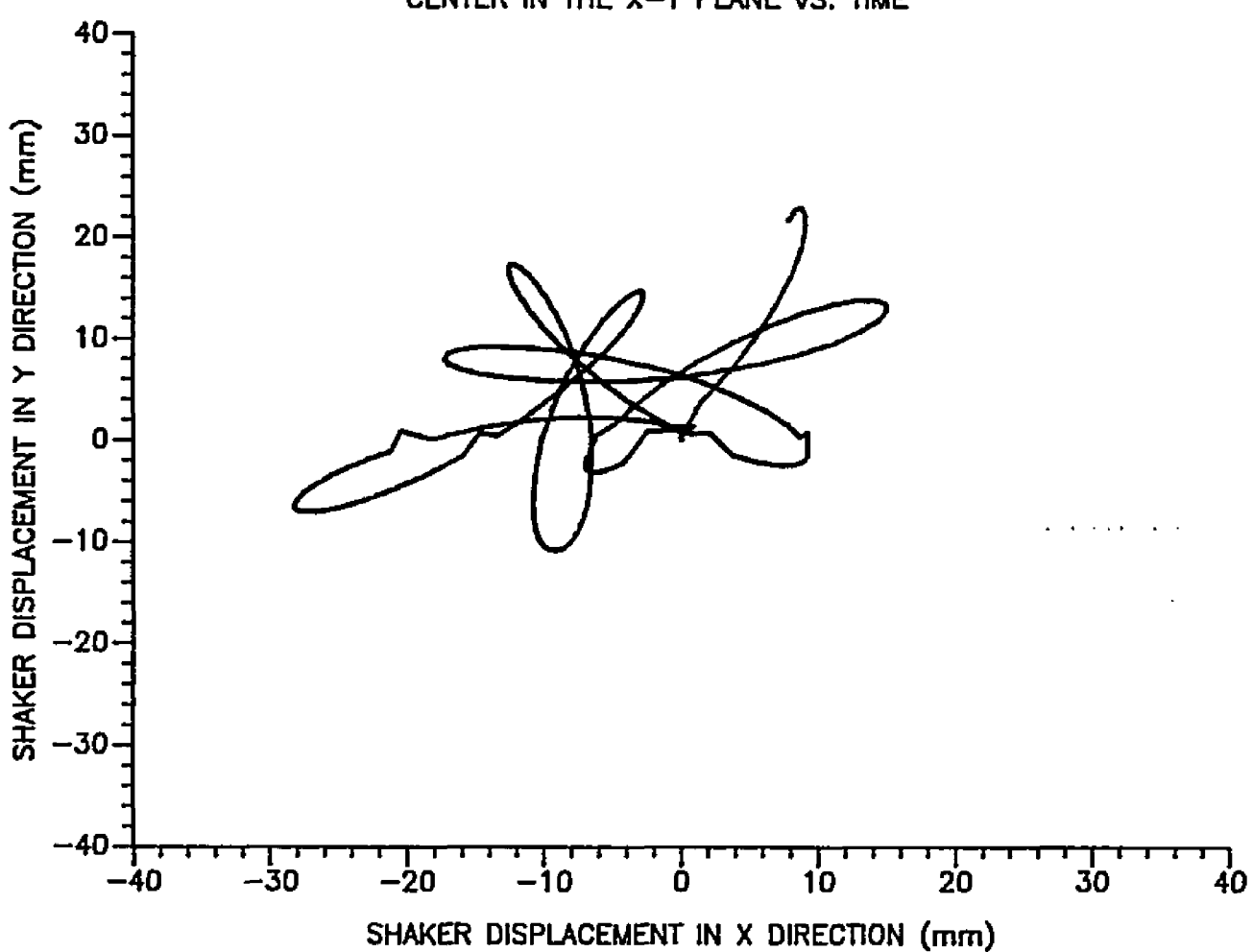


FIGURE 6.54 SHAKER DISPLACEMENT IN THE X-Y PLANE. MASSES ARE RUNNING AT ACCELERATIONS OF 298 AND 216 rad/s.s. AT A STARTING PHASE ANGLE OF 0 DEGREES.

#### CHAPTER 7

#### 7. SUMMARY AND CONCLUSIONS

#### 7.1 SUMMARY

In recent years, growers have reported that cherry tree decline (loss of vigor and yield, resulting in early replacement of the orchard) is an increasing problem where mechanical harvesting of cherries is being practiced. Trunk bark damage (crushed cambium, split and torn bark) often occurs during trunk shaking, and can result in tree decline. A possible cause of this damage is the transmission of high dynamic forces between the shaker and the bark during shaker operation.

A computer program entitled Integrated Mechanisms Program (IMP) was selected as a tool for modeling a Friday C-clamp trunk shaker that is widely used for cherry harvesting. The goals of the study were to simulate the shaker displacements with and without tree attachment, and to study the affects on shaker displacement behavior caused by changing some shaker physical properties or operating procedures.

During the 1985 cherry harvesting season, some physical properties for both sweet and sour cherry trees were measured and analyzed. The properties determined were:

true center of gravity above ground, tree mass above ground, trunk stiffness coefficients (linear and torsional), and tree damping coefficients as related to trunk diameter.

The physical properties of a Friday C-clamp trunk shaker were measured and analyzed to determine the shaker housing mass, mass moment of inertia, rotating mass, mass eccentricity, linear and torisonal stiffness and damping of the suspension bars, and the physical dimensions of the shaker.

These tree and shaker physical properties were then used as parameters in the free-shake and shaker-tree IMP simulation models. The displacement results obtained from the free-shake vibration model during the frequency stage were compared. The simulation indicated a maximum displacement in the x direction of 23 mm (0.90 in.), only 2 mm (0.07 in.) less than the value obtained from a photographic study conducted by others. The total shaker shift simulated by the shaker model was 11 mm (0.43 in.) and the shaker drift was 15 mm (0.59 in.), 5 mm (0.19 in.) less than the value obtained from the photographic study. During steady state simulation at a frequency of 15 Hz displacement was 25 mm (1 in.), almost the same displacement obtained from the photographic study. The shaker shift simulated by the model was 9 mm (0.35 in.) while the drift was 34 mm (1.33 in.), only 5 mm (0.19 in.) larger than that

found in the photographic study. Thus, the IMP model appears to agree closly with the results obtained during actual free-shaking operation.

The shaker-tree model, with no tree stiffness or damping was used to simulate tree trunk displacement. The results indicated maximum x displacements of 20 to 25 mm (0.78 to 1 in.) at three steady state frequencies of 5, 10, and 15 Hz. When the tree stiffness and damping were introduced in the model, the program simulation stopped before it reached the specified simulation time. After testing the IMP program in several ways it was concluded that the stiffness matrix algorithm was not accurate, thus tests requiring a nonzero stiffness matrix (the shaker-tree model) could not be conducted.

Tests of several shaker physical property changes and their affect on the shaker displacement behavior indicated that: the average ratio of the shaker displacement increase to the shaker housing mass decrease was 11 mm/100 kg (0.19 in./100 lbs); the average ratio of the shaker displacement decrease to the rotating mass decrease was 4.4 mm/ 10 kg (0.08 in./10 lbs); the average ratio of the shaker shift or drift increase to the shaker housing decrease was 4.4 mm/100 kg (0.07 in./100 lbs); the average shaker shift or drift decrease to the shaker rotating mass decrease was 1.5 mm/10 kg (0.027 in./10 lbs).

The shaker displacement was simulated using different transient accelerations for the rotating masses. The results indicated that there was no relationship between the magnitude of equal accelerations for the rotating masses and the shaker drift. However, using unequal accelerations for the inside and outside rotating masses did change the phase angle between the masses, the drift of the shaker, and the displacement behavior of the shaker.

A uniform, or regular, increase in shaker displacement is believed to be desirable when starting the shaking operation. The affect of using movable rotating masses (change eccentricity from zero to a maximum during shaker startup) was simulated. The displacement was found to increase uniformly, and shaker shift and drift were minimized.

Finally, to determine if shaker shift, drift and gallop could be minimized, different rotating mass starting phase angles were tested using the free-shake model. The maximum shift, drift and gallop occured at a starting phase angle of zero degrees and the minimum occured at 225 degrees. This shift, drift and gallop was found to be related only to the rotating mass starting phase angles. Starting acceleration or final steady state frequency did not have a significant affect on shaker shift, drift or gallop.

#### 7.2 Conclusions

According to the results obtained from using the IMP program to model the Friday C-clamp trunk shaker displacement behavior, the following conclusions were drawn:

- 1- The IMP program was a useful tool in modeling the displacements of the C-clamp trunk shaker because of the following:
  - a. The IMP model predicted the free-shake displacements, shift, and drift.
  - b. The IMP model was capable of testing different shaker physical property changes and their effect on the shaker displacement behavior.
- 2- The average ratio of the shaker displacement increase to the shaker housing mass decrease was 11 mm/100 kg (0.19 in./ 100 lbs).
- 3- There was no relationship between the magnitude of acceleration of the rotating masses and the shaker shift or drift.
- 4- The average ratio of the shaker displacement decrease to the rotating mass decrease was 4.4 mm/10 kg (0.78 in./10 lbs).
- 5- The average ratio of the shaker shift or drift increase to the shaker housing decrease was 4.4

- mm/100 kg (0.07 in./100 lbs).
- 6- The average ratio of the shaker shift or drift decrease to the shaker rotating mass decrease was 1.5 mm/10 kg (0.027 in./10 lbs).
- 7- The shaker gallop, shift and drift behavior during the transient startup of the shaker could be controlled by using a movable mass eccentricity that is zero when the shaker starts and a maximum within 0.353 to 0.45 s after startup. Similar results were also obtained when the shaker was initially running at the steady state frequency of 15 Hz.
- 8- The shaker gallop, shift and drift during startup could be minimized by using a particular starting position for the inside mass and a starting phase angle of 225 degrees counterclockwise between it and the starting position of the outside mass.
- 9- The largest shaker gallop, shift and drift occured at a starting phase angle of zero degrees between the masses.
- 10- The shaker shift and drift was related only to the starting phase angle between the rotating masses.
- 11- The IMP program was not able to modelthe shakertree displacements. The program was not able to

numerically handle the tree stiffness in the shaker-tree model.

#### 7.2-1 Scope And Limitations

Some limitations were encountered during this study, which can be summarized as follows:

- 1- The IMP program can only handle a limited number of degrees-of-freedom in a vibration system. My analysis involved a 9 degree-of-freedom system, which is larger than the IMP designers had previously tested.
- 2- The stiffness algorithm apparently is nonfunctional in the dynamic mode of the IMP program.
- 3- Because of the stiffness algorithm problem, the shaker-tree displacement behavior could not be simulated as planned.

#### 7.2-2 Future Research Needs

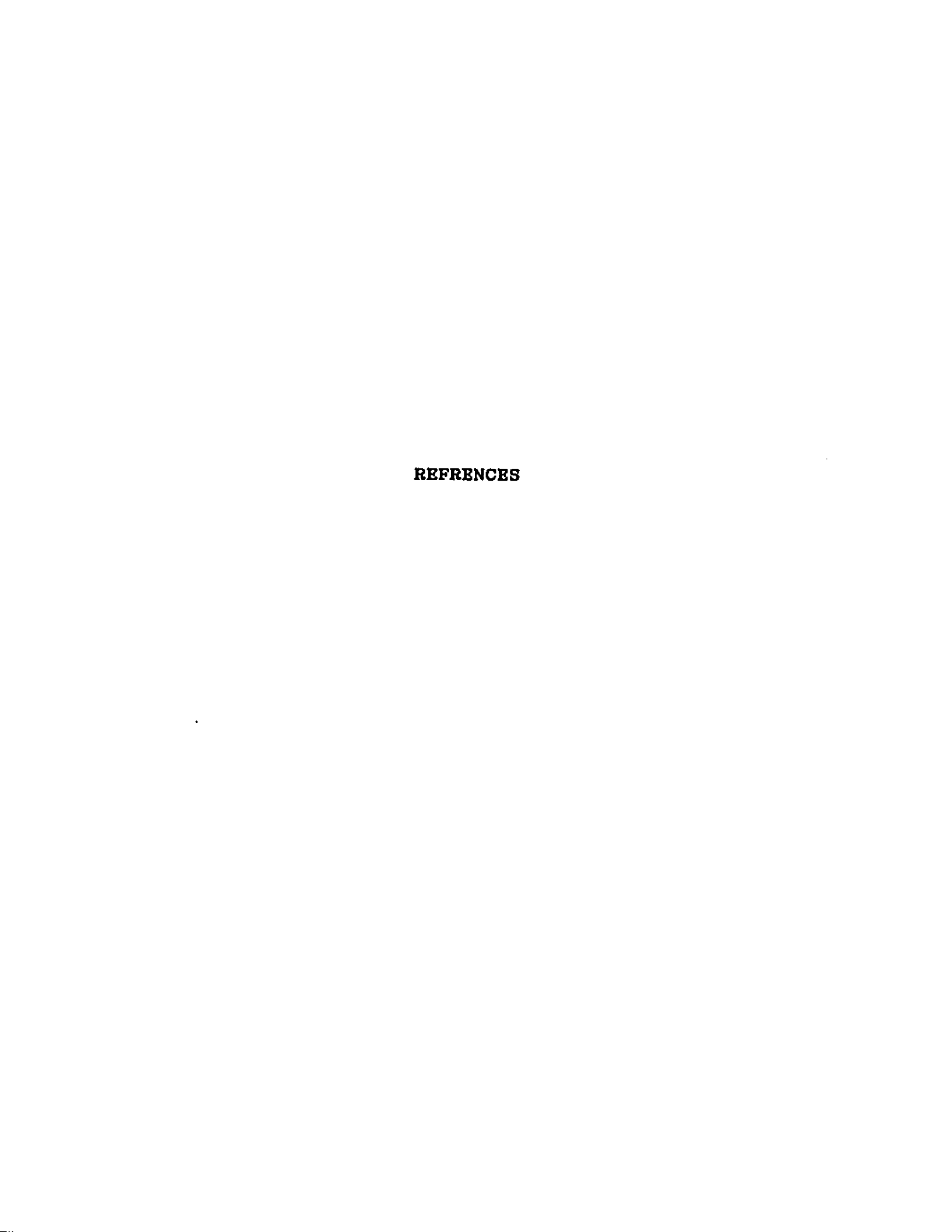
The author believes that further simulation and field research is needed in the following areas:

- 1- Since the tractor which carries the shaker was modeled as a fixed mass (ground) in the IMP shaker model, a more accurate model could be developed taking into consideration the tractor vibration contribution into the shaker-tree system. However, the IMP program capability must be increased before the tractor contribution can be modeled.
- 2- During the modeling stage, some shaker physical properties were ignored, such as the stiffness and damping of the pad used between the shaker and the trunk in the tree-shaker model, suspension bar stiffness and damping, and clamping cylinder stiffness and damping. These properties should be evaluated in future studies.
- 3- Studies are needed which measure the dynamic forces generated between the shaker clamp pads and the tree trunk, and the corresponding shaker and tree displacements. Careful analysis of that information might lead to a better shaker design

and result in reduce trunk bark damage.

- 4- More information on the actual displacements observed when shaking cherry tree trunks of various diameters would be very helpful for verification of simulation results.
- 5- The displacement of cherry tree trunks might be modeled more accurately using a different modeling procedure, such as finite element analysis.

  Appropriate forcing functions, from 3 above, applied to the finite element model might better describe trunk behavior.
- 6- A three dimensional model for the shaker-tree system is needed to take into consideration the shaker and tree properties in all three dimensions (x, y, and z), and to investigate the shaker and tree displacements in all three dimensions.
- 7- The apparent benefits of reduced shaker gallop and drift should be tested by redesigning the trunk shaker to: permit starting the rotating masses at a phase angle of 225 degrees on each trunk, and; permit increasing the eccentricity from zero to maximum during the startup phase on each trunk. These two changes appear to offer the best chance for eliminating the shaker gallop and drift that are believed to contribute to bark damage.



#### References

- 1. Adrian, P. A. and R. B. Fridley. Mechanical Fruit Tree Shaking. California Agriculture 12(10): 3, 1958.
- 2. Adrian, P. A. Forced Vibration Of A Tree Limb, ASAE Paper No. 63-642 D, 1963.
- 3. Adrian, P. A. and R. B. Fridley. Dynamics And Design Criteria Of Inertia-type Tree Shaker. Transactions of the ASAE 8(1):12-14, 1965.
- 4. Adrian, P. A., R. B. Fridley, D. H. Chaney. and K. Uriu. Shaker-Clamp Injury to Fruit and Nut Trees. Calif. Agric. 19(8):8-10, 1965.
- 5. Affeldt, H. A. Digital Analysis Of The Dynamic Response Within Trunk Shaker Harvester Systems. M.S. Thesis, Agr. Eng. Dept., Mich. State Univ., E. Lansing, MI 48824. 226 p. 1984.
- 6. Alper, Y., A. Foux and U. M. Peiper. Experimental Investigation of Orange Tree Dynamics Under Mechanical Shaking. J. Agr. Eng. Res. 21(2):121-131, 1976.
- 7. Beljakove, V., P. Manolov and A. Nikolov. Effect of Mechanical Harvesting Using Tree Shakers On The Root System And Physiological Processes of Fruit Trees. Selskostopanska Tehnika 16(6):3-14, 1979.
- 8. Berlage, A. G., and Willmonth, F. M. Fruit Removal Potential Of High Frquency Vibrations. Transactions of the ASAE 17(2):233-234, 1974.
- 9. Brown, G. K. Some Factors Affecting The Longitudinal Shear of Bark From Fruit Tree Limbs. M. S. Thesis. Agr. Eng. Dept., Univ. of California, Davis, 1965.
- 10. Brown, G. K. Harvest Mechanization Status For Horticultural Crops. ASAE Paper No. 80 1045, 1980.
- 11. Brown, G. K., J. K. Frahm, R. L. Ledebuhr, and B. F, Cargill. Bark Damage When Trunk Shaking Cherry Trees. ASAE paper No. 82-1557, 1982.
- 12. Brown, G. K., J. R. Frahm, L. J. Segerlind, and B. F.

- Cargill. Shaker Damage To Cherry Bark--Causes & Cures. Proc. Int'l Symp. Fruit, Nut, and Veg. Harv. Mech., Spec. pub. 5-84, ASAE, 2950 Niles Rd., St. Joseph, MI 49085. p. 364-371, 1984.
- Brown G. K., L. J. Segerlind, and P. L. Richey. Bark Stress Caused By Trunk Shaker Displacements. ASAE paper, No. 84-1066, 1984.
- 14. Cargill, B. F., G. K. Brown and M. J. Bukovac. Factors Affecting Bark Damage To Cherry Trees By Harvesting Machines. Mich. State Univ., CES, AEIS Bull. No. 471. June, 6 pp. 1982.
- 15. Cook, J. R., and R. H. Rand. Vibratory Fruit Harvesting: A Linear Theory Of Fruit-Stem Dynamics. J. Agr. Eng. Res. 14(3): 323-330, 1968.
- 16. Devay, J. E., W. H. English, F. L. Lukezic and H. J. O' Reilly. Mallet Wound Canker of Almond Trees. Calif. Agric. 14(8):8-9, 1960
- 17. Diener, R. G., F. H. Buelow, and G. E. Mase. Viscoelastic Analysis Of The Behavior And Properties Of Cherry Bark And Wood Under Static And Dynamic Loading. Transactions of the ASAE 11(3): 323-330, 1968.
- 18. Diener, R. G., J. H. Levin, and B. R. Tennes. Directional Strength Properties Of Cherry, Apple, and Peach Bark And The Influence Of Limb Mass And Diameter On Bark Damage. Transactions Of the ASAE 11(6): 788 and 791, 1968.
- 19. Drake, S. R. Introduction to The Symposium- The Influence Of Mechanical Harvesting On The Quality Of Horticultural Crops. Hort. Sci. 18(4): Spec. Insert p.406, 1983.
- 20. Esau, K. Plant Antatomy. John Wiley and Sons, Inc., New York, 1965.
- 21. Frahm, J. R., G. K. Brown, and L. J. Segerlind. Mechanical Properties Of Trunk Shaker Pads. ASAE Paper No. 83-1078, 1983.
- 22. Fridley, R. B., and P. A. Adrian. Some Aspects Of Vibratory Fruit Harvesting. Agr. Eng. 41(1):28-31, January, 1960.
- 23. Fridley, R. B., G. K. Brown, and P. A. Adrian. Strength Characteristics of Fruit Tree Bark, Hilgardia 40(8):205-222, August, 1970.

- 24. Halderson, J. L. 1966. Fundamental Factors in Mechanical Cherry Harvesting. Transactions of the ASAE, 9(5):481-684, 1966.
- 25. Hoag, D. L., J. R. Hutchinson, and R. B. Fridley. Effect of Proportional, Nonproportional and Nonlinear Damping On Dynamic Response Of Tree Limbs. Transactions of the ASAE 13(6): 879-884, 1970.
- 26. Hoag, D. L., R. B. Fridley, and J. R. Hutchinson. Experimental Measurement Of Internal and External Damping Properties Of Tree Limbs. Transactions of the ASAE 14(1): 20-24, 1971.
- 27. Hussain, A. A. M., G. E Rehkugler, and W. W. Gunkel. Tree Limb Response To Periodic Discontinuous Sinusoidal Displacement. Transactions of the ASAE 18(4): 614-615, 1975.
- 28. Khalilian, A., and W. J. Chancellor. Analysis and Testing Of A Spring-Load Tree Shaker. ASAE Paper No. 78-1019, June, 1978.
- 29. Kirk, D. E., and D. E. Booster. Identifying Damage Sources In Mechanically Harvested Sweet Cherries. Transactions of the ASAE 22(1): 21-26, 1979.
- 30. Kirk, D. E., L. C. Jenson, and D. E. Booster. To Measure Tree Trunk Movement During Mechanical Cherry Harvest. Agr. Eng. 61(11): 15-17, November 1980.
- 31. Kronenberg, H. G. Possibilities For Mechanical Fruit Harvesting. J. Agr. Eng. Res. 9 (2):194-196, 1964.
- 32. Levin, J. H., H. P. Gaston, S. L. Hedden and R. T. Whittenberger. Mechanizing The Harvest Of Red Tart Cherries. Quart Bull. 42(4):42-60. Mich. State Univ. Agr. Expt. Sta. E. Lansing, MI 48824. May, 1960.
- 33. Marshall, D. E Determining motion of mechanical harvesting system with photographic techniques. ASAE Paper No. 86-1556, 1986.
- 34. Mitchell, A. E., and J. H. Levin. Tart Cherries Growing, Harvesting, and Processing for Good Quality. Ext. Bull. E-654, Farm Science Series, 1969.
- 35. Moini, S., and J. A. Miles. Simulation Of Tree Response To Vibration. ASAE Paper No. 80-3526, 1980.

- 36. Michigan Department Of Agriculture. Michigan Agricultural Statistics. 80 pp. P. O. Box 20008, Lansing, Mi 48901, 1985.
- 37. Ortiz-Canavate, J., J. R. Gil, and F. J. Juste. Design and Testing Of Tree Shaker. ASAE Paper No. 80-1045, 1980.
- 38. Peterson, D. L. and G. E. Monroe. Continuously Moving Shake-Catch Harvester. Transactions of the ASAE 20(2): 202-205, 209, 1977.
- 39. Phillips, A. L., J. R. Hutchinson, and R. B. Fridley. Formulation of Forced Vibrations of Tree Limbs With Secondary Branches. Transactions of the ASAE 13(1): 138-142, 1970.
- 40. Upadhyaya, S. K., J. R. Cooke, and R. H. Rand. Limb Impact Harvesting, Part 1. Finite Element Analysis. ASAE Paper No. 79-1054, 1979.
- 41. Young, C., and R. B. Fridley. Simulation Of Vibration Of Whole Tree Systems Using Finite Elements. Transactions of the ASAE 8(3):475-481, 1975.

### APPENDIX A

Free Vibration C-Clamp Trunk Shaker Model

```
POINT(L1)=P7,P8,P9,P10,P7,P2,
DATA POINT(P7,ABS)=50,10,0
DATA POINT(P8,ABS)=59,10,0
DATA POINT(P9,ABS)=59,33,0
DATA POINT(P10,ABS)=50,33,0
POINT(L1)=P10,P11,P12,P4,P10
DATA POINT(P11,ABS)=50,38,0
DATA POINT(P12,ABS)=20,38,0
                                                                                                            SPHERE(L5, FRAME)=J7

DATA LINK(L5,J7)=22.5,41

DATA LINK(FRAME,J7)=22.5

SPHERE(L1,L6)=J8

DATA LINK(L1,J8)=28,87,0

DATA LINK(L6,J8)=28,87,0

SPHERE(L6,FRAME)=J9

DATA LINK(L6,J9)=28,87,1

DATA LINK(L6,J9)=28,87,1

DATA LINK(FRAME,J9)=28,87,1

DATA LINK(FRAME,J9)=28,87,1
                                                                                                                                                                                                                                                                                                              ******************
                                                                                                                                                                                                                                                                                       ******
                                                                                                                                                                              DATA LINK(
SPHERE(L1,
DATA LINK(
                                                                                                                                                            DATA LI
SPHERE(
DATA LI
                                                                                                                                                                                                SPHEI
DATA
                                                                                                                                                                                                                  SPHERE(L1,L4)=J4
DATA LINK(L1,J4)=64,41.
DATA LINK(L4,J4)=64,41.
                                                                                                                                                                                                                                         REVOLUTE(L1,L2)=J2
DATA REVOLUTE(J2)=
REVOLUTE(L1,L3)=J3
                                                                               DATA
                                                                                     DATA
                                                                                                                                                                                                                                    DATA REVOLUTE(J3)=
                                                                          DATA
                                                                                           POINT(L1)=P1
DATA POINT(P
                                                                                                                                                                                                                                                             GROUND=FRAME
                                                                                                                                                                                                                                                                         REMARK
                                                       POINT(L1)=P5,P6
DATA POINT(P6,A
                                                                    DATA
                                                                                                                                                                                                       PHERE
                                                                  VT(L1)=P1, P2, P3, P4, P5, P1

A POINT(P1, ABS)=20, 10, 0

A POINT(P2, ABS)=49, 10, 0

A POINT(P3, ABS)=49, 33, 0

A POINT(P4, ABS)=20, 33, 0

A POINT(P5, ABS)=20, 18, 0
                                                                                                                                                                   E(LS
                                                                                                                                                                                                 LINK
                                                       POINT (P6, ABS)
                                                                                                                                                                                                       *
                                                                                                                                                                                                                                                                         INTRODUCING
                                                                                                                                                                                                                                                                                      ((FRAME, J
|, L5)=J6
|
|((L1,J6)=|
                                                                                                                                                                                                (L4,J5)=J5
                                                                                                                                                                                           , J5
                                                                                                                                                                   )=22
)=22
)=J7
                                                                                                                                                                                                                                                                                                       FRIDAY
                                                                                                                                                                                                                                     :27
                                                                                                                                                                                                                                                 41
                                                         Ħ
                                                                                                                                                                                           ·
                                                                                                                                                                                           100
                                                                                                                                                                                                                                                                         THE
                                                                                                                                                                              .
                                                        4
                                                                                                                                                                        ប្រាប់
                                                                                                                                                                                                41.
                                                        Ö
                                                                                                                                                                                                                                     •
                                                                                                                                                                                                                                                 ٠
                                                                                                                                                                                                                                     G
                                                                                                                                                                                                                                                 Çī
                                                                                                                                                                                            Ā
                                                       •
                                                                                                                                                       54
                                                                                                                                                                         41.
                                                       18
                                                                                                                        -
                                                                                                                                     ~ ~
                                                                                                             ,14;32,84,;
,87,14;28,8
SHAKER HOL
                                                                                                                                      00
                                                                                                                                                                                            4 5
                                                                                                                                                                                                                   បា បា
                                                                                                                                                                                                                                                 N
                                                                                                                                                                                                                                     N
                                                                                                                                                                                                                                                                         SHAKER
                                                                                                                                                                                                                                                                                                       C-CLAMP
                                                                                                                                                                                           ~
                                                                                                                                     40 40
                                                                                                                                                       •
                                                                                                                                                            •
                                                                                                                                                                                                                   • •
                                                                                                                                                                                                                                     S
                                                                                                                                                                                                                                                 Ç
                                                                                                                                                                                                                   0;64
                                                                                                                                                                                           . _
                                                                                                                                                                         បា បា
                                                                                                                                                        D 4
                                                                                                                                                                                                                                                 •
                                                        0
                                                                                                                                      W N
                                                                                                                                                                                                                                     ٠
             io
O
                                                                                                                                                                                           S in
                                                                                                                                                                                                                                     ű
                                                                                                                                                                                                                                                 Ç
                                                                                                                                      N @
                                                                                                                                                       _
                                                                                                                                                                         • •
                                                                                                                                                       14
                                                                                                                                                                         00
                                                                                                                                                                                                **
                                                                                                                                                                                                                                                 •
                                                                                                                                     • •
                                                                                                                                                                                           •
                                                                                                                                                                                                                                    •
                                            N
                                                                                                                                                                                          64,10
,14;64
                                                                                                                                                                                                                                                ,0;41.
                                                                                                                                                                                                                                     0
                                                                                                                                      87
84
                                                                                                                                                                         ** **
                                                                                                                                                                         22.
22.
                                           P3, P10
                                                                                                                                                                                                                  10,0;
                                                                                                                                                                                                                                                                         JOINTS
                                                                                                              SOOH
                                                                                                                                     ~ ~
                                                                                                                                                       F N
                                                                                                                                                                                                                                     27
                                                                                                                                    .0
10
                                                                                                                                                        $ 8
                                                                                                             14;28
,87,0;
OUSING
                                                                                                                                                                                                                                                                                                 BY
                                                                                                                                                                                                                                                                                                       TRUNK
                                                                                                                                                       ** *
                                                                                                                                                                          ហហ
                                                                                                                                                                                                                                     ហ
                                                                                                                                                                                                                                                 ហ
                                                                                                                                      N
                                                                                                                                                       NO
                                                                                                                                                                        •
                                                                                                                                                                              \sim
                                                                                                                                                                                                •
                                                                                                                                                      2.5
                                                                                                                                                                         10,
                                                                                                                                                                                           14;
                                                                                                                                    .
Β΄ ω
-
                                                                                                                                                                                                                  10;
                                                                                                                                                                                                                                                 N
                                                                                                                                                                                                                                     2
                                                                                                                                      ∞-`
                                                                                                                                                                                                                                     Ü
                                                                                                                                                                                                                                                 Ġ
                                                                                                             8,87,0
32,84,
SHAPE
                                                                                                                                                                         0 5
                                                                                                                                                                                           \omega \omega
                                                                                                                                      78
                                                                                                                                                       •
                                                                                                                                                                                                                                     ٠
                                                                                                                                                                                                                                                 ٠
                                                                                                                                                       14
41
                                                                                                                                                                                                                   64,
                                                                                                                                                                                                                                                                                                       SHAKER MODEL
                                                                                                                                           4
                                                                                                                                                                         ~~ ~
                                                                                                                                                                                                 Š
                                                                                                                                                                                                                                     បា
                                                                                                                                                                                                                                                 ហ
                                                                                                                                                                                           •
                                                                                                                                                                                                                                                                                                              ******************
                                                                                                                                                                         10;
                                                                                                                                                                                           0-
                                                                                                                                                                                                                                    •
                                                                                                                                                                                                                                                 •
                                                                                                                                                                                                                                                 10
                                                                                                                                      00
                                                                                                                                                       ٠
                                                                                                                                                            70
                                                                                                                                                                                           ~•
                                                                                                                                                                                                 4
                                                                                                                                                                                                                                     10
                                                                                                                                                                                                                   5,
                                                                                                                                                                                           σË
                                                                                                                                                       S
                                                                                                                                                                         •
                                                                                                                                                                                                                                                                                       ×
                                                                                                                                                                        ,22.5
5,41
                                                                                                                                                                                          ..5,0
4,10
                                                                                                                                                            N
                                                                                                                                                                                                                                     ٠.
                                                                                                                                                                                                                                                 **
                                                                                                                                                                                                                                                                                       ******
                                                                                                                                                       •
                                                                                                                                                                                                                   •
                                                                                                                                                                                                                   1,0
                                                                                                                                                      0.5
                                                                                                                                                                                                                                                 41
                                                                                                                  14
                                                                                                                                                                                                                                     N
                                                                                                                                                                                                                                      J
                                                                                                                                                       N=
                                                                                                                                                       241
                                                                                                                                                                                                                                     G
                                                                                                                                                                                                                                                 បា
                                                                                                                                                                              •
                                                                                                                                                                        50
                                                                                                                                                                                           ш
                                                                                                                                                                                                                                                 •
                                                                                                                                                       55
                                                                                                                                                                                                                                     10
                                                                                                                                                                                                                                                 10
                                                                                                                                                                                            ۵
                                                                                                                                                                         100
                                                                                                                                                       100
                                                                                                                                                                                                                                                 •
                                                                                                                                                                                                                                     0
                                                                                                                                                                                                                                                 0
                                                                                                                                                                                                                                                                                       *
                                                                                                                                                                                                                                     ٠.
                                                                                                                                                                                                                                                 ٠.
                                                                                                                                                                                                                                                 4
                                                                                                                                                       14
                                                                                                                                                                                                                                     N
                                                                                                                                                                                                                                                                                       *
                                                                                                                                                                                                                                                 \vdash
                                                                                                                                                                                                                                                                                       ***
                                                                                                                                                                                                                                     G
                                                                                                                                                                                                                                                 G
                                                                                                                                                                                                                                     ഗ
                                                                                                                                                                                                                                                 ហ
                                                                                                                                                                                                                                                                                       *
                                                                                                                                                                                                                                                 •
                                                                                                                                                                                                                                     0
                                                                                                                                                                                                                                                 0
                                                                                                                                                                                                                                                                                       *
                                                                                                                                                                                                                                                                                       *
                                                                                                                                                                                                                                                                                       **
```

```
POINT(L1)=P12,P13,P14,P15,P12
DATA POINT(P13,ABS)=20,45,0
DATA POINT(P14, ABS)=64,45,0
DATA POINT(P15, ABS)=69,38,0
POINT(L1)=P19,P18,P16,P17
DATA POINT(P16,ABS)=47,45,0
DATA POINT(P17, ABS)=41,83,0
DATA POINT(P18, ABS)=45,45,0
DATA POINT(P19, ABS)=40,76,0
POINT(L1)=P23,P22,P20,P21
DATA POINT(P20, ABS) = 28,45,0
DATA POINT(P21, ABS)=34,76,0
DATA POINT(P22, ABS)=26,45,0
DATA POINT(P23, ABS)=33,83,0
POINT(L1)=P17,P25,P24,P23,P17
DATA POINT(P24, ABS)=33,76,0
DATA POINT(P25, ABS)=41,76,0
POINT(L1)=P26,P27,P28,P29
DATA POINT(P26, ABS)=35,83,0
DATA POINT(P27, ABS)=28,89,0
DATA POINT(P28, ABS)=26,87,0
DATA POINT(P29, ABS)=33,81,0
POINT(L1)=P30,P31,P32,P33,P34,P35,P36,P37,P30
DATA POINT(P30, ABS)=50,36,0
DATA POINT(P31, ABS) = 75,36,0
DATA POINT(P32, ABS) = 75,38,0
DATA POINT(P33,ABS)=78,38,0
DATA POINT(P34,ABS)=78,13,0
DATA POINT(P35, ABS)=75,10,0
DATA POINT(P36, ABS)=75,35,0
DATA POINT(P37,ABS)=50,35,0
POINT(L1)=P38,P39,P40,P41,P42,P35,P38,P41
DATA POINT(P38, ABS)=74,10,0
DATA POINT(P39, ABS)=66,10,0
DATA POINT(P40,ABS)=66,33,0
DATA POINT(P41, ABS) = 74,33,0
DATA POINT(P42, ABS) = 75,33,0
REMARK INTRODUCING THE INSIDE ROTATING MASS SHAPE....
POINT(L2)=P50,P51,P52,P53,P54,P55,P56,P57,P58,P59,P57,P50
DATA POINT(P50, ABS)=41.5,19,0
DATA POINT(P51,ABS)=38,20,0
DATA POINT(P52, ABS)=36,22,0
DATA POINT(P53, ABS) = 35, 25.5, 0
DATA POINT(P54, ABS)=36,29,0
DATA POINT(P55, \DeltaBS)=38,31,0
DATA POINT(P56, ABS) = 41.5,32,0
DATA POINT(P57,ABS)=41.5,25.5,0
DATA POINT(P58, ABS)=43,25.5,0
DATA POINT(P59, ABS)=40,25.5,0
POINT(L1)=P500
```

```
DATA POINT(P500, ABS)=59,22,0
REMARK INTRODUCING THE OUTSIDE ROTATING MASS SHAPE.....
POINT(L3)=P60,P61,P62,P63,P64,P65,P66,P67,P68,P69,P67,P60
DATA POINT(P60, ABS) = 27.5, 19,0
DATA POINT(P61, ABS)=24,20,0
DATA POINT(P62, ABS) = 22, 22, 0
DATA POINT(P63, ABS)=21,25.5,0
DATA POINT(P64, ABS) = 22, 29, 0
DATA POINT(P65, ABS)=24,31,0
DATA POINT(P66, ABS) = 27.5, 32,0
DATA POINT(P67, ABS)=27.5,25.5,0
DATA POINT(P68, ABS) = 29, 25.5, 0
DATA POINT(P69, ABS)=26,25.5,0
POINT(L1)=P70.P74.P78.P82.P70
DATA POINT(P70, ABS)=65,41.5,0
DATA POINT(P74, ABS) = 64,40.5,0
DATA POINT(P78, ABS)=63,41.5,0
DATA POINT(P82, ABS) = 64,42.5,0
POINT(L1)=P71,P75,P79,P83,P71
DATA POINT(P71, ABS)=65,41.5,1
DATA POINT(P75, ABS)=64,40.5,1
DATA POINT(P79, ABS)=63,41.5,1
DATA POINT(P83, ABS) = 64,42.5,1
POINT(L1)=P70.P71
POINT(L1)=P74,P75
POINT(L1)=P78,P79
POINT(L1)=P82.P83
REMARK INTRODUCING THE RIGHT SIDE SUSPENSION BAR SHAPE....
POINT(L4)=P72,P76,P80,P84,P72
DATA POINT(P72, ABS)=65,41.5,.25
DATA POINT(P76, ABS)=64,40.5,.25
DATA POINT(P80, ABS)=63,41.5,.25
DATA POINT(P84, ABS)=64,42.5,.25
POINT(L4)=P73,P77,P81,P85,P73
DATA POINT(P73,ABS)=65,41.5,13.75
DATA POINT(P77, ABS)=64,40.5,13.75
DATA POINT(P81,ABS)=63,41.5,13.75
DATA POINT(P85, ABS) = 64,42.5,13.75
POINT(L4)=P72,P73
POINT(L4)=P76,P77
POINT(L4)=P80,P81
POINT(L4)=P85,P73
POINT(FRAME)=P86,P88,P90,P92,P86
DATA POINT(P86, ABS) = 65,41.5,13
DATA POINT(P88, ABS) = 64,40.5,13
DATA POINT(P90, ABS) = 63,41.5,13
DATA POINT(P92, ABS) = 64,42.5,13
POINT(FRAME)=P87,P89,P91,P93,P87
DATA POINT(P87, ABS)=65,41.5,14
DATA POINT(P89, ABS) = 64,40.5,14
DATA POINT(P91, ABS)=63,41.5,14
DATA POINT(P93, ABS)=64,42.5,14
```

```
POINT(FRAME)=P86,P87
POINT(FRAME)=P88,P89
POINT(FRAME)=P90,P91
POINT(FRAME)=P92,P93
POINT(FRAME)=P94,P95,P96,P97,P94
DATA POINT(P94, ABS) = 70, 47, 14
DATA POINT(P95, ABS) = 70,37,14
DATA POINT(P96, ABS) = 60, 37, 14
DATA POINT(P97, ABS) = 60,47,14
POINT(L1)=P100,P101,P102,P103,P100
DATA POINT(P100, ABS)=23.5,41.5,0
DATA POINT(P101,ABS)=22.5,40.5,0
DATA POINT(P102,ABS)=21.5,41.5,0
DATA POINT(P103,ABS)=22.5,42.5,0
POINT(L1)=P104,P105,P106,P107,P104
DATA POINT(P104, ABS) = 23.5, 41.5,1
DATA POINT(P105, ABS) = 22.5, 40.5, 1
DATA POINT(P106, ABS) = 21.5, 41.5, 1
DATA POINT(P107, ABS) = 22.5, 42.5,1
POINT(L1)=P100,P104
POINT(L1)=P101,P105
POINT(L1)=P102,P106
POINT(L1)=P103,P107
REMARK INTRODUCING THE LEFT SIDE SUSPENSION BAR SHAPE....
POINT(L5)=P108,P109,P110,P111,P108
DATA POINT(P108, ABS) = 23.5,41.5,.25
DATA POINT(P109, ABS)=22.5,40.5,.25
DATA POINT(P110, ABS)=21.5,41.5,.25
DATA POINT(P111, ABS) = 22.5, 42.5, .25
POINT(L5)=P112,P113,P114,P115,P112
DATA POINT(P112, ABS)=23.5,41.5,13.75
DATA POINT(P113, ABS) = 22.5, 40.5, 13.75
DATA POINT(P114, ABS)=21.5,41.5,13.75
DATA POINT(P115, ABS)=22.5, 42.5, 13.75
POINT(L5)=P108,P112
POINT(L5)=P109,P113
POINT(L5)=P110,P114
POINT(L5)=P111,P115
POINT(FRAME)=P116,P117,P118,P119,P116
DATA POINT(P116, ABS)=23.5,41.5,13
DATA POINT(P117,ABS)=22.5,40.5,13
DATA POINT(P118, ABS)=21.5,41.5,13
DATA POINT(P119,ABS)=22.5,42.5,13
POINT(FRAME)=P120,P121,P122,P123,P120
DATA POINT(P120, ABS) = 23.5,41.5,14
DATA POINT(P121, ABS) = 22.5, 40.5, 14
DATA POINT(P122, ABS) = 21.5, 41.5, 14
DATA POINT(P123, ABS) = 22.5, 42.5, 14
POINT(FRAME)=P116,P120
POINT(FRAME)=P117,P121
```

```
POINT(FRAME)=P118,P122
POINT(FRAME)=P119,P123
POINT(FRAME)=P124,P125,P126,P127,P124
DATA POINT(P124, ABS) = 25,48,14
DATA POINT(P125, ABS) = 25,37,14
DATA POINT(P126, ABS)=15,37,14
DATA POINT(P127, ABS)=15,48,14
POINT(L1)=P130,P131,P132,P133,P130
DATA POINT(P130, ABS)=29,87,0
DATA POINT(P131, ABS)=28,86,0
DATA POINT(P132, ABS)=27,87,0
DATA POINT(P133, ABS)=28,88,0
POINT(L1)=P134,P135,P136,P137,P134
DATA POINT(P134, ABS)=29,87,1
DATA POINT(P135, ABS)=28,86,1
DATA POINT(P136, ABS)=27,87,1
DATA POINT(P137, ABS) = 28,88,1
POINT(L1)=P130,P134
POINT(L1)=P131,P135
POINT(L1)=P132,P136
POINT(L1)=P133,P137
REMARK INTRODUCING THE REAR SUSPENSION BAR SHAPE.....
POINT(L6)=P138,P139,P140,P141,P138
DATA POINT(P138, ABS) = 29,87,.25
DATA POINT(P139, ABS) = 28,86,.25
DATA POINT(P140, ABS)=27,87,.25
DATA POINT(P141, ABS) = 28,88,.25
POINT(L6)=P142,P143,P144,P145,P142
DATA POINT(P142, ABS)=29,87,13.75
DATA POINT(P143, ABS)=28,86,13.75
DATA POINT(P144, ABS)=27,87,13.75
DATA POINT(P145, ABS) = 28,88,13.75
POINT(L6)=P13B,P142
POINT(L6)=P139,P143
POINT(L6)=P140,P144
POINT(L6)=P141,P145
POINT(FRAME)=P146,P147,P148,P149,P146
DATA POINT(P146, ABS) = 29,87,13
DATA POINT(P147, ABS) = 28,86,13
DATA POINT(P148, ABS) = 27,87,13
DATA POINT(P149, ABS) = 28,88,13
POINT(FRAME)=P150,P151,P152,P153,P150
DATA POINT(P150, ABS) = 29,87,14
DATA POINT(P151, ABS) = 28,86,14
DATA POINT(P152, ABS)=27,87,14
DATA POINT(P153, ABS) = 28,88,14
POINT(FRAME)=P146,P150
POINT(FRAME)=P147,P151
POINT(FRAME)=P148,P152
POINT(FRAME)=P149,P153
POINT (FRAME)=P154,P155,P156,P157,P154
DATA POINT(P154, ABS)=32,92,14
```

```
DATA POINT(P155, ABS) = 32, 80, 14
DATA POINT(P156, ABS) = 23,80,14
DATA POINT(P157, ABS)=23,92,14
REMARK INTRODUCING THE SHAKER MASSES........
UNIT MASS=.002591
DATA GRAVITY=0,0,-386.1
DATA MASS(L1,J2)=1.813;-5,-1,0
DATA MASS(L2,J2)=.2279;0,-3,0
DATA MASS(L3,J3)=.2279;0,-3,0
DATA MASS(L4.J4)=.0259,0,0,7
DATA MASS(L5,J6)=.0259,0,0,7
DATA MASS(L6,J8)=.0259,0,0,7
REMARK INTRODUCING THE SHAKER MOMENT OF INERTIA.....
DATA INERTIA(L4,J4)=.8625,.8625,0,0,0,0
DATA INERTIA(L5,J6)=.8625,.8625,0,0,0,0
DATA INERTIA(L6,J8)=.8625,.8625,0,0,0,0
DATA INERTIA(L2,J2)=1.39,1.39,2.79,0,0,0
DATA INERTIA(L1,J8)=6423.8,1115.36,10761,0,0,0
DATA INERTIA(L3,J3)=1.39,1.39,2.79,0,0,0
REMARK INTRODUCING DYNAMIC MODE SOLUTION.....
FIND DYNAMIC
REMARK INTRODUCING THE TIME INTERVAL AND INTEGRATION TIME....
DATA TIME=.5,.002,.002
REMARK INTRODUCING THE ROTATING MASS FREQUENCY......
VALUE (SP1)=164*TIME*TIME
VALUE (SP2)=-123*TIME*TIME
DATA MOTION(J2)=SP1
DATA MOTION(J3)=SP2
REMARK INTRODUCING SOME CONTROL STATEMENTS......
ZERO SPRING=.00001
ZERO FORCE=.07..7
ZERO POSITION=.0001
ZERO DATA=.00001
ZERO INERTIA=.0001
ZERO SYSTEM=.00001
LIST POSITION(P500)
PRINT ON = SP1
RETURN
```

# APPENDIX B C-Clamp Trunk Shaker-Tree Model

```
**********************
*
           FRIDAY C-CLAMP TRUNK SHAKER-TREE MODEL
                           BY
*
                    GHASSAN AL-SOBOH
*********************
REMARK INTRODUCING THE SHAKER JOINTS...........
GROUND=FRAME
REVOLUTE(L1,L3)=J2
DATA REVOLUTE(J2)=41.5,25.5,0;41.5,25.5,10;41.5,10,0;41.5,5,0
REVOLUTE(L1,L4)=J3
DATA REVOLUTE(J3)=27.5,25.5,0;27.5,25.5,10;27.5,10,0;27.5,5,0
SPHERE(L1.L5)=J4
DATA LINK(L1,J4)=64,41.5,0;64,41.5,10;64,10,0
DATA LINK(L5,J4)=64,41.5,0;64,10,0;64,41.5,10
SPHERE (L5, FRAME) = J5
DATA LINK(L5,J5)=64,41.5,14;64,10,14;64,41.5,0
DATA LINK(FRAME, J5)=64,41.5,14;64,41.5,0;64,10,14
SPHERE(L1,L6)=J6
DATA LINK(L1,J6)=22.5,41.5,0;22.5,41.5,10;22.5,10,0
DATA LINK(L6,J6)=22.5,41.5,0;22.5,10,0;22.5,41.5,10
SPHERE (L6, FRAME) = J7
DATA LINK(L6,J7)=22.5,41.5,14;22.5,10,14;22.5,41.5,0
DATA LINK(FRAME, J7) = 22.5,41.5,14;22.5,41.5,0;22.5,10,14
SPHERE(L1.L7)=J8
DATA LINK(L1,J8)=28,87,0;28,87,10;32,84,0
DATA LINK(L7,J8)=28,87,0;32,84,0;28,87,10
SPHERE(L7, FRAME)=J9
DATA LINK(L7,J9)=28,87,14;32,84,14;28,87,0
DATA LINK(FRAME, J9) = 28,87,14;28,87,0;32,84,14
REMARK INTRODUCING THE TREE JOINT.....
REVOLUTE(L1,L9)=J11
DATA REVOLUTE(J11)=62.5,22,0;62.5,22,10;70,22,0;62.5,30,0
REMARK INTRODUCING THE SHAKER HOUSING SHAPE.......
POINT(L1)=P1,P2,P3,P4,P5,P1
DATA POINT(Pl,ABS)=20,10,0
DATA POINT(P2,ABS)=49,10,0
DATA POINT(P3, ABS)=49,33,0
DATA POINT(P4, ABS)=20,33,0
DATA POINT(P5, ABS)=20,18,0
POINT(L1)=P5,P6
DATA POINT(P6, ABS)=49,18,0
POINT(L1)=P7,P8,P9,P10,P7,P2,P3,P10
DATA POINT(P7, ABS)=50,10,0
DATA POINT(P8, ABS)=59,10,0
DATA POINT(P9, ABS)=59,33,0
DATA POINT(P10, ABS) = 50,33,0
POINT(L1)=P10,P11,P12,P4,P10
DATA POINT(P11, ABS) = 50.38.0
DATA POINT(P12, ABS) = 20,38,0
```

```
POINT(L1)=P26,P27,P28,P29
DATA POINT(P26,ABS)=35,83,0
DATA POINT(P27,ABS)=28,89,0
DATA POINT(P28,ABS)=26,87,0
DATA POINT(P29,ABS)=33,81,0
POINT(L1)=P30,P31,P32,P33,P34,
DATA POINT(P33,ABS)=75,36,0
DATA POINT(P34,ABS)=75,36,0
DATA POINT(P35,ABS)=75,10,0
DATA POINT(P35,ABS)=75,15,0
DATA POINT(P37,ABS)=75,35,0
DATA POINT(P37,ABS)=50,35,0
DATA POINT(P31,ABS)=50,36,0
DATA POINT(P31,ABS)=75,36,0
DATA POINT(P32,ABS)=75,36,0
DATA POINT(P34,ABS)=75,36,0
DATA POINT(P35,ABS)=75,36,0
DATA POINT(P35,ABS)=75,36,0
DATA POINT(P35,ABS)=75,36,0
DATA POINT(P36,ABS)=75,35,0
DATA POINT(P37,ABS)=76,35,0
DATA POINT(P38,ABS)=74,10,0
DATA POINT(P40,ABS)=66,33,0
DATA POINT(P41,ABS)=66,33,0
DATA POINT(P41,ABS)=66,33,0
DATA POINT(P41,ABS)=75,33,0
DATA POINT(P41,ABS)=66,25,5,5,0
DATA POINT(P401,ABS)=66,25,5,5,0
DATA POINT(P401,ABS)=66,25,25,5,0
DATA POINT(P403,ABS)=62.5,25,5,0
DATA POINT(P403,ABS)=62.5,25,5,0
DATA POINT(P403,ABS)=62.5,25,6,0
                                                                                                                                                                                                                                                                                                                                                                                                                                                                                                                                                                                                                                                                           POINT(L1)=P12,P13,P14,P15,P
DATA POINT(P13,ABS)=20,45,0
DATA POINT(P15,ABS)=64,45,0
DATA POINT(P15,ABS)=69,38,0
POINT(L1)=P19,P18,P16,P17
DATA POINT(P16,ABS)=47,45,0
DATA POINT(P17,ABS)=41,83,0
DATA POINT(P19,ABS)=40,76,0
POINT(L1)=P23,P22,P20,P21
DATA POINT(P20,ABS)=28,45,0
DATA POINT(P21,ABS)=34,76,0
DATA POINT(P21,ABS)=34,76,0
DATA POINT(P23,ABS)=33,83,0
POINT(L1)=P17,P25,P24,P23,P
DATA POINT(P24,ABS)=33,76,0
DATA POINT(P24,ABS)=33,76,0
DATA POINT(P25,ABS)=33,76,0
                                                                                                                                                                                                                                                                                                                                                                                                                                                                                                                                                                                                                                                                                   000000
                                                                                                                                                                                                                                                                                                                                                                                                                                                                                                                                                                                                                                                                                                                                                                                                                               0000
                                                                                                                                                                                                                                                                                                                                                                                                                                                                                                                                                                                                                                                                                                                                                                                                                                                                                                                             0007
                                                                                                                                                                                                                                                                                                                                                                                                                                                                                                                                                                                                                                                                                                                    17
                                                                                                                                                                                                                                                                                                                                                                                                                                                                                                                                                                                                                                                                                                                                                                                                                                                                                                                                                                                    12
                                                     ັ້ນ
                                                                                                                                                                                                                                                                                                                                                                                                                                                                                                                                               , P35,
                                                                                            P405
                                                                                                                                                                                                      P35, P38, P41
                                                                                                                                                                                                                                                                                                                                                                             Û
                                                                                                                                                                                                                                                                                                                                                                                                                                                                                                                                                P36, P37, P30
                                                                                         ,P401
                                                                                                                                                                                                                                                                                                                                                                             <u>5</u>
                                                                                                                                                                                                                                                                                                                                                                           37,
```

```
DATA POINT(P404, ABS)=62.5, 18.5, 0
DATA POINT(P405, ABS) = 66, 18.5, 0
REMARK INTRODUCING THE INSIDE ROTATING MASS SHAPE...
POINT(L3)=P50,P51,P52,P53,P54,P55,P56,P57,P58,P59,P57,P50
DATA POINT(P50, ABS) = 41.5,19,0
DATA POINT(P51,ABS)=38,20,0
DATA POINT(P52, ABS)=36,22,0
DATA POINT(P53, ABS) = 35,25.5,0
DATA POINT(P54, ABS)=36,29,0
DATA POINT(P55, ABS)=38,31,0
DATA POINT(P56, ABS) = 41.5, 32, 0
DATA POINT(P57, ABS)=41.5,25.5,0
DATA POINT(P58, ABS) = 43, 25.5, 0
DATA POINT(P59, ABS)=40,25.5,0
POINT(L1)=P500
DATA POINT(P500, ABS)=59,22,0
INTRODUCING THE OUTSIDE ROTATING MASS SHAPE......
POINT(L4)=P60,P61,P62,P63,P64,P65,P66,P67,P68,P69,P67,P60
DATA POINT(P60, ABS) = 27.5, 19.0
DATA POINT(P61, ABS) = 24,20,0
DATA POINT(P62, ABS)=22,22,0
DATA POINT(P63,ABS)=21,25.5,0
DATA POINT(P64, ABS)=22,29,0
DATA POINT(P65, ABS) = 24,31,0
DATA POINT(P66, ABS) = 27.5,32,0
DATA POINT(P67, ABS) = 27.5, 25.5, 0
DATA POINT(P68, ABS) = 29, 25.5, 0
DATA POINT(P69, ABS) = 26, 25.5, 0
POINT(L1)=P70,P74,P78,P82,P70
DATA POINT(P70, ABS)=65,41.5,0
DATA POINT(P74, ABS)=64,40.5,0
DATA POINT(P78, ABS) = 63,41.5,0
DATA POINT(P82, ABS) = 64,42.5,0
POINT(L1)=P71,P75,P79,P83,P71
DATA POINT(P71,ABS)=65,41.5.1
DATA POINT(P75,ABS)=64,40.5,1
DATA POINT(P79, ABS)=63,41.5,1
DATA POINT(P83, ABS) = 64,42.5,1
POINT(L1)=P70,P71
POINT(L1)=P74,P75
POINT(L1)=P78,P79
POINT(L1)=P82,P83
REMARK INTRODUCING THE RIGHT SIDE SUSPENSION BAR SHAPE....
POINT(L5)=P72,P76,P80,P84,P72
DATA POINT(P72, ABS)=65,41.5,.25
DATA POINT(P76, ABS)=64,40.5,.25
DATA POINT(P80, ABS) = 63,41.5,.25
DATA POINT(P84,ABS)=64,42.5,.25
POINT(L5)=P73,P77,P81,P85,P73
DATA POINT(P73,ABS)=65,41.5,13.75
DATA POINT(P77, ABS)=64,40.5,13.75
```

```
DATA POINT(P81,ABS)=63,41.5,13.75
DATA POINT(P85, ABS)=64,42.5,13.75
POINT(L5)=P72,P73
POINT(L5)=P76,P77
POINT(L5)=P80,P81
POINT(L5)=P85,P73
POINT(FRAME)=P86,P88,P90,P92,P86
DATA POINT(P86, ABS)=65,41.5,13
DATA POINT(P88, ABS) = 64,40.5,13
DATA POINT(P90, ABS)=63,41.5,13
DATA POINT(P92, ABS)=64,42.5,13
POINT(FRAME)=P87,P89,P91,P93,P87
DATA POINT(P87, ABS)=65,41.5,14
DATA POINT(P89, ABS)=64,40.5,14
DATA POINT(P91, ABS)=63,41.5,14
DATA POINT(P93, ABS)=64,42.5,14
POINT(FRAME)=P86,P87
POINT(FRAME)=P88,P89
POINT(FRAME)=P90,P91
POINT(FRAME)=P92,P93
POINT(FRAME)=P94, P95, P96, P97, P94
DATA POINT(P94, ABS) = 70,47,14
DATA POINT(P95, ABS)=70,37,14
DATA POINT(P96, ABS)=60,37,14
DATA POINT(P97, ABS) = 60,47,14
POINT(L1)=P100,P101,P102,P103,P100
DATA POINT(P100, ABS) = 23.5,41.5,0
DATA POINT(P101, ABS) = 22.5,40.5,0
DATA POINT(P102, ABS)=21.5,41.5,0
DATA POINT(P103, ABS) = 22.5, 42.5, 0
POINT(L1)=P104,P105,P106,P107,P104
DATA POINT(P104, ABS)=23.5,41.5,1
DATA POINT(P105, ABS)=22.5,40.5,1
DATA POINT(P106, ABS)=21.5,41.5,1
DATA POINT(P107, ABS)=22.5,42.5,1
POINT(L1)=P100,P104
POINT(L1)=P101,P105
POINT(L1)=P102,P106
POINT(L1)=P103,P107
REMARK INTRODUCING THE LEFT SIDE SUSPENSION BAR SHAPE.....
POINT(L6)=P108,P109,P110,P111,P108
DATA POINT(P108, ABS) = 23.5,41.5,.25
DATA POINT(P109, ABS) = 22.5,40.5,.25
DATA POINT(P110, ABS) = 21.5,41.5,.25
DATA POINT(P111, ABS) = 22.5, 42.5, .25
POINT(L6)=P112,P113,P114,P115,P112
DATA POINT(P112,ABS)=23.5,41.5,13.75
DATA POINT(P113, ABS)=22.5,40.5,13.75
DATA POINT(P114, ABS)=21.5,41.5,13.75
DATA POINT(P115, ABS) = 22.5, 42.5, 13.75
```

```
POINT(L6)=P108,P112
POINT(L6)=P109,P113
POINT(L6)=P110,P114
POINT(L6)=P111,P115
POINT(FRAME)=P116,P117,P118,P119,P116
DATA POINT(P116, ABS)=23.5,41.5,13
DATA POINT(P117, ABS)=22.5,40.5,13
DATA POINT(P118, ABS)=21.5,41.5,13
DATA POINT(P119, ABS)=22.5, 42.5, 13
POINT(FRAME)=P120,P121,P122,P123,P120
DATA POINT(P120, ABS) = 23.5, 41.5, 14
DATA POINT(P121, ABS)=22.5,40.5,14
DATA POINT(P122, ABS)=21.5,41.5,14
DATA POINT(P123, ABS)=22.5, 42.5, 14
POINT(FRAME)=P116,P120
POINT(FRAME)=P117,P121
POINT(FRAME)=P118,P122
POINT(FRAME)=P119,P123
POINT(FRAME)=P124,P125,P126,P127,P124
DATA POINT(P124, ABS) = 25,48,14
DATA POINT(P125, ABS) = 25, 37, 14
DATA POINT(P126, ABS)=15,37,14
DATA POINT(P127, ABS)=15,48,14
POINT(L1)=P130,P131,P132,P133,P130
DATA POINT(P130, ABS)=29,87,0
DATA POINT(P131, ABS) = 28,86,0
DATA POINT(P132, ABS) = 27,87,0
DATA POINT(P133, ABS) = 28,88,0
POINT(L1)=P134,P135,P136,P137,P134
DATA POINT(P134,ABS)=29,87,1
DATA POINT(P135, ABS) = 28, 86, 1
DATA POINT(P136, ABS)=27,87,1
DATA POINT(P137, ABS) = 28,88,1
POINT(L1)=P130,P134
POINT(L1)=P131.P135
POINT(L1)=P132,P136
POINT(L1)=P133,P137
REMARK INTRODUCING THE REAR SUSPENSION BAR SHAPE......
POINT(L7)=P138,P139,P140,P141,P138
DATA POINT(P138, ABS)=29,87,.25
DATA POINT(P139, ABS) = 28,86,.25
DATA POINT(P140, ABS) = 27,87,.25
DATA POINT(P141, ABS) = 28,88,.25
POINT(L7)=P142,P143,P144,P145,P142
DATA POINT(P142, ABS)=29,87,13.75
DATA POINT(P143, ABS) = 28,86,13.75
DATA POINT(P144, ABS)=27,87,13.75
DATA POINT(P145, ABS)=28,88,13.75
POINT(L7)≈P138,P142
POINT(L7)=P139,P143
POINT(L7)=P140,P144
POINT(L7)=P141,P145
```

```
POINT(FRAME)=P146,P147,P148,P149,P146
DATA POINT(P146, ABS) = 29.87.13
DATA POINT(P147, ABS) = 28, 86, 13
DATA POINT(P148, ABS) = 27,87,13
DATA POINT(P149, ABS) = 28,88,13
POINT(FRAME)=P150,P151,P152,P153,P150
DATA POINT(P150, ABS) = 29,87,14
DATA POINT(P151, ABS) = 28.86,14
DATA POINT(P152, ABS) = 27,87,14
DATA POINT(P153, ABS) = 28,88,14
POINT(FRAME)=P146,P150
POINT(FRAME)=P147,P151
POINT(FRAME)=P148.P152
POINT(FRAME)=P149,P153
POINT (L9)=P310,P311,P312,P313,P314,P315,P316,P317,P310
DATA POINT(P310,ABS)=59.22.0
DATA POINT(P311,ABS)=59.5,20,0
DATA POINT(P312, ABS)=62.5,18.5,0
DATA POINT(P313, ABS) = 65, 20, 0
DATA POINT(P314, ABS) = 66, 22, 0
DATA POINT(P315,ABS)=65,24,0
DATA POINT(P316, ABS) = 62.5, 25.5, 0
DATA POINT(P317, ABS) = 60, 24, 0
POINT (FRAME)=P154,P155,P156,P157,P154
DATA POINT(P154, ABS) = 32,92,14
DATA POINT(P155, ABS) = 32,80,14
DATA POINT(P156, ABS) = 23,80,14
DATA POINT(P157, ABS) = 23,92,14
POINT(L1)≈P200
DATA POINT(P200, ABS) = 78,22,0
POINT(FRAME) = P201, P202, P203
DATA POINT(P201, ABS) = 83,24,0
DATA POINT(P202, ABS) = 83,22,0
DATA POINT(P203, ABS) = 83,20,0
POINT(FRAME)=P206,P207,P208
DATA POINT(P206, ABS) = 60,15,0
DATA POINT(P207, ABS) = 62.5, 15, 0
DATA POINT(P208, ABS) = 65,15,0
REMARK INTRODUCING THE TREE STIFFNESS AND DAMPING ......
REMARK IN THE X DIRECTION.....
SPRING(P200,P202)=PUL1
DATA SPRING(PUL1)=71,1
DAMPER(P200, P202) = DAM1
DATA DAMPER(DAM1)=0.5
REMARK INTRODUCING THE TREE STIFFNESS AND DAMPING......
REMARK IN THE Y DIRECTION.............
SPRING(P207.P312) = PUL2
DATA SPRING(PUL2)=71.1
DAMPER(P207, P312) = DAM2
DATA DAMPER(DAM2)=0.5
REMARK INTRODUCING SHAKER AND TREE MASSES.......
```

```
UNIT MASS=.002591
DATA GRAVITY=0,0,-386.1
DATA MASS(L1.J2)=2.6548;-5,-1.0
DATA MASS(L3,J2)=.2279;0,-3,0
DATA MASS(L4,J3)=.2279;0,-3,0
DATA MASS(L5,J4)=.0259,0,0,7
DATA MASS(L6,J6)=.0259,0,0,7
DATA MASS(L7,J8)=.0259,0,0,7
DATA MASS(L9,J11)=.0534;0,0,0
REMARK INTRODUCING SHAKER AND TREE MASS MOMENT OF INERTIA..
DATA INERTIA(L5,J4)=.8625,.8625,0,0,0,0
DATA INERTIA(L6,J6)=.8625,.8625,0,0,0,0
DATA INERTIA(L7,J8)=.8625,.8625,0,0,0,0
DATA INERTIA(L3,J2)=3.076,3.076,5.584,0,0,0
DATA INERTIA(L1,J8)=10524,1486,10761,0,0,0
DATA INERTIA(L4,J3)=3.076,3.076,5.584,0,0,0
DATA INERTIA(L9,J11)=73,73,.167,0,0,0
REMARK INTRODUCING THE ROTATING MASS SPEED.......
FIND DYNAMIC
DATA TIME=.5,.002,.002
VALUE (SP1)=94.2478*TIME
VALUE (SP2)=-94.2478*TIME
DATA MOTION(J2)=SP1
DATA MOTION(J3)=SP2
REMARK INTRODUCING THE MODEL CONTROL STATEMENTS......
ZERO SPRING=.00001
ZERO FORCE = .07,.7
ZERO POSITION=.0001
ZERO DATA=.00001
ZERO INERTIA=.001
ZERO SYSTEM=.00001
PRINT POSITION (J2,P500)
LIST POSITION(J2,P500)
PRINT ON=TR1
RETURN
```

### APPENDIX C

Optical Free Shaker Displacement Results

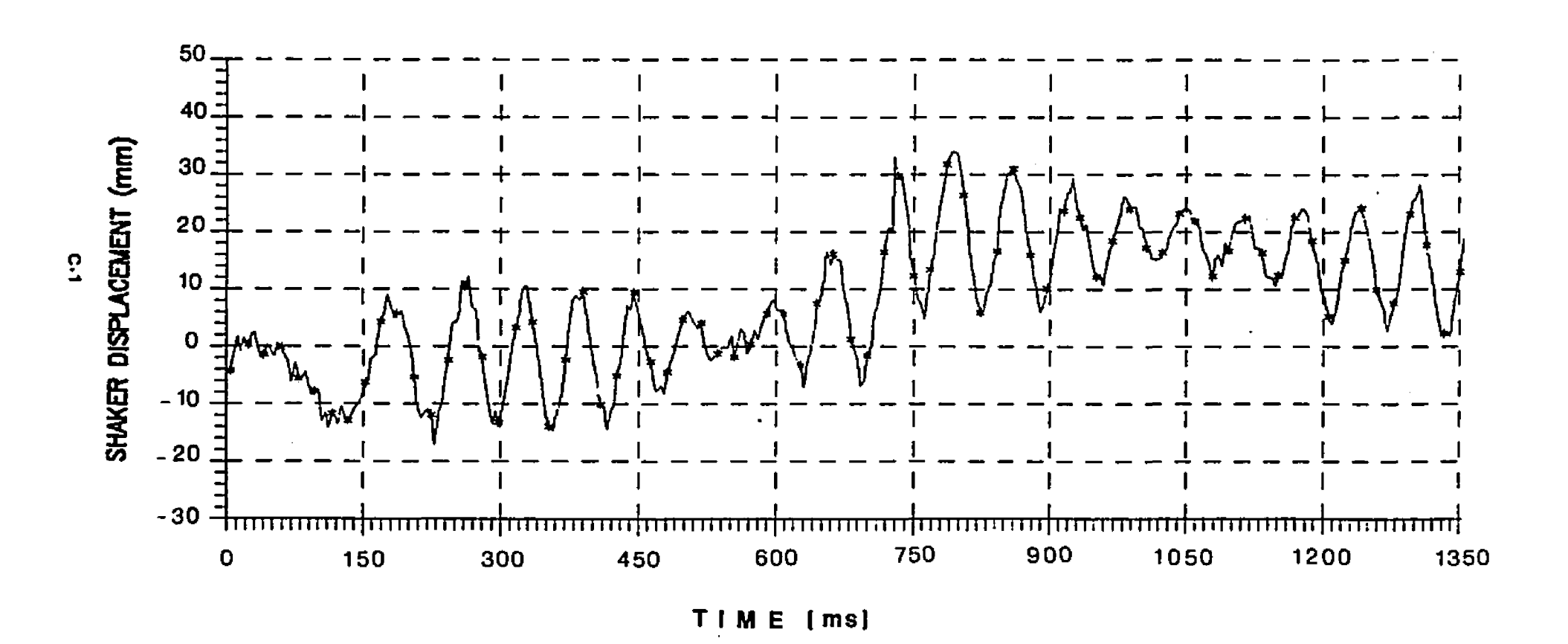
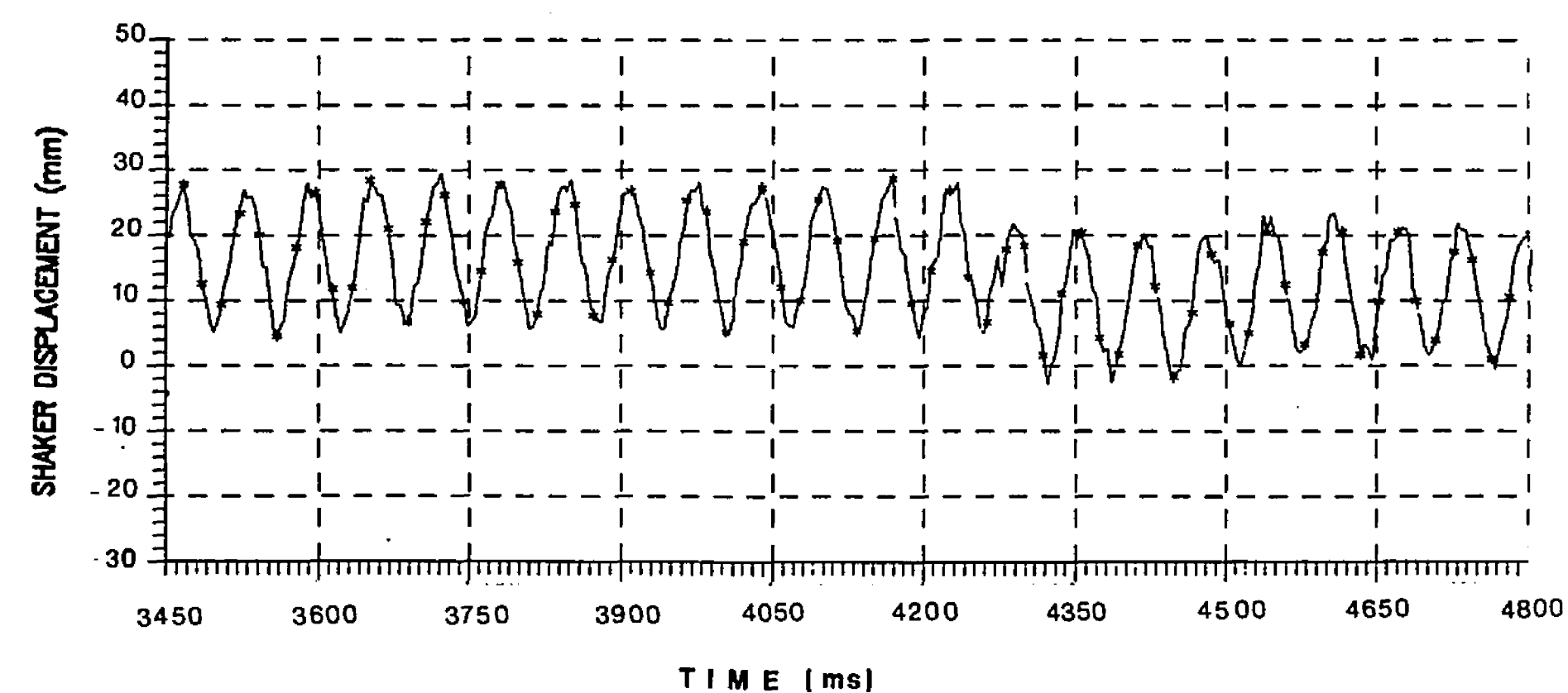


# FIGURE C.2 EXPERIMENTAL FREE SHAKER DISPLACEMENT VS. TIME AT THE PAD CENTER DURING SHAKER STEADY STATE FREQUENCY (MARSHALL, 1986).



## APPENDIX D

Optical Shaker-Tree Displacement Results

